An-Najah National University

Faculty of Graduate Studies

P-Delta Effect in Seismic Reinforced Concrete Portal Frames

By

Suhib Mohammad Abu Qbeitah

Supervisor

Dr. Abdul R. Touqan

This Thesis is Submitted in Partial Fulfillment of the Requirements for the Degree of Master of Structural Engineering, Faculty of Graduate Studies, at An-Najah National University, Nablus, Palestine.

2019

P-DELTA EFFECT IN SEISMIC REINFORCED CONCRETE PORTAL FRAMES

By

Suhib Mohammad Abu Qbeitah

This Thesis was defended successfully on 17/2/2019 and approved by:

Defense Committee Members	**Signature**
– **Dr. Abdul R. Touqan; Supervisor**	………………
– **Dr. Ghada Karaki / External Examiner**	………………
– **Dr. Monther Dwaikat / Internal Examiner**	………………

Dedication

To My Parents, My Brothers, and My Sisters

Acknowledgments

Initially, give Allah all the praise and all the recognition. As none of us can control of anything not even ourselves, and everything happens by his order.

I must mention my parents at the beginning of my thanks for providing me with the unfailing support and continuous encouragement throughout my years of study. They have provided me with the study's environment which otherwise I could not complete this research on time. O Allah, I ask you by your mercy which envelopes all things, that you forgive them.

I would like to thank Dr. Abdul R. Touqan whose office was always open whenever I ran into a trouble spot or had a question about my research or writing. Also his generosity that he provided me with his doctor of philosophy's dissertation is much appreciated. May Allah reward him immensely. Also I would like to thank my brothers Abdulhameed, Osayed and Muath and my sisters Fatima and Saja for their motivational efforts to complete my dissertation with the best quality that I can afford.

Thanks also go to my nephew Mohammad and my niece Jwana for their love. May Allah bless them, keep them and give them peace.

الإقرار

أنا الموقع أدناه مقدم الرسالة التي تحمل عنوان

P-Delta Effect in Seismic Reinforced Concrete Portal Frames

أقر بأن ما اشتملت عليه هذه الرسالة إنما هو نتاج جهدي الخاص، باستثناء ما تمت الإشارة اليه حيثما ورد، وأن هذه الرسالة ككل، أو أي جزء منها لم يقدم من قبل لنيل أية درجة أو لقب علمي أو بحثي لدى أية مؤسسة علمية أو بحثية أخرى.

Declaration

The work provided in this thesis, unless otherwise referenced, is the researcher's own work, and has not been submitted elsewhere for any other degree or qualification.

Student's Name: **اسم الطالب : صهيب محمد ابو قبيطة**

Signature: **التوقيع :**

Date: **التاريخ : 17/2/2019**

Table of Contents

List of Figures

List of Tables

P-Delta Effect in Seismic Reinforced Concrete Portal Frames
By
Suhib Mohammad Abu Qbeitah
Supervisor
Dr. Abdul R. Touqan

Abstract

P-Delta effect is a second-order nonlinear effect, which occurs in every structure when members are subjected to axial loads and bending moments and more eminent in high-rise buildings. ASCE 7 limits the base shear value using a certain period limit equation. The objective of this thesis is to prove that this limit if considered as a limit for the structure's period, which is not a code requirement; we will not run into problems of P-Delta to a certain number of storeys. Furthermore, although it is not a code requirement, the second objective of this thesis is to propose it as a code requirement.

Multi-storey buildings spread widely to accommodate the formidable number of people who need dwellings especially in metropolises. Thus, to study multi-storey effect on P-Delta analysis, P-Delta effect is investigated on six reinforced concrete portal frame multi-storey models from five-storey to thirty-storey which abide by the proposed equation versus three models from five-storey to fifteen-storey which do not abide by the proposed equation. Seismic loads are applied on all models which are determined using modal response spectrum analysis compatible with IBC 2015 and ASCE 7 codes.

As a final result, most probably, engineers will not run into problems with P-Delta if they build reinforced concrete portal frames until 25 storeys if the structure abides by the proposed equation and 8 storeys if the structure does not abide by the proposed equation for 10 percent increase between first-order and second-order analyses.

Chapter One

Introduction

1. 1 Preview

Beam-column is a structural member that is subjected to axial force and bending moment. In real structures, all members in a frame have both bending moments and axial forces. However, for simplicity, if the axial force effect is very small compared to the bending moment, it is more convenient to treat the member as a beam. Furthermore, if the bending moment effect is very small compared to axial force, it is more convenient to treat the member as a column. Therefore, beams or columns are special cases of beam-columns. The bending moments (and deflections) that are present in beam-columns consist of two types: primary bending moments (and deflections) which emerge from applied moments at the member and/or from transverse loads on the member; secondary bending moments (and deflections), which arise as a result of the axial force acting through the lateral displacement of the member, this phenomenon is called P-Delta effect. To account for P-Delta effect, a second-order analysis is needed.

First-order analysis is referring to writing the equilibrium and kinematic relationships on the original geometry of the structure, whilst, second-order analysis is referring to writing equilibrium and kinematic relationships on the deformed configuration of the structure. Generally, second-order analysis needs an iterative procedure to obtain the desired solution. The reason for that is the deformed configuration of the structure is not known and the solution needs to be repeated many times until reaching reasonable solution for the problem. The deformed configuration which is obtained from current phase is used as the basis for formulation of the subsequent phase of iterations.

There are two distinct types of P-Delta effect can be identified: the P-δ effect (member P-Delta effect), and the P-Δ effect (structure P-Delta effect). The P-δ effect has reference to the effects of the axial force in an individual member subjected to a deflection between its endpoints. P-Δ effect has reference to the effects of vertical loads acting on the laterally displaced structure. These secondary effects cause the member to deform more and induce additional stresses in the member. As a result, they have an undermining or destabilizing effect on the structure. So, in the seismic design of multi-storey structures allowance should be made for P-Delta effect.

This research deals with P-Delta effect in seismic portal frames, because Palestine and its conterminous countries are located in a highly seismic zone. Their seismicity derives from their location near the Dead Sea Fault, which has a length equals 1000Km. It extends from Al Aqaba Gulf northward along the Wade Araba, Dead Sea and Tiberias to central Lebanon, and fades away in the south of Turkey. Palestine has a long history in earthquakes over millennium of years. It has documentation and information of the historical earthquakes for almost 2000 years. One of the oldest documentations about earthquakes in Palestine is in the Bible. No region on earth has this long documentation and literature for earthquake events. Information about these ancient earthquakes can be found by archaeological findings. As a summary, Palestine has a long heritage of earthquakes which makes it a vulnerable region for major earthquakes at any time in the future.

Shear wall or dual systems are commonly used in Palestine to resist seismic loads, whereas moment resisting frames are less frequently used for such purposes. In this study, moment resisting frames are used. Moment resisting frames are rectilinear assemblages of columns and beams. Resistance to seismic loads is provided primarily by rigid frame action that-is, by developing bending moments and shear forces in frame members and joints. In moment resisting frames, the joints which connect beams and columns are designed to be rigid. This causes the columns and beams to bend during earthquakes.

1.2 Literature Review

Studies on the parameters the affect P-Delta analysis have been conducted on several fronts. Researchers have worked independently in understanding and quantifying these parameters as follows:

A. Gupta et al (2000) investigated the seismic response on three models of 3, 9, and 20 stories of ductile steel moment resisting frames located in regions with different seismicity levels (Los Angeles, Seattle and Boston), and subjected to seismic loads with different return periods (72,474 and

2475 years) and the seismic response was investigated. They concluded that the seismic response becomes very sensitive to building models when P-Delta was included.

U. Ashraf et al (2013) studied P-Delta effect in reinforced concrete portal frames with rigid joints. Their study was on 12 models with different heights, they observed that displacements change in exponential way when changing number of stories or structure's height under P-Delta effect. They concluded that P-Delta effect is necessary to be included in reinforced concrete high-rise buildings.

D. Yousuf et al (2013) studied the effect of global slenderness on P-Delta analysis in high-rise buildings. The structural analysis program STAAD Pro v8i was used to analyze 4 different models with different slenderness ratios and the percent variation between P-Delta analysis and first-order analysis is computed. It was concluded that due to wide displacement variation with increasing slenderness, P-Delta analysis is required for structures higher than 7 stories.

R. Vijayalakshmi et al (2017) presented a method of designing of P-Delta effects in high rise buildings. P-Delta effect for different number of stories from ten to forty stories was investigated. The load deflection curves and the results so obtained have been compared. The results of the analysis showed that P-Delta effect is more in the upper stories.

N. Pravin et al (2015) investigated the P-Delta effect on multi-storey buildings by taking three models (15, 20 and 25storey). If the change in bending moments is more than 10%, P-Delta should be considered in design. Earthquake load is applied for zone III in ETABS software. The results show that it is essential to consider the P-Delta effect for 25-storey building. So buildings having height more than or equal to 75m, should be designed considering P-Delta effect.

C. Konapure and P. Dhanshettei (2015) studied the P-Delta effect in multi-story buildings. Twelve models were analyzed using STAAD Pro V8i structural analysis program from 5 to 27 stories with 2-storey increment. Displacements, storey drifts, and column moment were computed. It was concluded that as number of stories increase, the P-Delta effect will become more predominant. Moreover, P-Delta effect is negligible up to 7-storey.

1.3 Objectives and Scope

The main objective of this dissertation is to prove that the period limit in ASCE 7 which limits the calculations of base shear (i.e. section 12.8.2, ASCE 7) has implicitly another meaning which is if the structure's period abides by this equation; the structure most probably will not run into problems of P-Delta. The ASCE 7 does not require satisfying this limit for the structure's fundamental period, so, the second objective of this thesis is to propose this limit as a code's requirement. This thesis aims to show that abiding by this limit will implicitly keep the structure away from P-Delta analysis to a certain number of storeys. Thus, if the structure is stiffened to abide by this proposed equation; the structure will not run into P-Delta problems.

1.4 Methodology

Six reinforced concrete models which abide by the proposed equation (i.e. section 12.8.2, ASCE 7) with different number of storeys (5-storey, 10-storey, 15-storey, 20-storey, 25-storey, and 30-storey) are analyzed on SAP2000 software by applying vertical loads and earthquake loads (i.e. response spectrum analysis) and the percent increase in second order moments compared to first order moments on all columns are determined and the critical column (i.e. the highest percent increase) is adopted. The previous analysis is repeated on the same models nevertheless are not abiding by the proposed equation. The relationships between percent increase and the number of storeys for the models which abide and defy by the proposed equation are drawn. The stability coefficients are also determined for all models and compared with the percent increase between first-order analysis and second-order analysis on the critical column.

Previous objectives are investigated on reinforced concrete portal frames models using SAP2000, version19.0 software with hand calculations when it is needed. International Building Code 2015 (IBC 2015) and Minimum Design Loads for Buildings and Other Structures (ASCE 7-10) are adopted in the entire course of this study.

1.5 Thesis's Structure

Chapter 2 expounds both member and structure P-Delta effects and reviews the methods which deal with P-Delta effect on an element or system levels, with clarifying the advantages and disadvantages of each method. Furthermore, it clarifies the main concepts that can be used in second-order analysis.

In Chapter 3, SAP2000, version 19.0.0 results in both static and dynamic analyses are verified. The verification on static results is made by computing the P-Delta effect on a portal frame by both SAP2000 software and hand calculations using approximate equations and the results from both methods are compared. The verification on dynamic results is made by computing the natural period for a portal frame by both SAP2000 software and hand calculations and the results are compared.

Chapter 4 deals with studying the effect of P-Delta analysis on a six models that abide by the proposed equation which increase number of storeys by five-storey increment from 5-storey to 30-storey subjected to response seismic analysis loads versus studying the same effect on another three models which also increase number of storeys by five-storey increment from 5-storey to 15-storey nevertheless they do not abide by the proposed equation. Moreover, the relationship between the percent increase between first-order analysis and second-order analysis and the number of storeys is drawn and tabulated. Furthermore, a comparison between the percent increase and stability coefficients is tabulated for both the abiding and defying models.

Chapter 5 summarizes the conclusions of this research and it suggests numerous recommendations for practicing engineers and future studies.

Chapter Two

Synthesis of Current Information

2. 1 Introduction

P-Delta effect, which is a second-order nonlinear effect, occurs in every structure where elements are subjected to axial load and bending moment and more prominent in tall buildings. P-Delta effect holds an essential role in analysis of the structure. The P-Delta effect is mainly dependent on the applied loads, building's material and structure geometry. Examples of geometry are the height, stiffness, and asymmetry of the structure. Building asymmetry leads to imbalance in distribution of mass, stiffness, etc. Buildings were constructed without considering the second order P-Delta effect and appropriate characteristic for seismic resistance constitute the main source of risk during an earthquake.

Studies on P-Delta effects have been conducted on several fronts. Researchers have worked independently in understanding and quantifying P-Delta effects and in developing methods to account for P-Delta effects. Secondary moments generally produce injurious effects to slender compression members and so they must be taken into consideration in design. The methods in which the secondary moments are integrated in the analysis and design of structural members in reinforced concrete portal frames are gathered in this and the following sections.

Many approaches to account for both member and structure P-Delta effects are discussed in this chapter. General comments on their advantages and disadvantages are also made.

2.2 P- δ Effect

To brief this effect which is called member P-Delta effect, a beam-column is shown in Fig. 2.1 with joint translation restrained and rotation permissible. The end-moments M_J and M_K and the point-load N will produce first-order moment M_1 and first-order deflection δ_1. When the beam-column's member is subjected to axial force P, the axial force will act on the first-order deflection to produce second-order moment M_2 and secondary deflection δ_2. These second-order moments and deflections have been caused by P-δ effect. Since P-δ effect will boost the instability of the member, it is mentioned here as the member instability effect.

The second-order effect can be accounted for by using one of the following methods of analysis:

Closed-form solution: The closed-form solution to account for member's P-Delta effect can be found by solving the governing differential equation which describes the behavior of beam-column after deformation in the elastic range with the proper boundary conditions as follows:

$$EI\,\frac{d^4v}{dx^4} + P\,\frac{d^2v}{dx^2} = w \qquad (2.1)$$

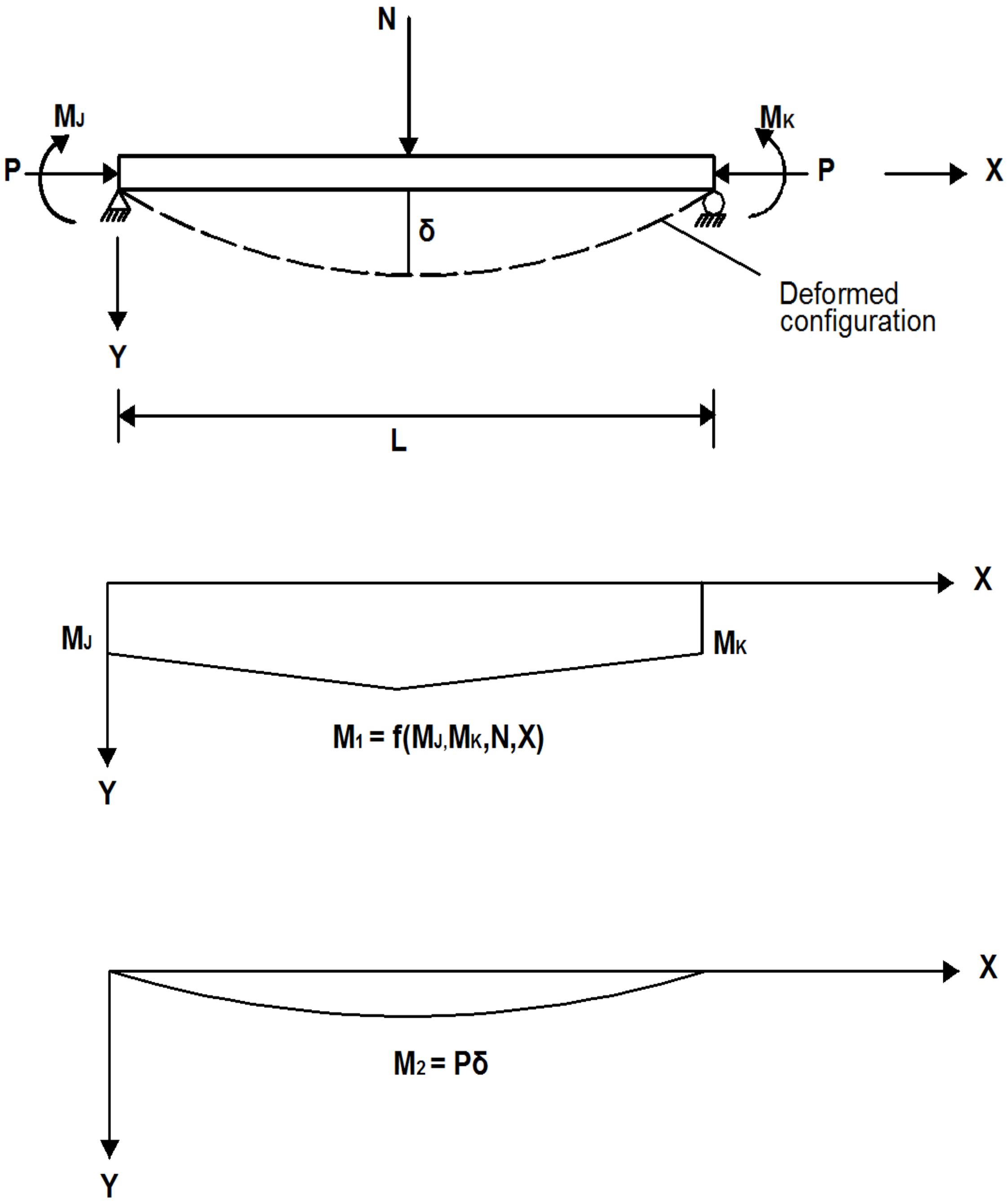

Figure 2.1 P-δ Effect [3].

Where

E = material's modulus of elasticity

I = section's moment of inertia

v = member's deflection in y-direction

x = variable distance along the member

w = transverse distributed load

P = axial force on the member

The closed-form solution is possible for members without material nonlinearity. If yielding or inelasticity occurs in the member, the moment-curvature-thrust relationship becomes non-linear. In such cases, the use of formal mathematics for the solution of the governing differential equation becomes intractable and engineers must move to numerical methods to obtain solutions. In some cases, closed-form solution is still possible if simplified assumptions have been made with respect to stress-strain relationship, and the deflection shape of the member. Generally, the numerical approaches are the best procedure to follow.

Numerical methods to account for P-δ effect: For simplicity, the yielding of the material is ignored and the focus of this study is on the elastic range of the member. Numerical methods in contrast to closed-form solution can account for P-δ effect in both elastic and inelastic range. In this section, four numerical methods to account for P-δ effect are discussed by the author: (1) the finite element approach, (2) the pseudo load approach, (3) the beam-columns approach, (4) moment amplification method. The following is a brief of each method:

Elastic analysis using finite element approach [37]: This approach gained a lot of approval in the engineering field. The finite element approach uses the energy theorem. There are different ways by which finite element can be created. The most common one is displacement-based formulation. In this approach, the displacement fields for both the axial deformation and transverse deformation are assumed for the element. The stiffness matrix which relates the nodal displacements to the nodal forces is attained by minimizing the total potential energy according to the principle of stationary potential energy, which states that equilibrium is attained when the variation of the potential energy vanishes. The main advantage of this approach is that it can solve complicated problems which do not have a closed-form solution. Its deficiency is in the chosen of element size which affects convergence characteristics, since if the member is subjected to large axial force; it is suitable to use small element size. The second deficiency of this method is the displacement fields for both axial and transverse deformations which their assumption does not represent the real element behavior. This method is used in SAP 2000 software to account for P-Delta effect.

We are all aware that a member has a larger lateral stiffness when subjected to tension force and a lower lateral stiffness when subjected to compression force. This general type of behavior is caused by change in the geometric stiffness of the structure. It is obvious that this stiffness is a function of the load in the member whether positive (tension) or negative (compression).

The fundamental equation for the geometric stiffness of a cable element is easy to derive. Consider the horizontal cable in Fig. 2.2 with length L and tension force T. If the cable is subjected to lateral displacements V_i and V_j, then forces F_i and F_j, shall be produced. Note that it is assumed all forces and displacements are positive in the up direction. Furthermore, it is assumed that the displacements are small and do not change the tension in the cable.

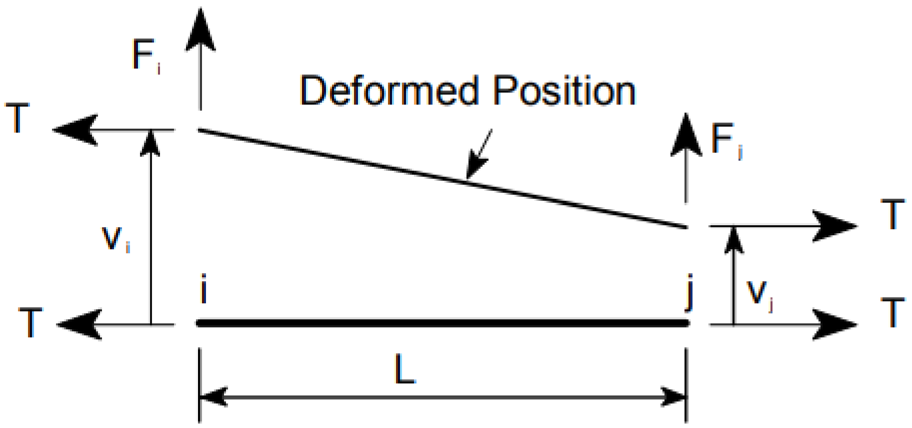

Figure 2.2 Forces Acting on a Cable Element

Taking moments about point j in the deformed position, the following equilibrium equation can be written.

$$F_i = \frac{T}{L}(v_i - v_j) \qquad (2.2)$$

The lateral forces can be expressed in the following matrix form:

$$\begin{bmatrix} F_i \\ F_j \end{bmatrix} = \frac{T}{L}\begin{bmatrix} 1 & -1 \\ -1 & 1 \end{bmatrix}\begin{bmatrix} v_i \\ v_j \end{bmatrix}$$

Or symbolically $F_g = k_g v$ (2.3)

Note that the geometric stiffness matrix is a function of element's length and the force in the element. The geometric stiffness for a beam element can be derived in the same way by adding bending properties in which the deformed shape is assumed to be a cubic function caused by rotations Φ_i and Φ_j at the ends, additional moments M_i and M_j are developed. The force-displacement relationship is given by the following matrix:

$$\begin{bmatrix} F_i \\ M_i \\ F_j \\ M_j \end{bmatrix} = \frac{T}{30L}\begin{bmatrix} 36 & 3L & -36 & 3L \\ 3L & 4L^2 & -3L & -L^2 \\ -36 & -3L & 36 & -3L \\ 3L & -L^2 & -3L & 4L^2 \end{bmatrix}\begin{bmatrix} v_i \\ \phi_i \\ v_j \\ \phi_j \end{bmatrix}$$

Or symbolically $F_G = k_G v$ (2.4)

Elastic analysis using pseudo load approach [38]: Pseudo approach uses analog between beam-column and a beam. Previous discussed approach (finite element approach) accounts for second-order effect by changing the stiffness matrix throughout the course of analysis, but pseudo load approach accounts for second-order effect in pseudo loads. This means that the same stiffness matrix can be used in all approach's cycles. Another advantage of this method over finite element approach is that the finite element cares about mesh size which affects the results, on the other hand, in pseudo load approach; the analysis does not depend on the way in which the member is divided. The main concept of this method is that the differential equation which governs beam-column with distributed load, end-moments and axial force is as discussed in Eq. 2.1, if the previous equation is rearranged, it can be written as follows:

$$EI\,\frac{d^4v}{dx^4} = w - P\,\frac{d^2v}{dx^2} \tag{2.5}$$

Where

$\frac{d^2v}{dx^2}$ = the second derivative of member's deflection with respect to variable distance along the member

E, I, w, P, v, x are as defined before

For small displacements, we can write:

$$\frac{d^2v}{dx^2} = -\,\frac{M}{EI} \tag{2.6}$$

Where

M = the bending moment.

Eq. 2.5 and Eq. 2.6 give

$$EI\,\frac{d^4v}{dx^4} = w + M\,\frac{P}{EI} \tag{2.7}$$

The differential equation of equilibrium for a beam member is as follows:

$$EI\,\frac{d^4v}{dx^4} = w \tag{2.8}$$

From the analog between Eq. 2.7 and Eq. 2.8, it can be concluded that, the difference between beam and beam column is the term $M\frac{P}{EI}$, so if the bending moment in each cycle is multiplied by the factor $\frac{P}{EI}$ to give the pseudo loads; the new moment can be determined. This process keeps repeating itself and the results of each cycle are used in the successive cycle until the value of M remains almost constant.

Elastic analysis using beam-columns approach [3]: In this method, the stiffness matrix which relates the member's forces and the member's displacements of a beam-column's member is created from the modified slope-deflection equations which take into account the effect of axial force on the member's bending stiffness. Second-order effect is accounted for in the stiffness matrix; this means that stiffness matrix is updated during the course of analysis. As a result, the solution can only be obtained by iterative procedure. The main disadvantages of this method are as follows: (1) its complexity, because in every case the stiffness matrix's formula needs to be modified. For example, if in-span loads apply at the member, the stiffness matrix formula must be changed, or if the member is not horizontally oriented, the stiffness matrix must be transformed into global coordinates, (2) the effect of curvature shortening (i.e. bowing effect) since if the bending moments are large, its effect on axial deformation must be included in the term EA/L in the stiffness matrix.

Moment amplification method [3]: In this method, the first-order moments obtained from a first-order analysis are magnified by amplification factors to account for member P-δ effect. The total moment (and deflection) is equal to the sum of primary and secondary moments. In this method, the form of secondary moment is assumed (e.g. half sine, parabola, etc.), and then after rearranging equations, the maximum moment is derived, which equals to the first-order moment multiplied by an amplification factor. The following amplification factor is derived based on secondary moment in the form of half sine wave (see theory of beam-columns Volume 1).

$$M_{max} = \left(\frac{C_m}{1-\frac{P}{P_{ek}}}\right)M_{1max} = B_1 M_{1max} \quad (2.9)$$

Where

M_{max} = maximum moment in the member

$C_m = 1 + \psi \frac{P}{P_e}$

$\psi = \frac{\delta_1 P_e}{M_{1max}} - 1$

P = axial load

$P_{ek} = \frac{\pi^2 EI}{(KL)^2}$ is the elastic buckling load considering end restraining conditions

B_1 = P-δ moment amplification factor

M_{1max} = maximum first-order moment

Table 2.1 summarizes C_m and ψ values for commonly beam-columns with transverse loading.

ψ is a factor with values equal or less than zero. It equals zero when the member is subjected to distributed load and the joint translation is prevented, which makes the member to deflect in a single curvature which implies maximum value for C_m factor which leads to maximum second-order effect. When the value of ψ increases in negative; this means the second-order effect will decrease (i.e. C_m will decrease).

C_m factor for beam-column subjected to end moments

C_m factor to beam-columns subjected to end moments is referred to the concept of equivalent moment factor; equations to account for P-Delta effect have been derived for the general case of a beam-column which is subjected to unequal end-moments. The maximum moment in the member may occur at the end of the member, or it may occur somewhere within its length. That's why the need came to use of the equivalent moment factor. The concept of equivalent moment factor is shown in Fig. 2.3. The end moments M_A and M_B are replaced by a couple of equal and opposite equivalent moment M_{Eq}. The magnitude of the equivalent moment is such that the maximum moment generated by it will be equal to that generated by M_A and M_B.

The equivalent moment factor C_m is a function of M_A, M_B and axial force P, where M_A is the smaller and M_B is the larger. M_A/M_B is positive when the member bends in double curvature (i.e. M_A and M_B rotate in the same direction) and negative when the member bends in single curvature (i.e. M_A and M_B rotate in opposite direction). Approximate expressions have been proposed that eliminate its dependency on axial force P as follows:

Table 2.1 Values of ψ and Cm [4].

Case	ψ	C_m
1 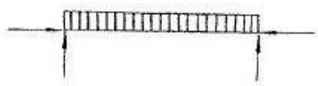	0	1.0
2 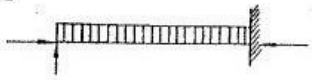	−0.4	$1-0.4\ P/P_{ek}$
3 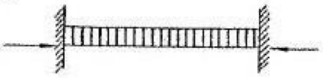	−0.4	$1-0.4\ P/P_{ek}$
4 	−0.2	$1-0.2\ P/P_{ek}$
5 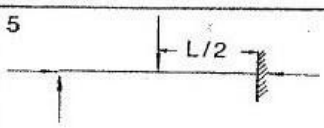	−0.3	$1-0.3\ P/P_{ek}$
6 	−0.2	$1-0.2\ P/P_{ek}$

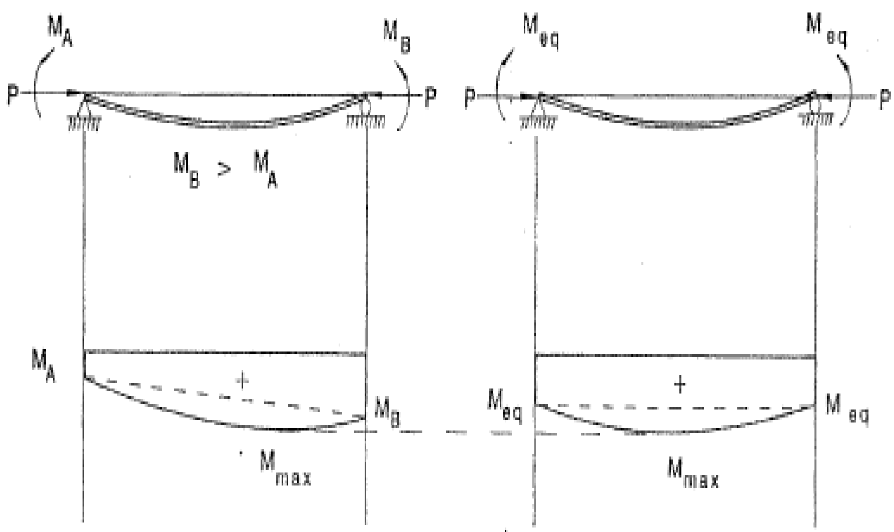

Figure 2.3 Representation of the Concept of Equivalent Moment [2].

Massonnet expression (1959)

Massonnet proposed the following equation:

$$C_m = \sqrt{(0.3\left(\frac{M_A}{M_B}\right)^2 - 0.4\left(\frac{M_A}{M_B}\right) + 0.3)} \qquad (2.10)$$

It is worth to be mentioned that C_m is not function of the axial force in Massonnet expression. When the axial force is large, the Massonnet expression gives reasonable results. However, when the axial force is small, it gives unreasonable results.

Austin expression (1961)

The Austin expression has the form

$$C_m = 0.6 - 0.4\left(\frac{M_A}{M_B}\right) \quad \geq 0.4 \qquad (2.11)$$

Similar to the Massonnet expression, in Austin expression C_m is not a function of the axial force in the member. In sway frames, the columns usually subjected to large axial force and bent in double curvature, which are the conditions at which the Austin expression gives conservative results. Furthermore, the Austin expression gives unconservative results if the axial force is small and if the columns bent in single curvature. Moreover, the condition that C_m must be equal or larger than 0.4 has been removed because it is a very conservative condition.

Duan-Sohal-Chen expression (1989)

As can be seen form Fig. 2.4, the Austin expression gives unconservative results for small axial forces (i.e. approximately $P/P_e \leq 0.68$ from Fig 2.4) and if M_A/M_B is negative (i.e. the member bents in singe curvature). To handle this unwanted situation, Duan-Sohal-Chen (1989) have proposed amended expression which takes into account the axial force's value as follows:

$$C_m = 1 + 0.25\left(\frac{P}{P_e}\right) - 0.6\left(\frac{P}{P_e}\right)^{\frac{1}{3}}\left(\frac{M_A}{M_B} + 1\right) \tag{2.12}$$

The various expressions for C_m are plotted in Fig. 2.5, as can be observed; the approximate expressions give to some extent a pretty approximation to the theoretical one. Because of its straightforwardness, the Austin expression has been adopted by numerous design codes.

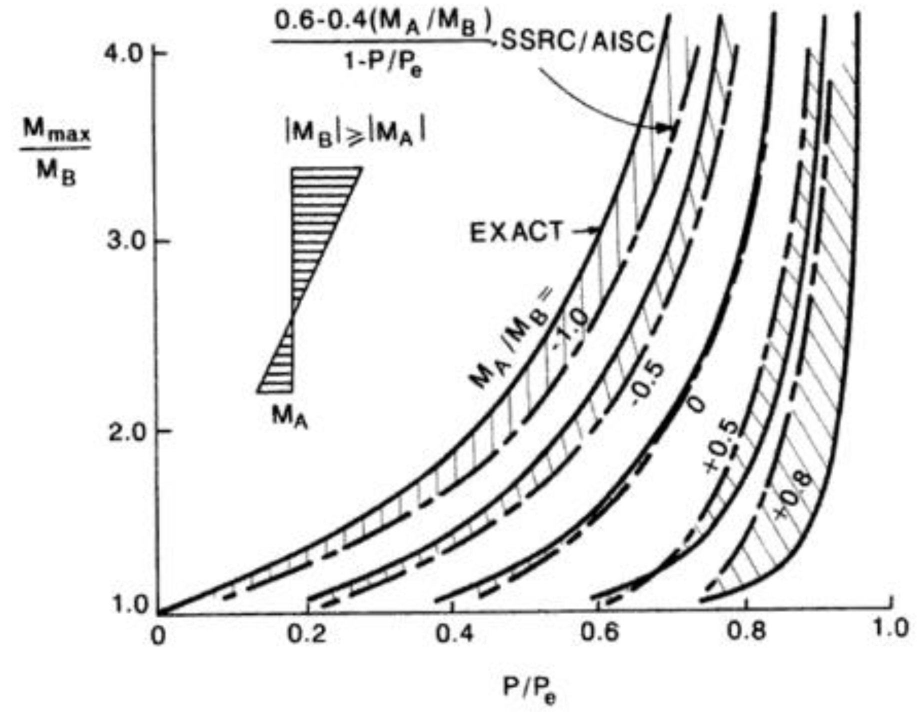

Figure 2.4 Comparison between Exact Amplification Factor and Austin's Expression [3].

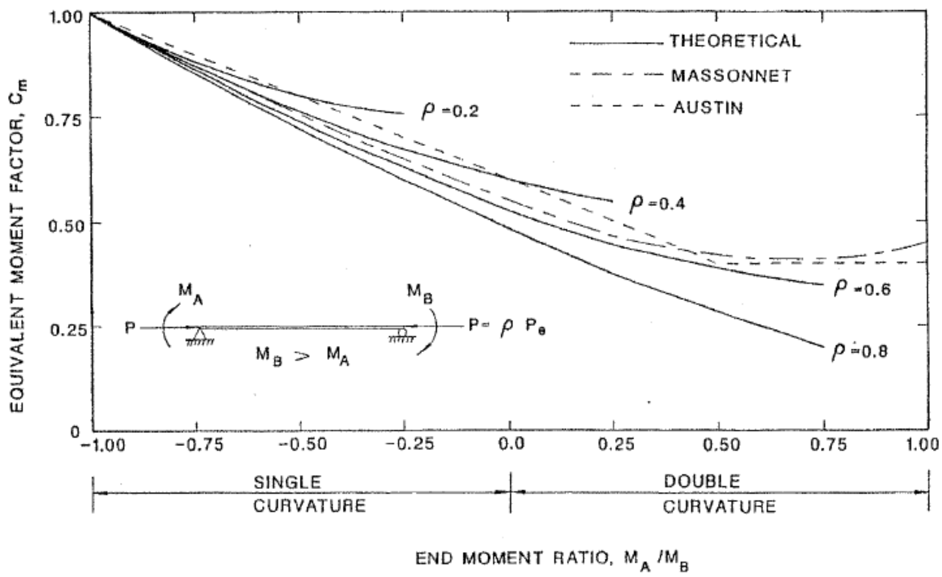

Figure 2.5 Comparison between Various Expressions of C_m and Theoretical Expression [2].

2.3 P-Δ effect

As a result of applying a horizontal force H, the frame moves until reaching an equilibrium position as shown in Fig. 2.6. The corresponding deflection which is computed on the un-deformed configuration is called the first-order deflection and is denoted by Δ_1. If a vertical force P is applied; it drifts the frame further by interaction with the lateral displacement Δ_1 caused by force H until reaching a new equilibrium position. The lateral deflection which coincides with the new equilibrium position is denoted by Δ (Fig. 2.7). The aforementioned incident by which the vertical axial force P interacts with the first-order deflection Δ_1 which is caused by the lateral force H is called the structure P-Delta effect, which leads to increase in both deflection and overturning moment. For the reason that the additional deflection and overturning moment have prejudicial effects on the stiffness and stability of the frame, they should be taken into account in analysis and design.

In order to calculate precisely the final deflection Δ and the second-order moment M taking into consideration the structure P-Δ effect, a nonlinear static analysis based on the deformed configuration of the structure is needed. Second-order analysis usually requires an iterative procedure. To account for P-Δ effect, it can be used either closed-form solution or approximate solutions.

Closed-form solution: The differential equation on the deformed configuration of the frame can be written with proper boundary conditions. However, closed-form procedure is highly complex for the entire frame and the required limitations are rarely met in reality. Thus, the numerical solutions are the best approaches to follow.

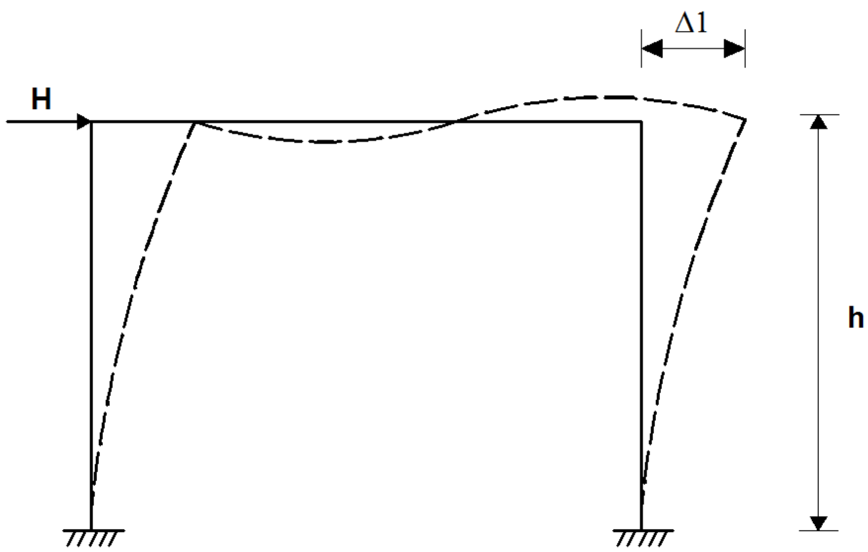

Figure 2.6 Equilibrium Position before P-Δ Effect [3].

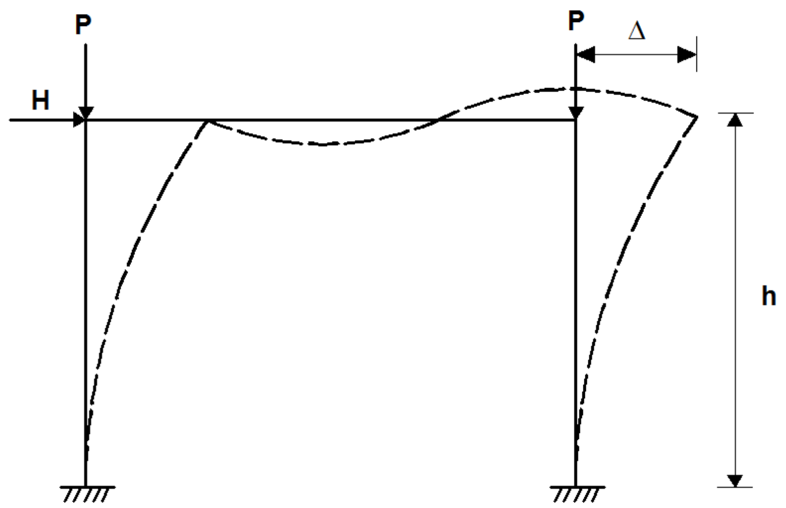

Figure 2.7 Equilibrium Position after P-Δ Effect [3].

Numerical methods to account for P-Δ effect: The previous explained approaches (i.e. finite element approach, pseudo load approach, and beam-column approach) still applicable to account for structure P-Δ effect. Two practical moment amplification methods are discussed in this section as follows:

Story magnifier method (Rosenblueth, 1965; Stevens, 1967; Cheong-Siat-Moy, 1972)

This method has been proposed by Rosenblueth in 1965 and then modified and developed by Stevens in 1967 and Cheong-Siat-Moy in 1972. This method contains two assumptions which facilitate the method of solution. The first assumption is that each story behaves independently of other stories. Second assumption is that the second-order moment which has resulted from P-Δ effect is equivalent to moment caused by a lateral force. From previous assumptions, we can say that, the story sway moments are directly proportional to the lateral deflections of the story.

$$M = \left(\frac{1}{1-\sum P\Delta_1/\sum Hh}\right) M_{1sway} = B_2 M_{1sway} \tag{2.13}$$

Where

M = maximum end moment accounting for P-Δ effect

M_{1sway} = maximum primary moment due to swaying of the story

B_2 = P-Δ moment amplification factor

Δ_1 = First-order deflection

$\sum P$ = summation of axial forces

$\sum H$ = summation of lateral forces

From Eq. (2.13), it can be concluded that to account for P-Δ effect, the first-order moment is computed and then multiplied by the moment amplification factor to account for second-order effect. This method gives acceptable results if the beams are stiff (i.e. inflection point exists in every column). The main disadvantage of this method is that it is a function of first-order deflection. Wherefore, to determine the second-order moment, a first-order analysis is needed.

Multiple-column magnifier method (Yura, 1971)

This method has been proposed by Yura in 1971. It has another name known as the modified effective length method. By assuming that the story sway moments are directly proportional to the lateral deflections of the story, the maximum end moments M accounting for the P-Δ effect can be written:

$$M = \left(\frac{1}{1-\sum P/\sum P_{ek}}\right) M_{1sway} = B_2 M_{1sway} \tag{2.14}$$

Where, M, M_{1sway}, B_2, $\sum P$ are as defined before

P_{ek} is elastic buckling load considering column end restraining conditions

The advantage of this method is that its simplicity since it is not function of first-order deflection. The main disadvantage of this method is that if the P-Δ effect is large, the story magnifier method will give preferable results.

2.4 Second-order analysis using solution algorithms:

In previous beam-column and finite element approaches, the account for nonlinear effect was by updating the stiffness matrix in every cycle. As the equilibrium configuration of the frame keeps changing, subsequently, the analysis can be carried out using a set of load increments. The states of equilibrium and kinematic relationships at the end of preceding load increment are used to formulate the stiffness relationships at the current load increment. Different schemes were made to determine the size of the load increment. As the size of the load increment has a strong impact on convergence of the problem and the solution time, it is assumed based on previous experiences. Two main used approaches are discussed in this section as follows: (1) load control method, (2) displacement control method. The main concept in both previous methods is to start with a known solution point on the equilibrium path to obtain another solution point on the path. The various solution schemes differ by the technique in which the load increment's size is determined and the manner in which iterations are carried out. By iterating the procedure, the whole load-deflection curve can be traced. The solution after x iterations will be converged, and the load and displacement are computed. The updated matrix can then be constructed and the solution steps to the next increment.

2.4.1 Load control method [3]

In this method, the load increment's size at every load step is determined as a percentage of total applied loads and this percentage is assumed based on the engineering decision and previous experiences. This method can be used in iterative or non-iterative procedures. If it is used in a non-iterative procedure, it is called simple incremental method, and if it used in an iterative procedure, it is called load control Newton-Raphson method.

2.4.1.1 Simple incremental method

As discussed before that the load increment's size is a percentage of total applied loads. The main concept of this method is that the stiffness matrix from preceding load step (i.e. i-1) and the load increment at load step *i* are used to determine the displacement at the load step i . Thereafter, the displacement is added to previous load step's displacement to obtain a new cumulative displacement. Eventually, the stiffness matrix for load step i can be updated and the solution can go ahead to the next step. The advantage of this method is that it does not imply any iteration; consequently, it is a straightforward procedure to follow. Simultaneously, the main disadvantage of this method is that it does not contain any iteration to eliminate the drift-off-error between actual equilibrium path and the calculated equilibrium path as shown in Fig. 2.8.

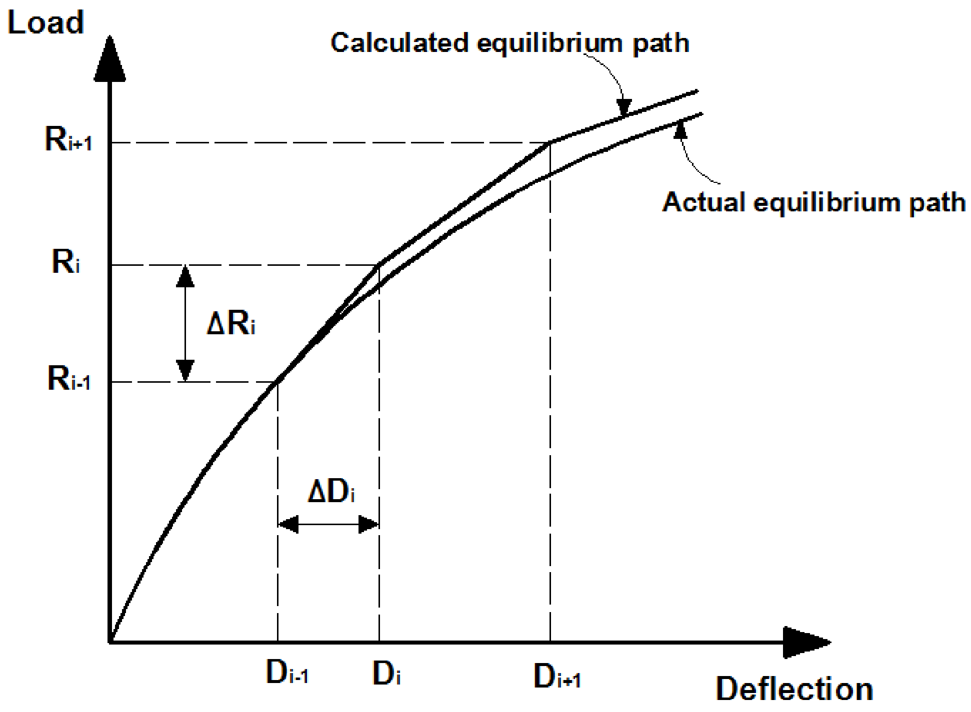

Figure 2.8 Drift-off-Error in Simple Incremental Method [3].

2.4.1.2 Load control Newton-Raphson method

This method has the same concept as simple incremental method. However it has iterations to eliminate the drift-off-error. The iterations in every load step continue until drift-off-error becomes negligibly small as shown in Fig. 2.9. The advantage of this method is that the correction is made by subjecting the frame to unbalanced forces (i.e. difference between internal and external forces). The disadvantages of this method are : (1) the solution diverges at the limit point and (2) a number of iterations and errors may be required to determine the appropriate load increment (3) the stiffness matrix need to be updated in every iteration during each load step.

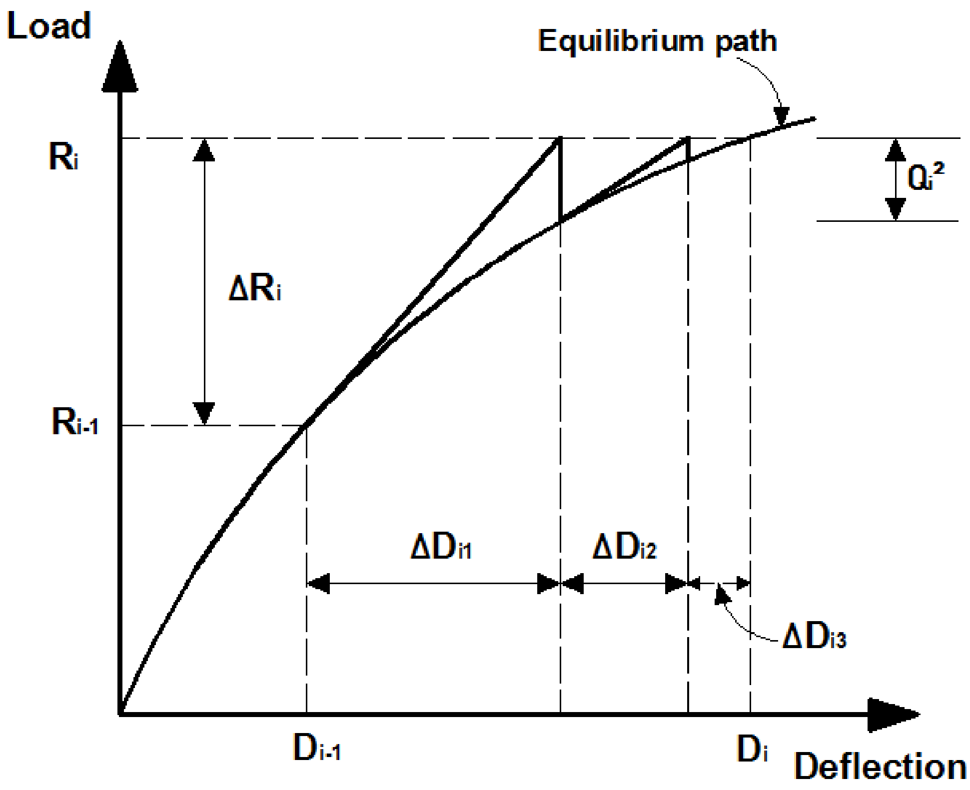

Figure 2.9 Load Control Newton-Raphson Method [3].

2.4.1.3 Modified Load control Newton-Raphson method

This method differs from load control Newton-Raphson method in that the same stiffness matrix is used for each load step and the stiffness matrix is updated occasionally which is considered an advantage for this method as shown in Fig. 2.10. Thereby, the computational time for the problem is decreased. The main deficiency of this method is that it has a slow rate of convergence.

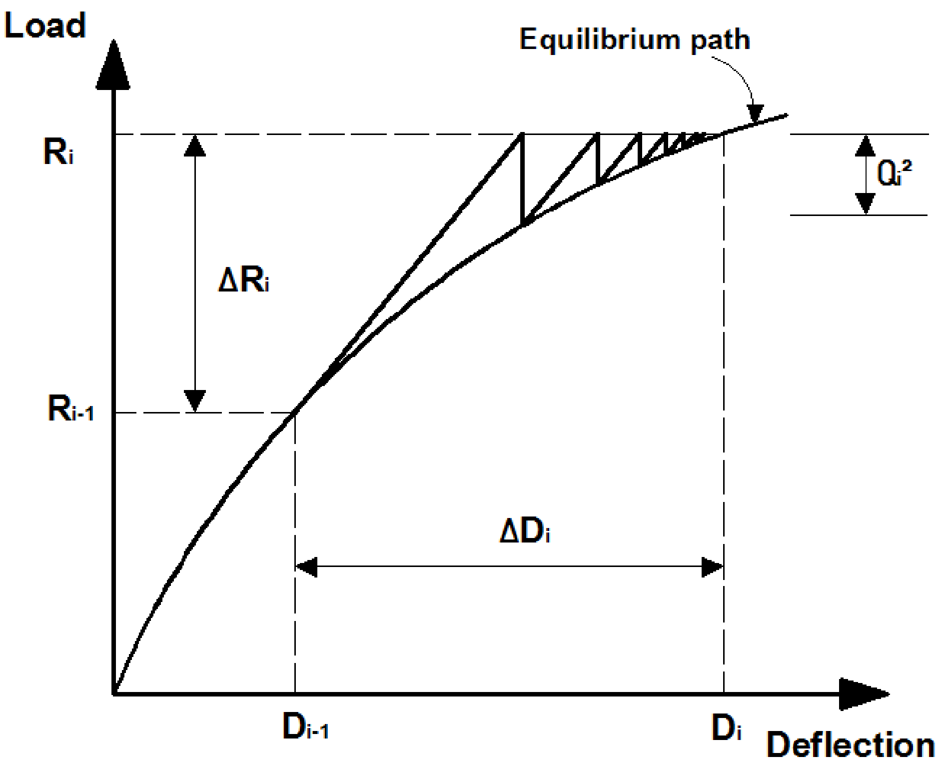

Figure 2.10 Modified Newton-Raphson Method [3].

2.4.2 Displacement control method [39]

This method implies a constant displacement instead of a constant load as such the case of simple incremental method or load control-Newton-Raphson method as shown in Fig. 2.11. A displacement variable is prescribed, and then applying equations to determine the load displacement increment for current iteration based on previous stiffness matrix iteration, then, the load increment factor for current iteration within the same load step is determined, thereafter, the displacement increment which includes displacement increment associated with unbalanced forces can be updated. The process keeps repeating until convergence is achieved, then a new load step can be started. The main advantage of this method is that because it is performed based on a constant displacement it is applicable for limit point. On the other hand, it has a deficiency in how to choose the proper control displacement which affects the convergence characteristics.

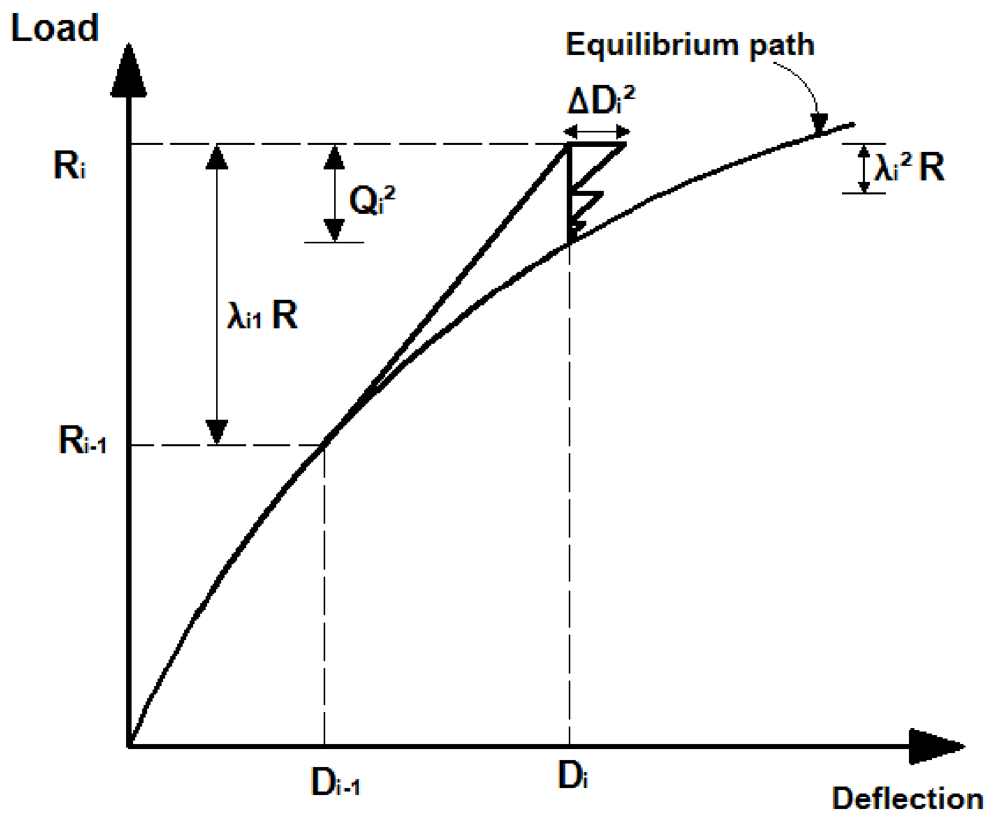

Figure 2.11 Displacement Control Method [3].

2.5 Moment-curvature-thrust relationship

The simplest cross section to obtain a closed-form solution for M-Φ-P relationship under uniaxial bending is a rectangular cross section. However, for general cross-sections under biaxial bending, numerical methods are used to obtain the moment-curvature-thrust relationship. For rectangular cross-section under uniaxial bending, the M-Φ-P relationship can be derived by using the integration for axial force and bending moment on the cross section area, then depending on the stress distribution (i.e. elastic, primary plastic and secondary plastic stress distribution); the moment-curvature-thrust relationship can be obtained. If the axial deformation is large, P-ε-M relationship (i.e. relationship between axial force P and axial deformation ε for certain values of bending moments) is needed. Generally, beam-columns have large flexural deformation compared to axial deformation; consequently, M-Φ-P relationship is required. Fig 2.12 shows M-Φ-P relationship for rectangular cross section. It can be seen that, the moment capacity of the member decreases as the magnitude of axial force increases which is a foreseeable result.

The derivation of preceding M-Φ-P curves for rectangular cross-section is done by assuming that:

(1) Plane sections before bending remain plane after bending (i.e. Euler-Bernoulli beam theory).

(2) The geometry of the cross-section does not change after section is subjected to loads.

(3) The material follows elastic-perfectly plastic behavior in stress-strain relationship.

For general cross-sections which the material manifests a more complex stress-strain behavior, closed-form solutions for M-Φ-P relationship become difficult. So, the M-Φ-P relationships can be derived by computer-based numerical procedures.

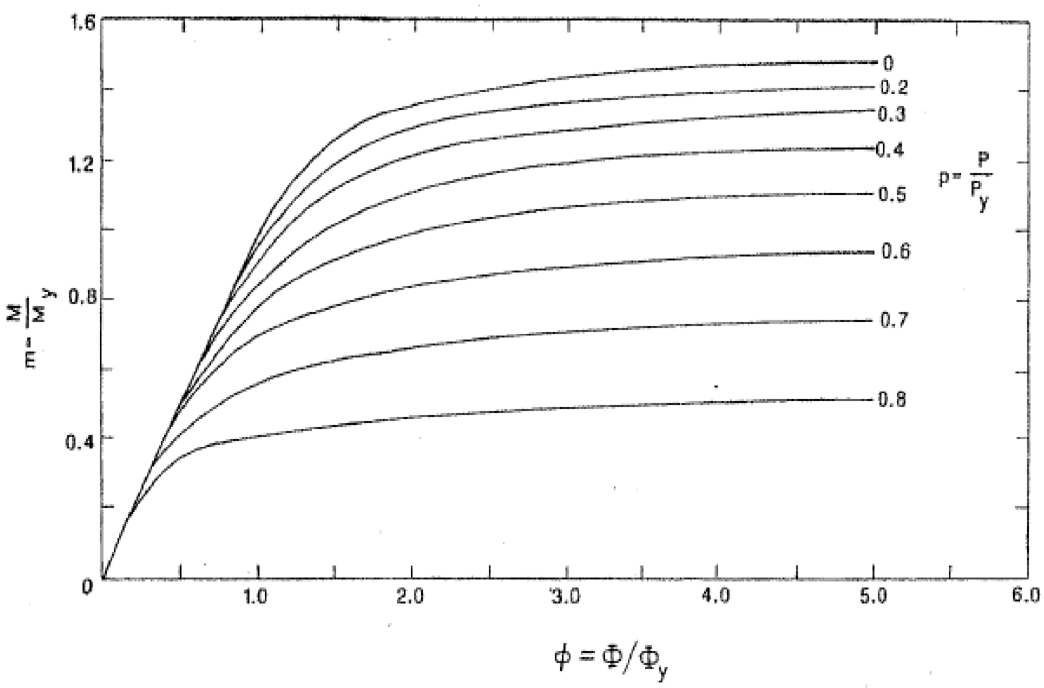

Figure 2.12 M-Φ-P Curves for Rectangular Cross-Section [2].

2.6 Effective length factor K

The effective length factor K is defined as a factor when multiplied by the member's length of end-restrained column; it gives the equivalent length of a pinned-pinned column as shown in Fig. 2.13. Furthermore, this equivalent length has the same buckling load as the end-restrained column. Since the moment at hinge equals zero, the effective length factor K is the distance between two adjacent points of zero curvature. Mathematically, the effective length factor K is given by the following formula:

$$K = \sqrt{\frac{Pe}{Pcr}} = \sqrt{\frac{\pi^2 EI}{L^2 Pcr}} \qquad (2.15)$$

Where

P_e = Euler buckling load

P_{cr} = elastic buckling load.

L = unsupported length of the column.

E and I are as defined before.

Table 2.2 summarizes some theoretical and recommended values for K-factor for isolated columns. As can be seen from this table, the recommended design values are greater than theoretical ones to be more conservative in design. With regards to columns in a framework, the effective length factor K theoretically can be determined from stability functions analysis (i.e. eigenvalue analysis). However, in practice, such analysis is not practical. Wherefore, a simple approach is discussed by the author that was developed by Julian and Lawrence (1959). This procedure has been adopted by many design codes among them ACI 318, AISC, and AASHTO specifications. This method is rather simple and straightforward to obtain the effective length factor K by using the proper alignment chart. In order to clarify the idea, the determination of K-factor for member in both braced and in an unbraced frame is discussed separately. The design of a beam-column starts with the determination of the stiffness ratio of columns and girders G_A and G_B, from which the effective length factor K is determined.

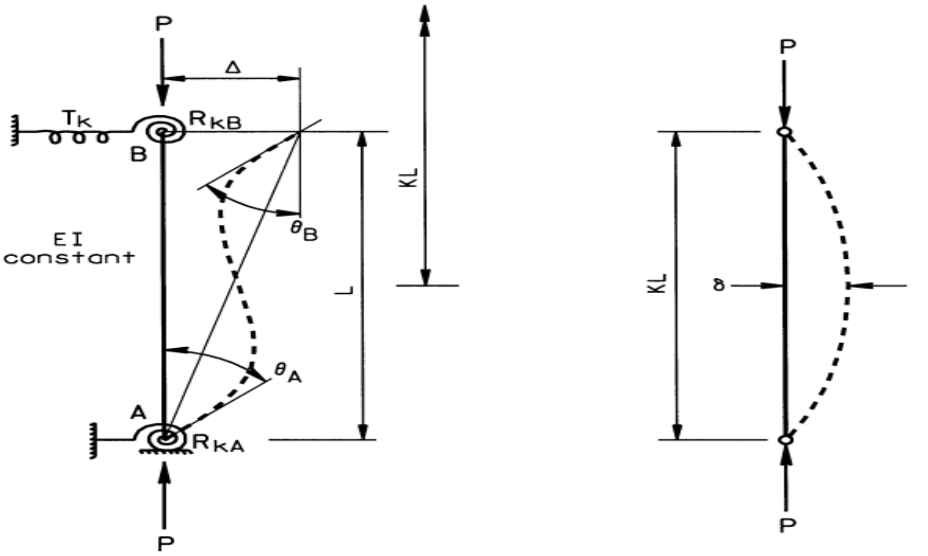

(a) End-restrained Columns (b) Pin-ended Column

Figure 2.13 Isolated Column [18].

Table 2.2 Theoretical and Recommended K Factor [18].

Buckled shape of column shown by dashed line	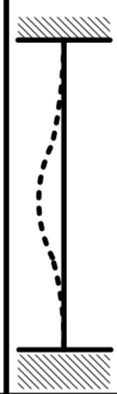	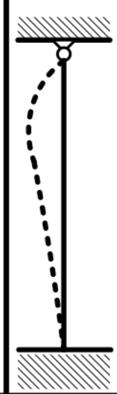		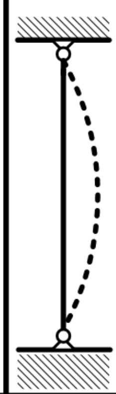	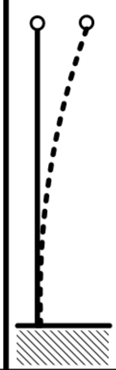	
Theoretical K value	0.5	0.7	1.0	1.0	2.0	2.0
Recommended design value K	0.65	0.80	1.2	1.0	2.10	2.0
End condition key	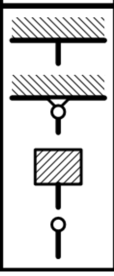	Rotation fixed and translation fixed Rotation free and translation fixed Rotation fixed and translation free Rotation free and translation free				

2.6.1 Braced frames

Braced frames are the frames in which the side way is prevented as shown in Fig. 2.14, and, therefore, the K-factor is never greater than 1.0. The structural model employed for determination of K-factor for a framed column braced against sideway is shown in Fig. 2.14.

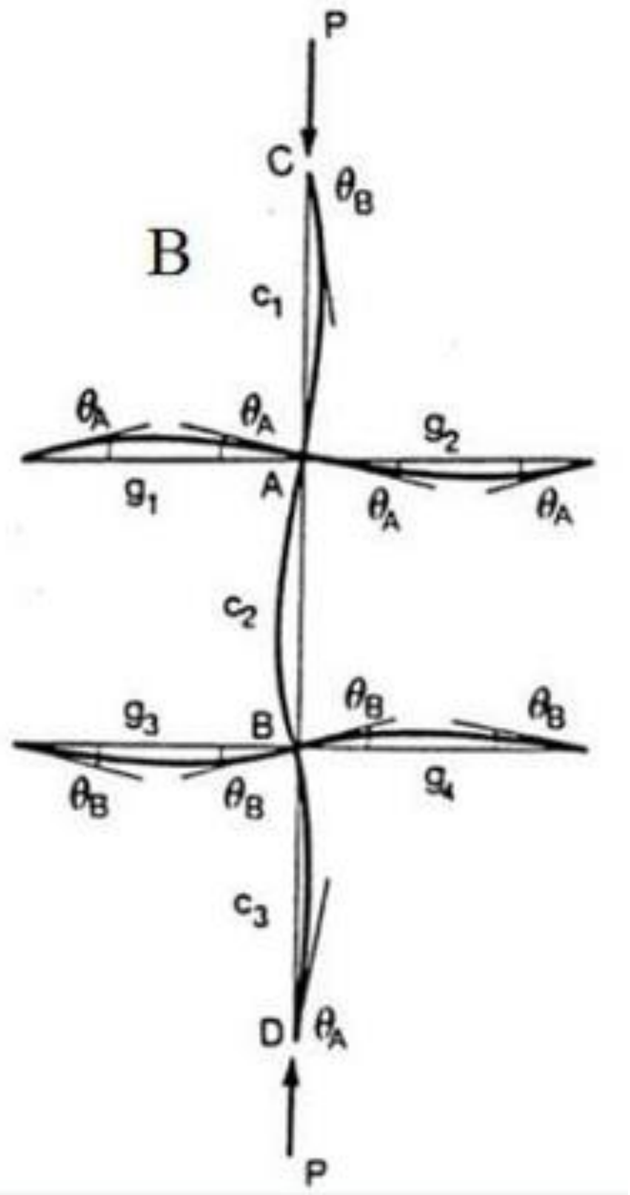

Figure 2.14 Model for Braced Frame [18].

The assumptions used in this model are:

1. All members have a constant cross section and behave elastically.
2. The axial forces in the beams are negligible.
3. All columns buckle simultaneously.
4. All joints are rigid.
5. At buckling, the rotations at the near and far ends of the beams are equal in magnitude and opposite in direction.
6. The restraining moment which is provided by the beam at joint is distributed on columns based on their stiffnesses.

To determine the K-factor using monograph form in Fig. 2.14 (Julian and Lawrence, 1959), G_A and G_B at A and B ends of the column under consideration are determined according to Eq. (2.16).

$$G = \frac{\sum\left(\frac{EI}{L}\right)\text{Columns}}{\sum\left(\frac{EI}{L}\right)\text{Beams}} \tag{2.16}$$

Where,

I = section's moment of inertia.

E = material's modulus of elaticity.

L = member's length.

G = end restraint factor.

Subscripts A and B = the joints at the two ends of the column section being considered.

Figs. 2.15 and 2.17 are widely used alignment charts in engineering practice to obtain the effective length factor K for the column under consideration. The minimum value of K (i.e. K=0.5) coincides with the case when girders are stiff so that the column's end conditions close to fixed supports. On the other hand, the maximum value of K (i.e. K=1) coincides with the case when girders are flexible so that the column's end conditions close to pin supports.

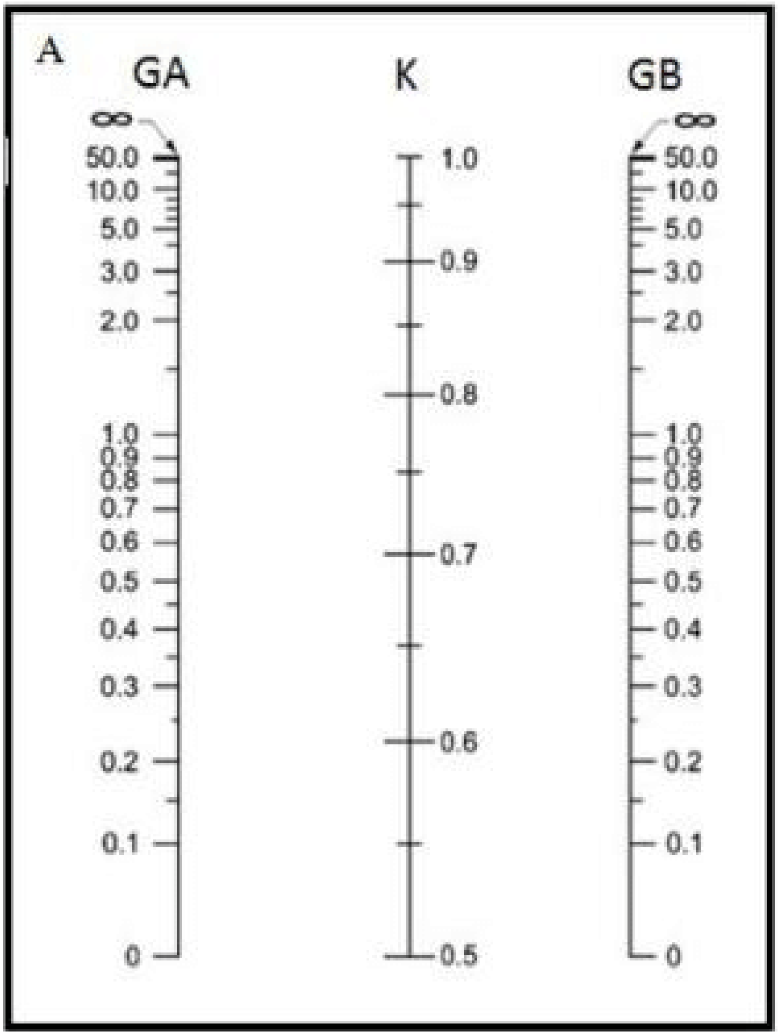

Figure 2.15 Alignment Chart for Braced Frame [18].

2.6.2 Unbraced frames

If a rigid frame depends solely on frame action to resist lateral forces, its side way is permitted as shown in Fig. 2.16. In this case, the K-factor is never smaller than 1.0 and its maximum value is infinity. The model for the determination of K-factor for a framed column subjected to sideway is shown in Fig. 2.16. The assumptions used for this model are the same as those used for the model of the braced frame, except that, for this model, the fifth assumption is modified as follows: the rotations at the near and far ends of the girders are equal in magnitude and direction.

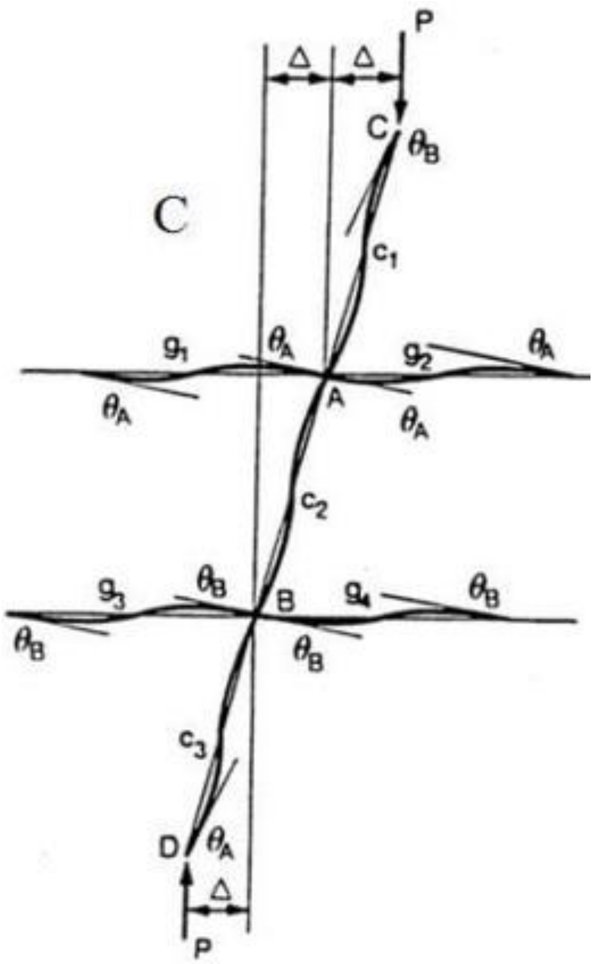

Figure 2.16 Model for Unbraced Frame [18].

To determine the K-factor using monograph form in Fig. 2.16 (Julian and Lawrence, 1959), G_A and G_B at A and B ends of the column under consideration are determined according to Eq. (2.16). The value of the effective length factor K is obtained as the intersection of the straight line with the K scale.

Note that, G equals zero when the column is connected rigidly to the footing. However, for practical design, a value of 1 is taken. Likewise, if the column is connected to the footing by a pinned support, G is infinity, but for practical design, a value of 10 is taken. The use of G equals 1 for a column which is rigidly attached to a properly designed footing and G equals 10 for a hinged support reflects the fact that an ideally fixed or hinged support condition will never be run across in a real frame.

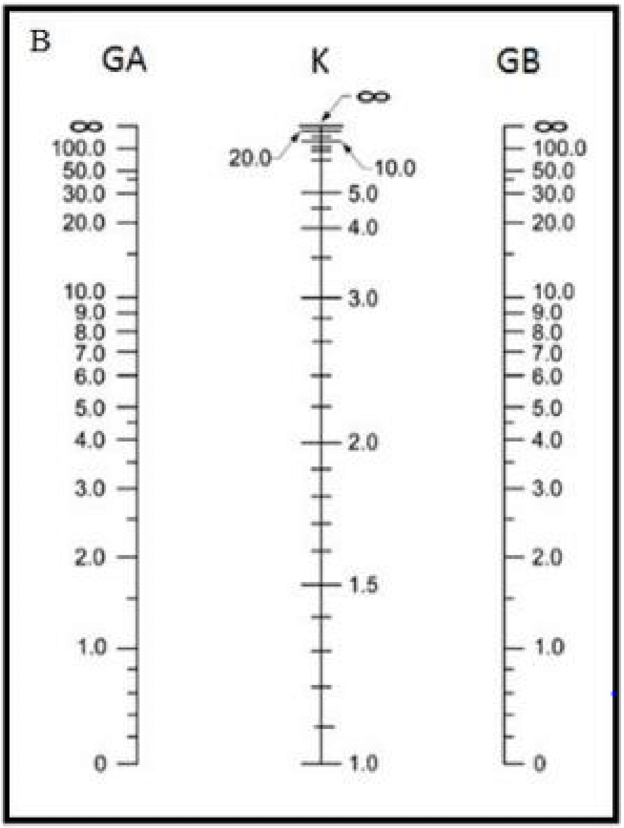

Figure 2.17 Alignment Chart for Unbraced Frame [18].

2.6.3 Modifications to alignment charts

In using previous alignment charts, the analyst must be aware of the assumptions that were used in developing these alignment charts. For example if the material is in inelastic range, Yura (1971) has developed a procedure to take into account the material nonlinearity effect on *K*-factor. Several modifications are briefed as follows:

Girders are not rigidly connected to columns: If the forth assumption in section 2.6.1 is violated which means that the end-conditions of restraining girder is not rigidly connected to column's end, the stiffness of the girder must be modified by the factor α_k in the determination of G_A and G_B which is developed by Duan et al (1996) as shown in Tables 2.3 and 2.4.

Table 2.3 Modification Factors αK for Braced Frames [18].

End conditions of restraining girder		
Near end	Far end	α_k
Rigid	Rigid	1.0
Rigid	Hinged	1.5
Rigid	Semi-rigid	$\left(1+\frac{6E_g I_g}{L_g R_{kF}}\right) / \left(1+\frac{4E_g I_g}{L_g R_{kF}}\right)$
Rigid	Fixed	2.0
Semi-rigid	Rigid	$1/\left(1+\frac{4E_g I_g}{L_g R_{kN}}\right)$
Semi-rigid	Hinged	$1.5/\left(1+\frac{3E_g I_g}{L_g R_{kN}}\right)$
Semi-rigid	Semi-rigid	$\left(1+\frac{6E_g I_g}{L_g R_{kF}}\right) / R^*$
Semi-rigid	Fixed	$2/\left(1+\frac{4E_g I_g}{L_g R_{kN}}\right)$

Note: $R^* = \left(1+\frac{4E_g I_g}{L_g R_{kN}}\right)\left(1+\frac{4E_g I_g}{L_g R_{kF}}\right) - \left(\frac{E_g I_g}{L_g}\right)^2 \frac{4}{R_{kN} R_{kF}}$

Table 2.4 Modification Factors αK for Unbraced Frames [18].

End conditions of restraining girder		
Near end	Far end	α_k
Rigid	Rigid	1
Rigid	Hinged	0.5
Rigid	Semi-rigid	$\left(1+\frac{2E_g I_g}{L_g R_{kF}}\right)/\left(1+\frac{4E_g I_g}{L_g R_{kF}}\right)$
Rigid	Fixed	2/3
Semi-rigid	Rigid	$1/\left(1+\frac{4E_g I_g}{L_g R_{kN}}\right)$
Semi-rigid	Hinged	$0.5/\left(1+\frac{3E_g I_g}{L_g R_{kN}}\right)$
Semi-rigid	Semi-rigid	$\left(1+\frac{2E_g I_g}{L_g R_{kF}}\right)/R^*$
Semi-rigid	Fixed	$(2/3)/\left(1+\frac{4E_g I_g}{L_g R_{kN}}\right)$

Note: $R^* = \left(1+\frac{4E_g I_g}{L_g R_{kN}}\right)\left(1+\frac{4E_g I_g}{L_g R_{kF}}\right) - \left(\frac{E_g I_g}{L_g}\right)^2 \frac{4}{R_{kN} R_{kF}}$

The beams sections are not prismatic: When the column is restrained by a girder with tapered rectangular section as shown in Fig. 2.18, a modified factor has been developed by King et al (1993). The factor is multiplied by the girder's stiffness in determination of G_A and G_B, which is a function of far end conditions and girder's tapering characteristics, r and a.

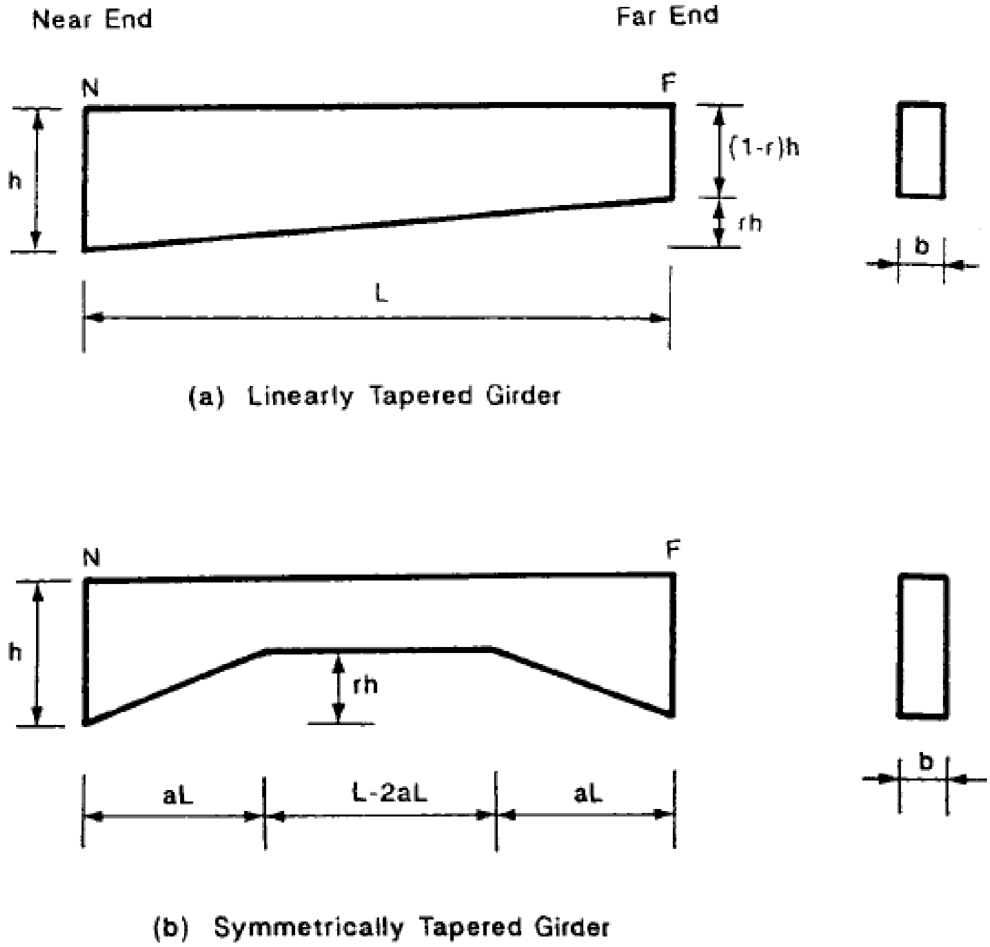

Figure 2.18 Tapered Rectangular Girders [18].

Unsymmetrical frames: When the columns differ in moment of inertia, height, or loads. Updating for the effective length factor K is needed. Chu and Chow (1969) have proposed a modification factor β as shown in Fig. 2.19. The formula has the form:

$$K_{\text{adjusted}} = \beta\, K_{\text{alignment chart}} \qquad (2.17)$$

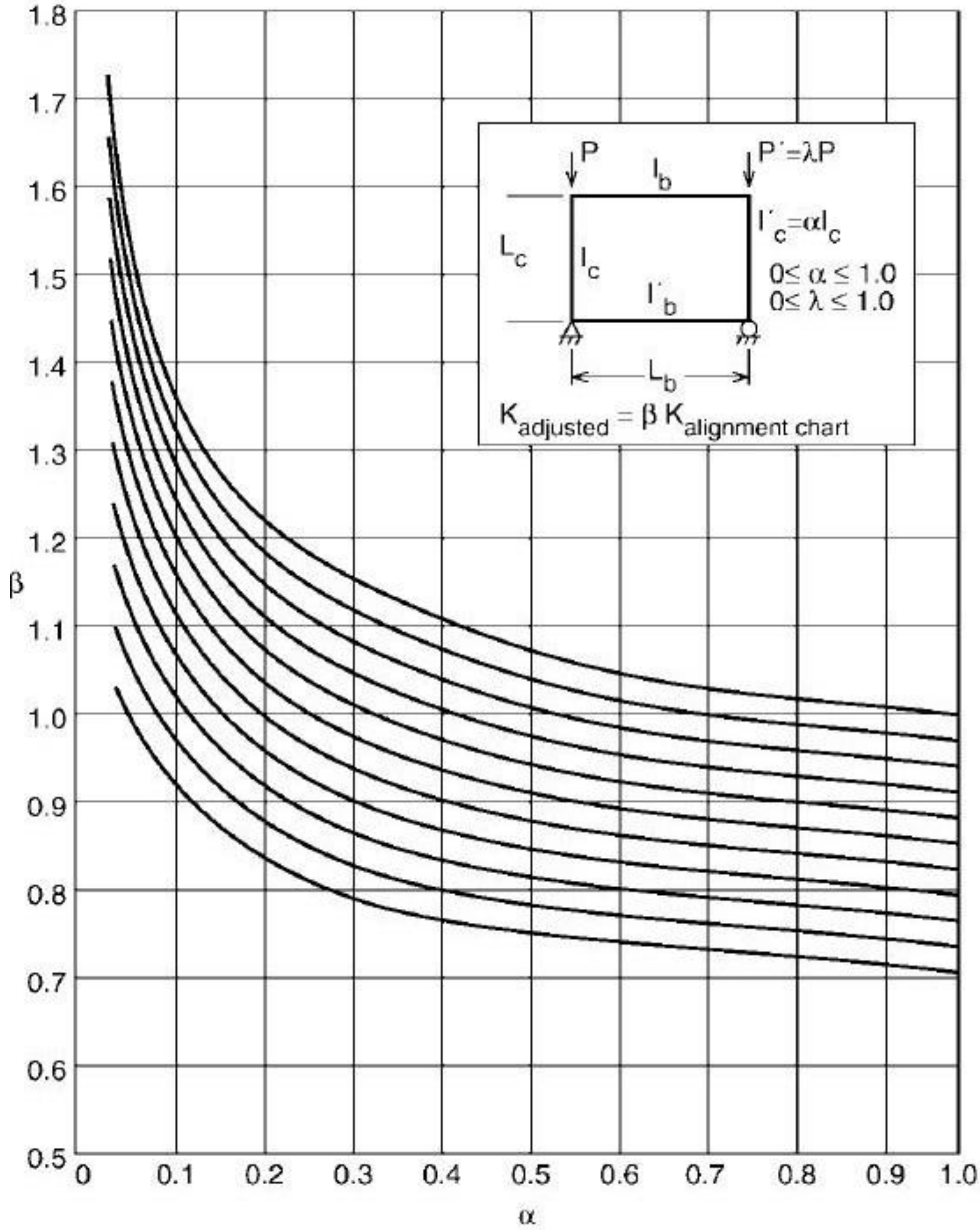

Figure 2.19 Chart for Modification Factor β in an Asymmetrical Frame [18].

Note that: every line corresponds to certain λ, where the upper line corresponds to λ =1 and the lower line corresponds to λ =0, and every line among upper and lower limits is at 0.1 increment.

2.7 Shear mode deformation in frames

Frames deflect in a shear mode which is similar to a beam with fixed support affected by support settlement as shown in Fig. 2.20. On the other hand, shear walls deflect in a cantilever mode which is similar to a cantilever beam with fixed support as shown in Fig. 2.21. If the frames were used solitary in the building to resist lateral loads, it will create bending moments in beams and columns to resist the applied shear force at each floor while the effect of overturning moment will be secondary and, in most, it will be negligible. The stories will stay level although the joints itself will rotate. Furthermore, if the shear walls were used solitary in the structure to resist lateral loads, it will generate bending moment at each level equal to the overturning moment at the same level. If both systems (i.e. frames and shear walls) were used to resist the lateral loads, each system will try to block the other from making its natural deflection and the final deflection shape will be between the two systems as shown in Fig. 2.22.

In the entire course of this study, reinforced concrete portal frames are used, which implies that, frames resist the seismic loads. Consequently, the typical deflection shape is shear mode deflection. As can be seen from shear mode deflection, the relative displacement will be maximum value at the ground columns, at the same time, the maximum axial force will be at the ground columns. Thus, the maximum P-Delta effect by sense in this special case is expected to be at the bottom floors. For this reason, the bending moment from both first order and second order analyses will be computed at all columns in all floors and the critical column will be adopted.

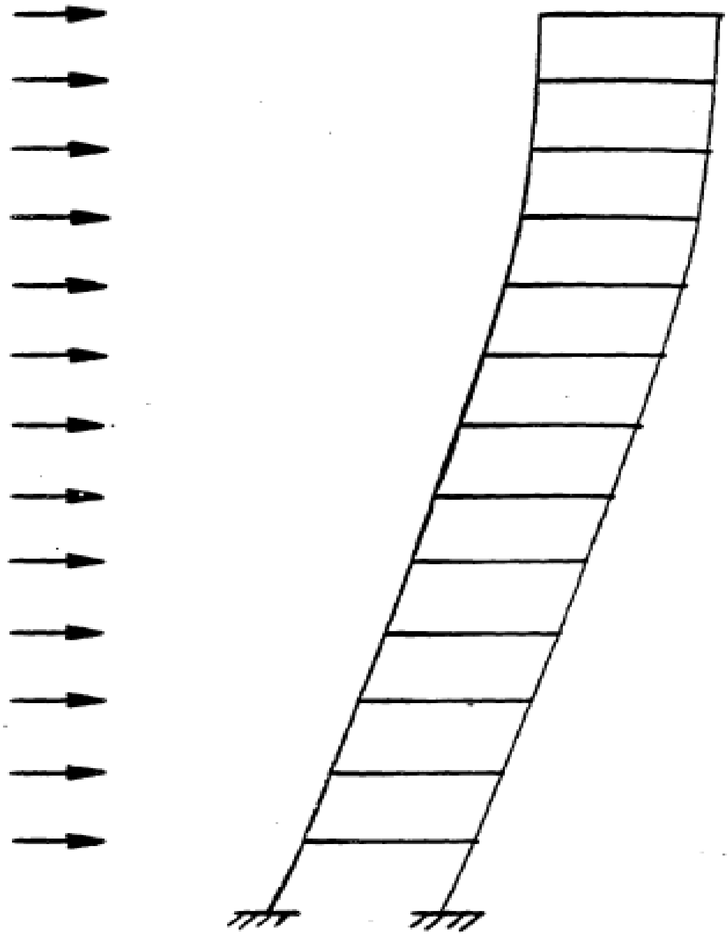

Figure 2.20 Shear Mode Deformation [9].

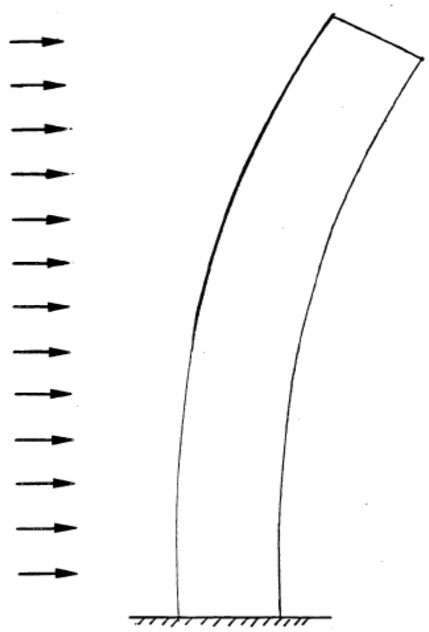

Figure 2.21 Cantilever Mode Deformation [9].

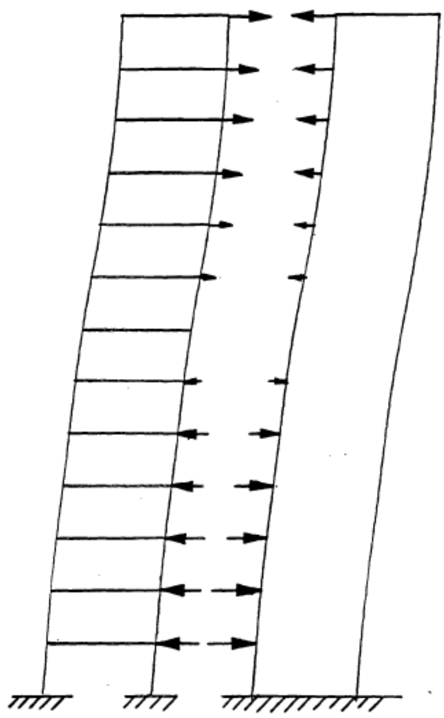

Figure 2.22 Frame-Shear Wall Interaction [9].

Chapter Three

Verification on SAP2000 Results

3.1 Introduction

It is vital to verify any software before it is used in calculations to make sure that the software works properly. During the entire course of this thesis SAP2000, version 19.0 is used. Consequently, it is verified in this chapter for both static and dynamic analyses. With regarded to static analysis a 2-D reinforced concrete portal frame model with both vertical and horizontal applied loads is used. This model is built on SAP2000, version 19.0 software with the given dimensions. The structure's geometry, material, section properties and load patterns are defined. Gravity and horizontal loads are applied. The bending moment on a chosen column from P-Delta analysis is determined and compared with bending moment determined from approximate equations. With regarded to dynamic analysis a 2-D portal frame's structural period is determined by both hand calculations and SAP2000, version 19.0.0 software and the results are compared. To make sure that SAP2000 software works properly, the resulting percentages between hand calculations and SAP2000 results must be equal or lower than five percent.

3.2 Verification on static results

In this section, the results of non-linear static analysis (i.e. geometric nonlinearity, material nonlinearity is out of scope of this research) using

SAP2000 software are compared to hand calculations using moment amplification methods. A 2-D frame model is used in this case which is illustrated in Fig. 3.1. It consists of two spans in x-direction with span length equals six meters. Moreover, the frame consists of three stories with each story height equals four meters. All columns sections properties are 0.15m× 0.25m in x-direction and y-direction respectively. The dimensions of beams are 0.20m×0.20m in depth and width. The loads divide into three types: distributed dead loads per unit length, distributed live loads per unit length and lateral loads. The distributed dead loads equal 10kN/m and 5kN/m on the first span and on the second span respectively. The distributed live loads equal 20kN/m and 10kN/m on the first span and on the second span respectively. Lateral loads increase from lower stories to the top stories with increment of 200kN. The column at which bending moment's magnitude is calculated from both SAP2000 and hand calculations is denoted by AB. Fixed supports (i.e. rigid support) are used which means it can resist vertical and horizontal forces as well as moment.

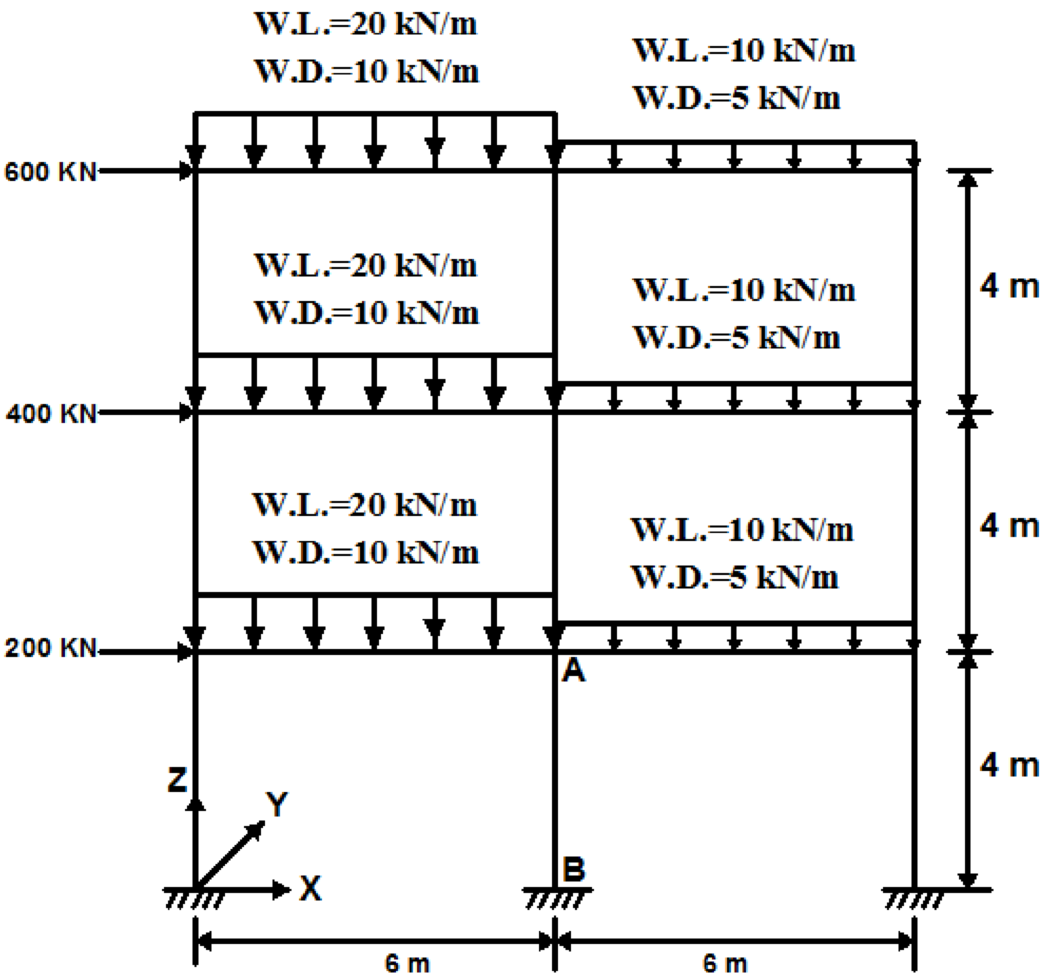

Figure 3.1 Frame Subjected to Horizontal and Vertical Loads

3.2.1 Hand calculations using moment amplification methods

3.2.1.1 P-Δ effect (structure P-Delta effect)

The frame is analyzed using SAP2000 software and the first-order analysis moments on column AB are shown in Fig. 3.2. Various moment amplification methods that can be used to account for P-Δ effect (e.g. story magnifier method, multiple-column magnifier method, etc.). Multiple-column magnifier method is chosen because it is a straightforward procedure and it is not function of first-order deflection of the frame as defined in Eq. 2.11 as follows:

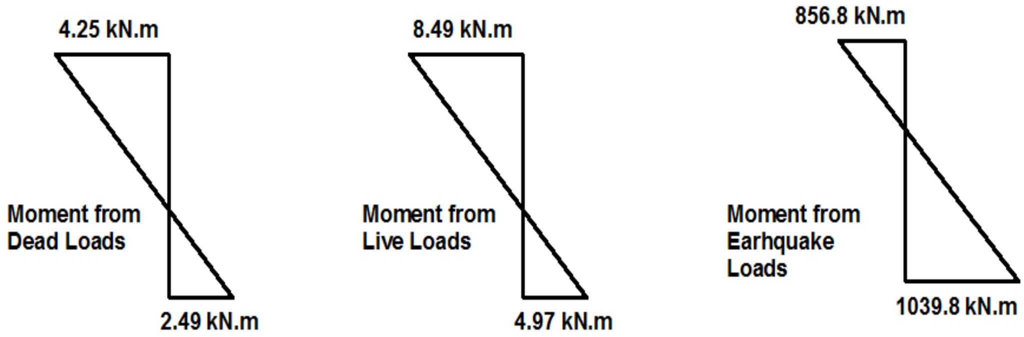

Figure 3.2 First-Order Moment Results for Column AB

$$M = \left(\frac{1}{1-\sum P/\sum P_{ek}}\right) M_{1sway} = B_2 M_{1sway}$$

Where

M = maximum end moment accounting for P-Δ effect.

M_{1sway} = maximum primary moment due to swaying of the story.

B_2 = P-Δ moment amplification factor.

$\sum P$= summation of axial forces.

P_{ek} is elastic buckling load considering column end restraining conditions.

$$\sum P = \big((20+10)\times 6 + (10+5)\times 6\big)\times 3 = 810\text{kN}$$

$$\sum P_{ek} = P_{ek\ middle} + 2\times P_{ek\ edge}$$

For middle:

$$G = \frac{\sum\left(\frac{EI}{L}\right)\text{Columns}}{\sum\left(\frac{EI}{L}\right)\text{Beams}}$$

Where, I is the moment of inertia, E is the moduls of elasticity, and L is the member's length.

$I_{Beam} = \frac{0.2^4}{12} = 1.33\times10^{-4}\ m^4$ $\quad I_{Column} = \frac{0.25\times0.15^3}{12} = 7.03\times10^{-5} m^4$

$G_A = \frac{7.03\times10^{-5}\times2/4}{1.33\times10^{-4}\times2/6} = 0.79$

$G_B = 0$

$$P_{ek} = \frac{\pi^2 EI}{(KL)^2}$$

Where, I is the moment of inertia, E is the moduls of elasticity, L is the member's length, and K is the effective length factor.

$E = 24.8\times10^6\ kN/m^2$

The effective length factor $K = 1.14$ (From Fig. 2.16)

$P_{ek\ middle} = \frac{\pi^2 EI}{(KL)^2} = \frac{\pi^2\times24.8\times10^6\times\ 7.03\times10^{-5}}{(1.14\times4)^2} = 828kN$

For edge:

$$G_A = \frac{\sum\left(\frac{EI}{L}\right)\text{Columns}}{\sum\left(\frac{EI}{L}\right)\text{Beams}} = \frac{7.03\times10^{-5}\times2/4}{1.33\times10^{-4}/6} = 1.58$$

$G_B = 0$

The effective length factor K = 1.24 (From Fig. 2.16).

$$P_{ek\ edge} = \frac{\pi^2 EI}{(KL)^2} = \frac{\pi^2 \times 24.8 * 10^6 \times 7.03 \times 10^{-5}}{(1.24 \times 4)^2} = 700kN$$

$$\sum P_{ek} = P_{ek\ middle} + 2 \times P_{ek\ edge} = 827.6 + 2 \times 699.55 = 2230kN$$

$$B_2 = \left(\frac{1}{1 - \sum P / \sum P_{ek}}\right) = \frac{1}{1 - 810/2230} = 1.57$$

3.2.1.2 P- δ Effect (member P-Delta effect)

The moment amplification method is used to account for P- δ Effect as defined in Eq. 2.6. From Austin expression (Austin, 1961), approximate expression for C_m factor is computed as defined in Eq. 2.8.

$$C_m = 0.6 - 0.4\left(\frac{M_A}{M_B}\right)$$

Where, M_B is the larger of the two end moments.

$M_A = M_{Dead} + M_{Live} = 4.97 + 2.49 = 7.46$kN.m

$M_B = M_{Dead} + M_{Live} = 8.49 + 4.25 = 12.80$kN.m

$$C_m = 0.6 - 0.4\left(\frac{7.46}{12.80}\right) = 0.365$$

$$P \approx 1.15\big((20 + 10) \times 3 + (10 + 5) \times 3\big) \times 3 = 466kN$$

$$G_A = 0.79$$

$$G_B = 0$$

The effective length factor K = 0.62 (From Fig. 2.14).

$$P_e = \frac{\pi^2 EI}{(KL)^2} = \frac{\pi^2 \times 24.8 \times 10^6 \times 7.03 \times 10^{-5}}{(0.62 \times 4)^2} = 2800kN$$

$$M_{max} = \left(\frac{C_m}{1 - \frac{P}{P_e}}\right) M_{1max} = B_1\ M_{1max}$$

$$B_1 = \frac{C_m}{1 - \frac{P}{P_e}} = \frac{0.365}{1 - \frac{465.75}{2800}} = 0.43 \text{ (Take } B_1 = 1)$$

$M_u = B_2 M_{1sway} + B_1\ M_{1non\text{-}sway} = 1.57 \times 857 + 1 \times (4.25 + 8.49) = 1360$kN.m

3.2.2 SAP2000 19 Results

The previous 2-D frame (Fig. 3.1) model is analyzed using SAP2000, version19.0.0 software by applying static non-linear load case with P-Delta geometric nonlinearity parameter as shown in Fig. 3.3. The P-Delta moment results for column AB are shown in Fig. 3.4 and the difference as percentage between hand calculations and SAP2000, version 19.0.0 is tabulated in Table 3.1.

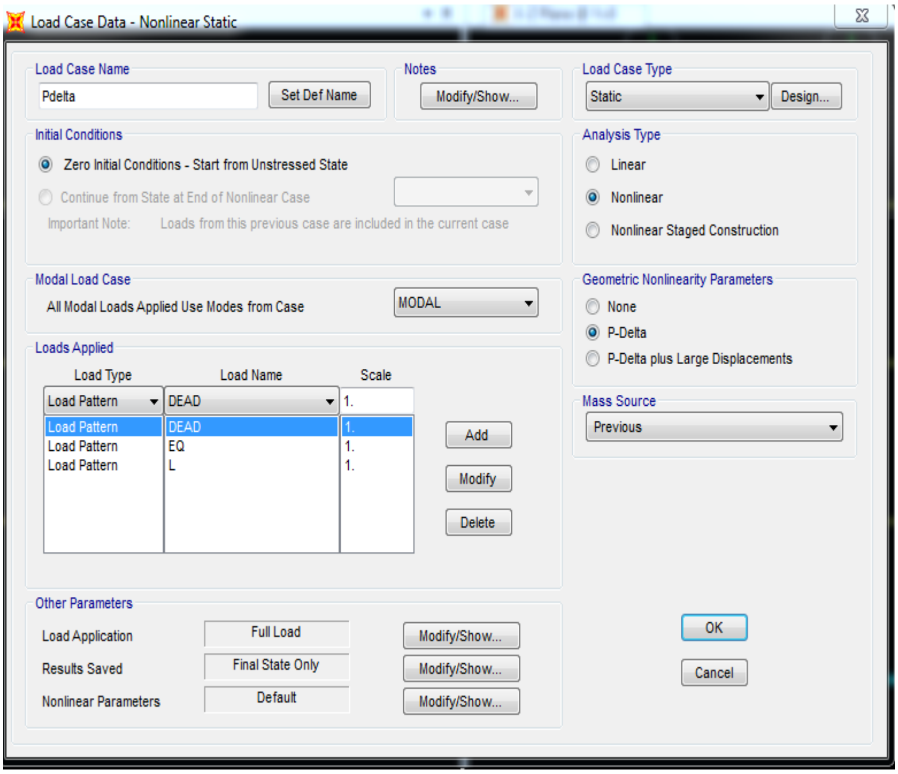

Figure 3.3 P-Delta Static Non-Linear Load Case

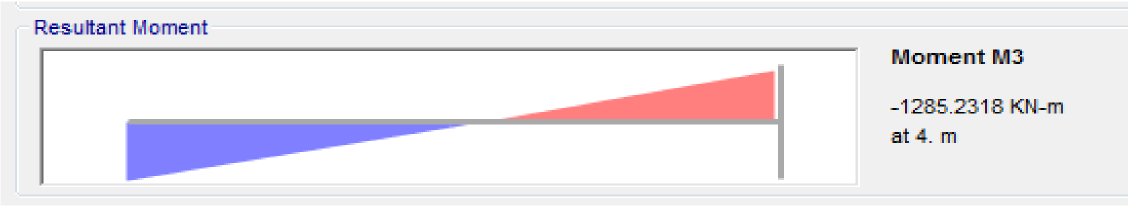

Figure 3.4 P-Delta Moment Results for Column AB Using SAP2000

Table 3.1 Difference between Hand Calculations and SAP2000 Results

Second-Order Moment Using Moment Amplification Method (kN.m)	Second-Order Moment Using SAP2000 (kN.m)	% Difference
1360	1285	5.35%

Based on the results in Table 3.1, the percent of difference between hand calculations and SAP2000 is almost five percent in computing P-Delta effect. These results give us reliability in SAP2000 software in static analysis.

3.3 Verification on dynamic results

3.3.1 Verification of the Fundamental Period

The portal frame which is under investigation is shown in Fig. 3.5, it is one-story portal frame with a story height equals three meters and one bay with a span length equals six meters. Beam's section is 0.6m × 0.3m in depth and width respectively. Column has 0.3m square section. The structural period of this frame is calculated by both; hand calculations and SAP2000 software. Reinforced concrete is used to build this portal frame with the following properties; concrete elasticity modulus equals 23GPa and Poisson's ratio equals 0.2. Weight of 670kN is applied on the portal frame as a line mass (i.e. mass = 670/9.81 ton). It is worth mentioning that, the source of mass in this study is the 670kN, which means that, the structure's own weight is zeroed by entering the weight per unit volume of concrete as zero.

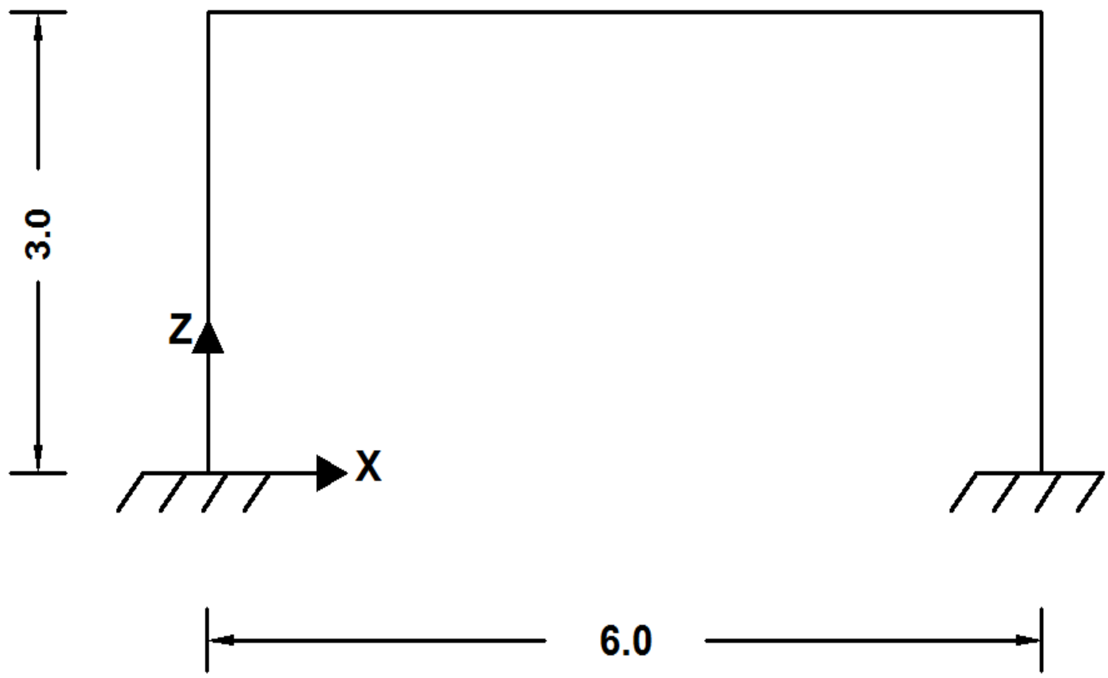

Figure 3.5 Portal Frame Dimensions (All dimensions are in meter)

3.3.1.1 Hand Calculations

Column's section moment of inertia (I) = $\frac{0.3^4}{12}$ = $6.75\times10^{-4}m^4$

EI = 23 $\times10^6\times6.75\times10^{-4}$ = 15500kN.m^2

Stiffness (K) = $\frac{2\times12\times EI}{h^3} = \frac{2\times12\times15500}{3^3}$ = 13800kN/m

Mass (m) = $\frac{weight}{9.81} = \frac{670}{9.81}$ = 68.3ton

The structural fundamental period can be found from the following equation:

$$T = 2\,\pi\sqrt{\frac{m}{K}} \quad = 2\,\pi\sqrt{\frac{68.3}{13800}} = 0.44\text{second}$$

3.3.1.2 Structural period using SAP2000 19

The mass is assigned on portal frame as line mass = $\frac{\text{m}}{\text{length}} = \frac{68.3}{6} =$ 11.38ton/m.

The beam's moment of inertia modifier about 3-axis is modified to 10, in order to make the beam as a rigid element.

Structural period using SAP2000 19 software = 0.45second (see Fig. 3.6).

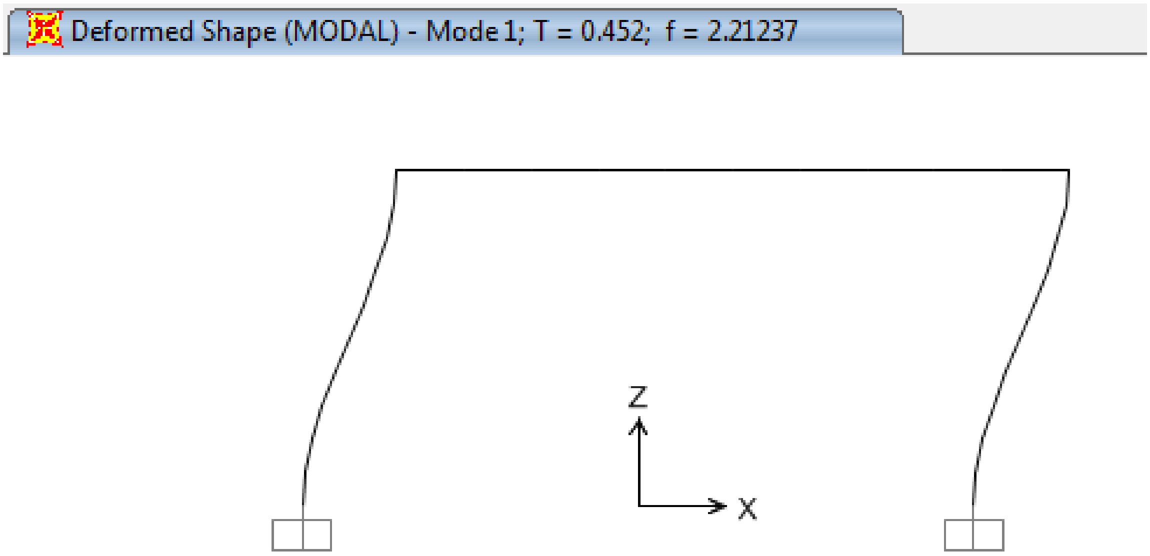

Figure 3.6 Structural Period Using SAP2000

The results are tabulated in Table 3.2 and the percent difference between hand calculations and SAP2000 results is calculated. It can be concluded that SAP2000 gives reasonable results with regarded to dynamic analysis because the percent difference is very small (i.e. less than five percent).

Table 3.2 Difference between Hand Calculations and SAP2000 Results

Structural Period Using Hand Calculations (seconds)	**Structural Period Using SAP2000 (seconds)**	**% Difference**
0.44	0.45	2%

3.3.2 Verification of Mode Shapes and the Fundamental Period for MDOF Structure

The model under investigation is the same as model in section 3.3.1, nevertheless, it consists of four storeys with the same mass on each storey which equals 11.38ton/m except the fourth floor has half mass of the previous value as shown in Fig. 3.7. The beam's moment of inertia modifier about 3-axis is modified to 10, in order to make the beam as a rigid element. To calculate the modal shapes and the natural frequencies; an eigenvalue problem must be solved (Eq. 3.1).

$$Ax = \lambda x \tag{3.1}$$

Where,

x_i = eigenvectors

λ_i = eigenvalues

$A = M^{-1}K$

M = mass matrix

K = stiffness matrix

The stiffness matrix can be constructed as follows,

Stiffness for Each Storey (Ks) = $\frac{2\times12\times EI}{h^3} = \frac{2\times12\times15500}{3^3}$ = 13800kN/m

$$\text{Stifness Matrix }(K) = \begin{bmatrix} 2Ks & -Ks & 0 & 0 \\ -Ks & 2Ks & -Ks & 0 \\ 0 & -Ks & 2Ks & -Ks \\ 0 & 0 & -Ks & Ks \end{bmatrix}$$

$$\text{Stifness Matrix }(K) = \begin{bmatrix} 2\cdot 13800 & -13800 & 0 & 0 \\ -13800 & 2\cdot 13800 & -13800 & 0 \\ 0 & -13800 & 2\cdot 13800 & -13800 \\ 0 & 0 & -13800 & 13800 \end{bmatrix}$$

$$\text{Mass Matrix }(m) = \begin{bmatrix} 68.3 & 0 & 0 & 0 \\ 0 & 68.3 & 0 & 0 \\ 0 & 0 & 68.3 & 0 \\ 0 & 0 & 0 & 34.15 \end{bmatrix}$$

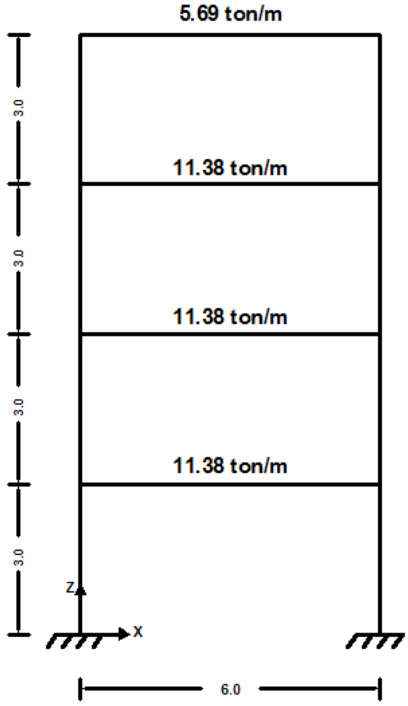

Figure 3.7 Model for Verification of Mode Shapes

Maple software can be used to get the eigenvalues and eigenvectors for this eigenvalue problem as follows,

$$\text{Eigenvalues} = \begin{bmatrix} 30.76 \\ 249.47 \\ 558.76 \\ 777.47 \end{bmatrix}$$

$$\text{Eigenvectors} = \begin{bmatrix} 0.38 & 0.92 & 0.92 & 0.38 \\ 0.71 & 0.71 & -0.71 & -0.71 \\ 0.92 & -0.38 & -0.38 & 0.92 \\ 1.00 & -1.00 & 1.00 & -1.00 \end{bmatrix}$$

Eigenvalues represent the squared natural frequencies (w^2) for every mode. Applying the following equation to get the natural period,

$$\text{Natural Period (T)} = \frac{2\,\pi}{w} \tag{3.2}$$

Where, w is the natural frequency.

Eigenvectors represent the mode shapes for every mode. Tables 3.3 and 3.4 summarize the natural period and mode shapes for every mode respectively from both hand calculations and SAP software.

Table 3.3 Natural Periods

Mode Number	T (Eq. 3.2)	T (SAP2000)	Percent Error
1	1.13	1.17	3.4%
2	0.40	0.41	2.4%
3	0.27	0.27	0.0%
4	0.23	0.23	0.0%

Table 3.4 Mode Shapes from Solving Eigenvalue Problem versus SAP Software

Mode1		Mode2		Mode3		Mode4	
Matrix	SAP2000	Matrix	SAP2000	Matrix	SAP2000	Matrix	SAP2000
0.38	0.37	0.92	0.90	0.92	0.93	0.38	0.41
0.71	0.69	0.71	0.71	-0.71	-0.67	-0.71	-0.76
0.92	0.91	-0.38	-0.35	-0.38	-0.41	0.92	0.96
1.00	1.00	-1.00	-1.00	1.00	1.00	-1.00	-1.00

From previous tables, it is obvious the matching of results.

Chapter Four

Multi-Storey Effect on P-Delta Analysis

4.1 Introduction

Three fundamental parameters affect P-Delta results, which are material of construction, loads and structure's geometry. In the entire course of this study the material is retained to be reinforced concrete. Number of stories is updated to investigate its effect on second-order analysis results. Section 4.2 deals with changing the number of storeys by taking six different models (i.e. 5-storey, 10-storey, 15-storey, 20-storey, 25-storey and 30-storey) with fundamental periods abide by the proposed equation (i.e. section 12.8.2, ASCE 7) and studying its effect on P-Delta results. Section 4.3 deals with changing the number of storeys by taking three different models (i.e. 5-storey, 10-storey, 15-storey) with fundamental periods greater than the proposed equation (i.e. section 12.8.2, ASCE 7) and studying its effect on P-Delta results. SAP2000, version 19.0.0 is used in this study with hand calculations when it is needed. All models are located in Nablus city. The seismic zone factor 0.2 is considered which falls under zone 2B. The soil which the structures are built on is considered as a rock. Wind loads or seismic loads act in the lateral direction. In this study, seismic loads are taken as the lateral applied loads. For purpose of second-order analysis a reasonable estimate of flexural rigidity may be made if I = 0.4 I_g for beams and 0.8 I_g for columns [40]. Thus, previous values are adopted for beams and columns in addition to coefficient equals 0.3 for slabs.

4.2 Multi-Storey Effect on P-Delta Analysis with Fundamental Period Abides by the Proposed Equation

On account of growing number of population with the shortage in suitable lands for construction especially in metropolises; people resort to build high-rise buildings to accommodate these formidable numbers of people who need dwellings. On the other hand, some countries compete with each other to have the tallest buildings in the world. Wherefore, the tendency of people to build high buildings is not neoteric tendency, it has been since the existence of human on this planet. The pyramids that have been built by pharaohs which are the only wonder of the seven wonders of the ancient world that has survived to the present day have been the tallest man-made structures on earth for millenniums of years until the competition of Lincoln Cathedral. Building high has difficulties and hardships which stimulate us into creative ways to be overcome. For instance, when people have built high-rise buildings, the need arose to the invention of elevators to carry people all the way up or down. Furthermore, constructing skyscrapers leads to thinking in ways to evacuate all these people in emergency cases from all the floors at the same time. Previous two examples of the difficulties and hardships that were created by high-rise buildings are also applied to structural engineering especially in P-Delta effect. P-Delta effect exists in low-rise as well as high-rise structures.

However, its amount in low-rise buildings can be neglected in contrast to high-rise buildings in which P-Delta effect must be included in design. The hardships accompanied with high-rise buildings must be overcome by designing for it. But the million dollar question is after how many regular storeys the P-Delta effect must be included in design. This question will be answered at the end of this chapter for reinforced concrete moment resisting frame structures.

P-Delta effect becomes a tremendous amount while increasing the building's height. In this section, the increase in difference between first-order analysis and second-order analysis is investigated due to increasing the building's height. Six models are used; model number one (M5) is a five-storey reinforced concrete portal frame and similarly M10, M15, M20, M25 and M30. The six models are assumed as standard occupancy structures. In the following sections, every model has been studied separately; and in the comments and conclusion section; the results from each model have been compared with each other. All models have the same plan, material properties, section properties, live loads and superimposed dead loads except number of stories and columns' sections.

4.2.1 Five-Storey model (M5)

M5 is a five-storey reinforced concrete portal frame with fixed supports. It consists from three spans in x-direction with span length equals 6m and three spans in y-direction with span length equals 6m as shown in Figs. 4.1 and 4.2. The beams' dimensions are 0.70m×0.75m in depth and width respectively. The columns are 0.75m×0.75m square section. The slab is solid with thickness equals 0.15m. All of the floors have a constant height which equals 3.40m with a total height equals 17m. Sections properties for frame's sections and area's section are summarized in Table 4.1. First-order moment and second-order moment are determined on all columns and the column which gives the maximum percent between first and second-order has been adopted.

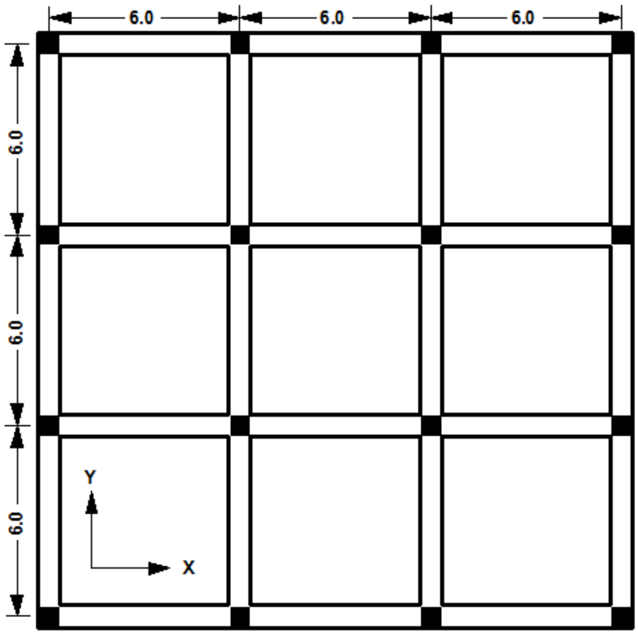

Figure 4.1 M5, M10, M15, M20, M25 and M30 Plan (All dimensions are in meter)

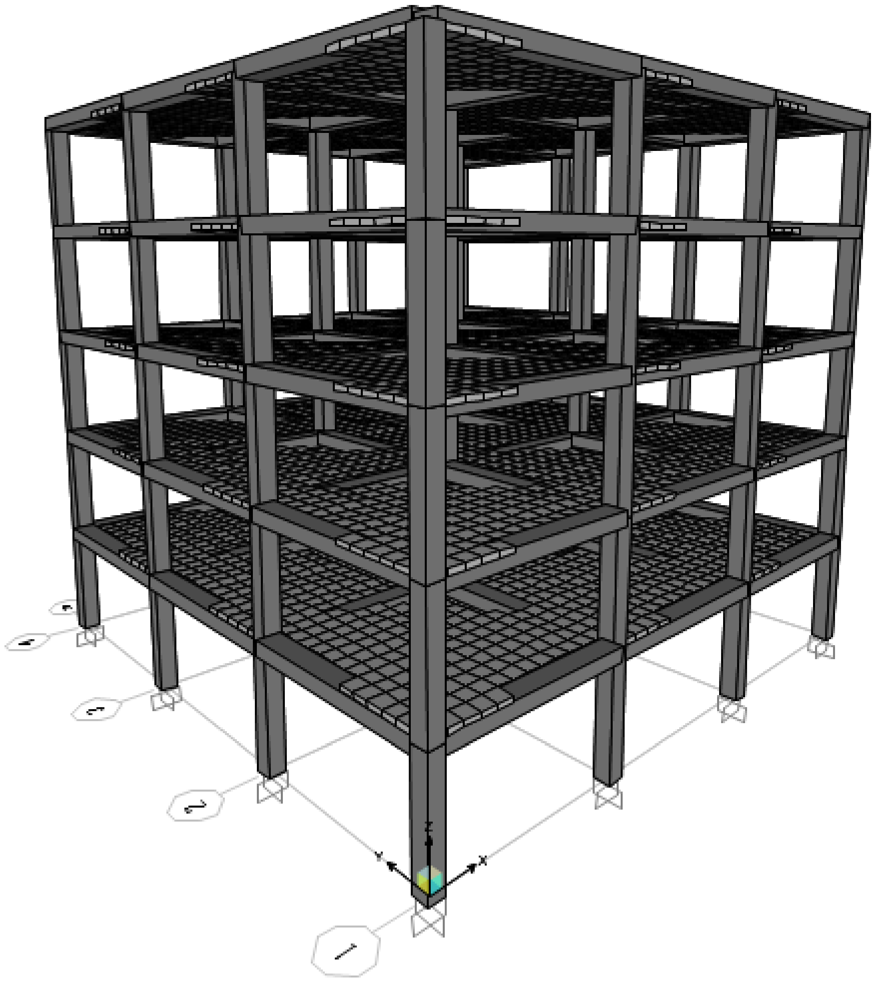

Figure 4.2 M5 Model in 3D view

Table 4.1 Sections Properties

Beam		Column		Slab
Depth(m)	**Width(m)**	**Depth(m)**	**Width(m)**	**Thickness(m)**
0.70	0.75	0.75	0.75	0.15

4.2.1.1 Material Properties

In the past, the construction materials consisted from thatch, adobe and wood. In the present era, there is two main materials can be used in construction, which are reinforced concrete and/or steel. The process which the material has been chosen for this research was based on the local practice. The construction material that is used in most projects in Palestine and in the contiguous countries is reinforced concrete material. Reinforced concrete predominates on other materials in construction in these countries because it does not need a high skilled workmanship like other materials (for example steel), also it does not need continuous maintenance (like steel). "Cast in place reinforced concrete offers outstanding resistance to explosion or impact. Moreover, it can endure very high temperatures from fire for long time without loss in structural integrity" (Alfred G. Gerosa, president of Concrete Alliance Inc.). In respect to wind loads, concrete has very high mass compared to steel, so it can resist wind loads more effectively. At the same time, steel is more ductile than reinforced concrete, which makes it a reasonable choice in seismic zones. "Steel framing does very well under high loads because it is ductile, which means it has the ability to bend without breaking and can absorb that kind of energy" (Larry Williams, president of the Washington, D.C.-based Steel Framing Alliance of cold-formed steel). In this study, the construction material was chosen to be reinforced concrete; its properties are tabulated in the following table, Table 4.2. For all structural elements, the yielding stress of steel (F_y) equals 420MPa.

Table 4.2 Concrete Properties

	Compressive Strength[1]	Compressive Strength[2]	Elasticity Modulus[1]	Elasticity Modulus[2]	Poisson's Ratio	Weight Per Unit Volume
Value	24MPa	32MPa	23GPa	26.6GPa	0.2	25kN/m^3

1 Concrete used for slabs and beams.
2 Concrete used for columns.

4.2.1.2 Vertical loads

The vertical loads are divided into two main categories: live loads and dead loads. Live loads refer to the loads that can change over time such as people, furniture, vehicles, and the like. It is measured as kilo newton per square meter (kN/m^2). Building codes prescribe minimum live loads requirements for various buildings and structures based on their type of usage. For example, the live load for a classroom differs from live load for a single family residence. Dead loads refer to the loads that do not change over time and it is divided into two types: structure's own weight, which refers to the weight of structural elements, and the superimposed dead load, which refers to the non-structural elements' weights such as, partitions, plumbing and HVAC (HVAC stands for Heating, Ventilation, and Air Conditioning). Table 4.3 summarizes live loads and dead loads that have been used in this study.

Table 4.3 Vertical Load Values

	Live Load	Dead Load	Superimposed Dead Load (SD)
Value	3kN/m^2	Structure's own weight	4.5kN/m^2

4.2.1.3 Seismic loads

Palestine is located in the Middle East region to the west of the Dead Sea basin. Series of major earthquakes occurred in the eastern Mediterranean region and in the Middle East. Seismicity in Palestine comes from the movement along the Dead Sea Transform-DST. The DST also known as the Dead Sea Fault System, is a north-south striking left-lateral shear zone extending from the incipient oceanic ridge (Red Sea) in the south to the Taurus plate collision in the north (Turkey). About 105-110 km of left-lateral displacement between the African and Arabian tectonic plates took place along this fault system during the last 15 million years. The average rate of motion during the last 5 million years is 5 millimeters per year (United States Geological Survey) as shown in Fig. 4.3. Fig. 4.4 shows the pressure ridges in the Araba Valley region in the south of Dead Sea basin.

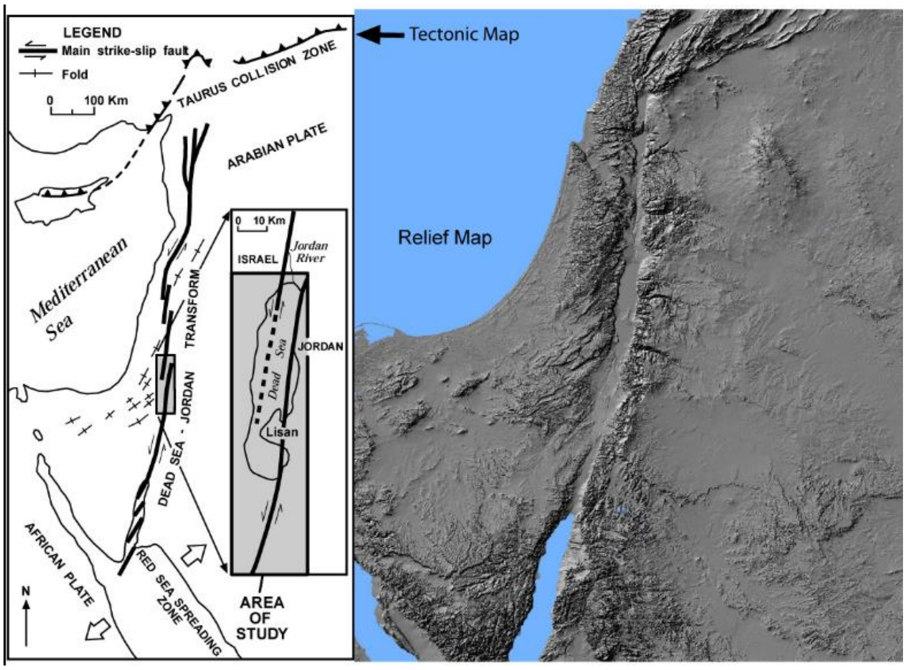

Figure 4.3 Tectonic Setting of the Dead Sea Transform (United States Geological Survey)

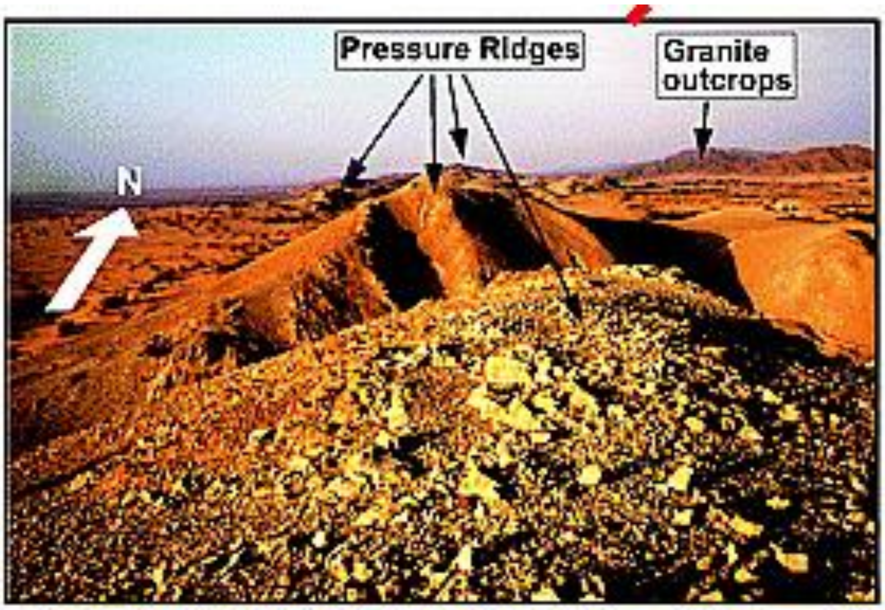

Figure 4.4 Pressure Ridges in the Araba Valley (Review of Geophysics, 2009)

Seismic forces threaten any structure on earth, not only in the highly seismic regions but everywhere on the planet can be affected by an earthquake. So every structure is designed to withstand these forces by following local or international building codes and regulations. Earthquake comes with uncertainty in magnitude, location and time. Many building codes tried to compute the maximum base shear that can apply on the structure based on numerous parameters such as seismic coefficients, zone factor, soil type, structure's weight and natural period of the structure. After computing the base shear on the structure, its value can be distributed on the floors based on their weights and cumulative heights. In this section and the following sections, the base shear is computed using modal response spectrum analysis compatible with International Building Code 2015 (IBC 2015) and ASCE 7 code. As stated previously, the six models are located in Nablus city on a rock soil. The direction at which the seismic forces are applied is x-direction. However, the plan is identical in both directions and the columns' sections are square sections, consequently, both directions will give the same results. Every structure, and portion thereof, including nonstructural components that are permanently attached to structures and their supports and attachments, shall be designed and constructed to resist the effects of earthquake motions in accordance with ASCE 7 (IBC 2015, section 1613.1). The exempted structures from previous phrase are very limited number of one and two-family dwellings which are located in very low seismic zones or for some structures that do not pose a risk on humans if they have been demolished during an earthquake (for example, agricultural storage structures intended only for incidental human occupancy).

The determination of base shear and its distribution on floors using IBC 2015 with accordance with ASCE 7 equations follows the steps bellow:

STEP 1 (Seismic Zone Factor)

The seismic zone factor (Z) is defined as the expected peak acceleration on the surface of a certain rock's type as a percent of gravity acceleration. Palestine is separated into four districts based on seismic zone factor as shown in Fig. 4.5 with 10% probability of exceedance in 50 years. Nablus is located in zone 2B with seismic zone factor (Z) equals 0.20. As can be seen from Fig. 4.5 the higher seismic zone factor is located in areas which are close to the Dead Sea Transform (for example, Jericho city), and its value diminishes with keeping away from Dead Sea Transform. It is worth mentioning that most West Bank districts are located in seismic zones 2A and 2B with seismic zone factor ranges from 0.15 to 0.2.

STEP 2 (Site Classification)

IBC 2015 states that based on the site soil properties, the site shall be classified in accordance with Chapter 20 of ASCE 7 as shown in Table 4.4. If the soil properties are not known, site class D shall be used unless there is information state that soil classes E or F are present. All models are located in Nablus city on a rock soil. According to Table 4.4, the site class is B.

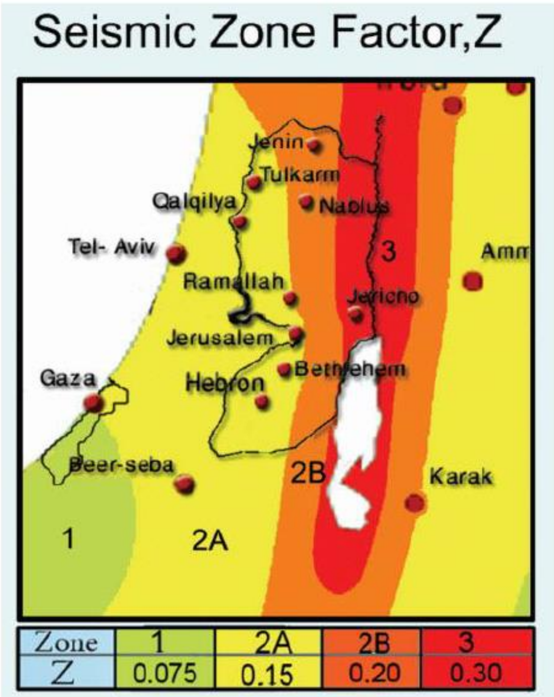

Figure 4.5 Palestine Seismic Map (Boore et al., 1997)

Table 4.4 Site Classification (Table20.3-1, ASCE 7)

Site Class	$\bar{v}_s$	$\bar{N}$ or $\bar{N}_{ch}$	$\bar{s}_u$
A. Hard rock	>5,000 ft/s	NA	NA
B. Rock	2,500 to 5,000 ft/s	NA	NA
C. Very dense soil and soft rock	1,200 to 2,500 ft/s	>50	>2,000 psf
D. Stiff soil	600 to 1,200 ft/s	15 to 50	1,000 to 2,000 psf
E. Soft clay soil	<600 ft/s	<15	<1,000 psf
	Any profile with more than 10 ft of soil having the following characteristics: —Plasticity index $PI > 20$, —Moisture content $w \geq 40\%$, —Undrained shear strength $\bar{s}_u < 500$ psf		
F. Soils requiring site response analysis in accordance with Section 21.1	See Section 20.3.1		

For SI: 1 ft/s = 0.3048 m/s; 1 lb/ft^2 = 0.0479 kN/m^2.

STEP 3 (Design Basis Earthquake, DBE)

The maximum considered earthquake (MCE) is divided into two types: S_s, which refers to MCE for short period (0.2 second), S_1, which refers to MCE for long period (1 second) for a 2% probability of exceedance in 50years. Design Basis Earthquake (DBE) defines the peak horizontal acceleration with 10% probability of exceedance in 50years. For a 10% probability of exceedance; S_{s*} can be taken as 2.5Z, and S_{1*} can be taken as 1.25Z (The National Steering Committee for Earthquake Preparedness, 2009).

$$S_{s*} = 2.5Z \qquad (4.1)$$

$$S_{1*} = 1.25Z \qquad (4.2)$$

Where, S_{s*} refers to an equivalent 0.67 MCE for 0.2-second period, S_{1*} refers to an equivalent 0.67 MCE for 1-second period and Z is the seismic zone factor.

By applying previous equations, we get:

$S_{s*} = 2.5Z = 2.5\times0.2 = 0.5$

$S_{1*} = 1.25Z = 1.25\times0.2 = 0.25$

Concerning the 2/3 reduction value, UBC97 was based on 10% probability of exceedance in 50 years. IBC adopts the same response spectrum but changes to 2% of exceedance in 50 years. The 2/3 term reduces the value to the same 10% of exceedance value. Whereas this works well in California where the 2% and 10% varies over period uniformly and where usually earthquake codes are developed, Eastern United States has no uniform variation between 2% and 10%. Thus they did not approve the 2/3 rule. Israeli code adopts IBC and 10% of exceedance and did not use the 2/3 reduction.

STEP 4 (Values of Site Coefficients)

It is substantial to consider the influence of soil conditions on the spectral design accelerations which can be achieved by site coefficient F_a at short period (0.2 second) and site coefficient F_v at long period (1second) as shown in Tables 4.5 and 4.6 respectively. It can be concluded from these tables that rock and hard rock do not amplify spectral design accelerations for both short period and long period, but on the contrary, hard rock minifies spectral design accelerations. On the other hand, soft clay, stiff soil or soft rock amplify the spectral design accelerations which can reach to tremendous amount in the case of soft clay soil.

For M5 model, with referring to step 2, the site class is B (thus values for F_a and F_v are equal to 1 for any value of S_s and S_1). Consequently, F_a equals 1 and F_v equals 1 (i.e. no change in spectral design accelerations).

Table 4.5 Values of Site Coefficient Fa (Table 1613.3.3(1), IBC 2015)

SITE CLASS	MAPPED SPECTRAL RESPONSE ACCELERATION AT SHORT PERIOD				
	$S_s \leq 0.25$	$S_s = 0.50$	$S_s = 0.75$	$S_s = 1.00$	$S_s \geq 1.25$
A	0.8	0.8	0.8	0.8	0.8
B	1.0	1.0	1.0	1.0	1.0
C	1.2	1.2	1.1	1.0	1.0
D	1.6	1.4	1.2	1.1	1.0
E	2.5	1.7	1.2	0.9	0.9
F	Note b	Note b	Note b	Note b	Note b

a. Use straight-line interpolation for intermediate values of mapped spectral response acceleration at short period, S_s.
b. Values shall be determined in accordance with Section 11.4.7 of ASCE 7.

Table 4.6 Values of Site Coefficient Fv (Table 1613.3.3(2), IBC 2015)

SITE CLASS	MAPPED SPECTRAL RESPONSE ACCELERATION AT 1-SECOND PERIOD				
	$S_1 \leq 0.1$	$S_1 = 0.2$	$S_1 = 0.3$	$S_1 = 0.4$	$S_1 \geq 0.5$
A	0.8	0.8	0.8	0.8	0.8
B	1.0	1.0	1.0	1.0	1.0
C	1.7	1.6	1.5	1.4	1.3
D	2.4	2.0	1.8	1.6	1.5
E	3.5	3.2	2.8	2.4	2.4
F	Note b	Note b	Note b	Note b	Note b

a. Use straight-line interpolation for intermediate values of mapped spectral response acceleration at 1-second period, S_1.
b. Values shall be determined in accordance with Section 11.4.7 of ASCE 7.

STEP 5 (Considering Soil Conditions)

The spectral design acceleration considering the influence of the soil conditions on-site in short periods (S_{DS}), and the spectral design acceleration considering the influence of the soil conditions on-site in period of one second (S_{D1}) can be determined from the following equations:

$$S_{DS} = F_a S_{s*} \tag{4.3}$$

$$S_{D1} = F_v S_{1*} \tag{4.4}$$

Where: S_{DS}, F_a, F_v, S_{s*} and S_{1*} are as defined before.

By applying previous equations, we get:

$S_{DS} = 1 \times 0.50 = 0.50$

$S_{D1} = 1 \times 0.25 = 0.25$

STEP 6 (Risk Category of the Structure)

IBC 2015 assigns the risk category of a certain structure based on the intended use of the structure. It is described by roman numerals from I to IV. Where, I risk category represents structures with low hazard to human lives in the event of failure (for example, agricultural facilities), and IV risk category represents essential facilities such as hospitals or fire stations. For M5 model, the risk category is II as shown in Table 4.7.

Table 4.7 Risk Category of Buildings and Other Structures (Table 1604.5, IBC 2015)

RISK CATEGORY	NATURE OF OCCUPANCY
I	Buildings and other structures that represent a low hazard to human life in the event of failure, including but not limited to: • Agricultural facilities. • Certain temporary facilities. • Minor storage facilities.
II	Buildings and other structures except those listed in Risk Categories I, III and IV.
III	Buildings and other structures that represent a substantial hazard to human life in the event of failure, including but not limited to: • Buildings and other structures whose primary occupancy is public assembly with an occupant load greater than 300. • Buildings and other structures containing Group E occupancies with an occupant load greater than 250. • Buildings and other structures containing educational occupancies for students above the 12th grade with an occupant load greater than 500. • Group I-2 occupancies with an occupant load of 50 or more resident care recipients but not having surgery or emergency treatment facilities. • Group I-3 occupancies. • Any other occupancy with an occupant load greater than 5,000.[a] • Power-generating stations, water treatment facilities for potable water, wastewater treatment facilities and other public utility facilities not included in Risk Category IV. • Buildings and other structures not included in Risk Category IV containing quantities of toxic or explosive materials that: Exceed maximum allowable quantities per control area as given in Table 307.1(1) or 307.1(2) or per outdoor control area in accordance with the *International Fire Code*; and Are sufficient to pose a threat to the public if released.[b]
IV	Buildings and other structures designated as essential facilities, including but not limited to: • Group I-2 occupancies having surgery or emergency treatment facilities. • Fire, rescue, ambulance and police stations and emergency vehicle garages. • Designated earthquake, hurricane or other emergency shelters. • Designated emergency preparedness, communications and operations centers and other facilities required for emergency response. • Power-generating stations and other public utility facilities required as emergency backup facilities for Risk Category IV structures. • Buildings and other structures containing quantities of highly toxic materials that: Exceed maximum allowable quantities per control area as given in Table 307.1(2) or per outdoor control area in accordance with the *International Fire Code*; and Are sufficient to pose a threat to the public if released.[b] • Aviation control towers, air traffic control centers and emergency aircraft hangars. • Buildings and other structures having critical national defense functions. • Water storage facilities and pump structures required to maintain water pressure for fire suppression.

a. For purposes of occupant load calculation, occupancies required by Table 1004.1.2 to use gross floor area calculations shall be permitted to use net floor areas to determine the total occupant load.

b. Where approved by the building official, the classification of buildings and other structures as Risk Category III or IV based on their quantities of toxic, highly toxic or explosive materials is permitted to be reduced to Risk Category II, provided it can be demonstrated by a hazard assessment in accordance with Section 1.5.3 of ASCE 7 that a release of the toxic, highly toxic or explosive materials is not sufficient to pose a threat to the public.

STEP 7 (Seismic Design Category)

The International Building Code 2015 (IBC 2015) determines the suitable seismic design category based on the spectral design accelerations after considering the influence of the soil conditions for short- period and 1-second period as shown in Tables 4.8 and 4.9 respectively. For M5 model, seismic design category is D.

Table 4.8 Seismic Design Category Based on Short-Period (0.2 second) Response Acceleration (Table 1613.3.5(1), IBC 2015)

VALUE OF S_{DS}	RISK CATEGORY		
	I or II	III	IV
$S_{DS} < 0.167g$	A	A	A
$0.167g \leq S_{DS} < 0.33g$	B	B	C
$0.33g \leq S_{DS} < 0.50g$	C	C	D
$0.50g \leq S_{DS}$	D	D	D

Table 4.9 Seismic Design Category Based on 1-Second Period Response Acceleration (Table 1613.3.5(2), IBC 2015)

VALUE OF S_{D1}	RISK CATEGORY		
	I or II	III	IV
$S_{D1} < 0.067g$	A	A	A
$0.067g \leq S_{D1} < 0.133g$	B	B	C
$0.133g \leq S_{D1} < 0.20g$	C	C	D
$0.20g \leq S_{D1}$	D	D	D

STEP 8 (Seismic Importance Factor)

Based on the suitable risk category of the structure in IBC 2015, the seismic importance factor can be determined from ASCE 7. The importance factor is multiplier that reflects the significance of the structure which increases or decreases the base shear value. The risk category and importance factor are intended to protect the public's safety. Consequently, risk category and importance factor are not intended to prevent the aesthetics or functionality aspects during and after strong earthquakes for low risk category structures. For this reason, ASCE 7 increases the importance factors for facilities which are intended to maintain its functionality after severe earthquakes such as hospitals. For M5 model, after referring to step 6 and Table 4.10, the seismic importance factor equals 1.

Table 4.10 Importance Factors by Risk Category of Buildings and Other Structures (Table 1.5-2, ASCE 7)

Risk Category from Table 1.5-1	Snow Importance Factor, I_s	Ice Importance Factor—Thickness, I_i	Ice Importance Factor—Wind, I_w	Seismic Importance Factor, I_e
I	0.80	0.80	1.00	1.00
II	1.00	1.00	1.00	$\boxed{1.00}$
III	1.10	1.25	1.00	1.25
IV	1.20	1.25	1.00	1.50

[a]The component importance factor, I_p, applicable to earthquake loads, is not included in this table because it is dependent on the importance of the individual component rather than that of the building as a whole, or its occupancy. Refer to Section 13.1.3.

STEP 9 (Permitted analytical procedure)

ASCE 7 permits three analytical procedures to determine the forces on the structure based on the seismic design category, irregularity, structural system and structure's height. The procedures are as follows; Equivalent Lateral Force Analysis, Modal Response Spectrum Analysis and Seismic Response History Procedure as shown in Table 4.11.

For M5 model; the seismic design category is D, and the structures does not include any irregularity condition and not exceeding 48.8m in structural height. As a result, both Modal Response Spectrum and Equivalent Lateral Force Analyses are permitted. Modal Response Spectrum Analysis is adopted in the entire course of this study, because it gives more reasonable shear force distribution. Likewise, it is permitted for all structures' heights.

Table 4.11 Permitted Analytical Procedures (Table 12.6-1, ASCE 7)

Seismic Design Category	Structural Characteristics	Equivalent Lateral Force Analysis, Section 12.8[a]	Modal Response Spectrum Analysis, Section 12.9[a]	Seismic Response History Procedures, Chapter 16[a]
B, C	All structures	P	P	P
D, E, F	Risk Category I or II buildings not exceeding 2 stories above the base	P	P	P
	Structures of light frame construction	P	P	P
	Structures with no structural irregularities and not exceeding 160 ft in structural height	P	P	P
	Structures exceeding 160 ft in structural height with no structural irregularities and with $T < 3.5T_s$	P	P	P
	Structures not exceeding 160 ft in structural height and having only horizontal irregularities of Type 2, 3, 4, or 5 in Table 12.3-1 or vertical irregularities of Type 4, 5a, or 5b in Table 12.3-2	P	P	P
	All other structures	NP	P	P

[a]P: Permitted; NP: Not Permitted; $T_s = S_{D1}/S_{DS}$.

STEP 10 (Design coefficients)

Design coefficients can be determined based on the seismic-force resisting system. As shown in Table 4.12. In M5 model case, the seismic-force resisting system is special reinforced concrete moment frames. The design coefficients can be summarized in Table 4.13.

Table 4.12 Design Coefficients and Factors for Seismic Force-Resisting Systems (Table 12.2-1, ASCE 7)

Seismic Force-Resisting System	ASCE 7 Section Where Detailing Requirements Are Specified	Response Modification Coefficient, R[a]	Overstrength Factor, Ω_0[g]	Deflection Amplification Factor, C_d[b]	Structural System Limitations Including Structural Height, h_n (ft) Limits[c]				
					Seismic Design Category				
					B	C	D[d]	E[d]	F[e]
C. MOMENT-RESISTING FRAME SYSTEMS									
1. Steel special moment frames	14.1 and 12.2.5.5	8	3	5½	NL	NL	NL	NL	NL
2. Steel special truss moment frames	14.1	7	3	5½	NL	NL	160	100	NP
3. Steel intermediate moment frames	12.2.5.7 and 14.1	4½	3	4	NL	NL	35[h]	NP[h]	NP[h]
4. Steel ordinary moment frames	12.2.5.6 and 14.1	3½	3	3	NL	NL	NP[i]	NP[i]	NP[i]
5. Special reinforced concrete moment frames[n]	12.2.5.5 and 14.2	8	3	5½	NL	NL	NL	NL	NL
6. Intermediate reinforced concrete moment frames	14.2	5	3	4½	NL	NL	NP	NP	NP

Table 4.13 M5 Design Coefficients and Factors

Response Modification Coefficient, R	Over Strength Factor, Ω_0	Deflection Amplification Factor, C_d
8	3	5.5

STEP 11 (Effective Seismic Weight)

In order to determine the base shear that applies on the structure, the total seismic dead load must be computed which includes the structure's own weight in addition to super imposed dead load. Beams' weights, columns' weights, slab's weight and super imposed dead loads in one floor are calculated and tabulated in Tables 4.14-4.17.

Table 4.14 Beams Weight in One Storey

	Number of Beams	Depth	Width	Length	Concrete Weight Per Unit Volume	Beams Weight
Calculations	24	0.55m*	0.75m	6m	25kN/m^3	1485kN

* 0.7-0.15 = 0.55m

Table 4.15 Columns Weight in One Storey

	Number of Columns	Depth	Width	Length	Concrete Weight Per Unit Volume	Columns Weight
Calculations	16	0.75m	0.75m	3.40m	25kN/m^3	765kN

Table 4.16 Slab Weight in One Storey

	Slab Area	Slab Thickness	Concrete Weight Per Unit Volume	Slab Weight
Calculations	324m^2	0.15m	25kN/m^3	1215kN

Table 4.17 Super Imposed Dead Load on One Storey

	Slab Area	SD Load Per Unit Area	SD Load
Calculations	324m^2	4.5kN/m^2	1458kN

The weight of each storey can be determined as the sum of beams' weights, columns' weights, slab's weight, and superimposed dead loads. The last storey is exempted from half columns' weights as tabulated in Table 4.18. The verification on an example of SAP2000 weight calculations is tabulated in Table 4.19 and Fig. 4.6.

Table 4.18 M5 Floors' Weights

Floor	Weight (kN)
1	4923
2	4923
3	4923
4	4923
5	4540
Total	24232

Table 4.19 M5-Super Imposed Dead Load

Super Imposed Dead Load Using Hand Calculations (kN)	Super Imposed Dead Load Using SAP2000 (kN)	%Error
7290	7290	0%

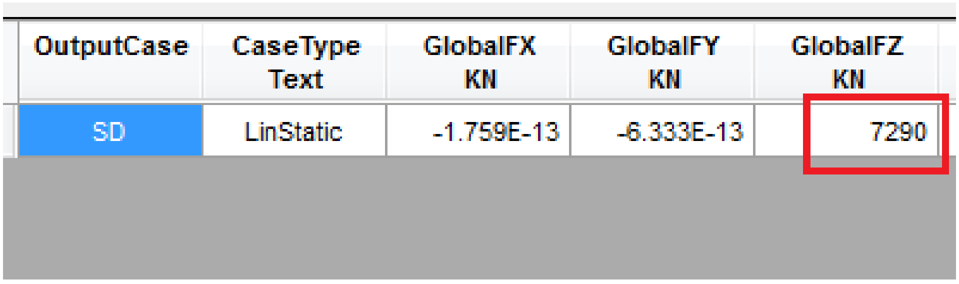

OutputCase	CaseType Text	GlobalFX KN	GlobalFY KN	GlobalFZ KN
SD	LinStatic	-1.759E-13	-6.333E-13	7290

Figure 4.6 M5-Super Imposed Dead Load Using SAP2000

STEP 12 (Fundamental Period of the Structure)

The natural period of the structure is defined as the time needed to complete one cycle of vibration, which is the inverse of structure's natural frequency. The structure's fundamental period is parameter which is of tremendous importance to earthquake engineering, because when the forcing period nears the natural period of the structure, it will endure the massive vibration and experience the largest loss. This phenomenon is called Resonance, which plays an essential part in survival or failure to survival of structure during and after earthquake. In this study, the fundamental period of the structure (T) is determined from SAP2000 software analysis. For M5 model, the fundamental period equals 0.69second.

Verification on SAP2000 fundamental period:

Rayleigh-Ritz method can be used for calculating an approximation to the fundamental periods for multi-degree structures using the following equation:

$$T = 2\pi\sqrt{\frac{\sum_{i=1}^{n} W_i {\delta_i}^2}{g\sum_{i=1}^{n} f_i \delta_i}} \tag{4.5}$$

Where, δ_i is lateral displacement of storey i, f_i is the horizontal load applied at storey i, W_i is the weight of storey i, n is number of storeys in the structure. The values of f_i represent any lateral force distribution in accordance with the principles of structural mechanics. The elastic deflections, δ_i, shall be calculated using the applied lateral forces as shown in Table 4.20.

Table 4.20 M5-Verification on SAP2000 Fundamental Period

Storey	W_i(kN)	f_i (kN)[a]	δ_i(m)[b]	δ_i^2	$f_i\ \delta_i$	$W_i\ \delta_i^2$
1	4923	1000	0.006	3.12E-05	5.59	0.15
2	4923	1000	0.015	0.00021	14.54	1.04
3	4923	1000	0.022	0.00050	22.45	2.48
4	4923	1000	0.028	0.00079	28.17	3.91
5	4540	1000	0.032	0.00100	31.67	4.55
					102.42	12.14

a Assumed forces

b Deflections corresponding to the assumed forces

By applying Eq. 4.5 with Table 4.20, we get:

T = 0.69 second

$$\% \text{ error} = \frac{\text{SAP Period} - \text{Approximated Period}}{\text{SAP Period}} \times 100\%$$

$$= \frac{0.69 - 0.69}{0.69} \times 100\% = 0.0\%$$

STEP 13 (Maximum Period Limit)

ASCE 7 in section 12.8.2 states that, the fundamental period, T, shall not exceed the product of the coefficient for upper limit on calculated period (C_u) from Table 4.21 and the approximate fundamental period, T_a.

$$T_a = C_t h_n^x \qquad (4.6)$$

Where, h_n is the structural height and the coefficients C_t and x are determined from Table 4.22.

Table 4.21 Coefficient for Upper Limit on Calculated Period (Table 12.8-1, ASCE 7)

Design Spectral Response Acceleration Parameter at 1 *s*, S_{D1}	Coefficient C_u
≥ 0.4	1.4
0.3	1.4
0.2	1.5
0.15	1.6
≤ 0.1	1.7

Table 4.22 Values of Approximate Period Parameters Ct and x (Table 12.8-2, ASCE 7)

Structure Type	C_t	x
Moment-resisting frame systems in which the frames resist 100% of the required seismic force and are not enclosed or adjoined by components that are more rigid and will prevent the frames from deflecting where subjected to seismic forces:		
Steel moment-resisting frames	0.028 (0.0724)[a]	0.8
Concrete moment-resisting frames	0.016 (0.0466)[a]	0.9
Steel eccentrically braced frames in accordance with Table 12.2-1 lines B1 or D1	0.03 (0.0731)[a]	0.75
Steel buckling-restrained braced frames	0.03 (0.0731)[a]	0.75
All other structural systems	0.02 (0.0488)[a]	0.75

[a]Metric equivalents are shown in parentheses.

After referring to Table 4.22

C_t = 0.0466 (Concrete moment-resisting frame)

$x = 0.9$

h_n = number of storeys× storey's height = 5×3.40 = 17m

Apply previous values in Eq. 4.6, we get

$T_a = 0.0466 \times 17^{0.9} = 0.597$seconds

After referring to Table 4.21

$S_{D1} = 0.25$

Interpolation between S_{D1} equals 0.20 and S_{D1} equals 0.30, we get

$C_u = 1.45$

$C_u \times T_a = 1.45 \times 0.597 = 0.87$second > 0.69second OK

STEP 14 (Response Spectrum Graph)

In earthquake engineering, there is many tools that can be used in designing of structures to support seismic loads, one of these tools is the response spectrum which is a graph relates the response parameter (i.e. acceleration, displacement or velocity) with natural period or natural frequency of the structure for single degree of freedom oscillator as shown in Figs. 4.7 and 4.8. The parameters in the response spectrum can be determined from the following equations:

$$T_0 = 0.2\,\frac{S_{D1}}{S_{DS}} \qquad (4.7)$$

$$T_S = \frac{S_{D1}}{S_{DS}} \qquad (4.8)$$

Where, S_{DS} and S_{D1} are as defined before, long-period transition period (T_L) for Palestine equals 4 second.

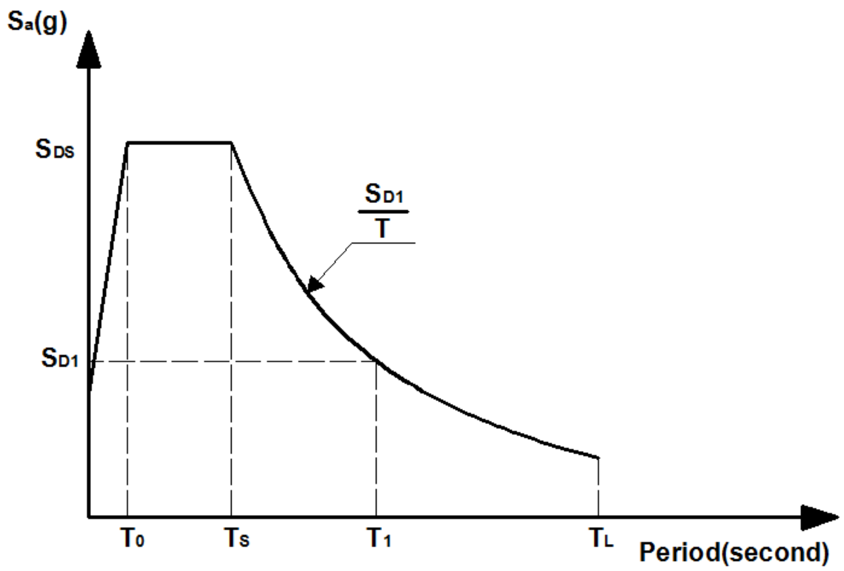

Figure 4.7 Generic Elastic Response Spectrum

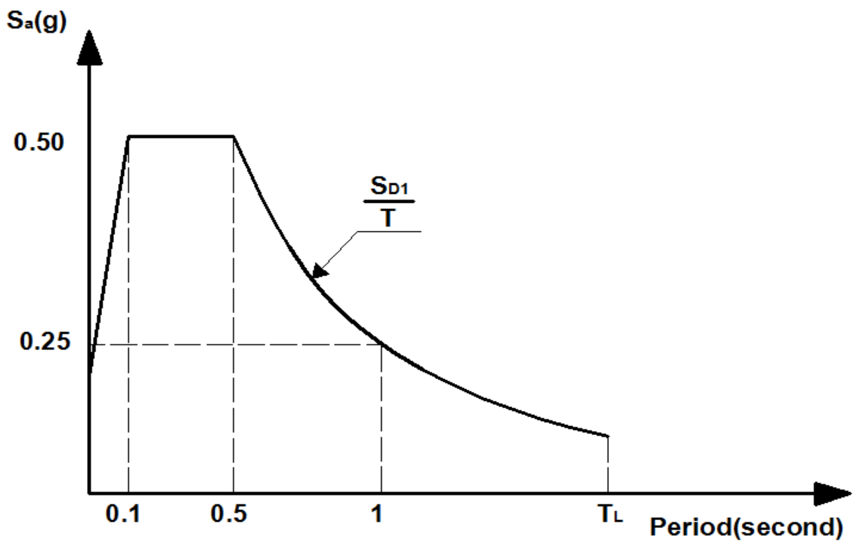

Figure 4.8 M5-Elastic Response Spectrum

In determining the base shear value and for design purposes; the inelastic response spectrum is used by dividing the elastic response accelerations by the response modification coefficient and multiplying it with the seismic importance factor as shown in Figs. 4.9 and 4.10.

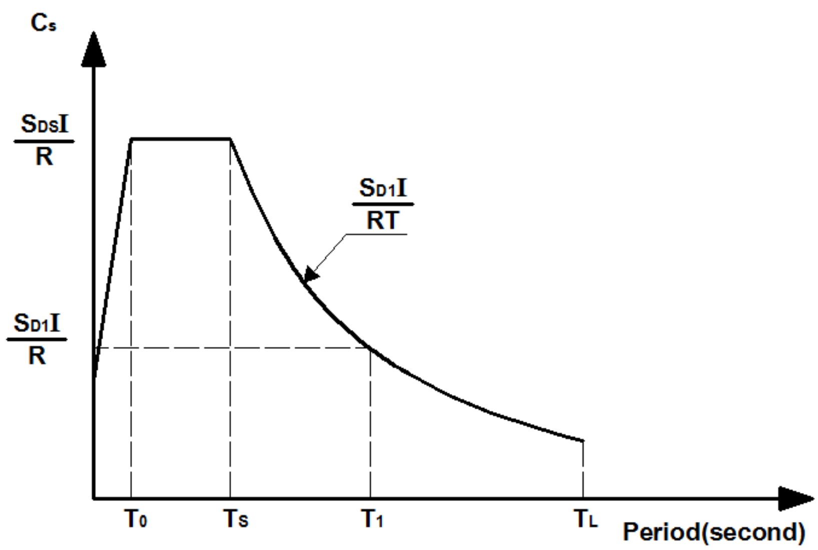

Figure 4.9 Generic Inelastic Response Spectrum

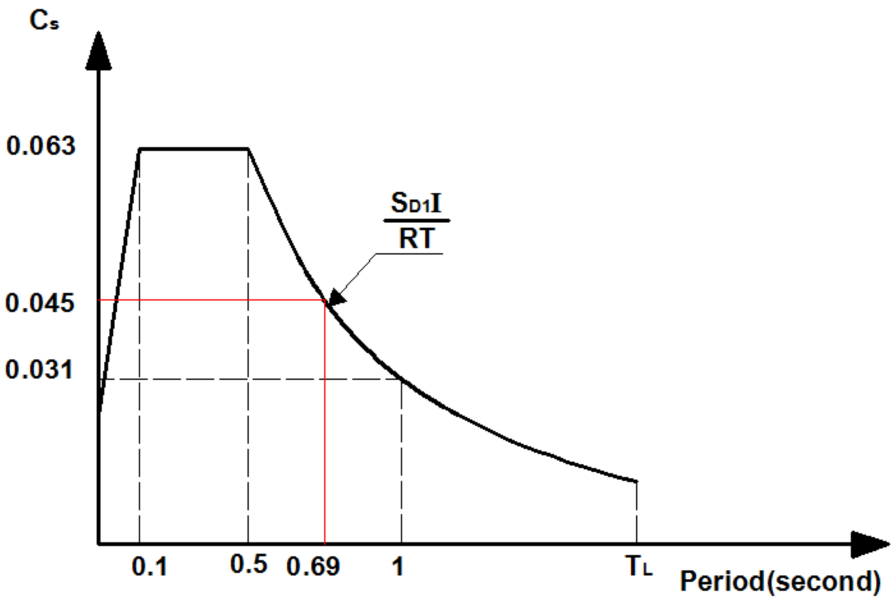

Figure 4.10 M5-Inelastic Response Spectrum

STEP 15 (Determination of Seismic Base Shear using Equivalent Lateral Force Analysis)

The seismic base shear (V) in a given direction is determined in accordance with the following equation:

$$V = C_s W \tag{4.9}$$

Where:

W is the effective seismic weight

C_s is the minimum of $\begin{cases} \frac{S_{DS}\times I}{R} \\ \frac{S_{D1}\times I}{R\times T} \end{cases} = \begin{cases} \frac{0.50\times 1}{8} \\ \frac{0.25\times 1}{8\times 0.69} \end{cases} = \begin{cases} 0.063 \\ 0.045 \end{cases} = 0.045$

S_{DS}, S_{D1}, I, R and T are as defined before.

By applying Eq. 4.9, we get:

V = 0.045×24232 = 1090kN

STEP 16 (Determination of Seismic Base Shear using Modal Response Spectrum Analysis)

As stated earlier, Modal Response Spectrum Analysis was used using SAP2000 analysis software after defining the response spectrum function with the appropriate parameters as shown in Fig. 4.11. After applying the modal response spectrum analysis on the structure as a load case, the base shear (V) has been computed by using section cut at columns of ground floor and the result is as follows,

V = 936kN

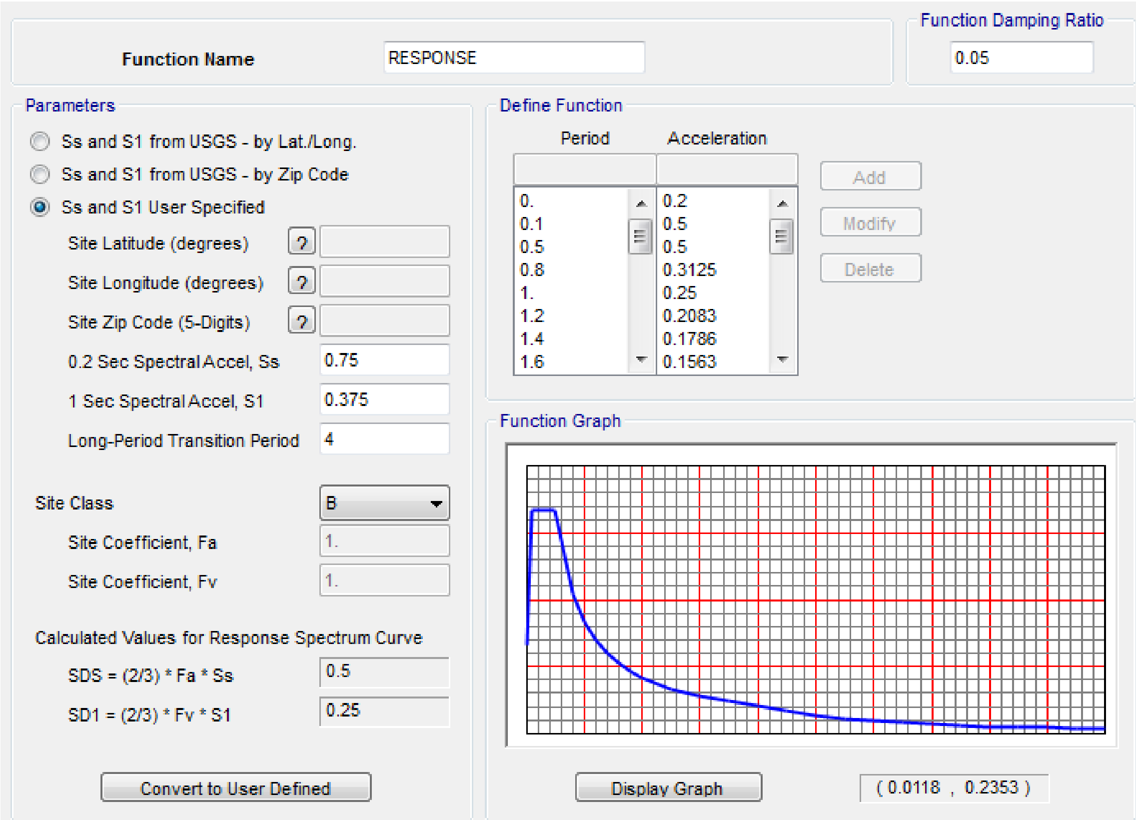

Figure 4.11 Response Spectrum Function Using SAP2000

ASCE 7 section 12.9.4.1 states that, the base shear (V) using the modal response spectrum procedure shall not be less than 85 percent of the calculated base shear (V) using the equivalent lateral force procedure as shown in Table 4.23.

Table 4.23 M5-Base Shear Selection

Base shear using MRSA[1] (kN)	Base shear using ELF[2] (kN)	0.85×ELF[2] (kN)
936	1090	926

1 Modal Response Spectrum Analysis
2 Equivalent Lateral Force

The base shear using modal response spectrum analysis is larger than 85 percent of the calculated base shear using equivalent lateral force procedure. Thus, base shear equals 936kN.

STEP 17 (Vertical Distribution of Seismic Base Shear)

Seismic base shear distribution can be computed using SAP2000 by making section cut and reading the shear force from response analysis case at each level as shown in Table 4.24.

Table 4.24 M5-Base Shear Distribution on Floors

Floor	h(m)	Shear Force (kN)	Force on each Floor (kN)
1	3.40	936	57
2	6.80	879	131
3	10.2	748	188
4	13.6	560	254
5	17.0	306	306

Verification of SAP2000 response shear results:

To verify response shear results which are created by SAP2000 software, new expressions shall be defined as follows:

$$\beta_n = \frac{\sum_{i=1}^{N} W_i \phi_{in}}{\sum_{i=1}^{N} W_i {\phi_{in}}^2} \tag{4.10}$$

Where

β_n = participation factor for mode n

i = level number

n = mode number

N = total number of storeys

W_i = weight at level i

Φ_{in} = mode shape value at level i in mode n

$$W_{en} = \frac{\left(\sum_{i=1}^{N} W_i \phi_{in}\right)^2}{\sum_{i=1}^{N} W_i {\phi_{in}}^2} \tag{4.11}$$

Where

W_{en} = effective weight in mode n

i, n, N, W_i and Φ_{in} are as defined before

$$F_{in} = aWi\beta_n\Phi_{in} \tag{4.12}$$

Where

F_{in} = force at each level i for mode n

a = spectral acceleration of SDOF system with a period corresponding to mode n

$\beta_n\Phi_{in}$ = the product of participation factor and mode shape, it is called participation function

Note: For reader's convenience previous symbols correspond with the book of Dynamics of Structures “Theory and Applications to Earthquake Engineering” by Anil K. Chopra as follows:

$\beta_n = \Gamma_n$

$\sum_{i=1}^{N} W_i \emptyset_{in} = L_n$

$\sum_{i=1}^{N} W_i \emptyset_{in}^{\;2} = W_n$

$W_{en} = W_n^*$

The applying of previous equations (Eqs.4.10, 4.11 and 4.12) is summarized in Tables 4.25-4.28.

Table 4.25 M5-Mode 1 Modal Mass Participation Ratio

Mode 1					
Level	W_i (kN)	Φ_i	Φ_i^2	$W_i\ \Phi_i$	$W_i\Phi_i^2$
1	4923	0.15	0.02	744.2	112.5
2	4923	0.42	0.17	2050.5	854.1
3	4923	0.67	0.45	3317.6	2235.8
4	4923	0.87	0.76	4300.1	3755.9
5	4540	1.00	1.00	4540.0	4540.0
			Σ	14952.4	11498.3
$\beta_1 = \frac{14952.4}{11498.3} = 1.3$					
$W_{e1} = \frac{14952.4^2}{11498.3} = 19444$kN					
Modal mass participation ratio of Mode 1 = $\frac{W_{e1}}{\text{total weight}}\times 100\%$ $= \frac{19444}{24232}\times 100\% = 80.2$ %					

Table 4.26 M5-Mode 1 Shear Distribution

Mode 1						
Level	T (second)	a*	W (kN)	β Φ_i	Force (kN)	Shear (kN)
1	0.69	0.045	4923	0.197	43.5	874.7
2	0.69	0.045	4923	0.541	120.0	831.2
3	0.69	0.045	4923	0.876	194.1	711.2
4	0.69	0.045	4923	1.136	251.6	517.1
5	0.69	0.045	4540	1.300	265.6	265.6

* response acceleration corresponding to mode period

Table 4.27 M5-Mode 2 Modal Mass Participation Ratio

Mode 2					
Level	W_i (kN)	Φ_i	Φ_i^2	$W_i\ \Phi_i$	$W_i\Phi_i^2$
1	4923	0.513	0.263	2525.2	1295.2
2	4923	1.000	1.000	4923.0	4923.0
3	4923	0.760	0.578	3741.6	2843.7
4	4923	-0.098	0.010	-481.9	47.2
5	4540	-0.998	0.995	-4529.1	4518.2
			$\sum$	6178.8	13627.4
$\beta_2 = \frac{6178.8}{13627.4} = 0.453$					
$W_{e2} = \frac{6178.8^2}{13627.4} = 2802\text{kN}$					
Modal mass participation ratio of Mode 2 = $\frac{W_{e2}}{\text{total weight}} \times 100\%$ $= \frac{2802}{24232} \times 100\% = 11.6\%$					

Table 4.28 M5-Mode 2 Shear Distribution

Mode 2						
Level	T (second)	a*	W (kN)	β Φ_i	Force (kN)	Shear (kN)
1	0.21	0.063	4923	0.232	72.1	176.3
2	0.21	0.063	4923	0.453	140.5	104.3
3	0.21	0.063	4923	0.344	106.8	-36.2
4	0.21	0.063	4923	-0.044	-13.8	-143.0
5	0.21	0.063	4540	-0.452	-129.3	-129.3

* response acceleration from response spectrum corresponding to mode period

Analysis shall include a sufficient number of modes to obtain a combined modal participation of at least 90% of the actual mass in each orthogonal level (ASCE 7, section 12.9.1). For M5 case, mode1 and mode 2 give 91.8% of the actual mass. Thus, mode1 and mode2 are sufficient for shear calculations. The difference between hand calculations and SAP2000 is carried out for the first and second storeys as shown in Table 4.29. There are different ways in which results from the modes are combined to arrive at the final response, such as: CQC, SRSS or Absolute. CQC method is used to account for some interaction of modes when the modes are closely spaced. While the square root of sum of squares (SRSS) is used when the modes spaced far apart. Absolute is rarely used because it is quite unconservative. It was noted that the modes are spaced far apart so SRSS is adopted in this research.

Table 4.29 M5-Shear Force Determination Using Both Hand Calculations and SAP2000

Level	Shear Using Hand Calculations (kN)	Shear Using SAP2000 (kN)	Percent of Error*
1	893	936	4.5%
2	838	879	4.6%

***** acceptance limit is 10%

4.2.1.4 P-Delta Effect

Two load cases on SAP2000 software are created. Number one: a linear load case which includes dead loads, live loads and seismic forces; Number two: a nonlinear load case with geometric nonlinearity which includes dead loads, live loads and seismic forces. The bending moment is determined on all columns in all floors and the column which gives the maximum percent difference between first-order analysis and second-order analysis is adopted as tabulated in Table 4.30. Fig. 4.12 shows the numbering sequence for all columns in all models.

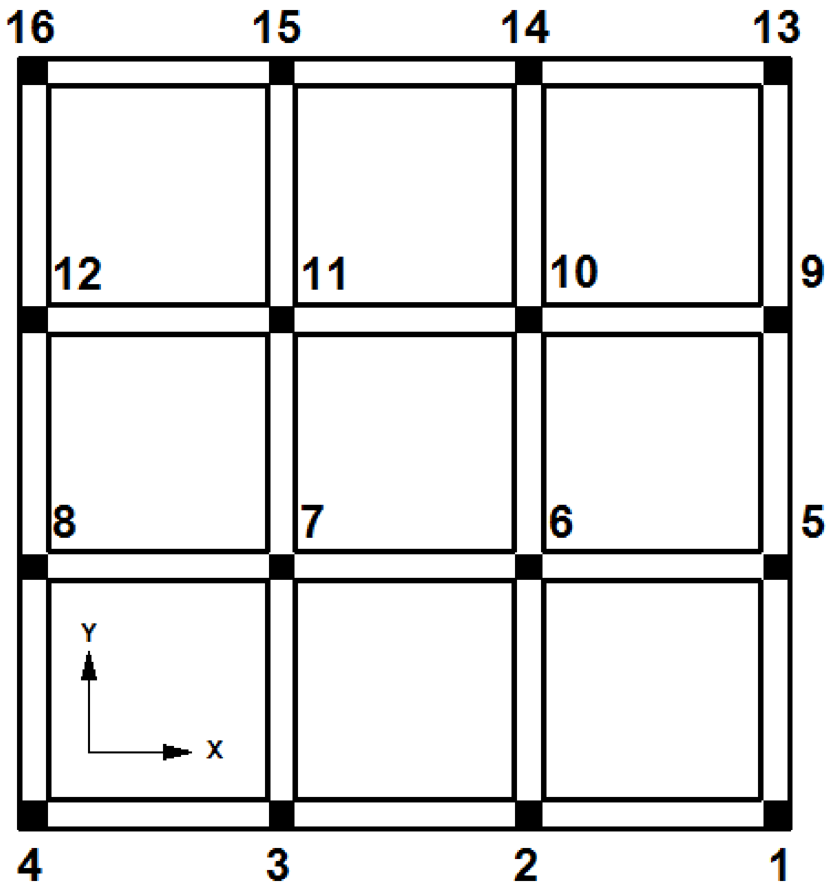

Figure 4.12 Models Numbering Sequence

Table 4.30 M5 Percent Difference between First-Order and Second-Order

M5						
Column	**M_{SD+D+L}**	**$M_{POSITIVE}$ EQ.**	**$M_{NEGATIVE}$ EQ.**	**First-Order Moment**	**Second-Order Moment**	**Percent**
1	26.7	164.1	-164.1	190.8	192.6	0.96
2	0.2	179.7	-179.7	179.9	181.9	1.07
3	-0.2	179.7	-179.7	-179.9	-181.9	1.07
4	-26.7	164.1	-164.1	-190.8	-192.6	0.96
5	44.1	165.0	-165.0	209.1	210.9	0.83
6	0.1	180.7	-180.7	180.8	182.6	0.96
7	-0.1	180.7	-180.7	-180.8	-182.6	0.96

8	-44.1	165.0	-165.0	-209.1	-210.9	0.83
9	44.1	165.0	-165.0	209.1	210.9	0.83
10	0.1	180.7	-180.7	180.8	182.6	0.96
11	-0.1	180.7	-180.7	-180.8	-182.6	0.96
12	-44.1	165.0	-165.0	-209.1	-210.9	0.83
13	26.7	164.1	-164.1	190.8	192.6	0.96
14	0.2	179.7	-179.7	179.9	181.9	1.07
15	-0.2	179.7	-179.7	-179.9	-181.9	1.07
16	-26.7	164.1	-164.1	-190.8	-192.6	0.96
17	72.4	80.2	-80.2	152.5	153.8	0.81
18	-0.4	127.0	-127.0	-127.4	-129.3	**1.46**
19	0.4	127.0	-127.0	127.4	129.3	**1.46**
20	-72.4	80.2	-80.2	-152.5	-153.8	0.81
21	123.0	81.3	-81.3	204.3	205.5	0.61
22	-0.2	129.3	-129.3	-129.5	-131.4	1.43
23	0.2	129.3	-129.3	129.5	131.4	1.43
24	-123.0	81.3	-81.3	-204.3	-205.5	0.61
25	123.0	81.3	-81.3	204.3	205.5	0.61
26	-0.2	129.3	-129.3	-129.5	-131.4	1.43
27	0.2	129.3	-129.3	129.5	131.4	1.43
28	-123.0	81.3	-81.3	-204.3	-205.5	0.61
29	72.4	80.2	-80.2	152.5	153.8	0.81
30	-0.4	127.0	-127.0	-127.4	-129.3	**1.46**
31	0.4	127.0	-127.0	127.4	129.3	**1.46**
32	-72.4	80.2	-80.2	-152.5	-153.8	0.81
33	66.4	44.3	-44.3	110.8	111.2	0.40
34	2.6	90.3	-90.3	92.9	93.9	1.13
35	-2.6	90.3	-90.3	-92.9	-93.9	1.13
36	-66.4	44.3	-44.3	-110.8	-111.2	0.40
37	112.8	45.6	-45.6	158.4	158.8	0.29
38	4.5	92.5	-92.5	97.0	98.1	1.11
39	-4.5	92.5	-92.5	-97.0	-98.1	1.11
40	-112.8	45.6	-45.6	-158.4	-158.8	0.29
41	112.8	45.6	-45.6	158.4	158.8	0.29
42	4.5	92.5	-92.5	97.0	98.1	1.11
43	-4.5	92.5	-92.5	-97.0	-98.1	1.11
44	-112.8	45.6	-45.6	-158.4	-158.8	0.29
45	66.4	44.3	-44.3	110.8	111.2	0.40
46	2.6	90.3	-90.3	92.9	93.9	1.13
47	-2.6	90.3	-90.3	-92.9	-93.9	1.13
48	-66.4	44.3	-44.3	-110.8	-111.2	0.40
49	67.2	19.6	-19.6	86.8	86.8	0.00
50	4.2	56.5	-56.5	60.7	61.1	0.62
51	-4.2	56.5	-56.5	-60.7	-61.1	0.62
52	-67.2	19.6	-19.6	-86.8	-86.8	0.00
53	113.7	20.7	-20.7	134.4	134.4	0.00
54	7.0	58.4	-58.4	65.3	65.8	0.64

55	-7.0	58.4	-58.4	-65.3	-65.8	0.64
56	-113.7	20.7	-20.7	-134.4	-134.4	0.00
57	113.7	20.7	-20.7	134.4	134.4	0.00
58	7.0	58.4	-58.4	65.3	65.8	0.64
59	-7.0	58.4	-58.4	-65.3	-65.8	0.64
60	-113.7	20.7	-20.7	-134.4	-134.4	0.00
61	67.2	19.6	-19.6	86.8	86.8	0.00
62	4.2	56.5	-56.5	60.7	61.1	0.62
63	-4.2	56.5	-56.5	-60.7	-61.1	0.62
64	-67.2	19.6	-19.6	-86.8	-86.8	0.00
65	80.5	-2.5	2.5	77.9	77.9	0.00
66	2.9	25.2	-25.2	28.1	28.2	0.20
67	-2.9	25.2	-25.2	-28.1	-28.2	0.20
68	-80.5	-2.5	2.5	-83.0	-83.2	0.22
69	137.3	-1.9	1.9	139.2	139.4	0.13
70	6.1	26.5	-26.5	32.7	32.8	0.26
71	-6.1	26.5	-26.5	-32.7	-32.8	0.26
72	-137.3	-1.9	1.9	-139.2	-139.4	0.13
73	137.3	-1.9	1.9	139.2	139.4	0.13
74	6.1	26.5	-26.5	32.7	32.8	0.26
75	-6.1	26.5	-26.5	-32.7	-32.8	0.26
76	-137.3	-1.9	1.9	-139.2	-139.4	0.13
77	80.5	-2.5	2.5	83.0	83.2	0.22
78	2.9	25.2	-25.2	28.1	28.2	0.20
79	-2.9	25.2	-25.2	-28.1	-28.2	0.20
80	-80.5	-2.5	2.5	-83.0	-83.2	0.22

* All calculations are on the bottom of columns

Verification of Second-Order Analysis

To verify second-order analysis results, it is required to determine both structure P-Delta effect and member P-Delta effect. Table 4.31 summarizes the first-order bending moments from all load cases on the column number four.

Table 4.31 M5-First-Order Moment Analysis on Column Number Four

	Moment on Base (kN.m)	Moment on Top (kN.m)
Live Load	-5.48	11.5
Super Imposed Load	-8.23	17.2
Dead Load	-12.9	27.1
Earthquake Load	-164	9.3

$\sum P$ = summation of axial forces = 29475kN

$I_{Column,Crack} = 0.8 \times I_{Column} = 0.8 \times \frac{0.75^4}{12} = 0.0211 m^4$

$I_{Beam,Crack} = 0.4 \times I_{Beam} = 0.4 \times \frac{0.75 \times 0.7^3}{12} = 8.58 \times 10^{-3}\ m^4$

$E_{Column} = 26.6 \times 10^6\ kN/m^2$

$E_{Beam} = 23 \times 10^6\ kN/m^2$

P-∆ effect (structure P-Delta effect)

For middle:

After applying Eq.2.13, we get:

$$G_A = \frac{26.6 \times 10^6 \times 0.0211 \times 2/3.4}{23 \times 10^6 \times 8.58 \times 10^{-3} \times 2/6} = 5.02$$

$G_B = 0$ (Fixed Support)

The effective length factor K = 1.5 (From Fig. 2.16)

$$P_{ek\ middle} = \frac{\pi^2 EI}{(KL)^2} = \frac{\pi^2 \times 26.6 \times 10^6 \times 0.0211}{(1.5 \times 3.4)^2} = 212970kN$$

For Edge:

After applying Eq.2.13, we get:

$$G_A = \frac{26.6 \times 10^6 \times 0.0211 \times 2/3.4}{23 \times 10^6 \times 8.58 \times 10^{-3}/6} = 10.03$$

$G_B = 0$ (Fixed Support)

The effective length factor K = 1.68 (From Fig. 2.16)

$$P_{ek\ edge} = \frac{\pi^2 EI}{(KL)^2} = \frac{\pi^2 \times 26.6 \times 10^6 \times 0.0211}{(1.68 \times 3.4)^2} = 169780\text{kN}$$

$$\sum P_{ek} = 8 \times P_{ek\ middle} + 8 \times P_{ek\ edge} = 3062000\text{kN}$$

After applying Eq.2.11, we get:

$$B_2 = \left(\frac{1}{1 - \sum P / \sum P_{ek}}\right) = \frac{1}{1 - 29475/3062000} = 1.01$$

P- δ Effect (member P-Delta effect)

By applying Eq. 2.8, we get

$$C_m = 0.6 - 0.4\left(\frac{M_A}{M_B}\right)$$

Where, M_B is the larger of the two end moments.

$M_A = M_{Live} + M_{SD} + M_{Dead} = -26.6\text{kN.m}$

$M_B = M_{Live} + M_{SD} + M_{Dead} = 55.8\text{kN.m}$

$$C_m = 0.6 - 0.4\left(\frac{26.6}{55.8}\right) = 0.41$$

P = axial load on prescribed column = 1057kN (SAP2000)

$$G_A = \frac{26.6 \times 10^6 \times 0.0211 \times 2/3.4}{23 \times 10^6 \times 6.25 \times 10^{-3}/6} = 10.03$$

$G_B = 0$ (Fixed Support)

The effective length factor K = 0.7 (From Fig. 2.14)

$$P_e = \frac{\pi^2 EI}{(KL)^2} = \frac{\pi^2 \times 26.6 \times 10^6 \times 0.0211}{(0.7 \times 3.4)^2} = 977935\text{kN}$$

By applying Eq. 2.6, we get

$$B_1 = \frac{C_m}{1-\frac{P}{P_e}} = \frac{0.41}{1-\frac{1057}{977935}} = 0.41 \text{ (Take } B_1\text{=1)}$$

$M_u = B_2 M_{1sway} + B_1\, M_{1non\text{-}sway} = 1.01 \times -164 - 5.48 - 8.23 - 12.9 = -192.3$kN.m

The second-order moment results for prescribed column from both hand calculations and SAP2000 are tabulated in Table 3.32.

Table 4.32 M5-Difference between Hand Calculations and SAP2000 Results on Column Number Four

	Second-Order Analysis Using Moment Amplification Method	**Second-Order Analysis Using SAP2000**	**Percent Difference**
Bending Moment (kN.m)	-192.3	-192.6	0. 1 %

4.2.1.5 Storey Drift Determination

The storey drift shall be computed as the difference of the deflections at the center of mass at the top and bottom of the storey under consideration (ASCE 7, section 12.8.6). Storey drift is an important indicator of structural behavior in performance-based seismic analysis especially for high-rise structures. During an earthquake, large lateral forces can be imposed on structures which require the designer to assess the effects of this deformation on both structural and non-structural elements. Storey drift has three primary effects on a structure; the movement can affect the structural elements (such as beams and columns); the movements can affect non-structural elements (such as the windows and cladding); and the movements can affect adjacent structures.

Design provisions for moment frame and eccentric braced frame structures have requirements to ensure the ability of the structure to sustain inelastic rotations resulting from deformation and drift. Without proper consideration of the expected movement of the structure, the lateral force resisting system might experience premature failure and a corresponding loss of strength. In addition, if the lateral deflections of any structure become too large, P-Δ effects can cause instability of the structure and potentially result in collapse. Thus, it is vital to determine the storey drift for every structure and making sure it is under the allowable limits prescribed in ASCE 7 as follows:

$$\Delta = \delta_x - \delta_{x-1} \tag{4.13}$$

$$\delta_x = \frac{C_d\,\delta_{xe}}{I_e} \tag{4.14}$$

Where

C_d = the deflection amplification factor in Table 12.2, ASCE 7

δ_{xe} = Elastic displacement

I_e = importance factor

The storey drifts are determined and checked for allowable limit and tabulated in Table 4.33.

Table 4.33 M5 Drift Check

Level	δ_{xe} (mm)[a]	δ_x (mm)[b]	Δ (mm)	$\Delta_{Allowable}$ (mm)[c]	Check
1	1.13	6.21	6.21	52	OK
2	3.10	17.06	10.85	52	OK
3	5.02	27.60	10.54	52	OK
4	6.53	35.91	8.30	52	OK
5	7.51	41.31	5.40	52	OK

a Elastic displacement from seismic load case
b Amplified displacement (ASCE 7, Eq. 12.8-15)
c $\Delta_{Allowable} = 0.0153h_{sx}$ (ASCE 7, Table 12.12-1)

4.2.1.6 Stability Coefficient

The stability coefficient is an indicator to indicate the need for considering P-Delta effect in the analysis. ASCE 7, section 12.8.7 states that P-Delta effects on story shears and moments, the resulting member forces and moments, and the story drifts induced by these effects are not required to be considered where stability coefficient (θ) as determined by the following equation is equal to or less than 0.10:

$$\theta = \frac{P_x \Delta I_e}{V_x h_{sx} C_d} \tag{4.15}$$

Where

P_x = the total vertical design load at and above level x in kN; where computing P_x, no individual load factor need exceed 1.0

Δ = the design story drift as defined in equation 4.13

I_e = importance factor

V_x = the seismic shear force acting between levels x and x-1

h_{sx} = the story height below level x

C_d = the deflection amplification factor in Table 12.2-1, ASCE 7

The Storeys' coefficients are determined and tabulated in Table4.34.

Table 4.34 M5 Stability Coefficient

M5						
Level	**P_x (kN)**	**Δ (mm)**	**V_x (kN)**	**h_{sx} (mm)**	**C_d**	**θ**
1	29475	6.21	936	3400	5.5	0.010
2	23580	10.85	879	3400	5.5	**0.016**
3	17685	10.54	748	3400	5.5	0.013
4	11790	8.30	560	3400	5.5	0.009
5	5130	5.40	306	3400	5.5	0.005

The maximum stability coefficient for model M5 is less than 0.10. Thus, P-Delta effect is not required to be considered. It is worth mentioning that the maximum difference between first-order moment and second-order moment on the critical column is very close to the stability coefficient's value. Furthermore, the stability coefficient gives more conservative value in this case.

4.2.2 Ten-Storey model (M10)

M10 is a ten-storey reinforced concrete portal frame with fixed supports with a total height equals 34m. M10 has the same plan, material properties, section properties, storey's height, live loads, and superimposed dead loads as M5 except number of stories and columns' sections. The columns' sections are as shown in Table 4.35. Elevation of M10 is illustrated in Fig. 4.13.

Table 4.35 M10-Columns' Sections

	Column	
Storey	**Depth (m)**	**Width (m)**
1-5	0.90	0.90
6-10	0.75	0.75

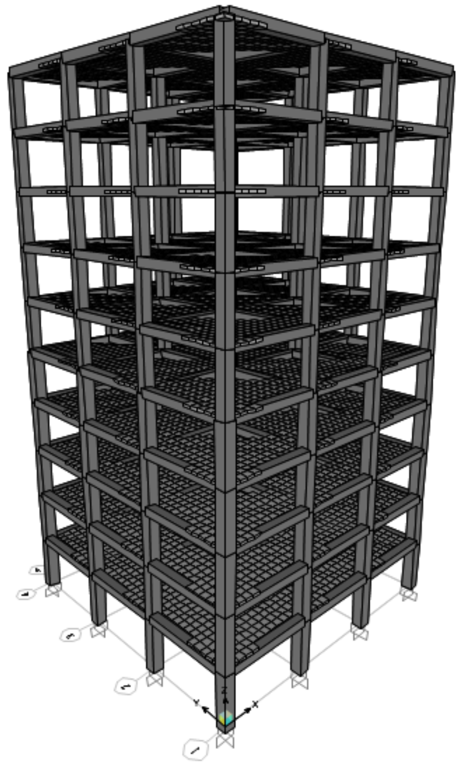

Figure 4.13 M10 Model in 3-D view

Parameters that can be used to determine the base shear using International Building Code 2015 (IBC 2015) in co-operation with ASCE 7 can be determined in the same way as M5 model. M10 has the same values as M5 from step 1 until step 10 as summarized in Table 4.36. The Calculations for the rest values are resumed from step 11.

Table 4.36 M10 Model Summary from Step One to Ten

Step	Parameter	Value
1	Seismic Zone Factor (Z)	0.20
2	Site Classification	B
3	S_S	0.50
	S_1	0.25
4	F_a	1
	F_v	1
5	S_{DS}	0.50
	S_{D1}	0.25
6	Risk Category of the Structure	II
7	Seismic Design Category	D
8	Seismic Importance Factor	1
9	Permitted Analytical Procedure	MRSA* is used
10	Response Modification Coefficient, R	8
	Over Strength Factor, Ω_0	3
	Deflection Amplification Factor, C_d	5.5

* Modal Response Spectrum Analysis

STEP 11(Effective Seismic Weight)

Each floor weight is determined in the same way as calculating M5 weights except for M10 model, the columns' sections are changing throughout the elevation. M10 columns' weights in each storey are determined and tabulated in Table 4.37. The weight of each storey can be determined as the sum of beams' weights, columns' weights, slab's weight, and superimposed dead loads. The last storey is exempted from half columns' weights as tabulated in Table 4.38.

Table 4.37 M10-Columns Weight in each Storey

Storey	Number of Columns	Depth	Width	Length	Concrete Weight Per Unit Volume	Columns Weight
1-5	16	0.9m	0.9m	3.40m	$25kN/m^3$	1102kN
6-10	16	0.75m	0.75m	3.40m	$25kN/m^3$	765kN

Table 4.38 M10-Floors' Weights

Floor	Weight (kN)
1	5260
2	5260
3	5260
4	5260
5	5260
6	4923
7	4923
8	4923
9	4923
10	4540
Total	50532

STEP 12 (Fundamental Period of the Structure)

The fundamental period of the structure (T) is determined from SAP2000, version 19.0.0 software analysis. For M10 model, the fundamental period equals 1.38second.

Verification on SAP2000 fundamental period:

Rayleigh-Ritz method can be used for calculating an approximation to the fundamental periods using the Eq. 4.5 as shown in Table 4.39.

By applying Eq. 4.5 with Table 4.39

T = 1.37 second

$$\% \text{ error} = \frac{\text{SAP Period} - \text{Approximated Period}}{\text{SAP Period}} \times 100\%$$

$$= \frac{1.38-1.37}{1.38} \times 100\% = 0.72\% < 10\% \text{ Acceptable}$$

Table 4.39 M10-Verification of SAP2000 Fundamental Period

Storey	**W_i(kN)**	**f_i (kN)[a]**	**δ_i(m)[b]**	**δ_i^2**	**$f_i\ \delta_i$**	**$W_i\ \delta i^2$**
1	5260	1000	0.008	7.03E-05	8.4	0.37
2	5260	1000	0.025	0.0006	24.9	3.25
3	5260	1000	0.043	0.0019	43.1	9.78
4	5260	1000	0.061	0.0037	60.7	19.37
5	5260	1000	0.077	0.0059	76.7	30.93
6	4923	1000	0.091	0.0084	91.4	41.16
7	4923	1000	0.103	0.0107	103.3	52.53
8	4923	1000	0.112	0.0126	112.4	62.15
9	4923	1000	0.119	0.0141	118.7	69.40
10	4540	1000	0.123	0.0151	122.8	68.41
				$\sum$	762.3	357.4

a Assumed forces

b The displacement corresponding to the assumed forces

STEP 13 (Maximum Period Limit)

After referring to Table 4.22

C_t = 0.0466 (Concrete moment-resisting frame)

x = 0.9

h_n = number of storeys× storey's height = 10×3.40 = 34m

Apply previous values in Eq. 4.6, we get

$T_a = 0.0466 \times 34^{0.9}$ = 1.11seconds

After referring to Table 4.21

S_{D1} = 0.25

Interpolation between S_{D1} equals 0.20 and S_{D1} equals 0.30, we get

C_u = 1.45

$C_u \times T_a = 1.45 \times 1.11 = 1.61\text{second} > 1.38\text{second}$ OK

STEP 14 (Response Spectrum Graph)

The elastic and inelastic response spectrums for M10 model are created in the same way as creating the response spectrums for M5 model as shown in Figs. 4.14 and 4.15 respectively.

STEP 15 (Determination of Seismic Base Shear using Equivalent Lateral Force Analysis)

The seismic base shear (V) in a given direction is determined by applying Eq. 4.9 as follows:

$$C_s \text{ is the minimum of } \begin{cases} \frac{S_{DS} \times I}{R} \\ \frac{S_{D1} \times I}{R \times T} \end{cases} = \begin{cases} \frac{0.50 \times 1}{8} \\ \frac{0.25 \times 1}{8 \times 1.38} \end{cases} = \begin{cases} 0.063 \\ 0.022 \end{cases} = 0.022$$

By applying Eq. 4.9, we get:

V = 0.022×50532= 1112kN

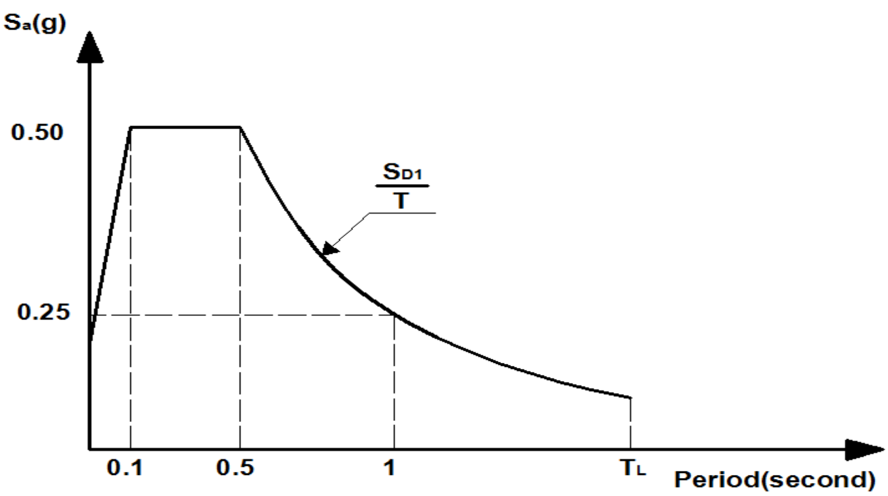

Figure 4.14 M10-Elastic Response Spectrum

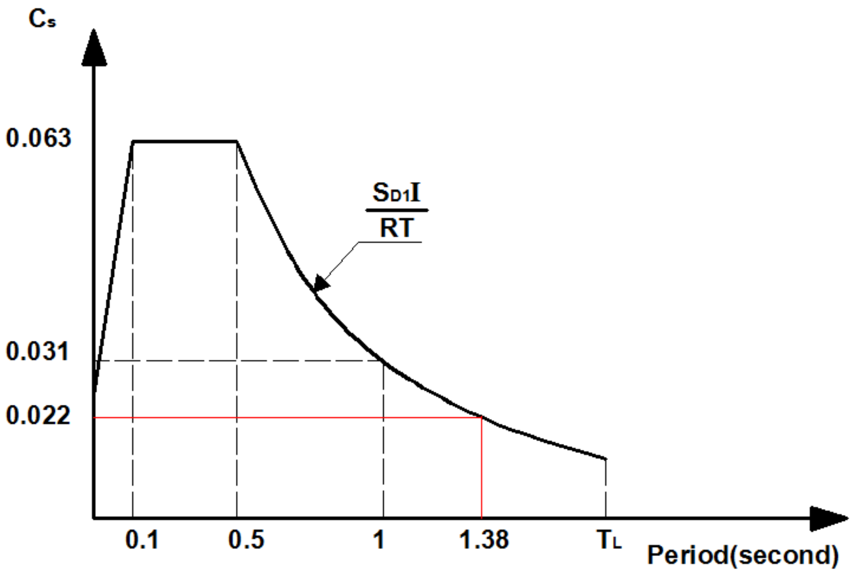

Figure 4.15 M10-Inelastic Response Spectrum

STEP 16 (Determination of Seismic Base Shear using Modal Response Spectrum Analysis)

The response spectrum was defined as for M5 model and the base shear (V) has been computed by using section cut at columns of ground floor for the response spectrum analysis case and the result is as follows,

V = 960kN

Table 4.40 summarizes the selection process for the appropriate base shear value based on ASCE 7 section 12.9.4.1

Table 4.40 M10-Base Shear Selection

Base shear using MRSA[1] (kN)	Base shear using ELF[2] (kN)	0.85×ELF[2] (kN)
960	1112	945

1 Modal Response Spectrum Analysis
2 Equivalent Lateral Force

The base shear using modal response spectrum analysis is larger than 85 percent of the calculated base-shear using equivalent lateral force procedure. Thus, base shear equals 960kN.

STEP 17 (Vertical Distribution of Seismic Base Shear)

Seismic base shear distribution can be computed using SAP2000 by making section cut and reading the shear force from response analysis case at each level as shown in Table 4.41.

Table 4.41 M10-Base Shear Distribution on Floors

Floor	h(m)	Shear Force (kN)*	Force on each Floor (kN)
1	3.40	960	26
2	6.80	934	59
3	10.2	875	70
4	13.6	805	71
5	17.0	734	68
6	20.4	666	69
7	23.8	597	88
8	27.2	509	119
9	30.6	390	169
10	34.0	221	221

* Verification is in appendix A

First-order moment and second-order moment are determined on all columns in all floors and they are annexed in appendix B and verified in appendix C. The critical column is tabulated in Table 4.42.

Table 4.42 M10-Bending Moment Results on Critical Column

	First-Order Analysis	Second-Order Analysis	Percent Difference
Bending Moment (kN.m)	168.7	173.8	3.05%

Storey drifts and stability coefficients for model M10 are calculated in the same way as were calculated for model M5 and tabulated in Tables 4.43 and 4.44 respectively.

Table 4.43 M10 Drift Check

Level	**δ_{xe} (mm)**	**δ_x (mm)**	**Δ (mm)**	**$\Delta_{Allowable}$ (mm)**	**Check**
1	0.85	4.69	4.69	52	OK
2	2.60	14.28	9.58	52	OK
3	4.61	25.35	11.08	52	OK
4	6.64	36.51	11.15	52	OK
5	8.59	47.22	10.71	52	OK
6	10.52	57.86	10.64	52	OK
7	12.24	67.33	9.48	52	OK
8	13.71	75.38	8.04	52	OK
9	14.84	81.61	6.23	52	OK
10	15.60	85.80	4.19	52	OK

Table 4.44 M10 Stability Coefficient

			M10			
Level	**P_x (kN)**	**Δ (mm)**	**V_x (kN)**	**h_{sx} (mm)**	**C_d**	**θ**
1	60633	4.69	960	3400	5.5	0.016
2	54401	9.58	934	3400	5.5	0.030
3	48170	11.08	875	3400	5.5	**0.033**
4	41938	11.15	805	3400	5.5	0.031
5	35707	10.71	734	3400	5.5	0.028
6	29475	10.64	666	3400	5.5	0.025
7	23580	9.48	597	3400	5.5	0.020
8	17685	8.04	509	3400	5.5	0.015
9	11790	6.23	390	3400	5.5	0.010
10	5130	4.19	221	3400	5.5	0.005

The P-Delta analysis is not required based on the stability coefficient which is less than 0.1. The maximum stability coefficient's value is very close to the percent difference between first and second-order analyses (Table 4.42) on the critical column. However, the stability coefficient gives more conservative result compared to the percent difference on the critical column.

4.2.3 Fifteen-Storey model (M15)

M15 is a fifteen-storey reinforced concrete portal frame with fixed supports with a total height equals 51m. M15 has the same plan, material properties, section properties, story's height, live loads, and superimposed dead loads as M5 except number of stories and columns' sections. The columns' sections are as shown in Table 4.45.

Table 4.45 M15-Columns' Sections

	Column	
Storey	**Depth (m)**	**Width (m)**
1-5	1.00	1.00
6-10	0.90	0.90
11-15	0.75	0.75

Elevation of M15 is illustrated in Fig. 4.16. Parameters that can be used to determine the base shear using International Building Code 2015 (IBC 2015) in co-operation with ASCE 7 can be determined in the same way as M5 model. M15 has the same values as M5 from step 1 until step 10 as summarized in Table 4.36. The Calculations for the rest values are resumed from step 11.

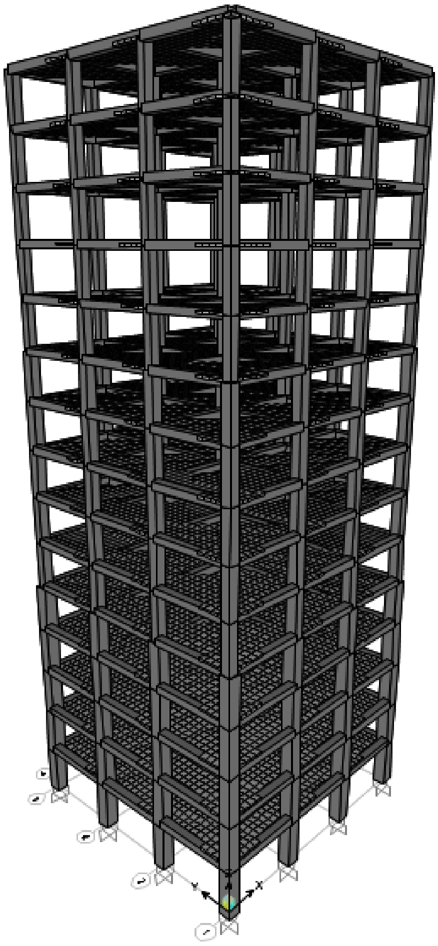

Figure 4.16 M15 Model in 3-D view

STEP 11 (Effective Seismic Weight)

The columns' sections change throughout the elevation. M15 columns' weights in each storey are determined and tabulated in Table 4.46. The weight of each storey can be determined as the sum of beams' weights, columns' weights, slab's weight, and superimposed dead loads. The last storey is exempted from half columns' weights as tabulated in Table 4.47.

Table 4.46 M15-Columns Weight in each Storey

Storey	Number of Columns	Depth	Width	Length	Concrete Weight Per Unit Volume	Columns Weight
1-5	16	1.0m	1.0m	3.40m	$25kN/m^3$	1360kN
6-10	16	0.9m	0.9m	3.40m	$25kN/m^3$	1102kN
11-15	16	0.75m	0.75m	3.40m	$25kN/m^3$	765kN

Table 4.47 M15-Floors' Weights

Floor	Weight (kN)
1	5518
2	5518
3	5518
4	5518
5	5518
6	5260
7	5260
8	5260
9	5260
10	5260
11	4923
12	4923
13	4923
14	4923
15	4540
Total	78122

STEP 12 (Fundamental Period of the Structure)

The fundamental period of the structure (T) is determined from SAP2000, version 19.0.0 software analysis. For M15 model, the fundamental period equals 2.09 second.

Verification of SAP2000 fundamental period:

Rayleigh-Ritz method can be used for calculating an approximation to the fundamental period using Eq. 4.5 as shown in Table 4.48.

By applying Eq. 4.5 with Table 4.48

Approximated period = 2.08 second

% error = $\frac{\text{Approximated Period} - \text{SAP Period}}{\text{SAP Period}} \times 100\% = 0.48\% < 10\%$

Acceptable

Table 4.48 M15-Verification of SAP2000 Fundamental Period

Storey	W_i(kN)	f_i (kN)[a]	δ_i(m)[b]	δ_i^2	$f_i\ \delta_i$	$W_i\ \delta i^2$
1	5518	1000	0.011	0.0001	10.7	0.6
2	5518	1000	0.033	0.0011	33.4	6.2
3	5518	1000	0.061	0.0037	60.7	20.3
4	5518	1000	0.089	0.0079	88.9	43.6
5	5518	1000	0.116	0.0136	116.5	74.9
6	5260	1000	0.143	0.0205	143.1	107.7
7	5260	1000	0.167	0.0280	167.5	147.5
8	5260	1000	0.189	0.0359	189.5	188.8
9	5260	1000	0.209	0.0437	209.1	230.0
10	5260	1000	0.227	0.0513	226.6	270.0
11	4923	1000	0.242	0.0588	242.4	289.3
12	4923	1000	0.255	0.0652	255.3	320.8
13	4923	1000	0.265	0.0704	265.3	346.5
14	4923	1000	0.273	0.0743	272.6	365.9
15	4540	1000	0.278	0.0771	277.6	349.8
				$\sum$	2559	2762

a Assumed forces

b The displacement corresponding to the assumed forces

STEP 13 (Maximum Period Limit)

After referring to Table 4.22

C_t = 0.0466 (Concrete moment-resisting frame)

x = 0.9

h_n = number of storeys× storey's height = 15×3.40 = 51m

Apply previous values in Eq. 4.6, we get

$T_a = 0.0466 \times 51^{0.9} = 1.60$seconds

After referring to Table 4.21

$S_{D1} = 0.25$

Interpolation between S_{D1} equals 0.20 and S_{D1} equals 0.30, we get

$C_u = 1.45$

$C_u \times T_a = 1.45 \times 1.60 = 2.32$second > 2.09second OK

STEP 14 (Response Spectrum Graph)

The elastic and inelastic response spectrums for M15 model are created in the same way as previously stated and the resulted graphs are as shown in Figs. 4.17 and 4.18 respectively.

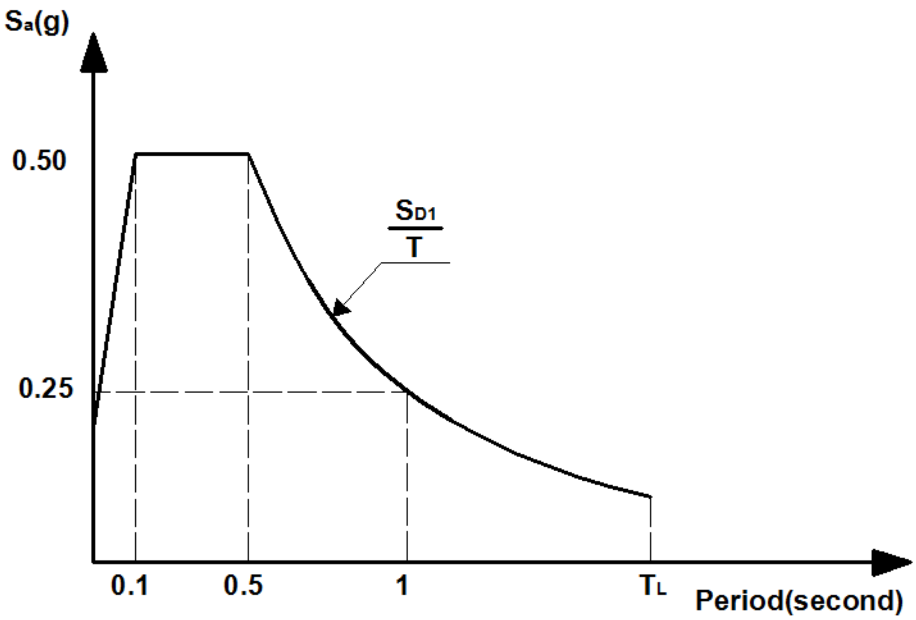

Figure 4.17 M15-Elastic Response Spectrum

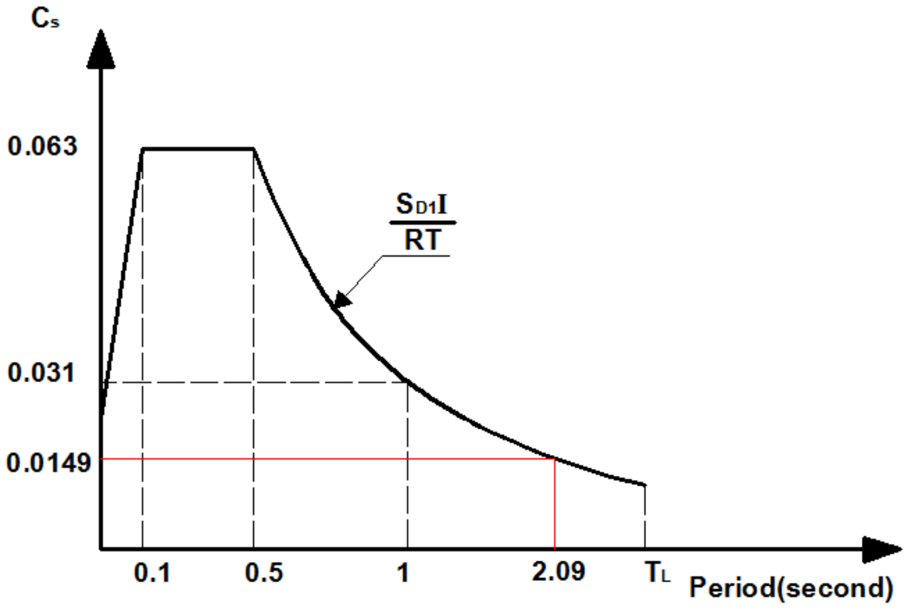

Figure 4.18 M15-Inelastic Response Spectrum

STEP 15 (Determination of Seismic Base Shear Using Equivalent Lateral Force Analysis)

The seismic base shear (V) in a given direction is determined by applying Eq. 4.9 as follows:

$$C_s \text{ is the minimum of } \begin{cases} \dfrac{S_{DS}\times I}{R} \\ \dfrac{S_{D1}\times I}{R\times T} \end{cases} = \begin{cases} \dfrac{0.50\times 1}{8} \\ \dfrac{0.25\times 1}{8\times 2.09} \end{cases} = \begin{cases} 0.063 \\ 0.0149 \end{cases} = 0.0149$$

By applying Eq. 4.9, we get:

V = 0.0149×78122= 1164kN

STEP 16 (Determination of Seismic Base Shear using Modal Response Spectrum Analysis)

The response spectrum was defined as for M5 model and the base shear (V) has been computed by using section cut at columns of ground floor and the result is as follows,

V = 1007kN

Table 4.49 summarizes the selection process for the appropriate base shear value based on ASCE 7 section 12.9.4.1

Table 4.49 M15-Base Shear Selection

Base shear using MRSA[1] (kN)	**Base shear using ELF[2] (kN)**	**0.85×ELF[2] (kN)**
1007	1164	989

1 Modal Response Spectrum Analysis
2 Equivalent Lateral Force

The base shear using modal response spectrum analysis is larger than 85 percent of the calculated base shear using equivalent lateral force procedure. Thus, base shear equals 1007kN.

STEP 17 (Vertical Distribution of Seismic Base Shear)

Seismic base shear distribution can be computed using SAP2000 by making section cut and reading the shear force from response analysis case at each level as shown in Table 4.50.

Table 4.50 M15-Base Shear Distribution on Floors

Floor	h(m)	Shear Force (kN)*	Force on each Floor (kN)
1	3.40	1007	14
2	6.80	993	39
3	10.2	954	53
4	13.6	901	52
5	17.0	849	46
6	20.4	803	44
7	23.8	759	45
8	27.2	714	45
9	30.6	669	46
10	34.0	623	51
11	37.4	572	61
12	40.8	511	75
13	44.2	436	105
14	47.6	331	151
15	51.0	180	180

* Verification is in appendix A

First-order moment and second-order moment are determined on all columns in all floors and they are annexed in appendix B and verified in appendix C. The critical column is tabulated in Table 4.51.

Table 4.51 Bending Moment Results for M15 Model on Critical Column

	First-Order Analysis	Second-Order Analysis	Percent Difference
Bending Moment (kN.m)	167.1	175.5	4.97%

Storey drifts and stability coefficients for model M15 are calculated in the same way as were calculated for model M5 and tabulated in Tables 4.52 and 4.53 respectively.

Table 4.52 M15 Drift Check

Level	δ_{xe} (mm)	δ_x (mm)	Δ (mm)	$\Delta_{Allowable}$ (mm)	Check
1	0.75	4.14	4.14	52	OK
2	2.40	13.19	9.04	52	OK
3	4.42	24.29	11.10	52	OK
4	6.56	36.06	11.77	52	OK
5	8.70	47.87	11.81	52	OK
6	10.85	59.69	11.82	52	OK
7	12.92	71.04	11.35	52	OK
8	14.88	81.86	10.82	52	OK
9	16.75	92.11	10.25	52	OK
10	18.51	101.82	9.71	52	OK
11	20.26	111.43	9.61	52	OK
12	21.82	120.02	8.59	52	OK
13	23.16	127.36	7.34	52	OK
14	24.20	133.12	5.76	52	OK
15	24.93	137.10	3.98	52	OK

Table 4.53 M15 Stability Coefficient

M15						
Level	**P_x (kN)**	**Δ (mm)**	**V_x (kN)**	**h_{sx} (mm)**	**C_d**	**θ**
1	93083	4.14	1007	3400	5.5	0.020
2	86593	9.04	993	3400	5.5	0.042
3	80103	11.1	954	3400	5.5	0.050
4	73613	11.77	901	3400	5.5	**0.051**
5	67123	11.81	849	3400	5.5	0.050
6	60633	11.82	803	3400	5.5	0.048
7	54401	11.35	759	3400	5.5	0.044
8	48170	10.82	714	3400	5.5	0.039
9	41938	10.25	669	3400	5.5	0.034
10	35707	9.71	623	3400	5.5	0.030
11	29475	9.61	572	3400	5.5	0.026
12	23580	8.59	511	3400	5.5	0.021
13	17685	7.34	436	3400	5.5	0.016
14	11790	5.76	331	3400	5.5	0.011
15	5130	3.98	180	3400	5.5	0.006

The P-Delta analysis is not required based on the stability coefficient which is less than 0.1. The maximum stability coefficient's value is very close to the percent difference between first and second-order analyses (Table 4.51) on the critical column. However, the stability coefficient gives more conservative result compared to the percent difference on the critical column.

4.2.4 Twenty-Storey model (M20)

M20 is a twenty-story reinforced concrete portal frame with fixed supports with a total height equals 68m. M20 has the same plan, material properties, section properties, story's height, live loads, and superimposed dead loads as M5 except number of stories and columns' sections. The columns' sections are shrunken to keep economical design as shown in Table 4.54. Elevation of M20 is illustrated in Fig. 4.19.

Table 4.54 M20-Columns' Sections

	Column	
Storey	**Depth (m)**	**Width (m)**
1-5	1.10	1.10
6-10	1.00	1.00
11-15	0.90	0.90
16-20	0.75	0.75

Parameters that can be used to determine the base shear using International Building Code 2015 (IBC 2015) in co-operation with ASCE 7 can be determined in the same way as M5 model. M20 has the same values as M5 from step 1 until step 10 as summarized in Table 4.36. The Calculations for the rest values are resumed from step 11.

STEP 11 (Effective Seismic Weight)

Each floor weight has determined in the same way as calculating M5 weights except for M20 model, the columns' sections are changing throughout the elevation. M20 columns' weights in each storey are determined and tabulated in Table 4.55. The weight of each storey can be determined as the sum of beams' weights, columns' weights, slab's weight, and superimposed dead loads. The last storey is exempted from half columns' weights as tabulated in Table 4.56.

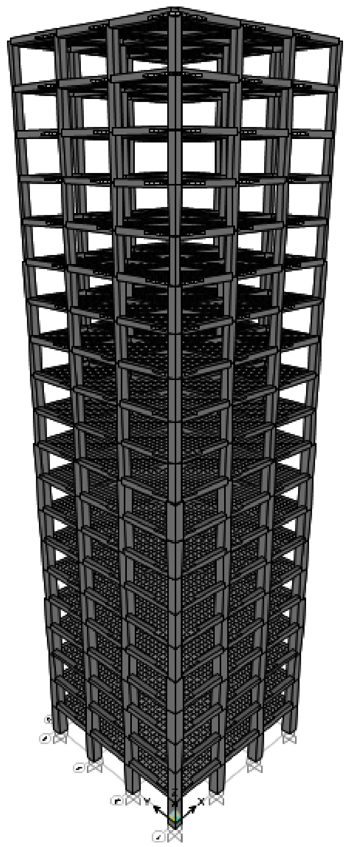

Figure 4.19 M20 Model in 3-D view

Table 4.55 M20-Columns Weight in each Storey

Storey	Number of Columns	Depth	Width	Length	Concrete Weight Per Unit Volume	Columns Weight
1-5	16	1.1m	1.1m	3.40m	25kN/m^3	1645kN
6-10	16	1.0m	1.0m	3.40m	25kN/m^3	1360kN
11-15	16	0.9m	0.9m	3.40m	25kN/m^3	1102kN
16-20	16	0.75m	0.75m	3.40m	25kN/m^3	765kN

Table 4.56 M20-Storeys' Weights

Storey	Weight (kN)
1	5803
2	5803
3	5803
4	5803
5	5803
6	5518
7	5518
8	5518
9	5518
10	5518
11	5260
12	5260
13	5260
14	5260
15	5260
16	4923
17	4923
18	4923
19	4923
20	4540
Total (kN)	107137

STEP 12 (Fundamental Period of the Structure)

The fundamental period of the structure (T) is determined from SAP2000, version 19.0.0 software analysis. For M20 model, the fundamental period equals 2.82second.

Verification on SAP2000 fundamental period

Rayleigh-Ritz method can be used for calculating an approximation to the fundamental period using Eq. 4.5 as shown in Table 4.57.

Table 4.57 M20-Verification on SAP2000 Fundamental Period

Storey	W_i(kN)	f_i (kN)[a]	δ_i(m)[b]	δ_i^2	$f_i\ \delta_i$	$W_i\ \delta i^2$
1	5803	1000	0.012	0.0001	12.2	0.9
2	5803	1000	0.040	0.0016	39.6	9.1
3	5803	1000	0.074	0.0055	74.2	32.0
4	5803	1000	0.112	0.0125	111.8	72.5
5	5803	1000	0.150	0.0225	149.9	130.4
6	5518	1000	0.188	0.0353	188.0	194.9
7	5518	1000	0.224	0.0504	224.5	278.0
8	5518	1000	0.259	0.0671	259.0	370.2
9	5518	1000	0.291	0.0850	291.5	468.9
10	5518	1000	0.322	0.1036	321.9	571.8
11	5260	1000	0.351	0.1229	350.6	646.7
12	5260	1000	0.377	0.1419	376.7	746.5
13	5260	1000	0.400	0.1602	400.3	842.8
14	5260	1000	0.421	0.1776	421.4	934.2
15	5260	1000	0.440	0.1939	440.3	1019.8
16	4923	1000	0.458	0.2095	457.7	1031.1
17	4923	1000	0.472	0.2228	472.0	1096.6
18	4923	1000	0.483	0.2337	483.4	1150.6
19	4923	1000	0.492	0.2423	492.2	1192.7
20	4540	1000	0.499	0.2486	498.6	1128.7
				$\sum$	6066	11918

a Assumed forces

b The displacement corresponding to the assumed forces

By applying Eq. 4.5 with Table 4.57

T = 2.81 second

% error = $\frac{\text{Approximated Period} - \text{SAP Period}}{\text{SAP Period}}$ ×100% = 0.35% $< 10\%$

Acceptable

STEP 13 (Maximum Period Limit)

After referring to Table 4.22

C_t = 0.0466 (Concrete moment-resisting frame)

x = 0.9

h_n = number of storeys× storey's height = 20×3.40 = 68m

Apply previous values in Eq. 4.6, we get

$T_a = 0.0466 \times 68^{0.9} = 2.07$seconds

After referring to Table 4.21

$S_{D1} = 0.25$

Interpolation between S_{D1} equals 0.20 and S_{D1} equals 0.30, we get

$C_u = 1.45$

$C_u \times T_a = 1.45 \times 2.07 = 3.0$second $>$ 2.82second OK

STEP 14 (Response Spectrum Graph)

The elastic and inelastic response spectrums for M20 model are created in the same way as creating the response spectrums for previous models as shown in Figs. 4.20 and 4.21 respectively.

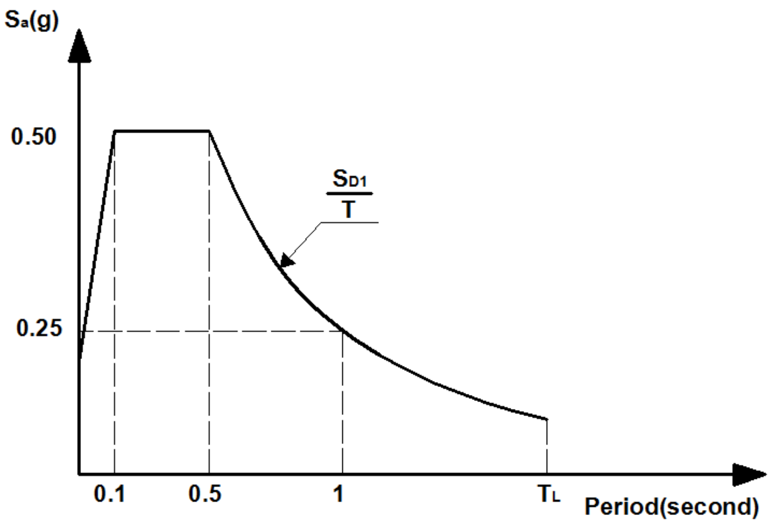

Figure 4.20 M20-Elastic Response Spectrum

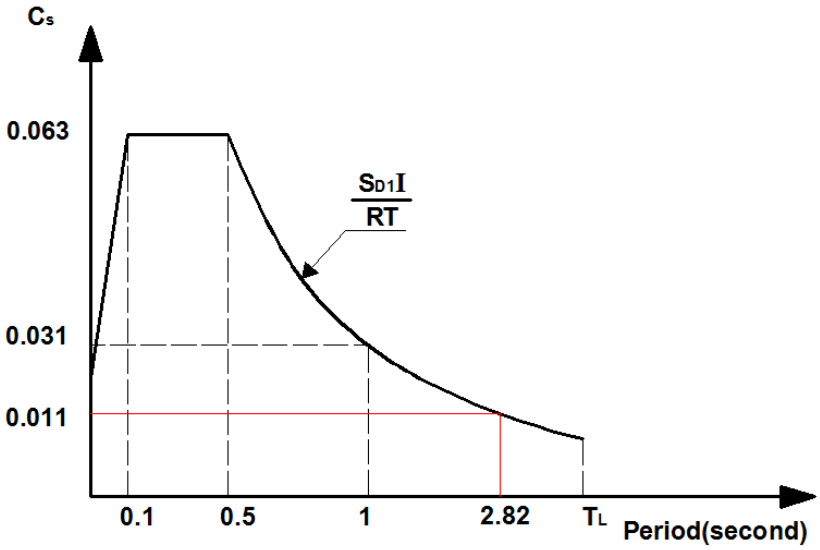

Figure 4.21 M20-Inelastic Response Spectrum

STEP 15 (Determination of Seismic Base Shear Using Equivalent Lateral Force Analysis)

The seismic base shear (V) in a given direction is determined by applying Eq. 4.9 as follows:

$$C_s \text{ is the minimum of } \begin{cases} \dfrac{S_{DS}\times I}{R} \\ \dfrac{S_{D1}\times I}{R\times T} \end{cases} = \begin{cases} \dfrac{0.50\times 1}{8} \\ \dfrac{0.25\times 1}{8\times 2.82} \end{cases} = \begin{cases} 0.063 \\ 0.011 \end{cases} = 0.011$$

By applying Eq. 4.9, we get:

V = 0.011×107137= 1178kN

STEP 16 (Determination of Seismic Base Shear using Modal Response Spectrum Analysis)

The response spectrum was defined as for M5 model and the base shear (V) has been computed by using section cut at columns of ground floor and the result is as follows,

V = 1030kN

Table 4.58 summarizes the selection process for the appropriate base shear value based on ASCE 7 section 12.9.4.1

Table 4.58 M20-Base Shear Selection

Base shear using MRSA[1] (kN)	Base shear using ELF[2] (kN)	0.85×ELF[2] (kN)
1030	1178	1001

1 Modal Response Spectrum Analysis
2 Equivalent Lateral Force

The base shear using modal response spectrum analysis is larger than 85 percent of the calculated base-shear using equivalent lateral force procedure. Thus, the base shear equals 1030kN.

STEP 17 (Vertical Distribution of Seismic Base Shear)

Seismic base shear distribution can be computed using SAP2000 by making section cut and reading the shear force from response analysis case at each level as shown in Table 4.59.

Table 4.59 M20-Base Shear Distribution on Floors

Floor	h(m)	Shear Force (kN)*	Force on each Floor (kN)
1	3.40	1030	10
2	6.80	1020	27
3	10.2	993	41
4	13.6	952	45
5	17.0	907	38
6	20.4	869	31
7	23.8	838	28
8	27.2	810	31
9	30.6	779	36
10	34.0	743	38
11	37.4	705	38
12	40.8	667	39
13	44.2	628	43
14	47.6	585	45
15	51.0	540	43
16	54.4	497	46
17	57.8	451	66
18	61.2	385	98
19	64.6	287	135
20	68.0	152	152

*Verification is in appendix A

First-order moment and second-order moment are determined on all columns in all floors and they are annexed in appendix B and verified in appendix C. The critical column is tabulated in Table 4.60.

Table 4.60 Bending Moment Results for M20 Model on Critical Column

	First-Order Analysis	Second-Order Analysis	Percent Difference
Bending Moment (kN.m)	165.9	178.1	7.35%

Storey drifts and stability coefficients for model M20 are calculated in the same way as were calculated for model M5 and tabulated in Tables 4.61 and 4.62 respectively.

Table 4.61 M20 Drift Check

Level	**δ_{xe} (mm)**	**δ_x (mm)**	**Δ (mm)**	**$\Delta_{Allowable}$ (mm)**	**Check**
1	0.66	3.61	3.61	52	OK
2	2.16	11.87	8.27	52	OK
3	4.09	22.48	10.61	52	OK
4	6.21	34.16	11.67	52	OK
5	8.40	46.22	12.06	52	OK
6	10.64	58.52	12.30	52	OK
7	12.85	70.69	12.17	52	OK
8	15.02	82.60	11.92	52	OK
9	17.13	94.21	11.61	52	OK
10	19.18	105.48	11.26	52	OK
11	21.19	116.56	11.09	52	OK
12	23.12	127.15	10.58	52	OK
13	24.95	137.21	10.07	52	OK
14	26.68	146.74	9.53	52	OK
15	28.32	155.76	9.02	52	OK
16	29.95	164.70	8.94	52	OK
17	31.42	172.79	8.09	52	OK
18	32.69	179.78	6.99	52	OK
19	33.70	185.35	5.56	52	OK
20	34.42	189.33	3.99	52	OK

Table 4.62 M20 Stability Coefficient

M20						
Level	**P_x (kN)**	**Δ (mm)**	**V_x (kN)**	**h_{sx} (mm)**	**C_d**	**θ**
1	126961	3.61	1030	3400	5.5	0.024
2	120185	8.27	1020	3400	5.5	0.052
3	113410	10.61	993	3400	5.5	0.065
4	106634	11.67	952	3400	5.5	0.070
5	99858	12.06	907	3400	5.5	**0.071**
6	93083	12.3	869	3400	5.5	0.070
7	86593	12.17	838	3400	5.5	0.067
8	80103	11.92	810	3400	5.5	0.063
9	73613	11.61	779	3400	5.5	0.059
10	67123	11.26	743	3400	5.5	0.054
11	60633	11.09	705	3400	5.5	0.051
12	54401	10.58	667	3400	5.5	0.046
13	48170	10.07	628	3400	5.5	0.041
14	41938	9.53	585	3400	5.5	0.037
15	35707	9.02	540	3400	5.5	0.032
16	29475	8.94	497	3400	5.5	0.028
17	23580	8.09	451	3400	5.5	0.023
18	17685	6.99	385	3400	5.5	0.017
19	11790	5.56	287	3400	5.5	0.012
20	5130	3.99	152	3400	5.5	0.007

The P-Delta analysis is not required based on the stability coefficient which is less than 0.1. The maximum stability coefficient's value is very close to the percent difference between first and second-order analyses (Table 4.60) on the critical column. However, the stability coefficient starts to give unconservative result compared to the percent difference on the critical column.

4.2.5 Twenty Five-Storey model (M25)

M25 is a twenty five-storey reinforced concrete portal frame with fixed supports with a total height equals 85m. M25 has the same plan, material properties, section properties, story's height, live loads, and superimposed dead loads as M5 except number of stories and columns' sections. The columns' sections are shrunken to keep economical design as shown in Table 4.63. Elevation of M25 is illustrated in Fig. 4.22.

Table 4.63 M25-Columns' Sections

	Column	
Storey	**Depth (m)**	**Width (m)**
1-5	1.20	1.20
6-10	1.10	1.10
11-15	1.00	1.00
16-20	0.90	0.90
21-25	0.75	0.75

Parameters that can be used to determine the base shear using International Building Code 2015 (IBC 2015) in co-operation with ASCE7-10 can be determined in the same way as M5 model. M25 has the same values as M5 from step 1 until step 10 as summarized in Table 4.36. The Calculations for the remaining values are resumed from step 11.

STEP 11 (Effective Seismic Weight)

Each floor weight has determined in the same way as calculating M5 weights except for M25 model, the columns' sections are changing throughout the elevation. M25 columns' weights in each storey are determined and tabulated in Table 4.64. The weight of each story can be determined as the sum of beams' weights, columns' weights, slab's weight, and superimposed dead loads. The last storey is exempted from half columns' weights as tabulated in Table 4.65.

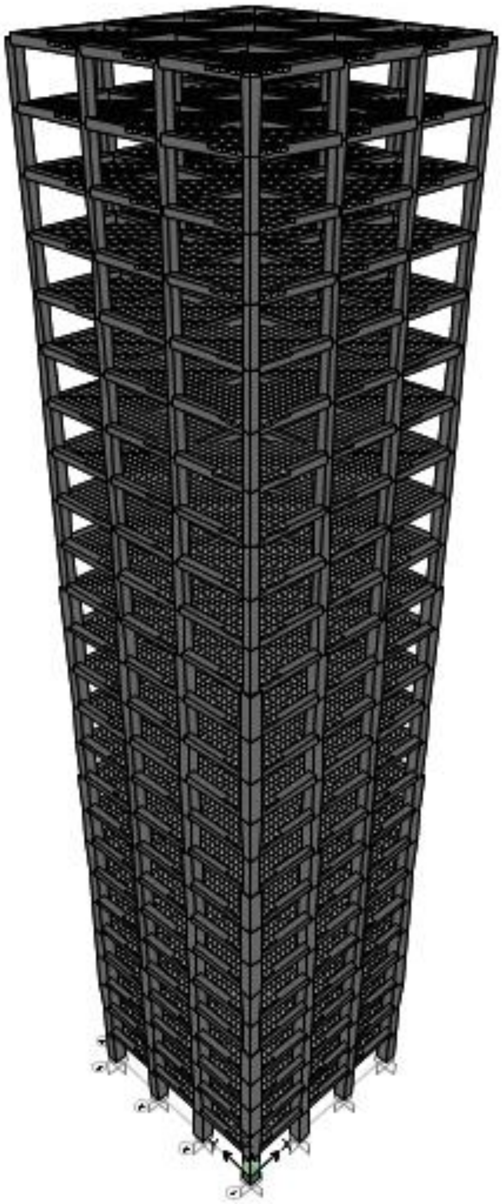

Figure 4.22 M25 Model in 3-D view

Table 4.64 M25-Columns Weight in each Storey

Storey	Number of Columns	Depth	Width	Length	Concrete Weight Per Unit Volume	Columns Weight
1-5	16	1.2m	1.2m	3.40m	$25kN/m^3$	1958kN
6-10	16	1.1m	1.1m	3.40m	$25kN/m^3$	1645kN
11-15	16	1.0m	1.0m	3.40m	$25kN/m^3$	1360kN
16-20	16	0.9m	0.9m	3.40m	$25kN/m^3$	1102kN
21-25	16	0.75m	0.75m	3.40m	$25kN/m^3$	765kN

Table 4.65 M25-Storeys' Weights

Storey	Weight (kN)
1	6116
2	6116
3	6116
4	6116
5	6116
6	5803
7	5803
8	5803
9	5803
10	5803
11	5518
12	5518
13	5518
14	5518
15	5518
16	5260
17	5260
18	5260
19	5260
20	5260
21	4923
22	4923
23	4923
24	4923
25	4540
Total (kN)	137717

STEP 12 (Fundamental Period of the Structure)

The fundamental period of the structure (T) is determined from SAP2000, version 19.0.0 software analysis. For M25 model, the fundamental period equals 3.57second.

Verification on SAP2000 fundamental period:

Rayleigh-Ritz method can be used for calculating an approximation to the fundamental period using Eq. 4.5 as shown in Table 4.66.

Table 4.66 M25-Verification on SAP2000 Fundamental Period

Storey	W_i(kN)	f_i (kN)[a]	δ_i(m)[b]	δ_i^2	$f_i\ \delta_i$	$W_i\ \delta i^2$
1	6116	1000	0.013	0.0002	13.1	1.1
2	6116	1000	0.044	0.0019	44.0	11.8
3	6116	1000	0.085	0.0071	84.5	43.7
4	6116	1000	0.130	0.0169	129.9	103.2
5	6116	1000	0.177	0.0315	177.4	192.5
6	5803	1000	0.226	0.0510	225.9	296.1
7	5803	1000	0.274	0.0749	273.7	434.8
8	5803	1000	0.320	0.1026	320.3	595.3
9	5803	1000	0.365	0.1334	365.2	773.9
10	5803	1000	0.408	0.1667	408.3	967.5
11	5518	1000	0.450	0.2024	449.9	1117.1
12	5518	1000	0.489	0.2393	489.2	1320.4
13	5518	1000	0.526	0.2768	526.1	1527.2
14	5518	1000	0.561	0.3144	560.7	1734.8
15	5518	1000	0.593	0.3519	593.2	1941.5
16	5260	1000	0.624	0.3892	623.9	2047.4
17	5260	1000	0.652	0.4251	652.0	2235.8
18	5260	1000	0.677	0.4590	677.5	2414.4
19	5260	1000	0.701	0.4908	700.6	2581.7
20	5260	1000	0.721	0.5205	721.4	2737.8
21	4923	1000	0.741	0.5487	740.7	2701.2
22	4923	1000	0.757	0.5730	757.0	2821.1
23	4923	1000	0.770	0.5935	770.4	2922.0
24	4923	1000	0.781	0.6102	781.1	3003.8
25	4540	1000	0.790	0.6233	789.5	2829.9
	137717			$\sum$	11876	37356

a Assumed forces

b The displacement corresponding to the assumed forces

By applying Eq. 4.5 with Table 4.58

T = 3.56 second

% error = $\frac{\text{Approximated Period} - \text{SAP Period}}{\text{SAP Period}}$ ×100% = 0.28% $< 10\%$

Acceptable

STEP 13 (Maximum Period Limit)

After referring to Table 4.22

C_t = 0.0466 (Concrete moment-resisting frame)

x = 0.9

h_n = number of storeys× storey's height = 25×3.40 = 85m

Apply previous values in Eq. 4.6, we get

$T_a = 0.0466 \times 85^{0.9} = 2.54$seconds

After referring to Table 4.21

$S_{D1} = 0.25$

Interpolation between S_{D1} equals 0.20 and S_{D1} equals 0.30, we get

$C_u = 1.45$

$C_u \times T_a = 1.45 \times 2.54 = 3.68$second > 3.57second OK

STEP 14 (Response Spectrum Graph)

The elastic and inelastic response spectrums for M25 model are created in the same way as creating the response spectrums for previous models as shown in Figs. 4.23 and 4.24 respectively.

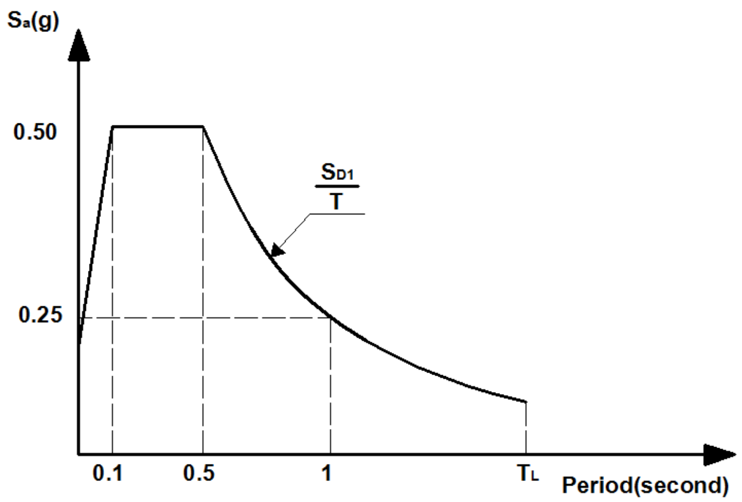

Figure 4.23 M25-Elastic Response Spectrum

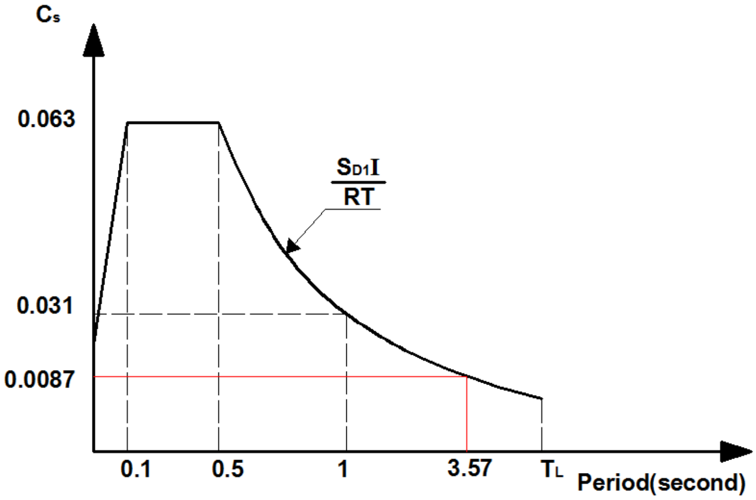

Figure 4.24 M25-Inelastic Response Spectrum

STEP 15 (Determination of Seismic Base Shear Using Equivalent Lateral Force Analysis)

The seismic base shear (V) in a given direction is determined by applying Eq. 4.9 as follows:

$$C_s \text{ is the minimum of } \begin{cases} \dfrac{S_{DS}\times I}{R} \\ \dfrac{S_{D1}\times I}{R\times T} \end{cases} = \begin{cases} \dfrac{0.50\times 1}{8} \\ \dfrac{0.25\times 1}{8\times 3.57} \end{cases} = \begin{cases} 0.063 \\ 0.0087 \end{cases} = 0.0087$$

By applying Eq. 4.9, we get:

V = 0.0087×137717 = 1198kN

STEP 16 (Determination of Seismic Base Shear using Modal Response Spectrum Analysis)

The response spectrum function was defined as for M5 model and the base shear (V) has been computed by using section cut at columns of ground floor and the result is as follows,

V = 1044kN

Table 4.67 summarizes the selection process for the appropriate base shear value based on ASCE 7 section 12.9.4.1

Table 4.67 M25-Base Shear Selection

Base shear using MRSA[1] (kN)	Base shear using ELF[2] (kN)	0.85×ELF[2] (kN)
1044	1198	1018

1 Modal Response Spectrum Analysis
2 Equivalent Lateral Force

The base shear using modal response spectrum analysis is larger than 85 percent of the calculated base-shear using equivalent lateral force procedure. Thus, the base shear equals 1044kN.

STEP 17 (Vertical Distribution of Seismic Base Shear)

Seismic base shear distribution can be computed using SAP2000 by making section cut and reading the shear force from response analysis case at each level as shown in Table 4.68.

Table 4.68 M25-Base Shear Distribution on Floors

Floor	h(m)	Shear Force (kN)*	Force on each Floor (kN)
1	3.40	1044	6
2	6.80	1038	19
3	10.2	1019	32
4	13.6	987	39
5	17.0	948	37
6	20.4	911	31
7	23.8	880	23
8	27.2	857	22
9	30.6	835	23
10	34.0	812	28
11	37.4	784	31
12	40.8	753	31
13	44.2	722	29
14	47.6	693	28
15	51.0	665	30
16	54.4	635	34
17	57.8	601	38
18	61.2	563	39
19	64.6	524	36
20	68.0	488	34
21	71.4	454	44
22	74.8	410	65
23	78.2	345	94
24	81.6	251	121
25	85.0	130	130

*Verification is in appendix A

First-order moment and second-order moment are determined on all columns in all floors and they are annexed in appendix B and verified in appendix C. The critical column is tabulated in Table 4.69.

Table 4.69 Bending Moment Results for M25 Model on Critical Column

	First-Order Analysis	Second-Order Analysis	Percent Difference
Bending Moment (kN.m)	195.8	215.0	9.82%

Storey drifts and stability coefficients for model M25 are calculated in the same way as were calculated for model M5 and tabulated in Tables 4.70 and 4.71 respectively.

Table 4.70 M25 Drift Check

Level	δ_{xe} (mm)	δ_x (mm)	Δ (mm)	$\Delta_{Allowable}$ (mm)	Check
1	0.57	3.15	3.15	52	OK
2	1.94	10.66	7.50	52	OK
3	3.75	20.63	9.97	52	OK
4	5.80	31.93	11.30	52	OK
5	7.98	43.88	11.95	52	OK
6	10.23	56.24	12.36	52	OK
7	12.49	68.68	12.44	52	OK
8	14.74	81.06	12.38	52	OK
9	16.96	93.31	12.24	52	OK
10	19.16	105.38	12.07	52	OK
11	21.34	117.36	11.99	52	OK
12	23.46	129.04	11.68	52	OK
13	25.52	140.39	11.35	52	OK
14	27.53	151.40	11.02	52	OK
15	29.47	162.11	10.71	52	OK
16	31.40	172.67	10.56	52	OK
17	33.23	182.79	10.11	52	OK
18	34.99	192.43	9.64	52	OK
19	36.65	201.59	9.17	52	OK
20	38.24	210.33	8.73	52	OK
21	39.82	219.02	8.69	52	OK
22	41.26	226.93	7.91	52	OK
23	42.51	233.79	6.86	52	OK
24	43.51	239.31	5.52	52	OK
25	44.26	243.42	4.10	52	OK

Table 4.71 M25 Stability Coefficient

M25						
Level	**P_x (kN)**	**Δ (mm)**	**V_x (kN)**	**h_{sx} (mm)**	**C_d**	**θ**
1	162403	3.15	1044	3400	5.5	0.026
2	155315	7.5	1038	3400	5.5	0.060
3	148226	9.97	1019	3400	5.5	0.078
4	141138	11.3	987	3400	5.5	0.086
5	134049	11.95	948	3400	5.5	0.090
6	126961	12.36	911	3400	5.5	**0.092**
7	120185	12.44	880	3400	5.5	0.091
8	113410	12.38	857	3400	5.5	0.088
9	106634	12.24	835	3400	5.5	0.084
10	99858	12.07	812	3400	5.5	0.079
11	93083	11.99	784	3400	5.5	0.076
12	86593	11.68	753	3400	5.5	0.072
13	80103	11.35	722	3400	5.5	0.067
14	73613	11.02	693	3400	5.5	0.063
15	67123	10.71	665	3400	5.5	0.058
16	60633	10.56	635	3400	5.5	0.054
17	54401	10.11	601	3400	5.5	0.049
18	48170	9.64	563	3400	5.5	0.044
19	41938	9.17	524	3400	5.5	0.039
20	35707	8.73	488	3400	5.5	0.034
21	29475	8.69	454	3400	5.5	0.030
22	23580	7.91	410	3400	5.5	0.024
23	17685	6.86	345	3400	5.5	0.019
24	11790	5.52	251	3400	5.5	0.014
25	5130	4.1	130	3400	5.5	0.009

The P-Delta analysis is not required based on the stability coefficient which is less than 0.1. The maximum stability coefficient's value is very close to the percent difference between first and second-order analyses (Table 4.69) on the critical column. However, the stability coefficient gives slightly unconservative result compared to the percent difference on the critical column.

4.2.6 Thirty-Storey model (M30)

M30 is a thirty-story reinforced concrete portal frame with fixed supports with a total height equals 102m. M30 has the same plan, material properties, section properties, story's height, live loads, and superimposed dead loads as M5 except number of stories and columns' sections. The columns' sections are shrunken to keep economical design as shown in Table 4.72. Elevation of M30 is illustrated in Fig. 4.25.

Table 4.72 M30-Columns' Sections

	Column	
Storey	**Depth (m)**	**Width (m)**
1-5	1.3	1.3
6-10	1.2	1.2
11-15	1.1	1.1
16-20	1.0	1.0
21-25	0.9	0.9
26-30	0.75	0.75

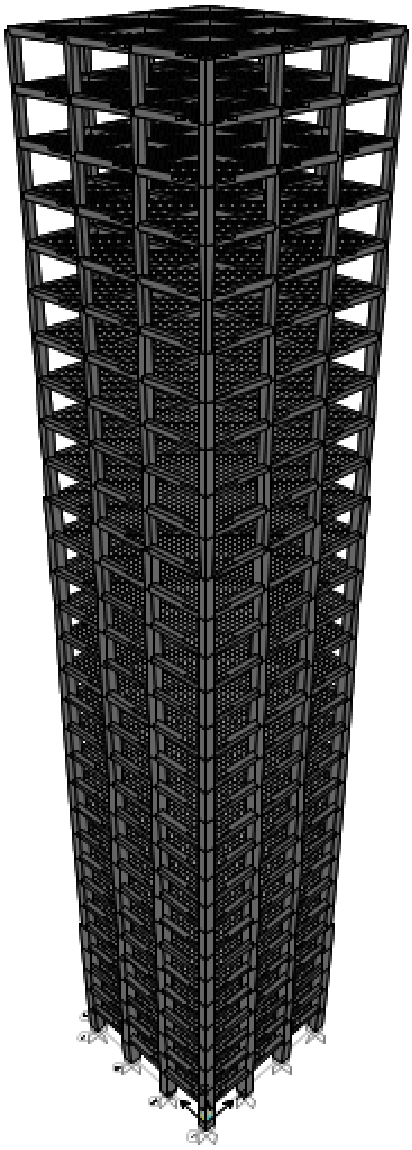

Figure 4.25 M30 Model in 3-D view

Parameters that can be used to determine the base shear using International Building Code 2015 (IBC 2015) in co-operation with ASCE7-10 can be determined in the same way as M5 model. M30 has the same values as M5 from step 1 until step 10 as summarized in Table 4.36. The Calculations for the rest values are resumed from step 11.

STEP 11 (Effective Seismic Weight)

Each floor weight has determined in the same way as calculating M5 weights except for M30 model, the columns' sections are changing throughout the elevation. M30 columns' weights in each storey are determined and tabulated in Table 4.73. The weight of each storey can be determined as the sum of beams' weights, columns' weights, slab's weight, and superimposed dead loads. The last story is exempted from half columns' weights as tabulated in Table 4.74.

Table 4.73 M30-Columns Weight in each Storey

Storey	**Number of Columns**	**Depth**	**Width**	**Length**	**Concrete Weight Per Unit Volume**	**Columns Weight**
1-5	16	1.3m	1.3m	3.40m	$25kN/m^3$	2298kN
6-10	16	1.2m	1.2m	3.40m	$25kN/m^3$	1958kN
11-15	16	1.1m	1.1m	3.40m	$25kN/m^3$	1645kN
16-20	16	1.0m	1.0m	3.40m	$25kN/m^3$	1360kN
21-25	16	0.9m	0.9m	3.40m	$25kN/m^3$	1102kN
26-30	16	0.75m	0.75m	3.40m	$25kN/m^3$	765kN

Table 4.74 M30-Storeys' Weights

Storey	Weight (kN)
1	6456
2	6456
3	6456
4	6456
5	6456
6	6116
7	6116
8	6116
9	6116
10	6116
11	5803
12	5803
13	5803
14	5803
15	5803
16	5518
17	5518
18	5518
19	5518
20	5518
21	5260
22	5260
23	5260
24	5260
25	5260
26	4923
27	4923
28	4923
29	4923
30	4540
Total (kN)	169997

STEP 12 (Fundamental Period of the Structure)

The fundamental period of the structure (T) is determined from SAP2000, version 19.0.0 software analysis. For M30 model, the fundamental period equals 4.33second.

Verification on SAP2000 fundamental period:

Rayleigh-Ritz method can be used for calculating an approximation to the fundamental period using Eq. 4.5 as shown in Table 4.75.

Table 4.75 M30-Verification on SAP2000 Fundamental Period

Storey	W_i(kN)	f_i (kN)[a]	δ_i(m)[b]	δ_i^2	$f_i\ \delta_i$	$W_i\ \delta i^2$
1	6456	1000	0.014	0.0002	13.7	1.2
2	6456	1000	0.047	0.0022	47.0	14.3
3	6456	1000	0.092	0.0085	92.1	54.8
4	6456	1000	0.144	0.0207	144.0	133.9
5	6456	1000	0.200	0.0398	199.6	257.1
6	6116	1000	0.257	0.0662	257.4	405.1
7	6116	1000	0.316	0.0997	315.7	609.5
8	6116	1000	0.374	0.1395	373.5	853.2
9	6116	1000	0.430	0.1851	430.3	1132.2
10	6116	1000	0.486	0.2359	485.7	1442.6
11	5803	1000	0.540	0.2914	539.8	1691.0
12	5803	1000	0.592	0.3503	591.9	2032.9
13	5803	1000	0.642	0.4120	641.8	2390.6
14	5803	1000	0.690	0.4757	689.7	2760.5
15	5803	1000	0.736	0.5411	735.6	3140.0
16	5518	1000	0.780	0.6081	779.8	3355.8
17	5518	1000	0.822	0.6750	821.6	3724.9
18	5518	1000	0.861	0.7413	861.0	4090.7
19	5518	1000	0.898	0.8066	898.1	4450.7
20	5518	1000	0.933	0.8705	933.0	4803.6
21	5260	1000	0.966	0.9335	966.2	4910.4
22	5260	1000	0.997	0.9934	996.7	5225.5
23	5260	1000	1.025	1.0500	1024.7	5522.9
24	5260	1000	1.050	1.1030	1050.2	5801.5
25	5260	1000	1.074	1.1524	1073.5	6061.7
26	4923	1000	1.095	1.1995	1095.2	5905.3
27	4923	1000	1.114	1.2408	1113.9	6108.7
28	4923	1000	1.130	1.2764	1129.8	6283.7
29	4923	1000	1.143	1.3063	1142.9	6430.8
30	4540	1000	1.154	1.3311	1153.7	6043.2
				$\sum$	20598	95638

a Assumed forces

b The displacement corresponding to the assumed forces

By applying Eq. 4.5 with Table 4.75

T = 4.32 second

% error = $\frac{\text{Approximated Period}-\text{SAP Period}}{\text{SAP Period}}$ ×100% = 0.23% $<$ 10% OK

STEP 13 (Maximum Period Limit)

After referring to Table 4.22

C_t = 0.0466 (Concrete moment-resisting frame)

x = 0.9

h_n = number of storeys× storey's height = 30×3.40 = 102m

Apply previous values in Eq. 4.6, we get

$T_a = 0.0466\times102^{0.9}$ = 3.0seconds

After referring to Table 4.21

S_{D1} = 0.25

Interpolation between S_{D1} equals 0.20 and S_{D1} equals 0.30, we get

C_u = 1.45

$C_u\times T_a$ = 1.45×3.0 = 4.35second $>$ 4.33second   OK

STEP 14 (Response Spectrum Graph)

The elastic and inelastic response spectrums for M30 model are created in the same way as creating the response spectrums for previous models as shown in Figs. 4.26 and 4.27 respectively.

STEP 15 (Determination of Seismic Base Shear Using Equivalent Lateral Force Analysis)

The seismic base shear (V) in a given direction is determined by applying Eq. 4.9 as follows:

$C_s = 0.0067$

By applying Eq. 4.9, we get:

$V = 0.0067 \times 169997 = 1140kN$

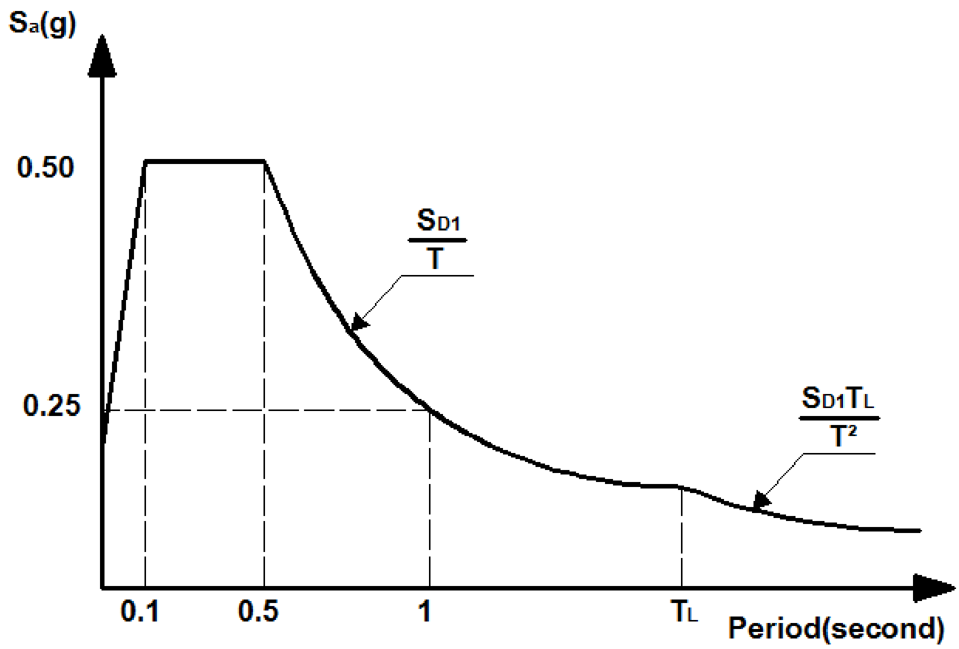

Figure 4.26 M30-Elastic Response Spectrum

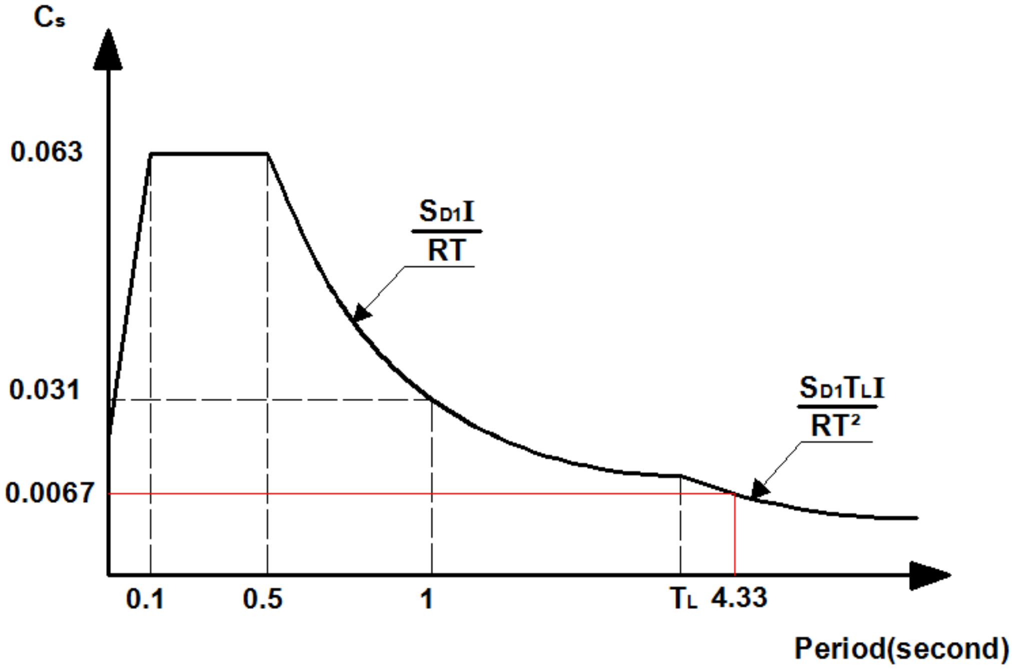

Figure 4.27 M30-Inelastic Response Spectrum

STEP 16 (Determination of Seismic Base Shear using Modal Response Spectrum Analysis)

The response spectrum function was defined as for M5 model and the base shear (V) has been computed by using section cut at columns of ground floor and the result is as follows,

V = 1005kN

Table 4.76 summarizes the selection process for the appropriate base shear value based on ASCE 7 section 12.9.4.1

Table 4.76 M30-Base Shear Selection

Base shear using MRSA[1] (kN)	Base shear using ELF[2] (kN)	0.85×ELF[2] (kN)
1005	1140	969

1 Modal Response Spectrum Analysis
2 Equivalent Lateral Force

The base shear using modal response spectrum analysis is larger than 85 percent of the calculated base shear using equivalent lateral force procedure. Thus, the base shear equals 1005kN.

STEP 17 (Vertical Distribution of Seismic Base Shear)

Seismic base shear distribution can be computed using SAP2000 by making section cut and reading the shear force from response analysis case at each level as shown in Table 4.77.

Table 4.77 M30-Base Shear Distribution on Floors

*

Floor	h(m)	Shear Force (kN)*	Force on each Floor (kN)
1	3.40	1005	5
2	6.80	1000	14
3	10.2	986	25
4	13.6	961	32
5	17.0	929	35
6	20.4	894	32
7	23.8	862	26
8	27.2	836	20
9	30.6	816	17
10	34.0	799	16
11	37.4	783	21
12	40.8	762	24
13	44.2	738	26
14	47.6	712	25
15	51.0	687	21
16	54.4	666	17
17	57.8	649	16
18	61.2	633	20
19	64.6	613	25
20	68.0	588	30
21	71.4	558	32
22	74.8	526	31
23	78.2	495	27
24	81.6	468	26
25	85.0	442	30
26	88.4	412	44
27	91.8	368	64
28	95.2	304	87
29	98.6	217	106
30	102	111	111

Verification is in appendix A

First-order moment and second-order moment are determined on all columns in all floors and they are annexed in appendix B and verified in appendix C. The critical column is tabulated in Table 4.78.

Table 4.78 Bending Moment Results for M30 Model on Critical Column

	First-Order Analysis	Second-Order Analysis	Percent Difference
Bending Moment (kN.m)	183.5	206.3	12.40%

Storey drifts and stability coefficients for model M30 are calculated in the same way as were calculated for model M5 and tabulated in Tables 4.79 and 4.80 respectively.

Table 4.79 M30 Drift Check

Level	δ_{xe} (mm)	δ_x (mm)	Δ (mm)	$\Delta_{Allowable}$ (mm)	Check
1	0.48	2.63	2.63	52	OK
2	1.65	9.09	6.45	52	OK
3	3.26	17.91	8.82	52	OK
4	5.12	28.14	10.23	52	OK
5	7.12	39.16	11.03	52	OK
6	9.22	50.72	11.56	52	OK
7	11.37	62.52	11.79	52	OK
8	13.52	74.37	11.85	52	OK
9	15.67	86.20	11.83	52	OK
10	17.81	97.96	11.76	52	OK
11	19.95	109.71	11.75	52	OK
12	22.05	121.30	11.59	52	OK
13	24.12	132.69	11.39	52	OK
14	26.16	143.86	11.18	52	OK
15	28.15	154.84	10.98	52	OK
16	30.14	165.75	10.91	52	OK
17	32.08	176.45	10.70	52	OK
18	33.99	186.94	10.49	52	OK
19	35.85	197.19	10.25	52	OK
20	37.67	207.19	10.00	52	OK
21	39.47	217.06	9.87	52	OK
22	41.19	226.54	9.48	52	OK
23	42.84	235.64	9.10	52	OK
24	44.43	244.37	8.73	52	OK
25	45.96	252.77	8.40	52	OK
26	47.48	261.15	8.38	52	OK
27	48.87	268.78	7.64	52	OK
28	50.08	275.43	6.65	52	OK
29	51.06	280.85	5.42	52	OK
30	51.82	285.00	4.16	52	OK

Table 4.80 M30 Stability Coefficient

M30						
Level	**P_x (kN)**	**Δ (mm)**	**V_x (kN)**	**h_{sx} (mm)**	**C_d**	**θ**
1	199545	2.63	1005	3400	5.5	0.028
2	192117	6.45	1000	3400	5.5	0.066
3	184688	8.82	986	3400	5.5	0.088
4	177260	10.23	961	3400	5.5	0.101
5	169831	11.03	929	3400	5.5	0.108
6	162403	11.56	894	3400	5.5	0.112
7	155315	11.79	862	3400	5.5	**0.114**
8	148226	11.85	836	3400	5.5	0.112
9	141138	11.83	816	3400	5.5	0.109
10	134049	11.76	799	3400	5.5	0.106
11	126961	11.75	783	3400	5.5	0.102
12	120185	11.59	762	3400	5.5	0.098
13	113410	11.39	738	3400	5.5	0.094
14	106634	11.18	712	3400	5.5	0.090
15	99858	10.98	687	3400	5.5	0.085
16	93083	10.91	666	3400	5.5	0.082
17	86593	10.7	649	3400	5.5	0.076
18	80103	10.49	633	3400	5.5	0.071
19	73613	10.25	613	3400	5.5	0.066
20	67123	10	588	3400	5.5	0.061
21	60633	9.87	558	3400	5.5	0.057
22	54401	9.48	526	3400	5.5	0.052
23	48170	9.1	495	3400	5.5	0.047
24	41938	8.73	468	3400	5.5	0.042
25	35707	8.4	442	3400	5.5	0.036
26	29475	8.38	412	3400	5.5	0.032
27	23580	7.64	368	3400	5.5	0.026
28	17685	6.65	304	3400	5.5	0.021
29	11790	5.42	217	3400	5.5	0.016
30	5130	4.16	111	3400	5.5	0.010

The P-Delta analysis is required based on the stability coefficient which is larger than 0.1 which is assured by the percent difference between first-order and second order analyses on the critical column also is larger than 0.1.The maximum stability coefficient's value is very close to the percent difference between first and second-order analyses (Table 4.78) on the critical column. However, the stability coefficient gives unconservative result compared to the percent difference on the critical column.

4.3 Multi-Storey Effect on P-Delta Analysis with Fundamental Period does not Abide by the Proposed Equation

In previous section, P-Delta effect on six models with different number of storeys was investigated taking into account that theirs fundamental periods are less than the proposed equation limit (Eq. 4.6). In this section, P-Delta effect on the same first three models is investigated taking into account that theirs fundamental periods are greater than the maximum proposed limit. To achieve this condition; the previous three models are investigated with the beam's section is switched to a smaller section which is 0.4m and 0.60m in depth and width respectively. Furthermore, columns have gotten smaller which is addressed in every model. The models are TM5, TM10 and TM15. For instance, TM5 refers to five-storey model with fundamental period greater the maximum proposed limit. It is worth mentioning that all other parameters are kept the same as previous models except beam's section and columns' sections are changed (for example TM5 is the same as M5 except the beam's section and columns' sections have gotten smaller). The bending moment from first-order analysis and second-order analysis are determined on all columns in all floors and the critical column is adopted.

4.3.1 Five-Storey model (TM5)

TM5's columns are 0.6m square section. In order to avoid repeating the same description of the model, refer to section 4.2.1 for more information about this model. It has the same results until step10; the calculations are continued from step11 as follows:

STEP 11 (Effective Seismic Weight)

Each floor weight has determined in the same way as calculating M5 weights and tabulated in Table 4.81.

Table 4.81 TM5-Floors' Weights

Floor	Weight (kN)
1	3704
2	3704
3	3704
4	3704
5	3459
Total	18275

STEP 12 (Fundamental Period of the Structure)

The fundamental period was computed using the analysis software SAP2000 which equals 1.23second.

Verification on SAP2000 fundamental period:

Rayleigh-Ritz method can be used for calculating an approximation to the fundamental period using Eq. 4.5 as shown in Table 4.82.

Table 4.82 TM5-Verification on SAP2000 Fundamental Period

Storey	W_i(kN)	f_i (kN)*	δ_i(m)	δ_i^2	$f_i\ \delta_i$	$W_i\ \delta i^2$
1	3704	1000	0.019	0.0004	19.3	1.4
2	3704	1000	0.055	0.0030	54.6	11.0
3	3704	1000	0.089	0.0079	88.9	29.3
4	3704	1000	0.116	0.0134	116.0	49.8
5	3459	1000	0.135	0.0182	134.9	63.0
				$\sum$	414	155

* Assumed forces

By applying Eq. 4.5 with Table 4.82

T = 1.23 second

$$\% \text{ error} = \frac{\text{Approximated Period} - \text{SAP Period}}{\text{SAP Period}} \times 100\% = 0\ \%$$

STEP 13 (Maximum Period Limit)

After referring to Table 4.22

C_t = 0.0466 (Concrete moment-resisting frame)

x = 0.9

h_n = number of storeys× storey's height = 5×3.40 = 17m

Apply previous values in Eq. 4.6, we get

$T_a = 0.0466 \times 17^{0.9} = 0.59$seconds

After referring to Table 4.21

$S_{D1} = 0.25$

Interpolation between S_{D1} equals 0.20 and S_{D1} equals 0.30, we get

$C_u = 1.45$

$C_u \times T_a = 1.45 \times 0.59 = 0.86$second $<$ 1.23second (Use T= 0.86second in base shear calculations).

STEP 14 (Response Spectrum Graph)

The elastic and inelastic response spectrums for TM5 model are created in the same way as creating the response spectrums for previous models as shown in Figs. 4.28 and 4.29 respectively.

STEP 15 (Determination of Seismic Base Shear Using Equivalent Lateral Force Analysis)

The seismic base shear (V) in a given direction is determined by applying Eq. 4.9 as follows:

$$C_s \text{ is the minimum of } \begin{cases} \dfrac{S_{DS} \times I}{R} \\ \dfrac{S_{D1} \times I}{R \times T} \end{cases} = \begin{cases} \dfrac{0.50 \times 1}{8} \\ \dfrac{0.25 \times 1}{8 \times 0.86} \end{cases} = \begin{cases} 0.063 \\ 0.0363 \end{cases} = 0.0363$$

By applying Eq. 4.9, we get:

V = 0.0363×18275 = 663kN

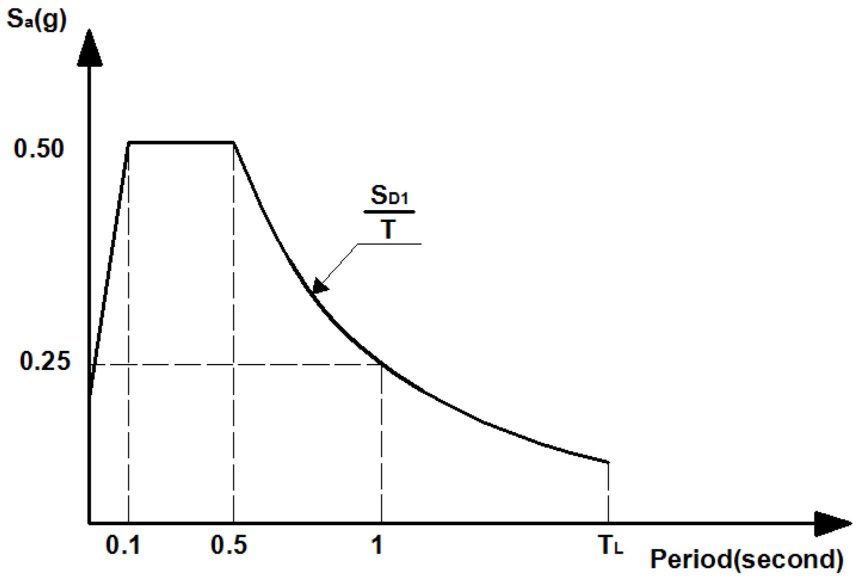

Figure 4.28 TM5-Elastic Response Spectrum

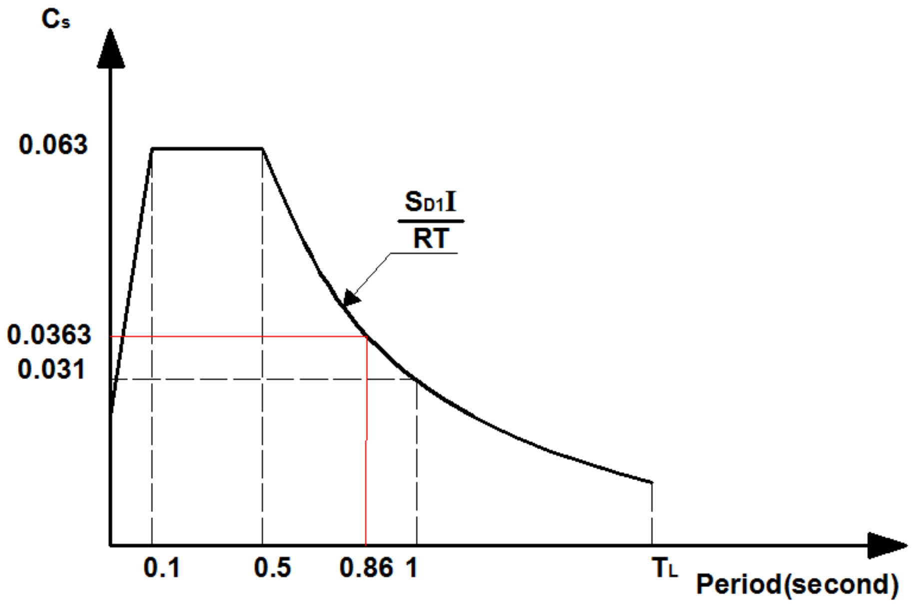

Figure 4.29 TM5-Inelastic Response Spectrum

STEP 16 (Determination of Seismic Base Shear using Modal Response Spectrum Analysis)

The response spectrum function was defined as previously mentioned and the base shear (V) has been computed by using section cut at columns of ground floor and the result is as follows,

V = 389kN

Table 4.83 summarizes the selection process for the appropriate base shear value based on ASCE 7 section 12.9.4.1

Table 4.83 TM5-Base Shear Selection

Base shear using MRSA[1] (kN)	**Base shear using ELF[2] (kN)**	**0.85×ELF[2] (kN)**
389	663	564

1 Modal Response Spectrum Analysis
2 Equivalent Lateral Force

The base shear using modal response spectrum analysis is less than 85 percent of the calculated base shear using equivalent lateral force procedure. Thus, the base shear has to scale to 0.85×ELF which equals 564kN.

STEP 17 (Vertical Distribution of Seismic Base Shear)

Seismic base shear distribution can be computed using SAP2000 by making section cut and reading the shear force from response analysis case at each level as shown in Table 4.84 and scale the value to 0.85×ELF.

Table 4.84 TM5-Base Shear Distribution on Floors

Floor	h(m)	Shear Force (kN)	Force on each Floor (kN)
1	3.40	564	45
2	6.80	519	86
3	10.2	434	81
4	13.6	352	128
5	17.0	225	225

First-order moment and second-order moment are determined on all columns in all floors and they are annexed in appendix B. The critical column is tabulated in Table 4.85.

Table 4.85 Bending Moment Results for TM5 Model n Critical Column

	First-Order Analysis	Second-Order Analysis	Percent Difference
Bending Moment (kN.m)	-84.0	-88.2	4.95%

Storey drifts and stability coefficients for TM5 model are calculated in the same way as were calculated for model M5 and tabulated in Tables 4.86 and 4.87 respectively.

Table 4.86 TM5 Drift Check

Level	δ_{xe} (mm)[a]	δ_x (mm)[b]	Δ (mm)	$\Delta_{Allowable}$ (mm)[c]	Check
1	2.40	13.20	13.20	52	OK
2	7.12	39.14	25.94	52	OK
3	12.11	66.62	27.48	52	OK
4	16.49	90.67	24.05	52	OK
5	19.85	109.18	18.51	52	OK

Table 4.87 TM5 Stability Coefficient

TM5						
Level	**P_x (kN)**	**Δ (mm)**	**V_x (kN)**	**h_{sx} (mm)**	**C_d**	**θ**
1	23373	13.20	564	3400	5.5	0.029
2	18698	25.94	519	3400	5.5	**0.050**
3	14024	27.48	434	3400	5.5	0.047
4	9349	24.05	352	3400	5.5	0.034
5	4185	18.51	225	3400	5.5	0.018

The P-Delta analysis is not required based on the stability coefficient which is less than 0.1 which is assured by the percent difference between first-order and second order analyses on the critical column which is also less than 0.1.The maximum stability coefficient's value is very close to the percent difference between first and second-order analyses (Table 4.85) on the critical column. However, the stability coefficient gives conservative result compared to the percent difference on the critical column.

4.3.2 Ten-Storey model (TM10)

TM10's columns' sections are square sections and are summarized in Table 4.88. TM10 has the same results as M10 until step 10; the calculations are resumed from step 11 as follows;

Table 4.88 TM10 columns' sections

Level	Depth	Width
1-5	0.7m	0.7m
6-10	0.6m	0.6m

STEP 11 (Effective Seismic Weight)

Each floor weight has determined in the same way as calculating M10 weights and tabulated in Table 4.89.

STEP 12 (Fundamental Period of the Structure)

The fundamental period of the structure (T) is determined from SAP2000, version 19.0.0 software analysis. For TM10 model, the fundamental period equals 2.56second.

Verification on SAP2000 fundamental period:

Rayleigh-Ritz method can be used for calculating an approximation to the fundamental period using Eq. 4.5 as shown in Table 4.90.

Table 4.89 TM10-Floors' Weights

Floor	**Weight (kN)**
1	3879
2	3879
3	3879
4	3879
5	3879
6	3704
7	3704
8	3704
9	3704
10	3459
Total	37670

Table 4.90 TM10-Verification on SAP2000 Fundamental Period

Storey	W_i(kN)	f_i (kN)[a]	δ_i(m)[b]	$\delta_i^2(10^{-3})$	$f_i\ \delta_i$	$W_i\ \delta i^2$
1	3879	1000	0.032	0.001	31.7	3.9
2	3879	1000	0.100	0.010	100.0	38.8
3	3879	1000	0.181	0.033	181.3	127.5
4	3879	1000	0.263	0.069	263.4	269.1
5	3879	1000	0.341	0.116	340.7	450.2
6	3704	1000	0.411	0.169	410.5	624.2
7	3704	1000	0.467	0.218	467.3	808.8
8	3704	1000	0.511	0.261	511.0	967.2
9	3704	1000	0.542	0.294	542.5	1090.0
10	3459	1000	0.564	0.318	563.9	1100.0
				$\sum$	3412	5480

a Assumed forces

b The displacement corresponding to the assumed forces

By applying Eq. 4.5 with Table 4.90

T = 2.54 second

% error = $\frac{\text{Approximated Period} - \text{SAP Period}}{\text{SAP Period}} \times 100\% = 0.8\% < 10\%$

Acceptable

STEP 13 (Maximum Period Limit)

After referring to Table 4.22

C_t = 0.0466 (Concrete moment-resisting frame)

x = 0.9

h_n = number of storeys× storey's height = 10×3.40 = 34m

Apply previous values in Eq. 4.6, we get

$T_a = 0.0466 \times 34^{0.9} = 1.11$seconds

After referring to Table 4.21

$S_{D1} = 0.25$

Interpolation between S_{D1} equals 0.20 and S_{D1} equals 0.30, we get

$C_u = 1.45$

$C_u \times T_a = 1.45 \times 1.11 = 1.61$second $<$ 2.56second (Use T=1.61second for base shear calculations).

STEP 14 (Response Spectrum Graph)

The elastic and inelastic response spectrums for TM10 model are created in the same way as creating the response spectrums for M10 model as shown in Figs. 4.30 and 4.31 respectively.

STEP 15 (Determination of Seismic Base Shear using Equivalent Lateral Force Analysis)

The seismic base shear (V) in a given direction is determined by applying Eq. 4.9 as follows:

$$C_s \text{ is the minimum of } \begin{cases} \dfrac{S_{DS} \times I}{R} \\ \dfrac{S_{D1} \times I}{R \times T} \end{cases} = \begin{cases} \dfrac{0.50 \times 1}{8} \\ \dfrac{0.25 \times 1}{8 \times 1.61} \end{cases} = \begin{cases} 0.063 \\ 0.0194 \end{cases} = 0.0194$$

By applying Eq. 4.9, we get:

$V = 0.0194 \times 37670 = 731$kN

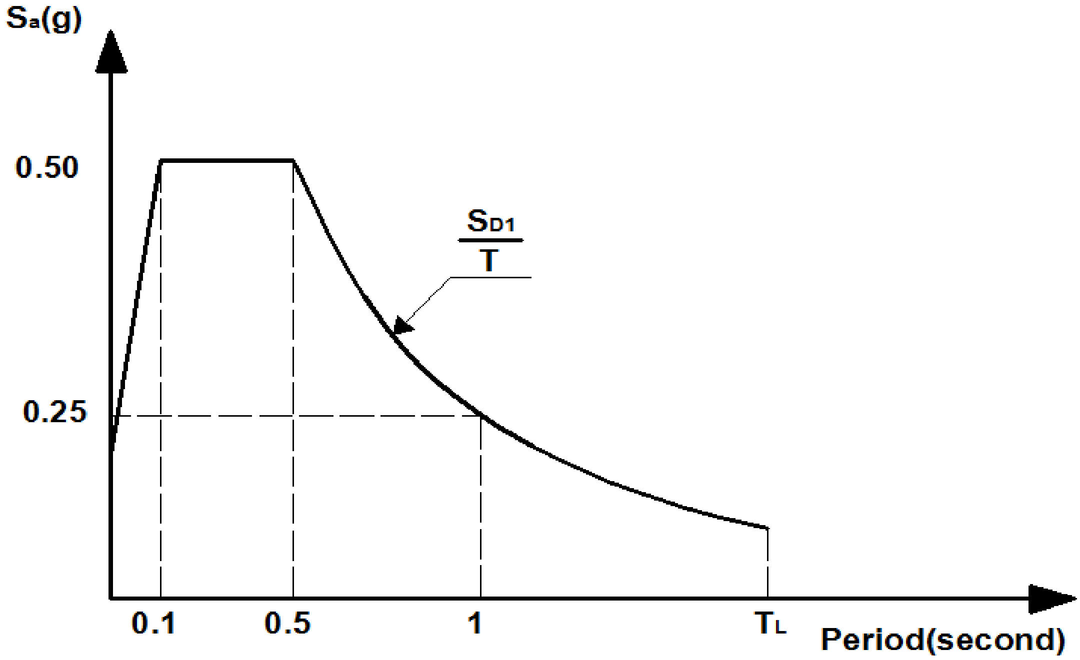

Figure 4.30 TM10-Elastic Response Spectrum

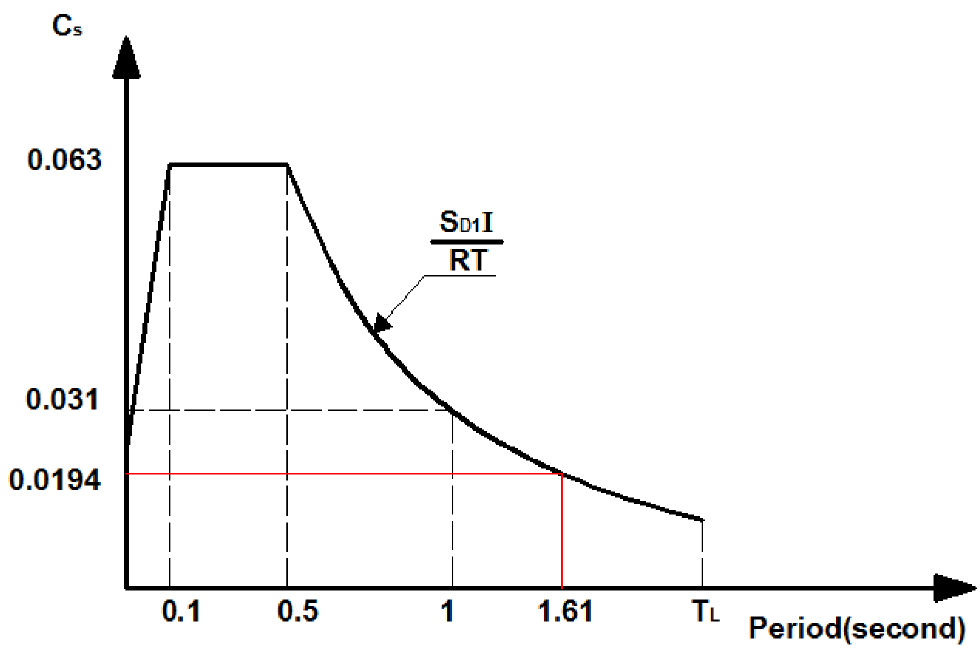

Figure 4.31 TM10-Inelastic Response Spectrum

STEP 16 (Determination of Seismic Base Shear using Modal Response Spectrum Analysis)

The response spectrum was defined as for M5 model and the base shear (V) has been computed by using section cut at columns of ground floor and the result is as follows,

V = 411kN

Table 4.91 summarizes the selection process for the appropriate base shear value based on ASCE 7 section 12.9.4.1

Table 4.91 TM10-Base Shear Selection

Base shear using MRSA[1] (kN)	**Base shear using ELF[2] (kN)**	**0.85×ELF[2] (kN)**
411	731	621

1 Modal Response Spectrum Analysis
2 Equivalent Lateral Force

The base shear using modal response spectrum analysis is less than 85 percent of the calculated base shear using equivalent lateral force procedure. Thus, the base shear has to scale to 0.85×ELF which equals 621kN.

STEP 17 (Vertical Distribution of Seismic Base Shear)

Seismic base shear distribution can be computed using SAP2000 by making section cut and reading the shear force from response analysis case at each level as shown in Table 4.92 and scale the value to 0.85×ELF.

Table 4.92 TM10-Base Shear Distribution on Floors

Floor	h(m)	Shear Force (kN)	Force on each Floor (kN)
1	3.40	621	26
2	6.80	595	53
3	10.2	542	44
4	13.6	499	35
5	17.0	464	39
6	20.4	425	39
7	23.8	385	48
8	27.2	337	53
9	30.6	284	97
10	34.0	187	187

First-order moment and second-order moment are determined on all columns in all floors and they are annexed in appendix B. The critical column is tabulated in Table 4.93.

Table 4.93 TM10-Bending Moment Results on Critical Column

	First-Order Analysis	Second-Order Analysis	Percent Difference
Bending Moment (kN.m)	90.7	102.5	12.91%

Storey drifts and stability coefficients for TM10 model are calculated in the same way as were calculated for model M5 and tabulated in Tables 4.94 and 4.95 respectively.

Table 4.94 TM10 Drift Check

Level	**δ_{xe} (mm)**	**δ_x (mm)**	**Δ (mm)**	**$\Delta_{Allowable}$ (mm)**	**Check**
1	2.09	11.49	6.46	52	OK
2	6.73	37.00	25.50	52	OK
3	12.41	68.28	31.28	52	OK
4	18.40	101.21	32.94	52	OK
5	24.34	133.88	32.67	52	OK
6	30.15	165.81	31.94	52	OK
7	35.42	194.83	29.01	52	OK
8	40.04	220.20	25.37	52	OK
9	43.85	241.19	20.99	52	OK
10	46.76	257.20	16.01	52	OK

Table 4.95 TM10 Stability Coefficient

TM10						
Level	**P_x (kN)**	**Δ (mm)**	**V_x (kN)**	**h_{sx} (mm)**	**C_d**	**θ**
1	47630	6.46	621	3400	5.5	0.026
2	42779	25.50	595	3400	5.5	0.098
3	37927	31.28	542	3400	5.5	**0.117**
4	33076	32.94	499	3400	5.5	**0.117**
5	28224	32.67	464	3400	5.5	0.106
6	23373	31.94	425	3400	5.5	0.094
7	18698	29.01	385	3400	5.5	0.075
8	14024	25.37	337	3400	5.5	0.056
9	9349	20.99	284	3400	5.5	0.037
10	4185	16.01	187	3400	5.5	0.019

The P-Delta analysis is required based on the stability coefficient which is larger than 0.1 which is assured by the percent difference between first-order and second order analyses on the critical column which is also larger than 0.1.The maximum stability coefficient's value is very close to the percent difference between first and second-order analyses (Table 4.93) on the critical column. However, the stability coefficient gives slightly unconservative result compared to the percent difference on the critical column

4.2.3 Fifteen-Storey model (TM15)

TM15's columns' sections are tabulated in Table 4.96. TM15 has the same results as M15 until step 10; the calculations are resumed from step 11 as follows;

Table 4.96 TM15 columns' sections

Level	Depth	Width
1-5	0.9m	0.9m
6-10	0.7m	0.7m
11-15	0.6m	0.6m

STEP 11 (Effective Seismic Weight)

Each floor weight has determined in the same way as calculating M15 weights and tabulated in Table 4.97.

Table 4.97 TM15-Floors' Weights

Floor	Weight (kN)
1	4314
2	4314
3	4314
4	4314
5	4314
6	3879
7	3879
8	3879
9	3879
10	3879
11	3704
12	3704
13	3704
14	3704
15	3459
Total	59240

STEP 12 (Fundamental Period of the Structure)

The fundamental period of the structure (T) is determined from SAP2000, version 19.0.0 software analysis. For TM15 model, the fundamental period equals 3.73second.

Verification on SAP2000 fundamental period:

Rayleigh-Ritz method can be used for calculating an approximation to the fundamental period using Eq. 4.5 as shown in Table 4.98.

Table 4.98 TM15-Verification on SAP2000 Fundamental Period

Storey	**W_i(kN)**	**f_i (kN)[a]**	**δ_i(m)[b]**	**$\delta_i^2(10^{-3})$**	**$f_i\ \delta_i$**	**$W_i\ \delta i^2$**
1	4314	1000	0.030	0.0009	30.1	3.9
2	4314	1000	0.103	0.0107	103.4	46.1
3	4314	1000	0.202	0.0407	201.6	175.4
4	4314	1000	0.313	0.0979	312.9	422.5
5	4314	1000	0.430	0.1846	429.7	796.4
6	3879	1000	0.550	0.3020	549.6	1171.5
7	3879	1000	0.664	0.4413	664.3	1711.8
8	3879	1000	0.770	0.5933	770.3	2301.5
9	3879	1000	0.866	0.7498	865.9	2908.5
10	3879	1000	0.951	0.9046	951.1	3508.9
11	3704	1000	1.026	1.0517	1025.5	3895.5
12	3704	1000	1.085	1.1769	1084.9	4359.4
13	3704	1000	1.130	1.2776	1130.3	4732.4
14	3704	1000	1.163	1.3530	1163.2	5011.6
15	3459	1000	1.186	1.4064	1185.9	4864.8
				$\sum$	10469	35910

a Assumed forces

b The displacement corresponding to the assumed forces

By applying Eq. 4.5 with Table 4.98

T = 3.72 second

$\% \text{ error} = \frac{\text{Approximated Period}-\text{SAP Period}}{\text{SAP Period}} \times 100\% = 0.3\% < 10\%$

Acceptable

STEP 13 (Maximum Period Limit)

After referring to Table 4.22

$C_t = 0.0466$ (Concrete moment-resisting frame)

$x = 0.9$

h_n = number of storeys× storey's height = 15×3.40 = 51m

Apply previous values in Eq. 4.6, we get

$T_a = 0.0466 \times 51^{0.9} = 1.60$seconds

After referring to Table 4.21

$S_{D1} = 0.25$

Interpolation between S_{D1} equals 0.20 and S_{D1} equals 0.30, we get

$C_u = 1.45$

$C_u \times T_a = 1.45 \times 1.60 = 2.32$second $<$ 3.73second (Use T=2.32second for base shear calculations).

STEP 14 (Response Spectrum Graph)

The elastic and inelastic response spectrums for TM15 model are created as previously mentioned as shown in Figs. 4.32 and 4.33 respectively.

STEP 15 (Determination of Seismic Base Shear Using Equivalent Lateral Force Analysis)

The seismic base shear (V) in a given direction is determined by applying Eq. 4.9 as follows:

C_s is the minimum of $\begin{cases} \frac{S_{DS}\times I}{R} \\ \frac{S_{D1}\times I}{R\times T} \end{cases} = \begin{cases} \frac{0.50\times 1}{8} \\ \frac{0.25\times 1}{8\times 2.32} \end{cases} = \begin{cases} 0.063 \\ 0.0135 \end{cases} = 0.0135$

By applying Eq. 4.9, we get:

V = 0.0135×59240= 800kN

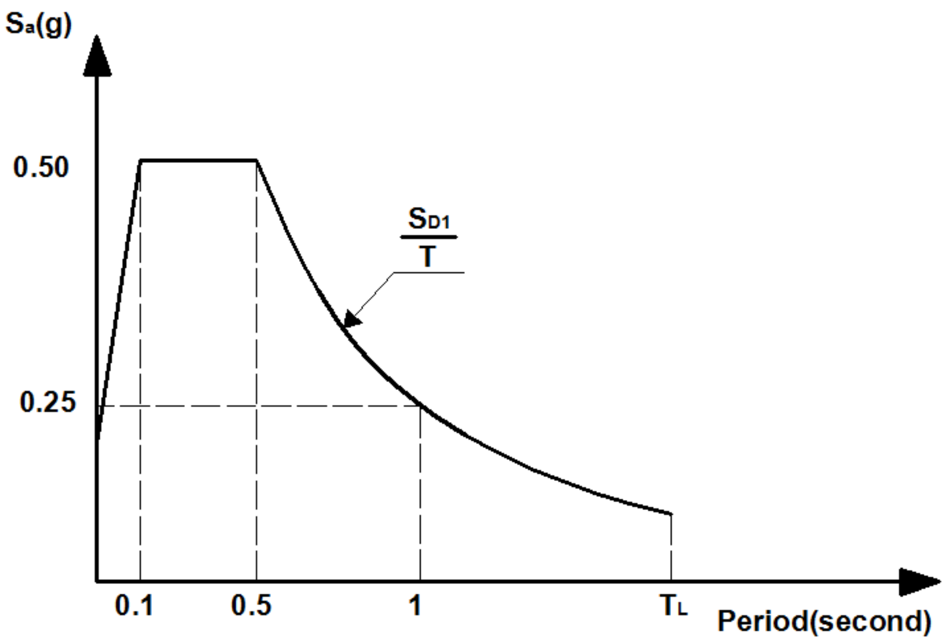

Figure 4.32 TM15-Elastic Response Spectrum

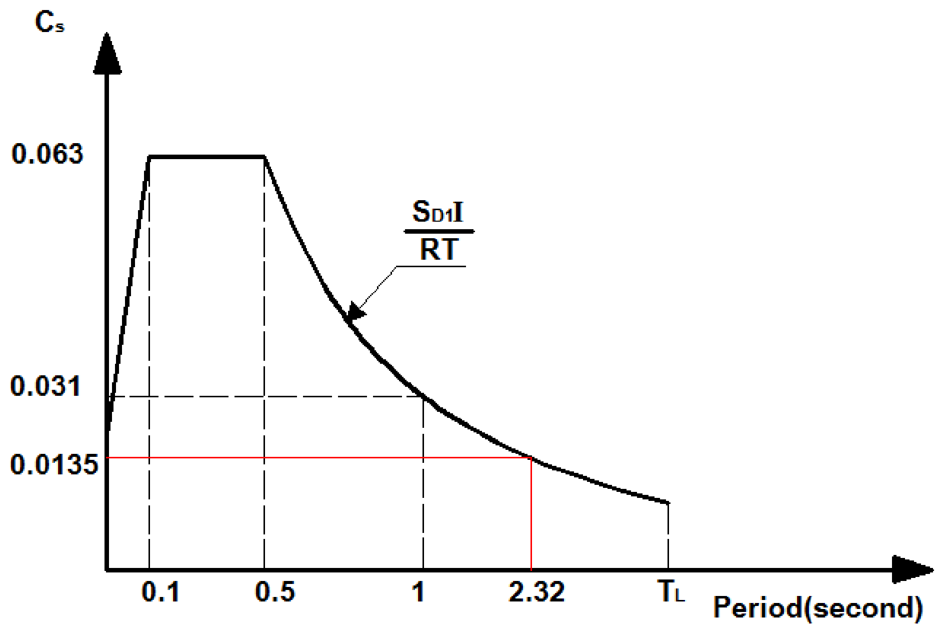

Figure 4.33 TM15-Inelastic Response Spectrum

STEP 16 (Determination of Seismic Base Shear using Modal Response Spectrum Analysis)

The response spectrum function was defined as previously mentioned and the base shear (V) has been computed by using section cut at columns of ground floor and the result is as follows,

V = 439kN

Table 4.99 summarizes the selection process for the appropriate base shear value based on ASCE 7 section 12.9.4.1.

Table 4.99 TM15-Base Shear Selection

Base shear using MRSA[1] (kN)	**Base shear using ELF[2] (kN)**	**0.85×ELF[2] (kN)**
439	800	680

1 Modal Response Spectrum Analysis
2 Equivalent Lateral Force

The base shear using modal response spectrum analysis is less than 85 percent of the calculated base shear using equivalent lateral force procedure. Thus, the base shear has to scale to 0.85×ELF which equals 680kN.

STEP 17 (Vertical Distribution of Seismic Base Shear)

Seismic base shear distribution can be computed using SAP2000 by making section cut and reading the shear force from response analysis case at each level as shown in Table 4.100 and scale the value to 0.85×ELF.

Table 4.100 TM15-Base Shear Distribution on Floors

Floor	h(m)	Shear Force (kN)	Force on each Floor (kN)
1	3.40	680	14
2	6.80	666	36
3	10.2	630	46
4	13.6	584	39
5	17.0	545	20
6	20.4	525	19
7	23.8	507	31
8	27.2	476	34
9	30.6	441	28
10	34.0	414	33
11	37.4	381	39
12	40.8	342	33
13	44.2	310	43
14	47.6	266	102
15	51.0	164	164

First-order moment and second-order moment are determined on all columns in all floors and they are annexed in appendix B. The critical column is tabulated in Table 4.101.

Table 4.101 Bending Moment Results for TM15 Model on Critical Column

	First-Order Analysis	Second-Order Analysis	Percent Difference
Bending Moment (kN.m)	126.5	152.7	20.72%

Storey drifts and stability coefficients for TM15 model are calculated in the same way as were calculated for model M5 and tabulated in Tables 4.102 and 4.103 respectively.

Table 4.102 TM15 Drift Check

Level	δ_{xe} (mm)	δ_x (mm)	Δ (mm)	$\Delta_{Allowable}$ (mm)	Check
1	1.45	7.98	4.55	52	OK
2	5.03	27.66	19.68	52	OK
3	9.89	54.41	26.75	52	OK
4	15.48	85.14	30.72	52	OK
5	21.44	117.91	32.78	52	OK
6	27.79	152.83	34.91	52	OK
7	34.20	188.12	35.29	52	OK
8	40.47	222.57	34.45	52	OK
9	46.47	255.56	33.00	52	OK
10	52.16	286.91	31.34	52	OK
11	57.60	316.81	29.90	52	OK
12	62.48	343.66	26.85	52	OK
13	66.77	367.23	23.57	52	OK
14	70.33	386.83	19.60	52	OK
15	73.04	401.73	14.90	52	OK

Table 4.103 TM15 Stability Coefficient

TM15						
Level	**P_x (kN)**	**Δ (mm)**	**V_x (kN)**	**h_{sx} (mm)**	**C_d**	**θ**
1	74063	4.55	680	3400	5.5	0.03
2	68776	19.68	666	3400	5.5	0.11
3	63490	26.75	630	3400	5.5	0.14
4	58203	30.72	584	3400	5.5	0.16
5	52917	32.78	545	3400	5.5	**0.17**
6	47630	34.91	525	3400	5.5	**0.17**
7	42779	35.29	507	3400	5.5	0.16
8	37927	34.45	476	3400	5.5	0.15
9	33076	33.00	441	3400	5.5	0.13
10	28224	31.34	414	3400	5.5	0.11
11	23373	29.90	381	3400	5.5	0.10
12	18698	26.85	342	3400	5.5	0.08
13	14024	23.57	310	3400	5.5	0.06
14	9349	19.60	266	3400	5.5	0.04
15	4185	14.90	164	3400	5.5	0.02

The P-Delta analysis is required based on the stability coefficient which is larger than 0.1 which is assured by the percent difference between first-order and second order analyses on the critical column which is also larger than 0.1. The maximum stability coefficient's value is to some extent close to the percent difference between first and second-order analyses (Table 4.101) on the critical column. However, the stability coefficient does not describe precisely the percent difference between first-order analysis and second order-analysis and gives lesser value and its value just indicates including or not including P-Delta analysis and this is noted for stability coefficient exceeds 0.1.

4.4 Seismic Design of Reinforced Concrete Special Moment Frames

Special Moment Resisting Frames (SMRFs) are used as a part of the seismic resisting system. SMRF concept was introduced in the United States discharge about 1960. Their use was very limited until 1973 where the Uniform Building Code first required use of the special frames in the highest seismicity regions. SMRF has more stringent requirements compared to Ordinary or Intermediate Moment Frames. The requirements in designing SMRF are addressed in ACI 318. Three types of elements are detailed to resist seismic loads without tremendous loss in stiffness or strength; these are beams, columns and beam-column joints [41]. They are detailed to resist internal forces (flexural, shear and axial forces) that result from imposed displacement as a result of earthquake ground shaking and to ensure that reinforced concrete special moment resisting frame maintains a high level of ductility and energy dissipation mechanism [43]. In this section, some special moment resisting frames main design regulations are explained and presented.

The good performance of SMRFs is greatly guaranteed if the following stringent design provisions are applied [42],

- The failure has to be a ductile failure; which means the designer shall avoid brittle failure such as shear failure.
- The flexural failure has to precede shear failure.
- Beam's distortion has to precede column's distortion.
- Joints are stronger than members.
- Use the concept of strong-column/weak-beam frame.

4.4.1 SMRFs Layout and Proportioning

Special Frame Beam Layout Requirements in ACI 318

- Comment 1: Beam clear span shall not be less than four times its effective depth.
- Comment 2: Width of beam web shall be larger than or equal the minimum of 0.3 of its depth, or 250mm.

Special Frame Column Layout Requirements in ACI 318

- Comment 1: The shortest cross-sectional dimension of the column shall be 300mm at least.
- Comment 2: The shortest cross-sectional dimension of the column shall be at least 0.4 of the other perpendicular dimension within the section.

Tables 4.104 and 4.105 summarize checking process on beams' and columns' dimensions respectively.

Table 4.104 Special Frame Beams Dimensions Checks

Model	Beam		Comment 2	Effective Depth	Clear Span	Comment 1
	Depth	Width				
M Models	0.7m	0.75m	> 0.21m	0.64m	4.7m	> 2.56m
TM Models	0.4m	0.6m	> 0.12 m	0.34m	4.8m	> 1.36m

Table 4.105 Special Frame Columns Dimensions Checks

Model	Base Column		Comment 1	Comment 2
	Depth(m)	Width(m)		
M5	0.75	0.75	> 0.3m	> 0.4 of other dimension
M10	0.9	0.9	> 0.3m	> 0.4 of other dimension
M15	1.0	1.0	> 0.3m	> 0.4 of other dimension
M20	1.1	1.1	> 0.3m	> 0.4 of other dimension
M25	1.2	1.2	> 0.3m	> 0.4 of other dimension
M30	1.3	1.3	> 0.3m	> 0.4 of other dimension
TM5	0.6	0.6	> 0.3m	> 0.4 of other dimension
TM10	0.7	0.7	> 0.3m	> 0.4 of other dimension
TM15	0.9	0.9	> 0.3m	> 0.4 of other dimension

4.4.2 SMRFs Material Properties

- ACI 318 states that "the specified concrete compressive strength shall be at least 21MPa". For all models in this research, a 24MPa concrete compressive strength is used for beams and slabs, and 32MPa compressive strength is used for columns which are both larger than 21MPa.
- ACI 318 states that "steel grades higher than 420MPa are not permitted". Yielding stress of 420MPa is utilized for all steel bars.

4.4.3 Longitudinal and Transverse Beam Reinforcement

In this section, a beam which is part of the special moment resisting frame in M5 model as shown in Fig.4.34 is designed and the ACI 318 provisions are checked.

4.4.3.1 Load Combinations

Structures, components, and foundations shall be designed so that their design strength equals or exceeds the effects of the factored loads in the following combinations (ASCE 7, section 2.3.2);

$$1.4D \qquad (4.16)$$

$$1.2D+1.6L \qquad (4.17)$$

$$1.2D+1.0L+1.0E \qquad (4.18)$$

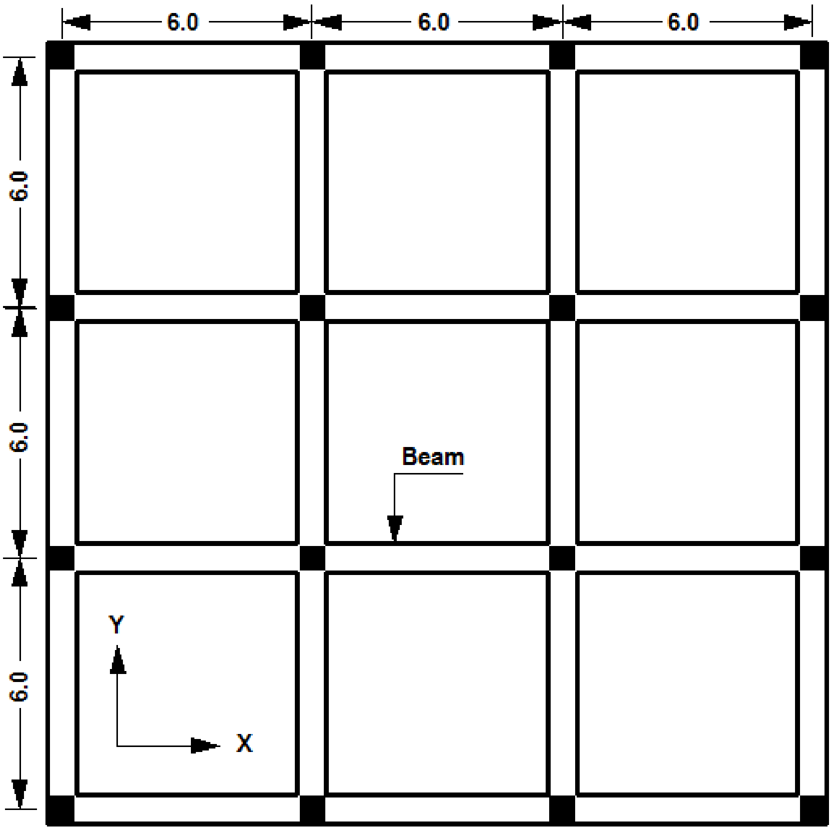

Figure 4.34 Location of Beam which is verified (All dimensions are in meter)

$$0.9D+1.0E \tag{4.19}$$

Where,

D = dead load

L = live load

E = for use in Eq. 4.18 and Eq. 4.19, shall be determined in accordance with Eq. 4.20 and Eq. 4.21 respectively (ASCE 7, section 12.4.2) as follows:

$$E = E_h+E_v \tag{4.20}$$

$$E = E_h-E_v \tag{4.21}$$

Where,

E_h = effect of horizontal seismic forces = ρQ_E

E_v = effect of vertical seismic forces = $0.2S_{DS}D$

Where,

ρ = redundancy factor = 1.3 (ASCE 7, section 12.3.4)

Q_E = seismic effect of orthogonal loading

S_{DS} and D are as defined before

Applying each quantity value in previous load combinations to get the final factored load pattern as follows:

$$1.4D \tag{4.22}$$

$$1.2D+1.6L \tag{4.23}$$

$$1.3D+1.0L+1.3Q_E \tag{4.24}$$

$$0.8D+1.3Q_E \tag{4.25}$$

During careful examination; Eq. 4.24 was giving the more critical values for the negative moment and Eq. 4.23 was giving the more critical values for the positive moment.

4.4.3.2 Beam Moments

The negative moment (M_{-ve}) = -300kN.m

The positive moment (M_{+ve}) = 124kN.m

Based on ACI 318, positive moment strength is not to be less than ½ of the negative moment strength provided at the face of the joint. Furthermore, the negative or positive moment at any section along the member is not to be less than ¼ of the maximum moment strength at face of either joint.

M_{+ve} = 0.5*300 = 150kN.m > 124kN.m (Take M_{+ve} = 150kN.m)

4.4.3.3 Factored Axial Force

Based on ACI 318, section 21.5.1; the factored axial compressive force is considered in the beam if $P_u > 0.1f_cA_g$

$P_u = 12.2kN < 1260kN$ (i.e. No need to consider axial force)

4.4.3.4 Longitudinal Reinforcement

$$d = h - C_c - d_h - 0.5d_b \tag{4.26}$$

Where,

d = member effective depth

h = member depth = 700mm

C_c = concrete cover = 40mm

d_h = hoop diameter ≈ 10mm (assumed)

d_b = bar diameter ≈ 20mm (assumed)

Applying previous values to Eq. 4.26 as follows:

d = 700 – 40 -10-10 = 640mm

The area of steel and minimum area of steel can be obtained from the following equations for M_u equals 300kN.m:

$$A_s = \frac{0.85f_c' b_w d}{fy}\left[1 - \sqrt{1 - \frac{2.61M_u}{f_c' b_w d^2}}\right]$$

$A_s = 1280mm^2$

$$A_{s,min} = \frac{0.25\sqrt{f_c'}}{fy} b_w d$$

$A_{s,min} = 1400mm^2$

$$A_{s,min} = \frac{1.4}{fy} b_w d$$

$A_{s,min} = 1600mm^2$

Take $A_s = 1600mm^2$ (8Φ16)

Based on ACI 318, section 21.5.2.3; lap splices of flexural reinforcement shall be permitted only if hoop or spiral reinforcement is provided over the lap length. Spacing of the transverse reinforcement enclosing the lap-spliced bars shall not exceed the smaller of d/4 or 100mm. Lap splices shall not be used:

a. Within the joints;
b. Within the distance of twice member depth from the face of the joint.
c. At locations where analysis indicates flexural yielding caused by inelastic lateral displacements of the frame.

In the beam under investigation; lap splices are used with implementing the previous requirements with spacing of the transverse reinforcement equals 100mm.

4.4.3.5 Shear Strength Requirements

The design shear force V_e is to be determined from consideration of the static forces on the portion of the member between faces of the joint. It is assumed that moments of opposite sign corresponding to probable flexural moment strength M_{pr} act at the joint faces and that the member is loaded with the factored tributary gravity load along its span (ACI 318, section

21.5.4). For calculations of M_{pr} it is assumed that tensile strength in the longitudinal bars is $1.25F_y$. The calculations are as follows:

V_g (shear force from factored gravity load) = 168kN

$$a = \frac{A_s 1.25F_y}{0.85f_c b_w} \tag{4.27}$$

Where,

a = depth of equivalent rectangular compressive block

A_s , F_y, f_c and b_w are as defined before

A_s = 1600mm^2, F_y = 420MPa, f_c = 24MPa, bw = 750mm, after applying these values in Eq. 12; we get:

a = 55mm

M_{pr} (+ve) = M_{pr} (-ve) = $A_s \times 1.25F_y \times$ (d-a/2)

= 515kN.m

$$V_d = \frac{M_{pr(+ve)} + M_{pr\,(-ve)}}{L_n} \tag{4.28}$$

Where,

V_d = design shear force

L_n = clear span length = 5.25m

V_d = 196kN

$$V_{e,max} = V_g + V_d \tag{4.29}$$

Where

$V_{e,max}$ = maximum required shear strength

V_g and V_d are as defined before

$V_{e,max}$ = 365kN

Based on ACI 318, section 21.5.4.2; transverse reinforcement over lengths identified in 21.5.3.1 shall be proportioned to resist shear assuming V_c =0 when the following conditions occur,

- The design shear force represents ½ or more of the maximum required shear strength within those lengths;
- The factored axial compressive force including earthquake effect is less than $0.05A_g f_c$.

Since both conditions met, the concrete nominal shear strength assumed to equal zero.

$V_s = \frac{V_u}{\emptyset} = \frac{365}{0.75} = 487\text{kN}$

To get the spacing, Eq. 4.30 can be used as follows:

$$V_s = \frac{A_v f_y d}{s} \qquad (4.30)$$

Where,

A_v = stirrup cross sectional area

For two-legged 10mm transverse reinforcement,

s = 87mm

Based on ACI 318, section 21.5.3.2, the first hoop is to be located at a distance not more than 50mm from the face of the supporting member. Maximum spacing of such reinforcement is not to exceed the smallest of: d/4, $6d_b$ where d_b is the diameter of the smallest longitudinal bars, and 150mm.

The smallest value of previous limits is $6d_b$ = 96mm

Use two-legged 10mm stirrup @ 80mm

For stirrups at other locations;

$V_c = 0.17\sqrt{f_c} b_w d = 400kN$

$V_u = 260kN$

Since $\frac{V_u}{\emptyset} < V_c$; $A_{v,min}$ /s shall be provided

$A_{v,min}$ /s shall be greater of :

a. $\frac{0.062\sqrt{f_c} b_w}{f_y}$ = 0.54mm^2/mm
b. $\frac{0.35 b_w}{f_y}$ = 0.625mm^2/mm

Use A_v/s = 0.625mm^2/mm

For two-legged 10mm transverse reinforcement; s= 250mm

Based on ACI 318, section 21.5.3.4, where hoops are not required, stirrups with seismic hooks at both ends are to be spaced at a distance not more than d/2 throughout the length of the member.

d/2 = 320mm > 200mm

Use two-legged 10mm stirrup @ 200mm

Previous results for the beam under consideration are detailed in Fig. 4.35.

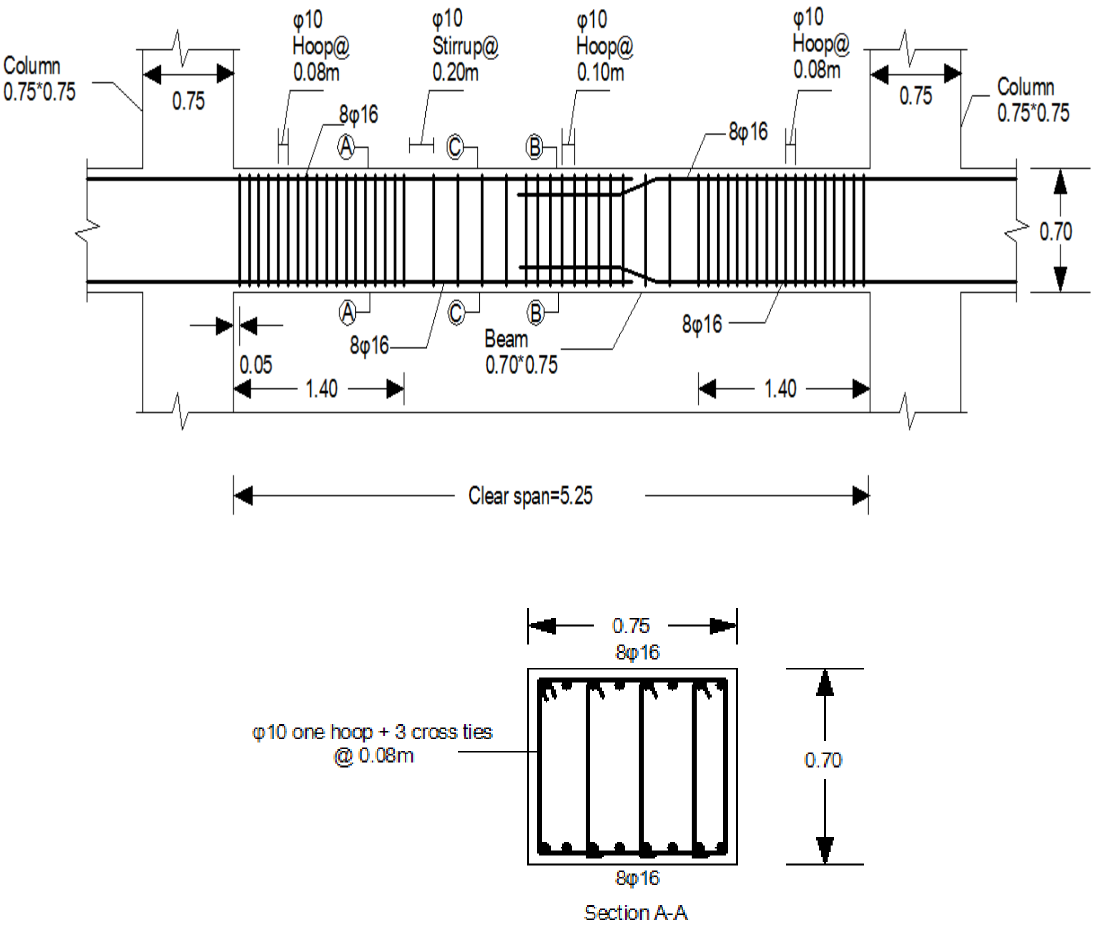

Figure 4.35 Longitudinal and Transverse Reinforcement for the Special Beam (All dimensions are in meter)

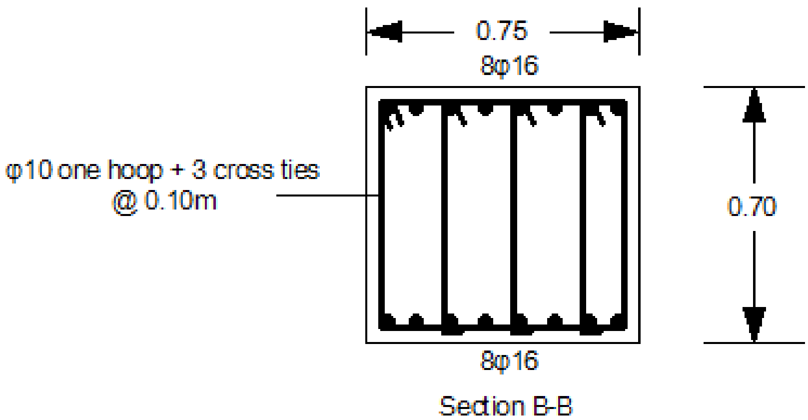

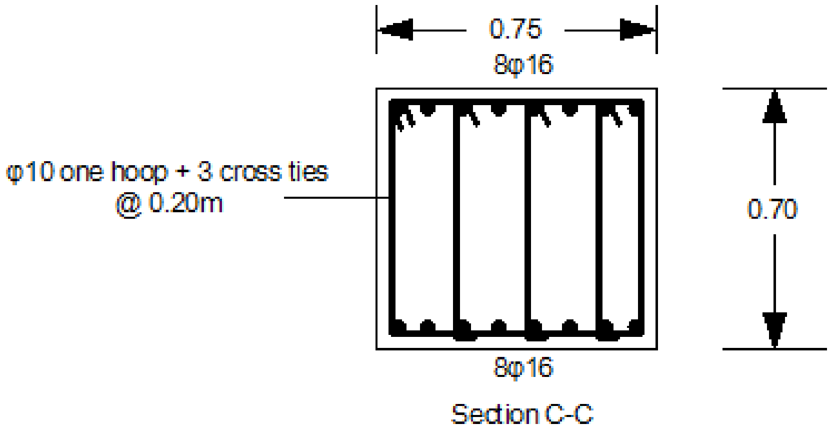

Section C-C

4.4.4 Design of Special Column

The columns which the beam in previous section is supported on; are designed, detailed and checked for ACI 318 special frame provisions.

P_u = 3588kN (from the critical load combination)

M_u = 235kN.m (from the critical load combination)

A_s (SAP2000) = 5625mm^2 (20Ø20mm)

$0.1f_cA_g$ = 1800kN < 3588kN

Thus, requirements of section 21.6.2 in ACI 318 must be satisfied.

Based on ACI318, section 21.6.2.2, the flexural strengths of the columns shall satisfy the following equation:

$$\sum M_{nc} \geq 1.2 \sum M_{nb} \tag{4.31}$$

Where,

$\sum M_{nc}$ = sum of nominal flexural strengths of columns framing into the joint, evaluated at the face of the joint

$\sum M_{nb}$ = sum of nominal flexural strengths of the beams framing into the joint, evaluated at the face of the joint

Considering the columns on both sides of the joint are of equal flexural strengths, the flexural strength of each column is determined using strength interaction diagrams using ρ equals 1%, γ equals 0.85, ∅ equals 0.65, P_u equals 3588kN.

M_u = 1270 kN.m (from strength interaction diagram)

$\sum M_{nc}$ = 1270+1270 = 2540kN.m

$a = \frac{A_s F_y}{0.85 f_c b_w}$ = 44mm (for previous beam)

M_b (+ve) = M_b (-ve) = $A_s \times F_y \times (d-a/2)$ = 415kN.m

$\sum M_{nb}$ = 415×4 = 1660

$\frac{\sum M_{nc}}{\sum M_{nb}} = \frac{2540}{1660} = 1.5 > 1.2$ (OK)

Based on ACI 318, section 21.6.3.1, the reinforcement ratio shall not be less than 0.01 and shall not exceed 0.06.

ρ = 0.01 (OK)

Based on ACI 318, section 21.6.3.3, lap splices are only permitted within the center half of the member length and shall be designed as tension lap splices enclosed within transverse reinforcement.

For class B lap splice, $L_{sp} = 1.3L_d = 1.3 \times \frac{0.59 \times f_y \times d_b}{\sqrt{f_c}} \geq 300$mm

= 1.15m (Use 1.2m)

Based on ACI 318, section 21.6.4.2, transverse reinforcement shall be spaced at a distance not exceeding (a) ¼ of the minimum member dimension (b) six times the diameter of the longitudinal reinforcement and

(c) S_x = 220-0.085h_x where h_x is the largest value of the distance from the centerline to centerline of tie legs.

(a) 0.25×750 = 187mm

(b) 6×20 = 120mm

(c) h_x = 126mm, S_x = 209mm

Use spacing equals 100mm between transverse reinforcement.

Based on ACI 318, section 21.6.4.4, the total cross section area of rectangular hoop reinforcement, A_{sh}, shall not be less than that required by Eqs. 4.32 and 4.33.

$$A_{sh,1} = 0.3\frac{sb_c f_c}{f_y}[(\frac{A_g}{A_{ch}})-1] \quad (4.32)$$

$$A_{sh,2} = 0.09\frac{sb_c f_c}{fy} \quad (4.33)$$

Where,

s = tie spacing

A_{ch} = core area

b_c = the core dimension perpendicular to the tie legs that constitute A_{ch}

s =100mm, b_c =670mm, A_{ch}= 670mm×670mm, A_g = 750mm×50mm, f_c = 32MPa

$A_{sh,1}$ = 388mm^2

$A_{sh,2}$ = 460mm^2

Use A_{sh} = 460mm^2

Use Ø12mm tie plus four Ø12mm cross tie @100mm

A_{sh} = 6×113 = 670mm^2 > 460mm^2 (OK)

Based on ACI 318, section 21.6.4.1, transverse reinforcement in amount specified before shall be provided over a length L_0 from each joint face and on both sides of any section where flexural yielding is likely to occur as a result of inelastic lateral displacements of the frame. The length L_0 shall not be less than the largest of the following:

a. the depth of the member at the joint face = 750mm
b. 1/6 of the clear span of the member = $\frac{1}{6}$×3250 = 542mm
c. 450mm

i.e. 750mm

Based on ACI 318, section 21.6.4.5, beyond L_0, the column shall contain spiral or hoop reinforcement with center to center spacing not exceeding the smaller of six times the diameter of the smallest longitudinal column bars and 150mm.

$S_{max,1}$ = 6×20 =120mm

$S_{max,2}$ = 150mm

i.e. S_{max} = 150mm

The design shear force, V_e, shall be determined from consideration of the maximum forces that can be generated at the faces of the joint at each end of the member. These forces shall be determined using the maximum probable moment strengths, M_{pr}, at each end of the member associated with the range of axial loads on the member (ACI 318, section 21.6.5.1).

P_u = 1300kN (factored axial load)

$$\gamma = \frac{h - 2*c}{h} \qquad (4.34)$$

Where,

h = column dimension perpendicular to the axis of rotation

c = concrete cover

From Eq. 4.34,

$$\gamma = \frac{h-2*c}{h} = \frac{750-2\times40}{750} = 0.9$$

$$\frac{P_u}{\emptyset A_g f_c} = \frac{1300\times1000}{0.65\times750\times750\times32} = 0.11$$

$$\rho = \frac{A_s}{b\times d} \tag{4.35}$$

Where,

A_s = area of steel

b = column width

d = column depth = 750-40-(20/2)-12 = 688mm

From Eq. 4.35,

$$\rho = \frac{A_s}{b\times d} = \frac{6283}{750\times688} = 0.012$$

Based on the previous values and the proper column interaction diagram with the indispensable interpolation; we can get the following values:

$$\frac{M_u}{\emptyset A_g f_c h} = 0.142$$

$$\frac{M_u}{\emptyset A_g f_c h} = \frac{M_u}{0.65\times750\times750\times32\times750} = 0.09 \rightarrow M_u = 790\text{kN.m}$$

$$V_e = \frac{790\times4\times0.5}{3.25} = 486\text{kN}$$

$$V_c = 0.17\sqrt{f_c}b_w d = 498\text{kN}$$

$$V_e/\emptyset > V_c$$

$V_s = V_e/\emptyset - V_c = 150kN$

$\frac{A_v}{s} = \frac{V_s}{F_y d} = 0.52\ mm^2/mm$

For spacing 100mm → $A_v = 52mm^2$

A_v (available within the length L_0) = $670mm^2 > 52mm^2$ (OK)

Previous results for the special column are detailed in Figs. 4.36 and 4.37.

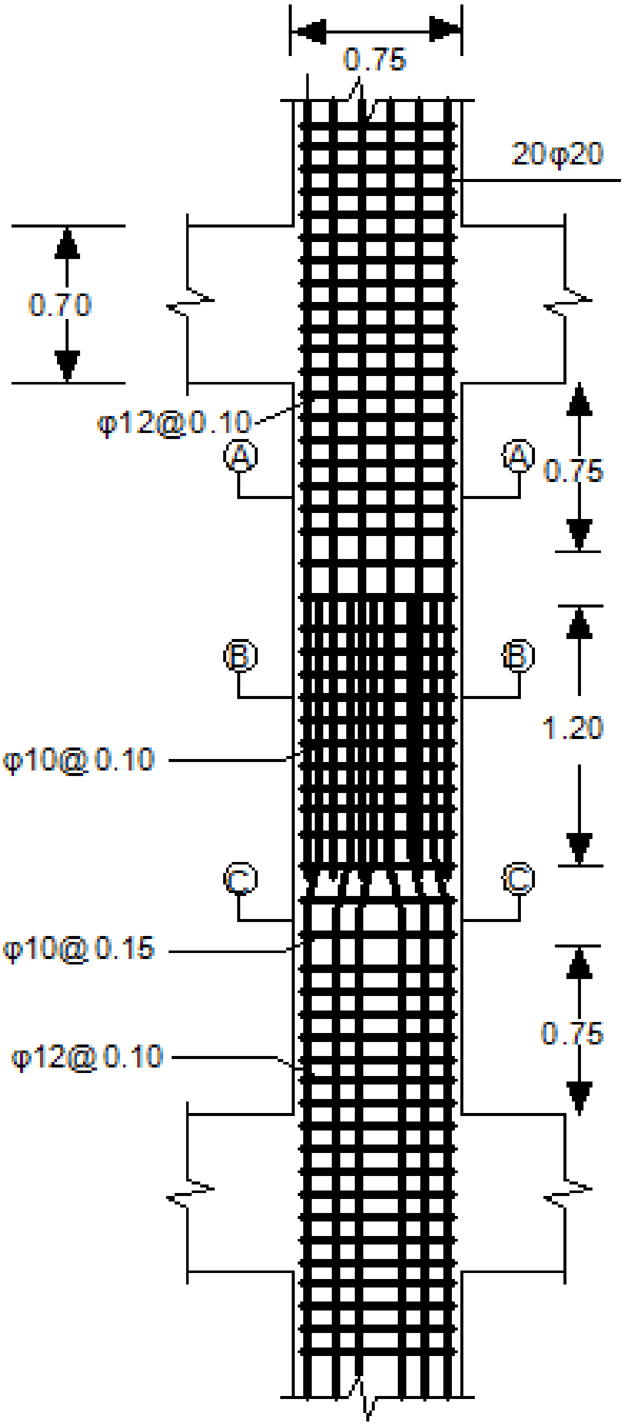

Figure 4.36 Special Column Detailing (All dimensions are in meter)

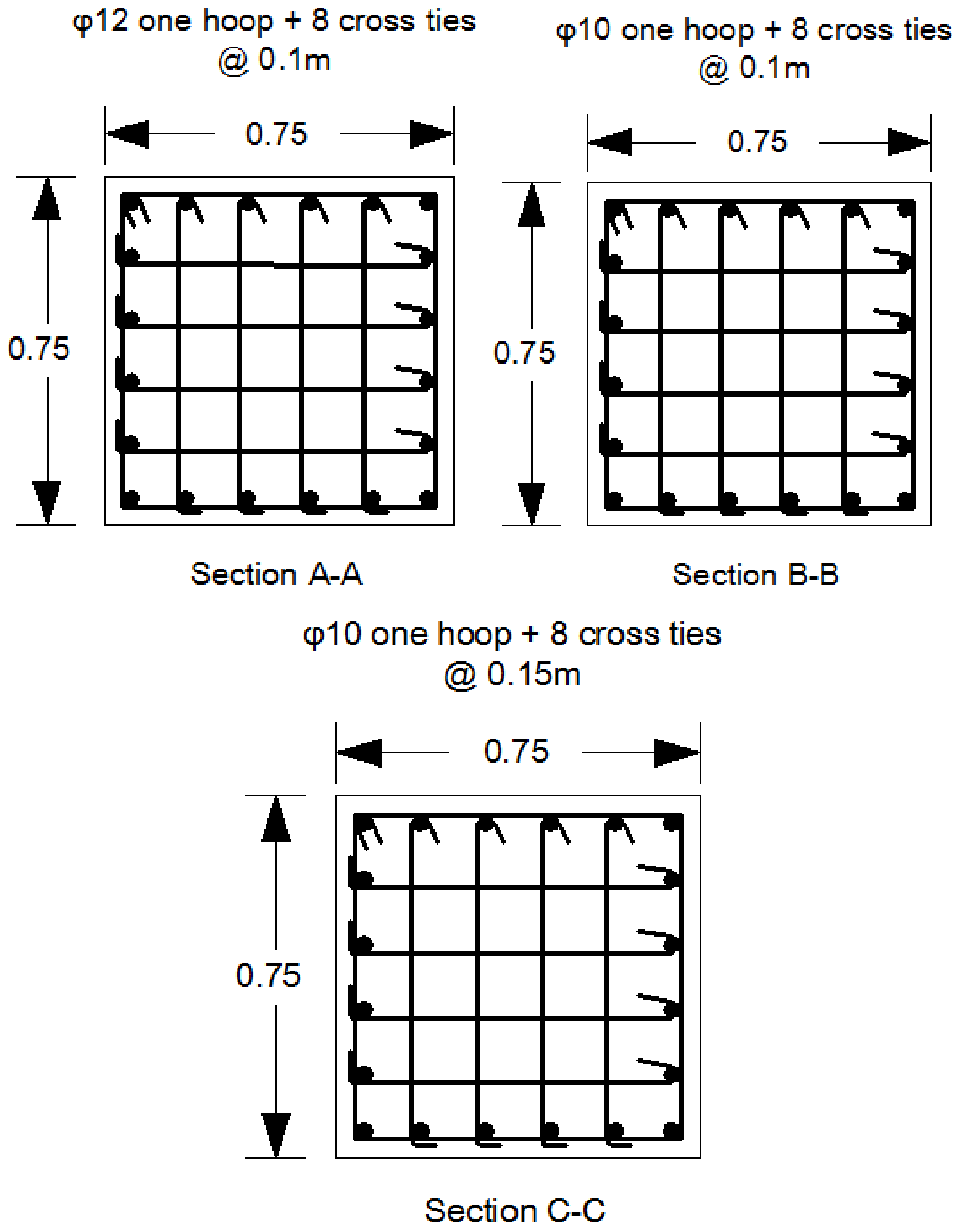

Figure 4.37 Special Column Cross Section (All dimensions are in meter)

4.4.5 Strong-Column/Weak-Beam Frame Concept

This concept means that columns are stiffer than the beams frame into them. The purpose of this concept in earthquake engineering is that when a building sways during an earthquake; if it has weak columns, drifts tend to concentrate in one or few stories as shown in Fig. 4.38-a, and may override the column drift limit. On the other hand, if the building has strong columns, the drifts will be more uniformly distributed as shown in Fig. 4.38-c. Furthermore, columns support the weight of the entire building, whereas beams support only the gravity loads of the floor which they form apart; thus, column's failure has a greater effect than failure of beam [41].

Studies (e.g. Kuntz and Browning 2003) have shown that the full beam mechanism can only be achieved if the column-to-beam strength ratio on the order of four. As this ratio is impractical in most cases; ACI 318 adopted this concept by specifying column-to-beam strength ratio of 1.2. Table 4.106 summarizes column-to-beam strength for previous example in model M5.

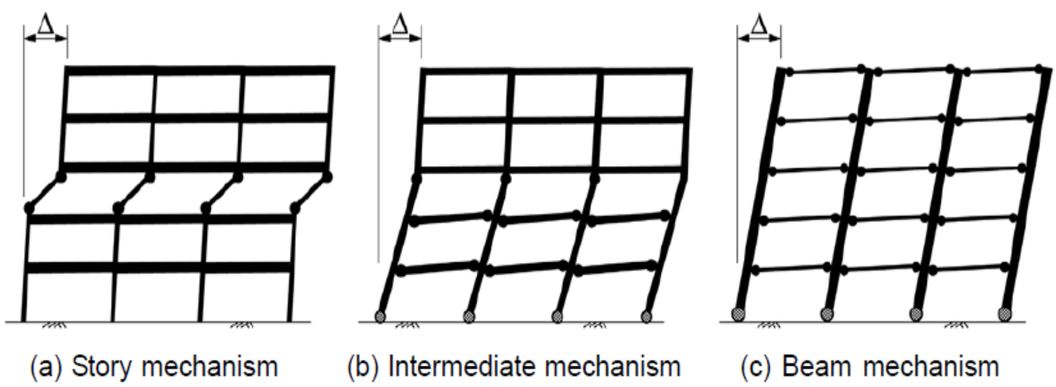

Figure 4.38 Strong-Column/Weak-Beam Concept Illustration

Table 4.106 Strong-Column/Weak-Beam Checks

Model	flexural capacity of the column (kN.m)	flexural capacity of the beam (kN.m)	column-to-beam strength	Comment
M5	790	515	1.53	>1.2

4.5 Results and discussion

For the models which abide by the proposed equation period limit; the relationship between the fundamental period and the maximum stability coefficient is drawn in Fig. 4.39. The relationship between the fundamental period and the maximum percent difference between first-order and second-order analyses (i.e. on the critical column) is drawn in Fig 4.40. Table 4.107 summarizes the maximum stability coefficient and the maximum percent difference. Table 4.108 tabulates the location of critical columns. For the models which do not abide by the proposed equation period limit; the relationship between the fundamental period and the maximum stability coefficient is drawn in Fig. 4.41. The relationship between the fundamental period and the maximum percent difference between first-order and second-order analyses (i.e. on the critical column) is drawn in Fig 4.42. Table 4.109 summarizes the maximum stability coefficient and the maximum percent difference. Table 4.110 tabulates the location of critical columns.

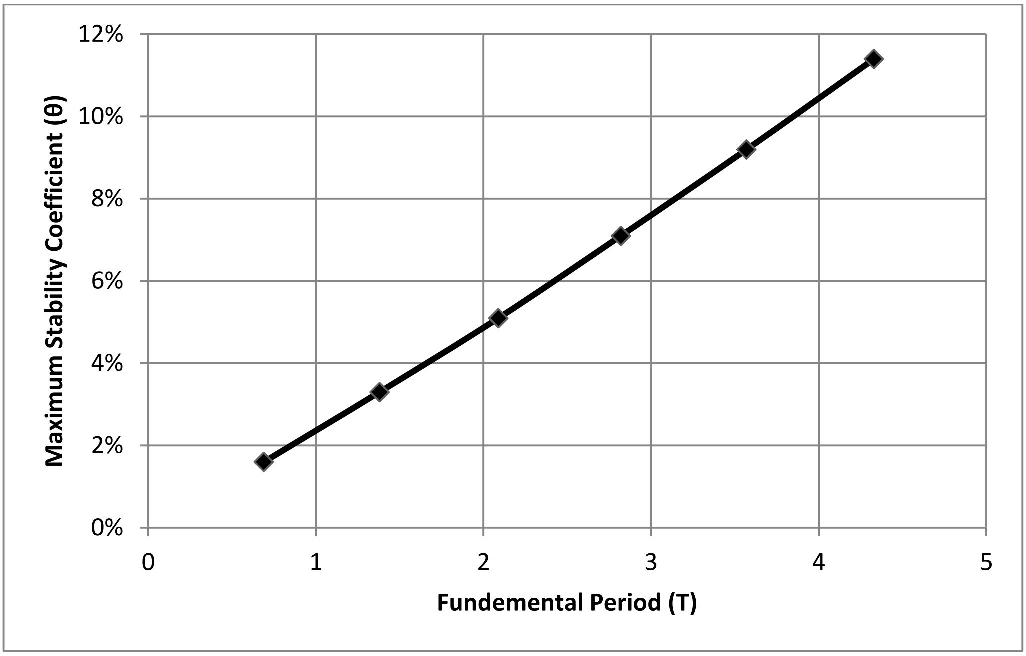

Figure 4.39 Maximum Stability Coefficient versus Fundamental Period for the Abiding Models by the Proposed Equation

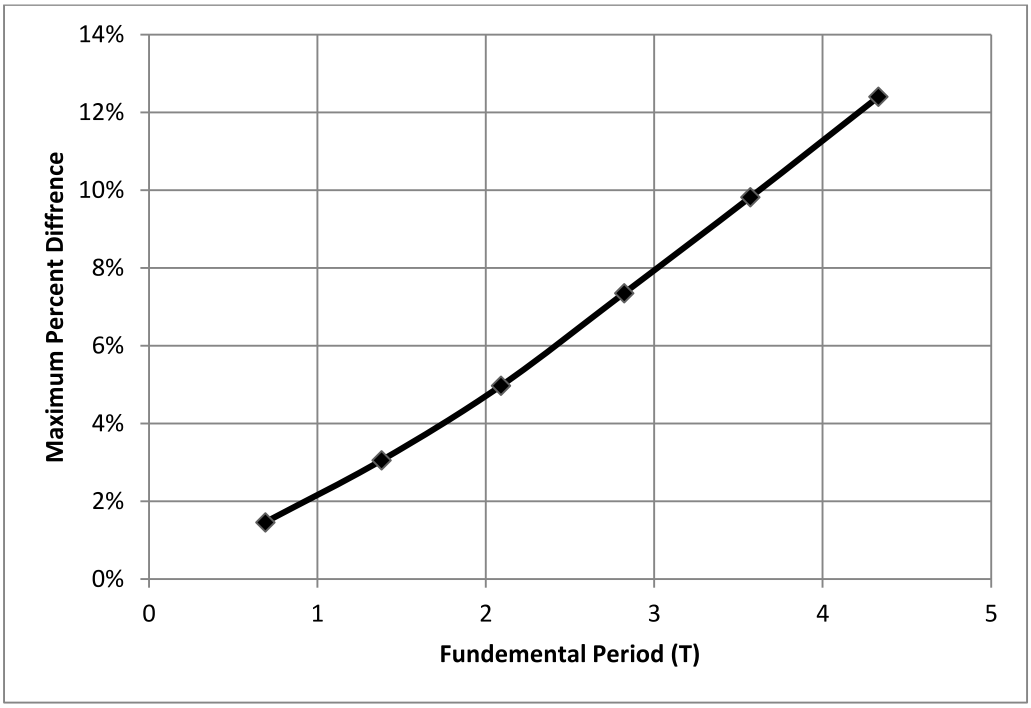

Figure 4.40 Maximum Percent Difference between First and Second-order Analyses on the Critical Column Versus the Fundamental Period for the Abiding Models by the Proposed Equation

Table 4.107 Maximum Stability Coefficient versus Maximum Percent Difference between First and Second-Order Analyses for the Abiding Models by the Proposed Equation

Model	Maximum Stability Coefficient (θ)	Maximum Percent Difference
M5	1.60%	1.46%
M10	3.30%	3.05%
M15	5.10%	4.97%
M20	7.10%	7.35%
M25	9.20%	9.82%
M30	11.40%	12.40%

Table 4.108 Location of critical Columns for the Abiding Models by the Proposed Equation

Model	Location of Critical Columns
M5	Second Storey
M10	Second Storey
M15	Third Storey
M20	Fourth Storey
M25	Fourth Storey
M30	Fifth Storey

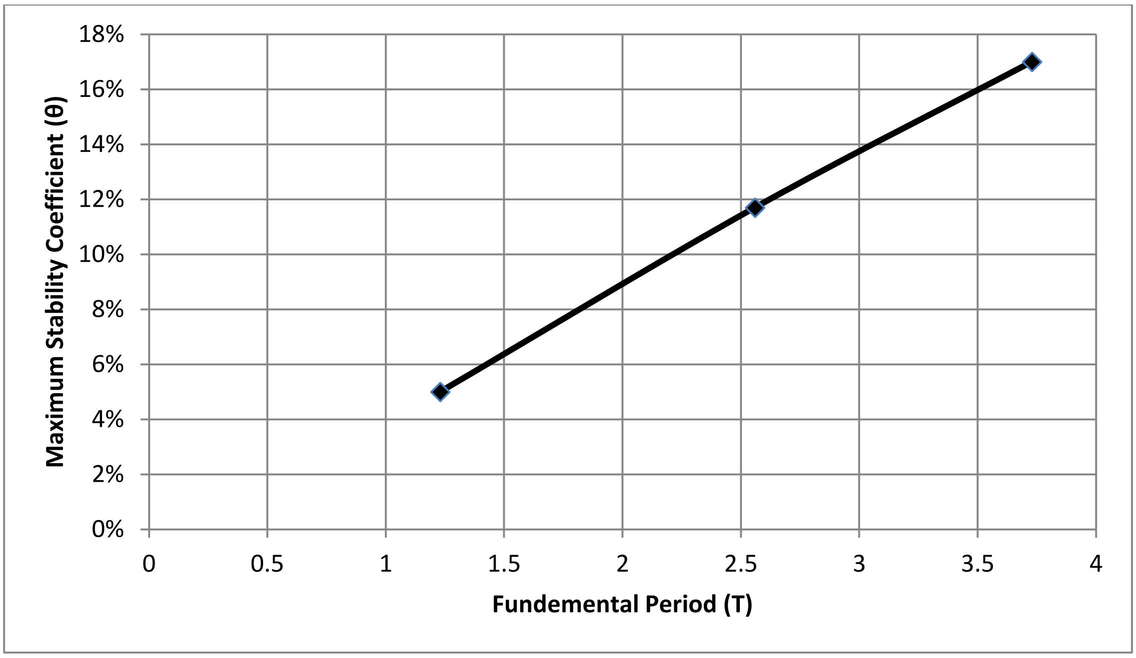

Figure 4.41 Maximum Stability Coefficient versus Fundamental Period for the non-Abiding Models by the Proposed Equation

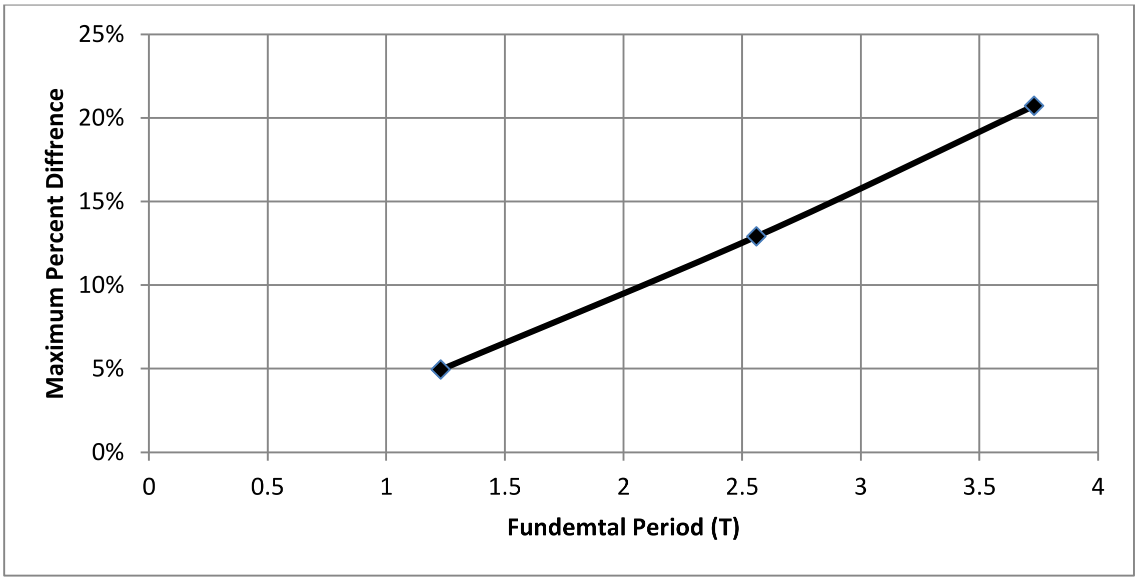

Figure 4.42 Maximum Percent Difference between First and Second-order Analyses on the Critical Column Versus the Fundamental Period for the non- Abiding Models by the Proposed Equation

Table 4.109 Maximum Stability Coefficient versus Maximum Percent Difference between First and Second-Order Analyses for the non-Abiding Models by the Proposed Equation

Model	Maximum Stability Coefficient (θ)	Maximum Percent Difference
TM5	5%	4.95%
TM10	11.7%	12.91%
TM15	17%	20.72%

Table 4.110 Location of Critical Columns for the non-Aboding Models by the Proposed Equation

Model	Location of Critical Columns
TM5	Second Storey
TM10	Third Storey
TM15	Fourth Storey

It can be noted from Figs. 4.39 and 4.41 that the period limits after which the P-Delta analysis must be included in the analysis (i.e. stability coefficient exceeds 10%) are 3.8second and 2.2second for the abiding and non-abiding models by the proposed equation respectively. It can be noted from Figs. 4.40 and 4.42 that the period limits after which the percent difference between first-order and second-order analyses exceeds 10% are 3.6second and 2.1second for the abiding and non-abiding models by the proposed equation respectively. It can be noticed from Tables 4.107 and 4.109 that for both the abiding and the non-abiding models to the proposed equation, the stability coefficient gives to some extent conservative results until 10%, and then, the percent difference on the critical column gives larger percentage (i.e. more conservative). Thus, it is concluded that when the stability coefficient exceeds 10%, its value does not describe precisely the percent difference between first-order and second-order analyses rather than its value indicates the urgent need to include the P-Delta effect in the analysis. Furthermore, it can be elicited from Tables 4.108 and 4.110 that in the non-abiding models to the proposed equation, the location of the critical column has the trend to go upward compared to the same number of storeys model nevertheless it abides by the proposed equation, concurrently; it remains in the same location in the plan. From Tables 4.107 and 4.109, it is noted that most likely engineers will not run into problems of P-Delta if they build reinforced concrete portal frames until 25storeys and 8storeys for abiding and non-abiding models by the proposed equation respectively.

Chapter Five

Summary, Conclusions, and Research Needs

5.1 Conclusions

5.1.1 General Conclusions

The research led to the following general conclusions:

1. When the number of storeys increases, the percent difference between first-order analysis and second-order analysis increases as well.
   - The percent difference between first-order analysis and second-order analysis is larger for the non-abiding models by the proposed equation (i.e. models that do not abide by Eq. 4.6).
2. When the number of storeys increases, the column which has the maximum percent difference between first-order and second-order moments (i.e. the critical column) goes upward.
   - The location of the critical column in the plan remains the same in the all models (i.e. in the edge). However, its level increases upward with increasing number of storeys.
   - The critical column has a larger willingness to go upward in the case of the non-abiding models by the proposed equation compared to the abiding models.
3. The drift is checked for all models and it is under the allowable limit, although there are problems in P-Delta above a certain number of

storeys which urges engineers not to neglect P-Delta if the drift is below the allowable limits.

4. The stability coefficient gives to some extent conservative results until 10%, and then, the percent difference on the critical column gives larger percentage (i.e. more conservative). Thus, it is concluded that when the stability coefficient exceeds 10%, its value does not describe precisely the percent difference between first-order and second-order analyses rather than its value indicates the urgent need to include the P-Delta effect in the analysis.
5. The ASCE 7 limits using Eq. 4.6 in calculations of base shear, but it was believed that this equation has implicitly another objective which is if the fundamental period of the structure abides by this equation; the structure will not run into problems of P-Delta which is proved in this thesis.
6. Abiding by Eq. 4.6 as a structure's fundamental period limit allows building approximately another 17 storeys without considering P-Delta effect.

5.1.2 Specific Conclusions

The research led to the following specific conclusions:

1. Most probably, engineers will not run problems with P-Delta if they build reinforced concrete portal frames until 25storeys for the models which abide by the proposed equation and 8storeys for the models which do not abide by the proposed equation for 10 percent of increase.

2. Most buildings in Palestine do not reach 15-storey which makes previous conclusion so valuable for structural engineers.
3. The period limits after which the P-Delta analysis must be included in the analysis are 3.6second and 2.1second for the abiding and non-abiding models by the proposed equation respectively.

5.2 Recommendations

In this research, it was decided to focus on well-defined problems for which accurate information could be obtained for deriving of the essential relationships. Research on the following topics is needed in order to generalize the results obtained in this research:

1. Variation of structural material from reinforced concrete to steel.
2. Examine other seismic force-resisting systems such as dual, shear wall systems and bracing.
3. Variation of plan and elevation configurations.
4. Study the interaction between torsion and P-delta effect.
5. Effect of inelasticity.
6. The ASCE 7-16 states that, the base shear using the modal response spectrum procedure shall not be less than 100 percent of the calculated base shear using the equivalent lateral force procedure. Thus, it is recommended to take this note into account in the future studies.

References

1) Chen, W.F. and Atsuta, T., ***Theory of beam-columns, Vol. 1: In-plane Behavior and Design,*** McGraw-Hill, New York, 1976.
2) Chen, W.F. and Lui, E.M., *Structural Stability-Theory and Implementation,* Elsevier, New York, 1987.
3) Chen, W.F. and Lui, E.M., ***Stability Design of Steel Frames***, CRC, New York, 1991.
4) ***Specification for Structural Steel Buildings***, American Institute of Steel Construction, 2016.
5) Touqan, Abdul R., ***P-Delta effect in portal frames***, PhD. Thesis, Department of Civil Engineering, Stanford University, 1989.
6) ***International Building Code 2015***, IBC 2015, International Code Council, Inc., October 2015.
7) ***Minimum Design Loads for Buildings and other Structures***, ASCE Standard ASCE/SEI 7-10, American Society of Civil Engineers, 2010.
8) Galambos, T.V., *Guide to stability design criteria for metal structures*, 5th edition, John Wiley and sons, 1998.
9) Patel, C.N., ***Cantilever Interaction of Shear Walls and Frames***, M.Sc. Thesis, Department of Civil Engineering, University of Arizona, 1968.
10) Davidson, B.J., Fenwick, R.C. and Chung, B.T., ***P-Delta effect in multi-storey structural design***, Earthquake Engineering, Tenth World Conference, 1992.

11) Didier Pettinga and Nigel Priestley, ***Accounting for P-Delta Effects in Structures when Using Direct Displacement-Based Design***, Earthquake Engineering, fourteenth World Conference, 2008.

12) Krawinkler, H. and Ibarra L.F., ***Global collapse of Frame Structures under Seismic Excitation***, Pacific Earthquake Engineering Research Center, 2005.

13) Lakshmi, s. and Sruthi, K., ***Influence of P-Delta Effect on Reinforced Concrete Buildings with Vertical Irregularity***, International research journal of engineering and technology, 2017.

14) Adams, P.F, ***Load-Deformations Relationships for simple frames***, Fritz laboratory report, 1964.

15) Rajath, R.T. and Ramegowda M., ***P-Delta analysis of multi-story reinforced concrete building***, International research journal of engineering and technology, 2016.

16) Dinar, Y., ***P-Delta effect in Reinforced Concrete Structures of Rigid Joint***, Journal of mechanical and civil engineering, 2013.

17) Salama, M.I., ***New simple equations for effective length factors***, Vol 10, Issue 2, HBRC journal, 2014.

18) Rave, J.F. and Blandon C.A., ***Structural response of buildings on mountain slopes subjected to earth pressure under seismic conditions***, 15 WCEE, 2012.

19) Duan, L. and Chen, W.F., ***Effective Length Factors of Compression Members***, structural engineering handbook, CRC Press LLC, 1999.

20) Duan, L. and Lu, Z.G., ***A modified G-factor for columns in semi-rigid frames***, research report, division of structures, California department of transportation, 1996.

21) N.N. Ambreseys, ***The seismic activity in Syria and Palestine during the middle of the 8the century; an amalgamation of historical earthquakes***, Journal of seismology, Volume 9, issue 1, 2005.

22) Gupta, A. and Krawinkler, H., ***Seismic demands for performance evaluation of steel moment resisting frame structures***, Report No.132, The John A. Blume Earthquake Engineering Center, Stanford University, 1999.

23) Pillai, S. and Chandran, N., ***Effectiveness of P-Delta Analysis in the Design of Tall Slender RC Structures,*** International Journal of Science and Research, Volume 5 Issue 6, 2016.

24) Dhadve, P. et al, ***Assessment of P-Delta Effect on High Rise Buildings***, International Journal on Recent and Innovation Trends in Computing and Communication, Volume 3, issue 5, 2015.

25) Moghadam, A. and Aziminejad, A., ***Interaction of Torsion and P-Delta Effects in Tall Buildings***, 13th World Conference on Earthquake Engineering, Vancouver, B.C., Canada, Paper No. 799, August 2004.

26) Hussein, A., Liang, R. and Nusier, Q., ***Seismicity of Jordan and Conterminous Countries***, International Conference on Recent Advances in Geotechnical Earthquake Engineering and Soil Dynamics, Missouri University of Science and Technology, 1995.

27) Kovach, R., and Andreasen, G., and Gettings, M., and Healy, J., ***Seismicity of Western Jordan***, United States geological survey, Open File Report 86-561, 1986.

28) Gupta, A. and Krawinkler, H., ***Behavior of Ductile SMRFS at Various Seismic Hazard Levels***, Journal of Structural Engineering, ASCE, Volume 126, NO. 1, January 2000.

29) Ashraf, U., Ayan B., Yousuf D., and Samiul K., ***P-Delta effect in Reinforced Concrete Structures of Rigid Joint,*** IOSR Journal of Mechanical and Civil Engineering, Volume 10, Issue 4, November 2013.

30) Mollik, M., ***Experimental study on P-Delta effect in RC high-rise building***, Journal of Civil Engineering, The institution of Engineers, Bangladesh, Vol CE 25, No.2, 1997.

31) Yousuf, D., Rahi, N., and Das, B., ***Variation of Deflection of Steel High-Rise Structure Due to P-Delta effect Considering Global slenderness Ratio***, International Journal of Emerging Technology and Advanced Engineering, Volume 3, Issue 12, December 2013.

32) Dubey, K., Sangamnerkar, P. and Soni, D., ***Dynamic Behavior of Reinforced Concrete Framed Buildings under Non Linear Analysis***, International Journal of Engineering Development and Research, Volume 2, Issue 4, 2014.

33) Malikarjuna, B. and Ranjith, A., ***Stability analysis of Steel frame structures: P-Delta analysis***, International Journal of Research in Engineering and Technology, Volume 3, Issue 8, August 2014.

34) Konapure, C. and Dhanshettei, P., ***Effect of P-Delta action on multi-story buildings***, International Journal of Engineering Research and Technology, Volume 4, Issue 1, January 2015.

35) El-Isa, Z., Eaton, D. and McKnight, S., ***Historical seismicity of the Jordan Dead Sea Transform region and seismotectonic implications***, Arabian Journal of Geosciences, Volume 8, Issue 6, June 2015.

36) Montgomery, C., ***Influence of P – Delta effects on seismic design***, Canadian Journal of Civil Engineering, Volume 8, Number 1, March 1981.

37) Zeinkiewicz, O.C. and Taylor, R.L., ***The Finite Element Method***, Volume1, the Basis, Butterworth-Heinemann, 2000.

38) Lui, E.M. and Zhang, ***Nonlinear frame analysis by the pseudo load method***, Computers and Structures, Volume 37, Issue 5, 1990.

39) Zienkiewicz, O.C., ***Incremental Displacement in Non-Linear Analysis***, International Journal for Numerical Methods in Engineering, Volume3, 1971.

40) Pauly, T., ***A Consideration of P-Delta Effects in Ductile Reinforced Concrete Frames***, The New Zealand National Society for Earthquake Engineering, Volume 11, NO. 3, 1978.

41) Moehle, J., Hooper, J. and Lubke, C., ***Seismic Design of Reinforced Concrete Special Moment Frames: A Guide for Practicing Engineers***, National Institute of Standards and Technology, 2008.

42) Duggal, S., ***Earthquake-resistant design of structures***, Oxford University Press, 2013.

43) Rafezy, B., ***What Makes a Special Moment Frame Special***, Steel Conference in San Antonio, 2017.

44) Vijayalakshmi R., Bindu N. and Vahini M., ***Effects of P-Delta on High Rise Buildings Located in Seismic Zones***, International Research Journal of Engineering and Technology, Volume4, 2017.

45) Pravin N. et al, ***Assessment of P-Delta Effect on High Rise Buildings***, International Journal on Recent and Innovation Trends in Computing and Communication, Volume3, 2015.

Appendix A

Verification of Response Shear Results

A. Verification of SAP2000 Response Shear Results

A.1 M10

Table A.1 M10-Mode 1 Modal Mass Participation Ratio

Mode1					
Level	**W_i (kN)**	**Φ_i**	**Φ_i^2**	**$W_i\ \Phi_i$**	**$W_i\Phi_i^2$**
1	5260	-0.056	0.003	-294.7	16.5
2	5260	-0.172	0.030	-904.0	155.4
3	5260	-0.308	0.095	-1619.5	498.6
4	5260	-0.446	0.199	-2347.6	1047.7
5	5260	-0.579	0.335	-3045.3	1763.1
6	4923	-0.707	0.500	-3482.8	2463.9
7	4923	-0.816	0.665	-4015.7	3275.6
8	4923	-0.901	0.812	-4435.6	3996.4
9	4923	-0.962	0.925	-4734.9	4554.0
10	4540	-1.000	1.000	-4540.0	4540.0
			$\sum$	-29420	22311
$\beta_1 = \frac{-29420}{22311} = -1.32$					
$W_{e1} = \frac{-29420^2}{22311} = 38794\text{kN}$					
Modal mass participation ratio of Mode 1 $= \frac{W_{e1}}{\text{total weight}} \times 100\%$ $= \frac{38794}{50532} \times 100\% = 77\ \%$					

Table A.2 M10-Mode1 Shear Distribution

Mode1						
Level	**T (second)**	**a**	**W (kN)**	**β Φ_i**	**Force (kN)**	**Shear (kN)**
1	1.38	0.022	5260	0.074	8.5	853.5
2	1.38	0.022	5260	0.227	26.2	844.9
3	1.38	0.022	5260	0.406	47.0	818.7
4	1.38	0.022	5260	0.589	68.1	771.7
5	1.38	0.022	5260	0.763	88.3	703.6
6	1.38	0.022	4923	0.933	101.0	615.3
7	1.38	0.022	4923	1.076	116.5	514.2
8	1.38	0.022	4923	1.188	128.7	397.7
9	1.38	0.022	4923	1.268	137.4	269.1
10	1.38	0.022	4540	1.319	131.7	131.7

Table A.3 M10-Mode 2 Modal Mass Participation Ratio

Mode 2					
Level	**W_i (kN)**	**Φ_i**	**Φ_i^2**	**$W_i\ \Phi_i$**	**$W_i\Phi_i^2$**
1	5260	0.173	0.030	909.7	157.3
2	5260	0.486	0.236	2555.1	1241.2
3	5260	0.758	0.575	3988.0	3023.7
4	5260	0.894	0.799	4701.7	4202.6
5	5260	0.859	0.737	4516.1	3877.3
6	4923	0.608	0.369	2991.1	1817.4
7	4923	0.185	0.034	910.7	168.5
8	4923	-0.292	0.085	-1438.1	420.1
9	4923	-0.711	0.506	-3501.1	2490.0
10	4540	-1.000	1.000	-4540.0	4540.0
	50532		$\sum$	11093	21938
$\beta_2 = \frac{11093}{21938} = 0.51$					
$W_{e2} = \frac{11093^2}{21938} = 5609\text{kN}$					
Modal mass participation ratio of Mode 2 $= \frac{W_{e2}}{\text{total weight}} \times 100\%$ $= \frac{5609}{50532} = 11.1\%$					

Table A.4 M10-Mode2 Shear Distribution

Mode 2						
Level	**T (second)**	**a**	**W (kN)**	**β Φ_i**	**Force (kN)**	**Shear (kN)**
1	0.44	0.063	5260	0.087	29.0	353.4
2	0.44	0.063	5260	0.246	81.4	324.4
3	0.44	0.063	5260	0.383	127.0	243.0
4	0.44	0.063	5260	0.452	149.8	116.0
5	0.44	0.063	5260	0.434	143.9	-33.8
6	0.44	0.063	4923	0.307	95.3	-177.7
7	0.44	0.063	4923	0.094	29.0	-273.0
8	0.44	0.063	4923	-0.148	-45.8	-302.0
9	0.44	0.063	4923	-0.360	-111.5	-256.2
10	0.44	0.063	4540	-0.506	-144.6	-144.6

For M10 case, mode1 and mode 2 give almost 90% of the actual mass. Thus, mode1 and mode2 are sufficient for shear calculations. The difference between hand calculations and SAP2000 is carried out for the first and second storeys as shown in Table A.5.

Table A.5 M10-Shear Force Determination Using Both Hand Calculations and SAP2000

Level	**Shear Using Hand Calculations (kN)**	**Shear Using SAP2000 (kN)**	**Percent of Error***
1	923.8	960	3.7%
2	905.0	934	3.1%

* Acceptance limit is 10%

A.2 M15

Table A.6 M15-Mode 1 Modal Mass Participation Ratio

Mode1					
Level	**W_i (kN)**	**Φ_i**	**Φ_i^2**	**$W_i\ \Phi_i$**	**$W_i\Phi_i^2$**
1	5518	-0.031	0.001	-172.1	5.4
2	5518	-0.100	0.010	-551.9	55.2
3	5518	-0.186	0.035	-1025.3	190.5
4	5518	-0.278	0.077	-1536.1	427.6
5	5518	-0.372	0.139	-2055.0	765.3
6	5260	-0.467	0.218	-2455.8	1146.5
7	5260	-0.557	0.310	-2930.1	1632.2
8	5260	-0.641	0.411	-3372.8	2162.7
9	5260	-0.718	0.516	-3778.8	2714.7
10	5260	-0.788	0.622	-4146.9	3269.4
11	4923	-0.853	0.728	-4201.0	3584.9
12	4923	-0.907	0.822	-4464.6	4049.0
13	4923	-0.949	0.900	-4671.5	4432.8
14	4923	-0.980	0.960	-4822.5	4724.0
15	4540	-1.000	1.000	-4540.0	4540.0
	78122		Σ	-44724	33700
$\beta_1 = \frac{-44724}{33700} = -1.33$					
$W_{e1} = \frac{-44724^2}{33700} = 59355\text{kN}$					
Modal mass participation ratio of Mode 1 $= \frac{W_{e1}}{\text{total weight}} \times 100\%$ $= \frac{59355}{78122} = 76\ \%$					

Table A.7M15-Mode1 Shear Distribution

Mode1						
Level	**T (second)**	**a**	**W (kN)**	**β Φ_i**	**Force (kN)**	**Shear (kN)**
1	2.09	0.0149	5518	0.041	3.4	884.4
2	2.09	0.0149	5518	0.133	10.9	881.0
3	2.09	0.0149	5518	0.247	20.3	870.1
4	2.09	0.0149	5518	0.369	30.4	849.8
5	2.09	0.0149	5518	0.494	40.6	819.4
6	2.09	0.0149	5260	0.620	48.6	778.8
7	2.09	0.0149	5260	0.739	57.9	730.2
8	2.09	0.0149	5260	0.851	66.7	672.3
9	2.09	0.0149	5260	0.953	74.7	605.6
10	2.09	0.0149	5260	1.046	82.0	530.9
11	2.09	0.0149	4923	1.132	83.1	448.9
12	2.09	0.0149	4923	1.204	88.3	365.8
13	2.09	0.0149	4923	1.259	92.4	277.5
14	2.09	0.0149	4923	1.300	95.4	185.1
15	2.09	0.0149	4540	1.327	89.8	89.8

Table A.8 M15-Mode 2 Modal Mass Participation Ratio

Mode2					
Level	**W_i (kN)**	**Φ_i**	**Φ_i^2**	**$W_i\ \Phi_i$**	**$W_i\Phi_i^2$**
1	5518	0.093	0.009	513.5	47.8
2	5518	0.286	0.082	1575.8	450.0
3	5518	0.499	0.249	2751.7	1372.2
4	5518	0.686	0.471	3786.2	2597.9
5	5518	0.821	0.675	4532.5	3722.9
6	5260	0.881	0.776	4632.5	4079.9
7	5260	0.845	0.714	4444.8	3756.0
8	5260	0.720	0.519	3788.2	2728.2
9	5260	0.520	0.271	2736.0	1423.2
10	5260	0.266	0.071	1397.7	371.4
11	4923	-0.046	0.002	-224.6	10.2
12	4923	-0.361	0.131	-1778.6	642.6
13	4923	-0.642	0.412	-3158.9	2026.9
14	4923	-0.858	0.736	-4224.1	3624.4
15	4540	-1.000	1.000	-4540.0	4540.0
	78122		Σ	16233	31394

$$\beta_2 = \frac{16233}{31394} = 0.52$$

$$W_{e2} = \frac{16233^2}{31394} = 8394\text{kN}$$

$$\text{Modal mass participation ratio of Mode 2} = \frac{W_{e2}}{\text{total weight}} \times 100\%$$

$$= \frac{8394}{78122} = 10.7\%$$

Table A.9 M15-Mode2 Shear Distribution

Mode 2						
Level	**T (second)**	**a**	**W (kN)**	**β Φ_i**	**Force (kN)**	**Shear (kN)**
1	0.69	0.045	5518	0.048	11.9	377.7
2	0.69	0.045	5518	0.148	36.7	365.8
3	0.69	0.045	5518	0.258	64.0	329.1
4	0.69	0.045	5518	0.355	88.1	265.1
5	0.69	0.045	5518	0.425	105.5	177.0
6	0.69	0.045	5260	0.455	107.8	71.5
7	0.69	0.045	5260	0.437	103.4	-36.3
8	0.69	0.045	5260	0.372	88.1	-139.7
9	0.69	0.045	5260	0.269	63.7	-227.9
10	0.69	0.045	5260	0.137	32.5	-291.5
11	0.69	0.045	4923	-0.024	-5.2	-324.0
12	0.69	0.045	4923	-0.187	-41.4	-318.8
13	0.69	0.045	4923	-0.332	-73.5	-277.4
14	0.69	0.045	4923	-0.444	-98.3	-203.9
15	0.69	0.045	4540	-0.517	-105.6	-105.6

Table A.10 M15-Mode 3 Modal Mass Participation Ratio

Mode3					
Level	**W_i (kN)**	**Φ_i**	**Φ_i^2**	**$W_i\ \Phi_i$**	**$W_i\Phi_i^2$**
1	5518	-0.165	0.027	-908.8	149.7
2	5518	-0.470	0.221	-2591.4	1217.0
3	5518	-0.730	0.533	-4028.6	2941.2
4	5518	-0.838	0.703	-4626.4	3878.8
5	5518	-0.755	0.570	-4164.6	3143.2
6	5260	-0.464	0.215	-2439.9	1131.7
7	5260	-0.030	0.001	-156.5	4.7
8	5260	0.420	0.177	2210.1	928.6
9	5260	0.764	0.584	4020.0	3072.2
10	5260	0.922	0.851	4851.7	4475.1
11	4923	0.806	0.650	3969.6	3200.9
12	4923	0.412	0.169	2026.7	834.3
13	4923	-0.122	0.015	-601.1	73.4
14	4923	-0.633	0.401	-3116.7	1973.1
15	4540	-1.000	1.000	-4540.0	4540.0
	78122		Σ	-10096	31564
$\beta_3 = \frac{-10096}{31564}$ =-0.32					
$W_{e3} = \frac{-10096^2}{31564}$ =3229kN					
Modal mass participation ratio of Mode 3 $= \frac{W_{e3}}{\text{total weight}} \times 100\%$ $= \frac{3229}{78122} = 4.1\ \%$					

Table A.11 M15-Mode3 Shear Distribution

Mode3						
Level	**T (second)**	**a**	**W (kN)**	**β Φ_i**	**Force (kN)**	**Shear (kN)**
1	0.38	0.063	5518	0.053	18.3	203.4
2	0.38	0.063	5518	0.150	52.2	185.1
3	0.38	0.063	5518	0.234	81.2	132.9
4	0.38	0.063	5518	0.268	93.2	51.7
5	0.38	0.063	5518	0.241	83.9	-41.5
6	0.38	0.063	5260	0.148	49.2	-125.4
7	0.38	0.063	5260	0.010	3.2	-174.6
8	0.38	0.063	5260	-0.134	-44.5	-177.7
9	0.38	0.063	5260	-0.244	-81.0	-133.2
10	0.38	0.063	5260	-0.295	-97.8	-52.2
11	0.38	0.063	4923	-0.258	-80.0	45.6
12	0.38	0.063	4923	-0.132	-40.8	125.6
13	0.38	0.063	4923	0.039	12.1	166.4
14	0.38	0.063	4923	0.202	62.8	154.3
15	0.38	0.063	4540	0.320	91.5	91.5

For M15 case, mode1, mode 2 and mode3 give 91% of the actual mass. Thus, mode1, mode2 and mode 3are sufficient for shear calculations. The difference between hand calculations and SAP2000 is carried out for the first and second storeys as shown in Table A.12.

Table A.12 M15-Shear Force Determination Using Both Hand Calculations and SAP2000

Level	**Shear Using Hand Calculations (kN)**	**Shear Using SAP2000 (kN)**	**Percent of Error***
1	983	1007	2.4%
2	972	993	2.1%

***** Acceptance limit is 10%

A.3 M20

Table A.13 M20-Mode 1 Modal Mass Participation Ratio

	Mode1				
Level	**W_i (kN)**	**Φ_i**	**Φ_i^2**	**$W_i\ \Phi_i$**	**$W_i\Phi_i^2$**
1	5803	0.020	0.0004	114.3	2.3
2	5803	0.065	0.0043	378.5	24.7
3	5803	0.124	0.0155	722.1	89.9
4	5803	0.191	0.0363	1106.2	210.9
5	5803	0.260	0.0676	1508.7	392.2
6	5518	0.331	0.1099	1828.9	606.2
7	5518	0.402	0.1620	2220.9	893.9
8	5518	0.472	0.2226	2603.3	1228.2
9	5518	0.539	0.2902	2972.6	1601.3
10	5518	0.603	0.3634	3326.6	2005.4
11	5260	0.665	0.4419	3496.7	2324.5
12	5260	0.722	0.5216	3798.9	2743.6
13	5260	0.775	0.6005	4076.2	3158.8
14	5260	0.823	0.6771	4328.2	3561.4
15	5260	0.866	0.7500	4555.2	3944.9
16	4923	0.906	0.8206	4459.6	4039.8
17	4923	0.939	0.8817	4622.5	4340.4
18	4923	0.965	0.9322	4753.1	4589.1
19	4923	0.986	0.9714	4852.0	4782.1
20	4540	1.000	1.0000	4540.0	4540.0
	107137		$\sum$	60264	45080
$\beta_1 = \frac{60264}{45080} = 1.34$					
$W_{e1} = \frac{60264^2}{45080} = 80564\text{kN}$					
Modal mass participation ratio of Mode 1 $= \frac{W_{e1}}{\text{total weight}} \times 100\%$ $= \frac{80564}{107137} = 75.2\%$					

Table A.14 M20-Mode1 Shear Distribution

Mode1						
Level	**T (second)**	**a**	**W (kN)**	**β Φ_i**	**Force (kN)**	**Shear (kN)**
1	2.82	0.011	5803	0.026	1.7	886.2
2	2.82	0.011	5803	0.087	5.6	884.5
3	2.82	0.011	5803	0.166	10.6	879.0
4	2.82	0.011	5803	0.255	16.3	868.3
5	2.82	0.011	5803	0.348	22.2	852.1
6	2.82	0.011	5518	0.443	26.9	829.9
7	2.82	0.011	5518	0.538	32.7	803.0
8	2.82	0.011	5518	0.631	38.3	770.3
9	2.82	0.011	5518	0.720	43.7	732.1
10	2.82	0.011	5518	0.806	48.9	688.3
11	2.82	0.011	5260	0.889	51.4	639.4
12	2.82	0.011	5260	0.966	55.9	588.0
13	2.82	0.011	5260	1.036	59.9	532.1
14	2.82	0.011	5260	1.100	63.6	472.2
15	2.82	0.011	5260	1.158	67.0	408.6
16	2.82	0.011	4923	1.211	65.6	341.6
17	2.82	0.011	4923	1.255	68.0	276.0
18	2.82	0.011	4923	1.291	69.9	208.0
19	2.82	0.011	4923	1.318	71.4	138.1
20	2.82	0.011	4540	1.337	66.8	66.8

Table A.15 M20-Mode 2 Modal Mass Participation Ratio

Mode2					
Level	**W_i (kN)**	**Φ_i**	**Φ_i^2**	**$W_i \Phi_i$**	**$W_i\Phi_i^2$**
1	5803	0.059	0.003	341.4	20.1
2	5803	0.189	0.036	1098.7	208.0
3	5803	0.348	0.121	2019.8	703.0
4	5803	0.508	0.258	2948.7	1498.4
5	5803	0.653	0.426	3788.1	2472.8
6	5518	0.768	0.590	4239.5	3257.3
7	5518	0.840	0.705	4633.9	3891.5
8	5518	0.863	0.745	4761.4	4108.5
9	5518	0.837	0.701	4618.6	3865.7
10	5518	0.765	0.585	4222.0	3230.4
11	5260	0.644	0.415	3387.3	2181.3
12	5260	0.479	0.230	2520.3	1207.6
13	5260	0.283	0.080	1488.9	421.5
14	5260	0.068	0.005	357.2	24.3
15	5260	-0.155	0.024	-814.4	126.1
16	4923	-0.388	0.151	-1911.8	742.4
17	4923	-0.601	0.361	-2956.9	1776.0
18	4923	-0.778	0.605	-3830.0	2979.6
19	4923	-0.911	0.830	-4486.2	4088.1
20	4540	-1.000	1.000	-4540.0	4540.0
	107137		Σ	21887	41342

$$\beta_2 = \frac{21887}{41342} = 0.53$$

$$W_{e2} = \frac{21887^2}{41342} = 11587\text{kN}$$

$$\text{Modal mass participation ratio of Mode 2} = \frac{W_{e2}}{\text{total weight}} \times 100\%$$

$$= \frac{11587}{107137} = 11\%$$

Table A.16 M20-Mode2 Shear Distribution

Mode 2						
Level	**T (second)**	**a**	**W (kN)**	**β Φ_i**	**Force (kN)**	**Shear (kN)**
1	0.94	0.033	5803	0.031	6.0	382.4
2	0.94	0.033	5803	0.100	19.2	376.4
3	0.94	0.033	5803	0.184	35.3	357.2
4	0.94	0.033	5803	0.269	51.5	321.9
5	0.94	0.033	5803	0.346	66.2	270.4
6	0.94	0.033	5518	0.407	74.1	204.2
7	0.94	0.033	5518	0.445	81.0	130.2
8	0.94	0.033	5518	0.457	83.2	49.2
9	0.94	0.033	5518	0.443	80.7	-34.0
10	0.94	0.033	5518	0.405	73.8	-114.7
11	0.94	0.033	5260	0.341	59.2	-188.4
12	0.94	0.033	5260	0.254	44.0	-247.6
13	0.94	0.033	5260	0.150	26.0	-291.6
14	0.94	0.033	5260	0.036	6.2	-317.6
15	0.94	0.033	5260	-0.082	-14.2	-323.9
16	0.94	0.033	4923	-0.206	-33.4	-309.7
17	0.94	0.033	4923	-0.318	-51.7	-276.3
18	0.94	0.033	4923	-0.412	-66.9	-224.6
19	0.94	0.033	4923	-0.482	-78.4	-157.7
20	0.94	0.033	4540	-0.529	-79.3	-79.3

Table A.17 M20-Mode3 Modal Mass Participation Ratio

Mode3					
Level	**W_i (kN)**	**Φ_i**	**Φ_i^2**	**$W_i\ \Phi_i$**	**$W_i\Phi_i^2$**
1	5803	0.102	0.010	592.0	60.4
2	5803	0.314	0.099	1824.3	573.5
3	5803	0.543	0.294	3148.1	1707.9
4	5803	0.724	0.524	4201.3	3041.6
5	5803	0.822	0.676	4770.4	3921.6
6	5518	0.804	0.646	4434.1	3563.1
7	5518	0.655	0.429	3614.4	2367.5
8	5518	0.402	0.162	2217.6	891.2
9	5518	0.083	0.007	458.7	38.1
10	5518	-0.255	0.065	-1409.3	359.9
11	5260	-0.569	0.323	-2991.2	1701.0
12	5260	-0.791	0.626	-4161.4	3292.2
13	5260	-0.886	0.785	-4659.7	4127.8
14	5260	-0.839	0.704	-4412.5	3701.6
15	5260	-0.662	0.439	-3483.7	2307.3
16	4923	-0.343	0.118	-1687.5	578.5
17	4923	0.057	0.003	280.8	16.0
18	4923	0.455	0.207	2237.7	1017.1
19	4923	0.781	0.610	3845.3	3003.4
20	4540	1.000	1.000	4540.0	4540.0
	107137		Σ	13359	40810

$$\beta_3 = \frac{13359}{40810} = 0.33$$

$$W_{e3} = \frac{13359^2}{40810} = 4373\text{kN}$$

Modal mass participation ratio of Mode 3 = $\frac{W_{e3}}{\text{total weight}} \times 100\% = \frac{4373}{107137} = 4.1\%$

Table A.18 M20-Mode3 Shear Distribution

Mode3						
Level	**T (second)**	**a**	**W (kN)**	**β Φ_i**	**Force (kN)**	**Shear (kN)**
1	0.53	0.059	5803	0.033	11.4	258.0
2	0.53	0.059	5803	0.103	35.2	246.6
3	0.53	0.059	5803	0.178	60.8	211.4
4	0.53	0.059	5803	0.237	81.1	150.6
5	0.53	0.059	5803	0.269	92.1	69.4
6	0.53	0.059	5518	0.263	85.6	-22.7
7	0.53	0.059	5518	0.214	69.8	-108.4
8	0.53	0.059	5518	0.132	42.8	-178.2
9	0.53	0.059	5518	0.027	8.9	-221.0
10	0.53	0.059	5518	-0.084	-27.2	-229.9
11	0.53	0.059	5260	-0.186	-57.8	-202.6
12	0.53	0.059	5260	-0.259	-80.4	-144.9
13	0.53	0.059	5260	-0.290	-90.0	-64.5
14	0.53	0.059	5260	-0.275	-85.2	25.5
15	0.53	0.059	5260	-0.217	-67.3	110.7
16	0.53	0.059	4923	-0.112	-32.6	178.0
17	0.53	0.059	4923	0.019	5.4	210.6
18	0.53	0.059	4923	0.149	43.2	205.2
19	0.53	0.059	4923	0.256	74.3	162.0
20	0.53	0.059	4540	0.327	87.7	87.7

For M20 case, mode1, mode 2 and mode 3 give 90.3% of the actual mass. Thus, mode1, mode 2 and mode 3 are sufficient for shear calculations. The difference between hand calculations and SAP2000 is carried out for the first and second storeys as shown in Table A.19.

Table A.19 M20-Shear Force Determination Using Both Hand Calculations and SAP2000

Level	Shear Using Hand Calculations (kN)	Shear Using SAP2000 (kN)	Percent of Error*
1	999	1030	3.0%
2	992	1020	2.7%

* Acceptance limit is 10%

A.4 M25

Table A.20 M25-Mode 1 Modal Mass Participation Ratio

Mode1					
Level	**W_i (kN)**	**Φ_i**	**Φ_i^2**	**$W_i\ \Phi_i$**	**$W_i\Phi_i^2$**
1	6116	0.013	0.0002	81.9	1.1
2	6116	0.045	0.0021	278.1	12.6
3	6116	0.089	0.0079	541.9	48.0
4	6116	0.138	0.0191	844.6	116.6
5	6116	0.191	0.0365	1169.0	223.4
6	5803	0.247	0.0609	1431.9	353.3
7	5803	0.303	0.0920	1760.3	534.0
8	5803	0.360	0.1294	2087.9	751.2
9	5803	0.416	0.1728	2411.9	1002.5
10	5803	0.470	0.2213	2729.8	1284.1
11	5518	0.525	0.2751	2894.3	1518.1
12	5518	0.577	0.3324	3181.5	1834.4
13	5518	0.626	0.3924	3456.7	2165.4
14	5518	0.674	0.4542	3718.9	2506.4
15	5518	0.719	0.5171	3968.2	2853.6
16	5260	0.762	0.5812	4009.9	3056.9
17	5260	0.802	0.6437	4220.0	3385.7
18	5260	0.839	0.7038	4412.7	3701.8
19	5260	0.872	0.7606	4587.4	4000.8
20	5260	0.902	0.8140	4745.8	4281.8
21	4923	0.930	0.8652	4579.2	4259.4
22	4923	0.954	0.9095	4695.0	4477.6
23	4923	0.973	0.9467	4790.0	4660.6
24	4923	0.988	0.9767	4865.3	4808.2
25	4540	1.000	1.0000	4540.0	4540.0
	137717		$\sum$	76002	56378
$\beta_1 = \frac{76002}{56378} = 1.35$					
$W_{e1} = \frac{76002^2}{56378} = 102458\text{kN}$					
Modal mass participation ratio of Mode 1 $= \frac{W_{e1}}{\text{total weight}} \times 100\% = \frac{102458}{137717} = 74.4\%$					

Table A.21 M25-Mode1 Shear Distribution

Mode1						
Level	**T (second)**	**a**	**W (kN)**	**β Φ_i**	**Force (kN)**	**Shear (kN)**
1	3.57	0.0087	6116	0.018	1.0	891.4
2	3.57	0.0087	6116	0.061	3.3	890.4
3	3.57	0.0087	6116	0.119	6.4	887.2
4	3.57	0.0087	6116	0.186	9.9	880.8
5	3.57	0.0087	6116	0.258	13.7	870.9
6	3.57	0.0087	5803	0.333	16.8	857.2
7	3.57	0.0087	5803	0.409	20.6	840.4
8	3.57	0.0087	5803	0.485	24.5	819.7
9	3.57	0.0087	5803	0.560	28.3	795.3
10	3.57	0.0087	5803	0.634	32.0	767.0
11	3.57	0.0087	5518	0.707	33.9	735.0
12	3.57	0.0087	5518	0.777	37.3	701.0
13	3.57	0.0087	5518	0.844	40.5	663.7
14	3.57	0.0087	5518	0.909	43.6	623.2
15	3.57	0.0087	5518	0.969	46.5	579.5
16	3.57	0.0087	5260	1.028	47.0	533.0
17	3.57	0.0087	5260	1.082	49.5	486.0
18	3.57	0.0087	5260	1.131	51.8	436.5
19	3.57	0.0087	5260	1.176	53.8	384.7
20	3.57	0.0087	5260	1.216	55.7	330.9
21	3.57	0.0087	4923	1.254	53.7	275.3
22	3.57	0.0087	4923	1.286	55.1	221.6
23	3.57	0.0087	4923	1.312	56.2	166.5
24	3.57	0.0087	4923	1.332	57.1	110.3
25	3.57	0.0087	4540	1.348	53.2	53.2

Table A.22 M25-Mode 2 Modal Mass Participation Ratio

Mode2					
Level	**W_i (kN)**	**Φ_i**	**Φ_i^2**	**$W_i\ \Phi_i$**	**$W_i\Phi_i^2$**
1	6116	-0.040	0.002	-246.7	10.0
2	6116	-0.134	0.018	-820.7	110.1
3	6116	-0.255	0.065	-1558.1	396.9
4	6116	-0.385	0.148	-2352.7	905.0
5	6116	-0.512	0.263	-3134.0	1605.9
6	5803	-0.629	0.396	-3652.2	2298.6
7	5803	-0.726	0.527	-4210.7	3055.4
8	5803	-0.797	0.635	-4622.6	3682.3
9	5803	-0.840	0.705	-4871.8	4090.0
10	5803	-0.854	0.729	-4955.8	4232.3
11	5518	-0.836	0.699	-4612.5	3855.6
12	5518	-0.783	0.613	-4320.0	3382.1
13	5518	-0.699	0.488	-3856.1	2694.7
14	5518	-0.588	0.345	-3243.1	1906.1
15	5518	-0.455	0.207	-2508.3	1140.1
16	5260	-0.299	0.089	-1571.6	469.6
17	5260	-0.128	0.016	-675.0	86.6
18	5260	0.049	0.002	258.3	12.7
19	5260	0.227	0.051	1193.4	270.8
20	5260	0.400	0.160	2101.9	839.9
21	4923	0.571	0.326	2810.0	1603.9
22	4923	0.720	0.519	3546.9	2555.4
23	4923	0.843	0.711	4151.9	3501.5
24	4923	0.936	0.876	4608.2	4313.5
25	4540	1.000	1.000	4540.0	4540.0
	137717		$\sum$	-28001	51559
$\beta_2 = \frac{-28001}{51559} = -0.54$					
$W_{e2} = \frac{-28001^2}{51559} = 15207\text{kN}$					
Modal mass participation ratio of Mode 2 = $\frac{W_{e2}}{\text{total weight}} \times 100\% = \frac{15207}{137717} = 11\ \%$					

Table A.23 M25-Mode2 Shear Distribution

Mode2						
Level	**T (second)**	**a**	**W (kN)**	**β Φ_i**	**Force (kN)**	**Shear (kN)**
1	1.19	0.026	6116	0.022	3.5	395.4
2	1.19	0.026	6116	0.073	11.6	391.9
3	1.19	0.026	6116	0.138	22.0	380.3
4	1.19	0.026	6116	0.209	33.2	358.3
5	1.19	0.026	6116	0.278	44.3	325.1
6	1.19	0.026	5803	0.342	51.6	280.8
7	1.19	0.026	5803	0.394	59.5	229.3
8	1.19	0.026	5803	0.433	65.3	169.8
9	1.19	0.026	5803	0.456	68.8	104.5
10	1.19	0.026	5803	0.464	70.0	35.8
11	1.19	0.026	5518	0.454	65.1	-34.2
12	1.19	0.026	5518	0.425	61.0	-99.4
13	1.19	0.026	5518	0.380	54.4	-160.4
14	1.19	0.026	5518	0.319	45.8	-214.8
15	1.19	0.026	5518	0.247	35.4	-260.6
16	1.19	0.026	5260	0.162	22.2	-296.0
17	1.19	0.026	5260	0.070	9.5	-318.2
18	1.19	0.026	5260	-0.027	-3.6	-327.7
19	1.19	0.026	5260	-0.123	-16.9	-324.1
20	1.19	0.026	5260	-0.217	-29.7	-307.2
21	1.19	0.026	4923	-0.310	-39.7	-277.6
22	1.19	0.026	4923	-0.391	-50.1	-237.9
23	1.19	0.026	4923	-0.458	-58.6	-187.8
24	1.19	0.026	4923	-0.508	-65.1	-129.2
25	1.19	0.026	4540	-0.543	-64.1	-64.1

Table A.24 M25-Mode 3 Modal Mass Participation Ratio

Mode3					
Level	**W_i (kN)**	**Φ_i**	**Φ_i^2**	**$W_i\ \Phi_i$**	**$W_i\Phi_i^2$**
1	6116	0.069	0.0048	423.0	29.3
2	6116	0.223	0.0498	1365.0	304.7
3	6116	0.407	0.1655	2488.4	1012.5
4	6116	0.581	0.3381	3556.3	2067.9
5	6116	0.721	0.5200	4410.1	3180.1
6	5803	0.801	0.6416	4648.4	3723.5
7	5803	0.802	0.6428	4652.5	3730.1
8	5803	0.723	0.5225	4194.8	3032.3
9	5803	0.572	0.3277	3321.7	1901.4
10	5803	0.365	0.1335	2120.6	775.0
11	5518	0.113	0.0128	624.9	70.8
12	5518	-0.157	0.0247	-867.3	136.3
13	5518	-0.415	0.1722	-2290.1	950.4
14	5518	-0.634	0.4019	-3498.4	2217.9
15	5518	-0.795	0.6321	-4387.0	3487.8
16	5260	-0.877	0.7686	-4611.4	4042.7
17	5260	-0.858	0.7370	-4515.6	3876.5
18	5260	-0.746	0.5564	-3923.7	2926.8
19	5260	-0.553	0.3054	-2906.8	1606.3
20	5260	-0.300	0.0899	-1576.8	472.7
21	4923	0.015	0.0002	74.9	1.1
22	4923	0.339	0.1146	1666.4	564.1
23	4923	0.628	0.3942	3090.9	1940.6
24	4923	0.852	0.7262	4195.3	3575.2
25	4540	1.000	1.0000	4540.0	4540.0
	137717		$\sum$	16796	50166
$\beta_3 = \frac{16796}{50166} = 0.33$					
$W_{e3} = \frac{16796^2}{50166} = 5624$ kN					
Modal mass participation ratio of Mode 3 = $\frac{W_{e3}}{\text{total weight}} \times 100\% = \frac{5624}{137717} = 4.1\ \%$					

Table A.25 M25-Mode3 Shear Distribution

Mode3						
Level	**T (second)**	**a**	**W (kN)**	**β Φ$_i$**	**Force (kN)**	**Shear (kN)**
1	0.67	0.047	6116	0.023	6.7	264.3
2	0.67	0.047	6116	0.075	21.5	257.7
3	0.67	0.047	6116	0.136	39.2	236.2
4	0.67	0.047	6116	0.195	56.0	197.0
5	0.67	0.047	6116	0.241	69.4	141.1
6	0.67	0.047	5803	0.268	73.1	71.7
7	0.67	0.047	5803	0.268	73.2	-1.5
8	0.67	0.047	5803	0.242	66.0	-74.7
9	0.67	0.047	5803	0.192	52.3	-140.7
10	0.67	0.047	5803	0.122	33.4	-193.0
11	0.67	0.047	5518	0.038	9.8	-226.4
12	0.67	0.047	5518	-0.053	-13.6	-236.2
13	0.67	0.047	5518	-0.139	-36.0	-222.5
14	0.67	0.047	5518	-0.212	-55.1	-186.5
15	0.67	0.047	5518	-0.266	-69.0	-131.5
16	0.67	0.047	5260	-0.294	-72.6	-62.4
17	0.67	0.047	5260	-0.287	-71.1	10.1
18	0.67	0.047	5260	-0.250	-61.7	81.2
19	0.67	0.047	5260	-0.185	-45.7	142.9
20	0.67	0.047	5260	-0.100	-24.8	188.7
21	0.67	0.047	4923	0.005	1.2	213.5
22	0.67	0.047	4923	0.113	26.2	212.3
23	0.67	0.047	4923	0.210	48.6	186.1
24	0.67	0.047	4923	0.285	66.0	137.5
25	0.67	0.047	4540	0.335	71.4	71.4

For M25 case, mode1, mode 2 and mode 3 give almost 90% of the actual mass. Thus, mode1 and mode2 and mode 3 are sufficient for shear calculations. The difference between hand calculations and SAP2000 is carried out for the first and second storeys as shown in Table A.26.

Table A.26 M25-Shear Force Determination Using Both Hand Calculations and SAP2000

Level	Shear Using Hand Calculations (kN)	Shear Using SAP2000 (kN)	Percent of Error*
1	1010	1044	3.3%
2	1006	1038	3.1%

* acceptance limit is 10%

A.5 M30

Table A.27 M30-Mode1 Modal Mass Participation Ratio

Mode1					
Level	**W_i (kN)**	**Φ_i**	**Φ_i^2**	**W_i Φ_i**	**$W_i\Phi_i^2$**
1	6456	-0.010	0.0001	-61.5	0.6
2	6456	-0.033	0.0011	-214.0	7.1
3	6456	-0.066	0.0043	-423.7	27.8
4	6456	-0.104	0.0108	-670.3	69.6
5	6456	-0.146	0.0212	-939.4	136.7
6	6116	-0.190	0.0361	-1161.6	220.6
7	6116	-0.236	0.0556	-1442.3	340.1
8	6116	-0.282	0.0797	-1727.2	487.7
9	6116	-0.329	0.1083	-2012.5	662.2
10	6116	-0.376	0.1410	-2296.8	862.5
11	5803	-0.422	0.1780	-2448.5	1033.1
12	5803	-0.467	0.2185	-2712.5	1267.9
13	5803	-0.512	0.2620	-2970.3	1520.3
14	5803	-0.555	0.3081	-3221.3	1788.1
15	5803	-0.597	0.3566	-3465.5	2069.6
16	5518	-0.638	0.4074	-3522.1	2248.2
17	5518	-0.678	0.4591	-3738.9	2533.4
18	5518	-0.715	0.5114	-3946.0	2821.8
19	5518	-0.751	0.5636	-4142.6	3110.1
20	5518	-0.784	0.6154	-4328.7	3395.8
21	5260	-0.817	0.6671	-4296.3	3509.2
22	5260	-0.847	0.7168	-4453.2	3770.2
23	5260	-0.874	0.7641	-4597.9	4019.2
24	5260	-0.899	0.8086	-4730.0	4253.4
25	5260	-0.922	0.8503	-4850.3	4472.5
26	4923	-0.943	0.8900	-4644.4	4381.5
27	4923	-0.962	0.9249	-4734.5	4553.3
28	4923	-0.977	0.9548	-4810.4	4700.4
29	4923	-0.990	0.9796	-4872.4	4822.4
30	4540	-1.000	1.0000	-4540.0	4540.0
	169997		$\sum$	-91975	67625
$\beta_1 = \frac{-91975}{67625} = -1.36$					
$W_{e1} = \frac{-91975^2}{67625} = 125093$ kN					
Modal mass participation ratio of Mode 1 $= \frac{W_{e1}}{\text{total weight}} \times 100\% = \frac{125093}{169997} = 74\%$					

Table A.28 M30-Mode1 Shear Distribution

	Mode1					
Level	**T (second)**	**a**	**W (kN)**	**β Φ_i**	**Force (kN)**	**Shear (kN)**
1	4.33	0.0067	6456	0.013	0.6	838.1
2	4.33	0.0067	6456	0.045	1.9	837.6
3	4.33	0.0067	6456	0.089	3.9	835.6
4	4.33	0.0067	6456	0.141	6.1	831.7
5	4.33	0.0067	6456	0.198	8.6	825.6
6	4.33	0.0067	6116	0.258	10.6	817.1
7	4.33	0.0067	6116	0.321	13.1	806.5
8	4.33	0.0067	6116	0.384	15.7	793.4
9	4.33	0.0067	6116	0.448	18.3	777.6
10	4.33	0.0067	6116	0.511	20.9	759.3
11	4.33	0.0067	5803	0.574	22.3	738.3
12	4.33	0.0067	5803	0.636	24.7	716.0
13	4.33	0.0067	5803	0.696	27.1	691.3
14	4.33	0.0067	5803	0.755	29.4	664.2
15	4.33	0.0067	5803	0.812	31.6	634.9
16	4.33	0.0067	5518	0.868	32.1	603.3
17	4.33	0.0067	5518	0.922	34.1	571.2
18	4.33	0.0067	5518	0.973	36.0	537.2
19	4.33	0.0067	5518	1.021	37.7	501.2
20	4.33	0.0067	5518	1.067	39.4	463.4
21	4.33	0.0067	5260	1.111	39.1	424.0
22	4.33	0.0067	5260	1.151	40.6	384.8
23	4.33	0.0067	5260	1.189	41.9	344.3
24	4.33	0.0067	5260	1.223	43.1	302.4
25	4.33	0.0067	5260	1.254	44.2	259.3
26	4.33	0.0067	4923	1.283	42.3	215.1
27	4.33	0.0067	4923	1.308	43.1	172.7
28	4.33	0.0067	4923	1.329	43.8	129.6
29	4.33	0.0067	4923	1.346	44.4	85.8
30	4.33	0.0067	4540	1.360	41.4	41.4

Table A.29 M30-Mode2 Modal Mass Participation Ratio

Mode2					
Level	**W_i (kN)**	**Φ_i**	**Φ_i^2**	**$W_i\ \Phi_i$**	**$W_i\Phi_i^2$**
1	6456	0.029	0.0008	187.9	5.5
2	6456	0.099	0.0098	640.4	63.5
3	6456	0.193	0.0372	1244.5	239.9
4	6456	0.298	0.0887	1922.8	572.7
5	6456	0.406	0.1650	2622.1	1065.0
6	6116	0.512	0.2619	3130.0	1601.9
7	6116	0.608	0.3698	3719.3	2261.8
8	6116	0.691	0.4778	4227.5	2922.2
9	6116	0.758	0.5751	4638.3	3517.6
10	6116	0.808	0.6533	4943.3	3995.5
11	5803	0.838	0.7018	4861.5	4072.8
12	5803	0.843	0.7114	4894.7	4128.5
13	5803	0.826	0.6827	4794.8	3961.8
14	5803	0.787	0.6200	4569.3	3597.9
15	5803	0.729	0.5313	4229.7	3083.0
16	5518	0.649	0.4215	3582.3	2325.6
17	5518	0.550	0.3021	3033.1	1667.2
18	5518	0.434	0.1886	2396.5	1040.8
19	5518	0.307	0.0940	1691.6	518.6
20	5518	0.170	0.0289	937.7	159.3
21	5260	0.024	0.0006	126.4	3.0
22	5260	-0.125	0.0155	-655.3	81.6
23	5260	-0.271	0.0737	-1427.7	387.5
24	5260	-0.413	0.1706	-2172.7	897.4
25	5260	-0.547	0.2992	-2877.1	1573.7
26	4923	-0.676	0.4575	-3329.9	2252.3
27	4923	-0.788	0.6209	-3879.1	3056.6
28	4923	-0.880	0.7736	-4330.0	3808.5
29	4923	-0.950	0.9020	-4675.5	4440.4
30	4540	-1.000	1.0000	-4540.0	4540.0
	169997		$\sum$	34506	61842
$\beta_2 = \frac{34506}{61842} = 0.56$					
$W_{e2} = \frac{34506^2}{61842} = 19254$ kN					
Modal mass participation ratio of Mode 2 $= \frac{W_{e2}}{\text{total weight}} \times 100\% = \frac{19254}{169997} = 11.3\ \%$					

Table A.30 M30-Mode2 Shear Distribution

Mode2						
Level	**T (second)**	**a**	**W (kN)**	**β Φ_i**	**Force (kN)**	**Shear (kN)**
1	1.46	0.021	6456	0.016	2.2	404.3
2	1.46	0.021	6456	0.055	7.5	402.1
3	1.46	0.021	6456	0.108	14.6	394.6
4	1.46	0.021	6456	0.166	22.5	380.0
5	1.46	0.021	6456	0.227	30.7	357.5
6	1.46	0.021	6116	0.286	36.7	326.8
7	1.46	0.021	6116	0.339	43.6	290.1
8	1.46	0.021	6116	0.386	49.5	246.5
9	1.46	0.021	6116	0.423	54.3	197.0
10	1.46	0.021	6116	0.451	57.9	142.6
11	1.46	0.021	5803	0.467	57.0	84.7
12	1.46	0.021	5803	0.471	57.4	27.8
13	1.46	0.021	5803	0.461	56.2	-29.6
14	1.46	0.021	5803	0.439	53.5	-85.8
15	1.46	0.021	5803	0.407	49.6	-139.3
16	1.46	0.021	5518	0.362	42.0	-188.9
17	1.46	0.021	5518	0.307	35.5	-230.9
18	1.46	0.021	5518	0.242	28.1	-266.4
19	1.46	0.021	5518	0.171	19.8	-294.5
20	1.46	0.021	5518	0.095	11.0	-314.3
21	1.46	0.021	5260	0.013	1.5	-325.3
22	1.46	0.021	5260	-0.070	-7.7	-326.8
23	1.46	0.021	5260	-0.151	-16.7	-319.1
24	1.46	0.021	5260	-0.230	-25.5	-302.4
25	1.46	0.021	5260	-0.305	-33.7	-276.9
26	1.46	0.021	4923	-0.377	-39.0	-243.2
27	1.46	0.021	4923	-0.440	-45.5	-204.2
28	1.46	0.021	4923	-0.491	-50.7	-158.7
29	1.46	0.021	4923	-0.530	-54.8	-108.0
30	1.46	0.021	4540	-0.558	-53.2	-53.2

Table A.31 M30-Mode3 Modal Mass Participation Ratio

Mode3					
Level	**W_i (kN)**	**Φ_i**	**Φ_i^2**	**$W_i\ \Phi_i$**	**$W_i\Phi_i^2$**
1	6456	0.050	0.0025	321.2	16.0
2	6456	0.166	0.0275	1071.0	177.7
3	6456	0.313	0.0981	2021.6	633.0
4	6456	0.466	0.2171	3008.4	1401.9
5	6456	0.606	0.3670	3911.0	2369.3
6	6116	0.716	0.5121	4376.7	3132.0
7	6116	0.780	0.6079	4768.4	3717.7
8	6116	0.792	0.6274	4844.4	3837.1
9	6116	0.752	0.5649	4596.9	3455.1
10	6116	0.662	0.4381	4048.0	2679.3
11	5803	0.522	0.2726	3029.5	1581.6
12	5803	0.339	0.1150	1968.0	667.4
13	5803	0.129	0.0165	746.1	95.9
14	5803	-0.094	0.0088	-545.7	51.3
15	5803	-0.314	0.0985	-1821.6	571.8
16	5518	-0.517	0.2676	-2854.5	1476.6
17	5518	-0.683	0.4667	-3769.5	2575.0
18	5518	-0.799	0.6391	-4411.2	3526.4
19	5518	-0.859	0.7378	-4739.6	4071.1
20	5518	-0.860	0.7398	-4746.1	4082.2
21	5260	-0.795	0.6322	-4182.4	3325.5
22	5260	-0.664	0.4407	-3491.7	2317.9
23	5260	-0.480	0.2301	-2523.4	1210.5
24	5260	-0.257	0.0662	-1353.7	348.4
25	5260	-0.013	0.0002	-67.4	0.9
26	4923	0.257	0.0659	1263.5	324.3
27	4923	0.511	0.2607	2513.6	1283.4
28	4923	0.727	0.5289	3580.3	2603.7
29	4923	0.891	0.7947	4388.5	3912.1
30	4540	1.000	1.0000	4540.0	4540.0
	169997		$\sum$	20490	59985
$\beta_3 = \frac{20490}{59985} = 0.34$					
$W_{e3} = \frac{20490^2}{59985} = 6999\text{kN}$					
Modal mass participation ratio of Mode 3 = $\frac{W_{e3}}{\text{total weight}} \times 100\% = \frac{6999}{169997} = 4.1\%$					

Table A.32 M30-Mode3 Shear Distribution

Mode3						
Level	**T (second)**	**a**	**W (kN)**	**β Φ_i**	**Force (kN)**	**Shear (kN)**
1	0.82	0.038	6456	0.017	4.2	266.0
2	0.82	0.038	6456	0.057	13.9	261.8
3	0.82	0.038	6456	0.107	26.2	247.9
4	0.82	0.038	6456	0.159	39.1	221.7
5	0.82	0.038	6456	0.207	50.8	182.6
6	0.82	0.038	6116	0.244	56.8	131.8
7	0.82	0.038	6116	0.266	61.9	75.0
8	0.82	0.038	6116	0.271	62.9	13.1
9	0.82	0.038	6116	0.257	59.7	-49.7
10	0.82	0.038	6116	0.226	52.5	-109.4
11	0.82	0.038	5803	0.178	39.3	-162.0
12	0.82	0.038	5803	0.116	25.5	-201.3
13	0.82	0.038	5803	0.044	9.7	-226.8
14	0.82	0.038	5803	-0.032	-7.1	-236.5
15	0.82	0.038	5803	-0.107	-23.6	-229.4
16	0.82	0.038	5518	-0.177	-37.1	-205.8
17	0.82	0.038	5518	-0.233	-48.9	-168.7
18	0.82	0.038	5518	-0.273	-57.3	-119.8
19	0.82	0.038	5518	-0.293	-61.5	-62.5
20	0.82	0.038	5518	-0.294	-61.6	-1.0
21	0.82	0.038	5260	-0.272	-54.3	60.6
22	0.82	0.038	5260	-0.227	-45.3	114.9
23	0.82	0.038	5260	-0.164	-32.8	160.2
24	0.82	0.038	5260	-0.088	-17.6	193.0
25	0.82	0.038	5260	-0.004	-0.9	210.5
26	0.82	0.038	4923	0.088	16.4	211.4
27	0.82	0.038	4923	0.174	32.6	195.0
28	0.82	0.038	4923	0.248	46.5	162.4
29	0.82	0.038	4923	0.305	57.0	115.9
30	0.82	0.038	4540	0.342	58.9	58.9

Table A.33 M30-Mode4 Modal Mass Participation Ratio

Mode4					
Level	**W_i (kN)**	**Φ_i**	**Φ_i^2**	**$W_i\ \Phi_i$**	**$W_i\Phi_i^2$**
1	6456	0.071	0.0051	460.1	32.8
2	6456	0.230	0.0530	1486.0	342.0
3	6456	0.417	0.1736	2689.8	1120.7
4	6456	0.586	0.3433	3782.6	2216.2
5	6456	0.707	0.4996	4563.5	3225.7
6	6116	0.750	0.5629	4588.5	3442.5
7	6116	0.697	0.4854	4261.1	2968.8
8	6116	0.552	0.3051	3378.1	1865.9
9	6116	0.335	0.1120	2047.0	685.1
10	6116	0.070	0.0049	429.8	30.2
11	5803	-0.213	0.0456	-1238.5	264.3
12	5803	-0.475	0.2256	-2756.4	1309.3
13	5803	-0.677	0.4585	-3929.4	2660.8
14	5803	-0.793	0.6286	-4601.0	3648.0
15	5803	-0.810	0.6560	-4700.0	3806.6
16	5518	-0.712	0.5075	-3931.0	2800.4
17	5518	-0.504	0.2541	-2781.7	1402.3
18	5518	-0.219	0.0481	-1210.7	265.7
19	5518	0.101	0.0102	557.3	56.3
20	5518	0.415	0.1723	2290.5	950.8
21	5260	0.682	0.4657	3589.6	2449.7
22	5260	0.848	0.7193	4461.0	3783.3
23	5260	0.888	0.7887	4671.4	4148.7
24	5260	0.798	0.6371	4198.4	3351.0
25	5260	0.595	0.3541	3129.9	1862.4
26	4923	0.270	0.0727	1327.8	358.1
27	4923	-0.116	0.0135	-571.7	66.4
28	4923	-0.490	0.2405	-2414.1	1183.8
29	4923	-0.795	0.6318	-3913.1	3110.4
30	4540	-1.000	1.0000	-4540.0	4540.0
	169997		$\sum$	15325	57948
$\beta_4 = \frac{15325}{57948} = 0.26$					
$W_{e4} = \frac{15325^2}{57948} = 4053\text{kN}$					
Modal mass participation ratio of Mode 4 = $\frac{W_{e3}}{\text{total weight}} \times 100\% = \frac{4053}{169997} = 2.4\ \%$					

Table A.34 M30-Mode4 Shear Distribution

Mode4						
Level	**T (second)**	**a**	**W (kN)**	**β Φ_i**	**Force (kN)**	**Shear (kN)**
1	0.56	0.055	6456	0.019	6.7	222.9
2	0.56	0.055	6456	0.061	21.6	216.2
3	0.56	0.055	6456	0.110	39.1	194.6
4	0.56	0.055	6456	0.155	55.0	155.5
5	0.56	0.055	6456	0.187	66.4	100.5
6	0.56	0.055	6116	0.198	66.7	34.1
7	0.56	0.055	6116	0.184	62.0	-32.7
8	0.56	0.055	6116	0.146	49.1	-94.6
9	0.56	0.055	6116	0.089	29.8	-143.8
10	0.56	0.055	6116	0.019	6.3	-173.6
11	0.56	0.055	5803	-0.056	-18.0	-179.8
12	0.56	0.055	5803	-0.126	-40.1	-161.8
13	0.56	0.055	5803	-0.179	-57.2	-121.7
14	0.56	0.055	5803	-0.210	-66.9	-64.5
15	0.56	0.055	5803	-0.214	-68.4	2.4
16	0.56	0.055	5518	-0.188	-57.2	70.7
17	0.56	0.055	5518	-0.133	-40.5	127.9
18	0.56	0.055	5518	-0.058	-17.6	168.4
19	0.56	0.055	5518	0.027	8.1	186.0
20	0.56	0.055	5518	0.110	33.3	177.9
21	0.56	0.055	5260	0.180	52.2	144.6
22	0.56	0.055	5260	0.224	64.9	92.4
23	0.56	0.055	5260	0.235	67.9	27.5
24	0.56	0.055	5260	0.211	61.1	-40.5
25	0.56	0.055	5260	0.157	45.5	-101.5
26	0.56	0.055	4923	0.071	19.3	-147.1
27	0.56	0.055	4923	-0.031	-8.3	-166.4
28	0.56	0.055	4923	-0.130	-35.1	-158.1
29	0.56	0.055	4923	-0.210	-56.9	-123.0
30	0.56	0.055	4540	-0.264	-66.0	-66.0

For M30 case, mode1, mode 2, mode 3 and mode 4 give 91.8% of the actual mass. Thus, mode1, mode2, mode 3 and mode 4 are sufficient for shear calculations. The difference between hand calculations and SAP2000 is carried out for the first and second storeys as shown in Table A.35.

Table A.35 M30-Shear Force Determination Using Both Hand Calculations and SAP2000

Level	Shear Using Hand Calculations (kN)	Shear Using SAP2000 (kN)	Percent of Error*
1	993	1005	1.2%
2	989	1000	1.1%

* acceptance limit is 10%

Appendix B

First and Second-Order Moments in All Columns

Table B.1 M10 First and Second-Order Moments

M10						
Column	**M_{SD+D+L}**	**$M_{POSITIVE\ EQ.}$**	**$M_{NEGATIVE\ EQ.}$**	**First-Order Moment**	**Second-Order Moment**	**Percent**
1	28.5	227.2	-227.2	255.6	260.3	1.85
2	1.5	241.2	-241.2	242.7	247.6	2.03
3	-1.5	241.2	-241.2	-242.7	-247.6	2.03
4	-28.5	227.2	-227.2	-255.6	-260.3	1.85
5	47.4	228.1	-228.1	275.5	280.0	1.65
6	1.9	242.2	-242.2	244.1	248.7	1.89
7	-1.9	242.2	-242.2	-244.1	-248.7	1.89
8	-47.4	228.1	-228.1	-275.5	-280.0	1.65
9	47.4	228.1	-228.1	275.5	280.0	1.65
10	1.9	242.2	-242.2	244.1	248.7	1.89
11	-1.9	242.2	-242.2	-244.1	-248.7	1.89
12	-47.4	228.1	-228.1	-275.5	-280.0	1.65
13	28.5	227.2	-227.2	255.6	260.3	1.85
14	1.5	241.2	-241.2	242.7	247.6	2.03
15	-1.5	241.2	-241.2	-242.7	-247.6	2.03
16	-28.5	227.2	-227.2	-255.6	-260.3	1.85
17	73.9	123.5	-123.5	197.4	201.4	2.03
18	1.5	167.1	-167.1	168.7	173.8	**3.05**
19	-1.5	167.1	-167.1	-168.7	-173.8	**3.05**
20	-73.9	123.5	-123.5	-197.4	-201.4	2.03
21	128.4	124.4	-124.4	252.8	256.8	1.59
22	3.0	169.5	-169.5	172.5	177.6	2.97
23	-3.0	169.5	-169.5	-172.5	-177.6	2.97
24	-128.4	124.4	-124.4	-252.8	-256.8	1.59
25	128.4	124.4	-124.4	252.8	256.8	1.59
26	3.0	169.5	-169.5	172.5	177.6	2.97
27	-3.0	169.5	-169.5	-172.5	-177.6	2.97
28	-128.4	124.4	-124.4	-252.8	-256.8	1.59
29	73.9	123.5	-123.5	197.4	201.4	2.03
30	1.5	167.1	-167.1	168.7	173.8	**3.05**
31	-1.5	167.1	-167.1	-168.7	-173.8	**3.05**
32	-73.9	123.5	-123.5	-197.4	-201.4	2.03
33	70.7	76.2	-76.2	146.8	149.4	1.73
34	6.0	128.4	-128.4	134.4	138.5	3.04
35	-6.0	128.4	-128.4	-134.4	-138.5	3.04
36	-70.7	76.2	-76.2	-146.8	-149.4	1.73
37	121.0	77.6	-77.6	198.6	201.1	1.28
38	9.8	131.0	-131.0	140.9	145.0	2.93
39	-9.8	131.0	-131.0	-140.9	-145.0	2.93
40	-121.0	77.6	-77.6	-198.6	-201.1	1.28
41	121.0	77.6	-77.6	198.6	201.1	1.28
42	9.8	131.0	-131.0	140.9	145.0	2.93

43	-9.8	131.0	-131.0	-140.9	-145.0	2.93
44	-121.0	77.6	-77.6	-198.6	-201.1	1.28
45	70.7	76.2	-76.2	146.8	149.4	1.73
46	6.0	128.4	-128.4	134.4	138.5	3.04
47	-6.0	128.4	-128.4	-134.4	-138.5	3.04
48	-70.7	76.2	-76.2	-146.8	-149.4	1.73
49	73.3	53.6	-53.6	126.9	128.3	1.13
50	7.9	106.4	-106.4	114.3	117.3	2.62
51	-7.9	106.4	-106.4	-114.3	-117.3	2.62
52	-73.3	53.6	-53.6	-126.9	-128.3	1.13
53	125.7	55.0	-55.0	180.7	182.2	0.82
54	13.1	109.1	-109.1	122.2	125.2	2.52
55	-13.1	109.1	-109.1	-122.2	-125.2	2.52
56	-125.7	55.0	-55.0	-180.7	-182.2	0.82
57	125.7	55.0	-55.0	180.7	182.2	0.82
58	13.1	109.1	-109.1	122.2	125.2	2.52
59	-13.1	109.1	-109.1	-122.2	-125.2	2.52
60	-125.7	55.0	-55.0	-180.7	-182.2	0.82
61	73.3	53.6	-53.6	126.9	128.3	1.13
62	7.9	106.4	-106.4	114.3	117.3	2.62
63	-7.9	106.4	-106.4	-114.3	-117.3	2.62
64	-73.3	53.6	-53.6	-126.9	-128.3	1.13
65	77.2	41.4	-41.4	118.6	119.4	0.66
66	9.8	94.3	-94.3	104.1	106.4	2.18
67	-9.8	94.3	-94.3	-104.1	-106.4	2.18
68	-77.2	41.4	-41.4	-118.6	-119.4	0.66
69	133.1	42.7	-42.7	175.8	176.6	0.47
70	16.6	97.0	-97.0	113.6	115.9	2.07
71	-16.6	97.0	-97.0	-113.6	-115.9	2.07
72	-133.1	42.7	-42.7	-175.8	-176.6	0.47
73	133.1	42.7	-42.7	175.8	176.6	0.47
74	16.6	97.0	-97.0	113.6	115.9	2.07
75	-16.6	97.0	-97.0	-113.6	-115.9	2.07
76	-133.1	42.7	-42.7	-175.8	-176.6	0.47
77	77.2	41.4	-41.4	118.6	119.4	0.66
78	9.8	94.3	-94.3	104.1	106.4	2.18
79	-9.8	94.3	-94.3	-104.1	-106.4	2.18
80	-77.2	41.4	-41.4	-118.6	-119.4	0.66
81	62.6	43.1	-43.1	105.7	106.5	0.74
82	9.2	80.4	-80.4	89.7	91.4	1.92
83	-9.2	80.4	-80.4	-89.7	-91.4	1.92
84	-62.6	43.1	-43.1	-105.7	-106.5	0.74
85	105.2	44.2	-44.2	149.4	150.2	0.55
86	14.8	82.2	-82.2	97.1	98.9	1.84
87	-14.8	82.2	-82.2	-97.1	-98.9	1.84
88	-105.2	44.2	-44.2	-149.4	-150.2	0.55
89	105.2	44.2	-44.2	149.4	150.2	0.55

90	14.8	82.2	-82.2	97.1	98.9	1.84
91	-14.8	82.2	-82.2	-97.1	-98.9	1.84
92	-105.2	44.2	-44.2	-149.4	-150.2	0.55
93	62.6	43.1	-43.1	105.7	106.5	0.74
94	9.2	80.4	-80.4	89.7	91.4	1.92
95	-9.2	80.4	-80.4	-89.7	-91.4	1.92
96	-62.6	43.1	-43.1	-105.7	-106.5	0.74
97	79.5	31.8	-31.8	111.3	111.6	0.26
98	11.9	74.3	-74.3	86.2	87.4	1.40
99	-11.9	74.3	-74.3	-86.2	-87.4	1.40
100	-79.5	31.8	-31.8	-111.3	-111.6	0.26
101	133.8	32.8	-32.8	166.6	166.9	0.19
102	19.6	76.2	-76.2	95.8	97.1	1.32
103	-19.6	76.2	-76.2	-95.8	-97.1	1.32
104	-133.8	32.8	-32.8	-166.6	-166.9	0.19
105	133.8	32.8	-32.8	166.6	166.9	0.19
106	19.6	76.2	-76.2	95.8	97.1	1.32
107	-19.6	76.2	-76.2	-95.8	-97.1	1.32
108	-133.8	32.8	-32.8	-166.6	-166.9	0.19
109	79.5	31.8	-31.8	111.3	111.6	0.26
110	11.9	74.3	-74.3	86.2	87.4	1.40
111	-11.9	74.3	-74.3	-86.2	-87.4	1.40
112	-79.5	31.8	-31.8	-111.3	-111.6	0.26
113	78.9	23.8	-23.8	102.7	102.8	0.06
114	13.5	58.8	-58.8	72.3	73.0	0.91
115	-13.5	58.8	-58.8	-72.3	-73.0	0.91
116	-78.9	23.8	-23.8	-102.7	-102.8	0.06
117	132.6	24.7	-24.7	157.3	157.4	0.05
118	22.1	60.4	-60.4	82.5	83.2	0.84
119	-22.1	60.4	-60.4	-82.5	-83.2	0.84
120	-132.6	24.7	-24.7	-157.3	-157.4	0.05
121	132.6	24.7	-24.7	157.3	157.4	0.05
122	22.1	60.4	-60.4	82.5	83.2	0.84
123	-22.1	60.4	-60.4	-82.5	-83.2	0.84
124	-132.6	24.7	-24.7	-157.3	-157.4	0.05
125	78.9	23.8	-23.8	102.7	102.8	0.06
126	13.5	58.8	-58.8	72.3	73.0	0.91
127	-13.5	58.8	-58.8	-72.3	-73.0	0.91
128	-78.9	23.8	-23.8	-102.7	-102.8	0.06
129	78.7	12.1	-12.1	90.8	90.7	-0.13
130	15.3	39.7	-39.7	54.9	55.2	0.47
131	-15.3	39.7	-39.7	-54.9	-55.2	0.47
132	-78.7	12.1	-12.1	-90.8	-90.7	-0.13
133	131.5	12.9	-12.9	144.4	144.3	-0.08
134	24.5	41.0	-41.0	65.5	65.7	0.43
135	-24.5	41.0	-41.0	-65.5	-65.7	0.43
136	-131.5	12.9	-12.9	-144.4	-144.3	-0.08

137	131.5	12.9	-12.9	144.4	144.3	-0.08
138	24.5	41.0	-41.0	65.5	65.7	0.43
139	-24.5	41.0	-41.0	-65.5	-65.7	0.43
140	-131.5	12.9	-12.9	-144.4	-144.3	-0.08
141	78.7	12.1	-12.1	90.8	90.7	-0.13
142	15.3	39.7	-39.7	54.9	55.2	0.47
143	-15.3	39.7	-39.7	-54.9	-55.2	0.47
144	-78.7	12.1	-12.1	-90.8	-90.7	-0.13
145	93.7	-2.1	2.1	95.8	96.0	0.18
146	15.7	19.3	-19.3	35.0	35.1	0.17
147	-15.7	19.3	-19.3	-35.0	-35.1	0.17
148	-93.7	-2.1	2.1	-95.8	-96.0	0.18
149	158.2	-1.7	1.7	159.9	160.1	0.11
150	26.5	20.3	-20.3	46.8	46.9	0.18
151	-26.5	20.3	-20.3	-46.8	-46.9	0.18
152	-158.2	-1.7	1.7	-159.9	-160.1	0.11
153	158.2	-1.7	1.7	159.9	160.1	0.11
154	26.5	20.3	-20.3	46.8	46.9	0.18
155	-26.5	20.3	-20.3	-46.8	-46.9	0.18
156	-158.2	-1.7	1.7	-159.9	-160.1	0.11
157	93.7	-2.1	2.1	95.8	96.0	0.18
158	15.7	19.3	-19.3	35.0	35.1	0.17
159	-15.7	19.3	-19.3	-35.0	-35.1	0.17
160	-93.7	-2.1	2.1	-95.8	-96.0	0.18

Table B.2 M15 First and Second-Order Moments

M15						
Column	**M_{SD+D+L}**	**$M_{POSITIVE\ EQ.}$**	**$M_{NEGATIVE\ EQ.}$**	**First-Order Moment**	**Second-Order Moment**	**Percent**
1	29.5	288.8	-288.8	318.3	327.4	2.85
2	2.2	302.1	-302.1	304.4	313.7	3.07
3	-2.2	302.1	-302.1	-304.4	-313.7	3.07
4	-29.5	288.8	-288.8	-318.3	-327.4	2.85
5	49.0	289.8	-289.8	338.7	347.5	2.59
6	2.8	303.0	-303.0	305.9	314.8	2.91
7	-2.8	303.0	-303.0	-305.9	-314.8	2.91
8	-49.0	289.8	-289.8	-338.7	-347.5	2.59
9	49.0	289.8	-289.8	338.7	347.5	2.59
10	2.8	303.0	-303.0	305.9	314.8	2.91
11	-2.8	303.0	-303.0	-305.9	-314.8	2.91
12	-49.0	289.8	-289.8	-338.7	-347.5	2.59
13	29.5	288.8	-288.8	318.3	327.4	2.85
14	2.2	302.1	-302.1	304.4	313.7	3.07
15	-2.2	302.1	-302.1	-304.4	-313.7	3.07
16	-29.5	288.8	-288.8	-318.3	-327.4	2.85
17	73.9	168.2	-168.2	242.1	250.3	3.35
18	2.3	209.6	-209.6	211.9	221.6	4.60
19	-2.3	209.6	-209.6	-211.9	-221.6	4.60
20	-73.9	168.2	-168.2	-242.1	-250.3	3.35
21	129.4	169.1	-169.1	298.5	306.6	2.73
22	4.2	211.9	-211.9	216.1	225.9	4.51
23	-4.2	211.9	-211.9	-216.1	-225.9	4.51
24	-129.4	169.1	-169.1	-298.5	-306.6	2.73
25	129.4	169.1	-169.1	298.5	306.6	2.73
26	4.2	211.9	-211.9	216.1	225.9	4.51
27	-4.2	211.9	-211.9	-216.1	-225.9	4.51
28	-129.4	169.1	-169.1	-298.5	-306.6	2.73
29	73.9	168.2	-168.2	242.1	250.3	3.35
30	2.3	209.6	-209.6	211.9	221.6	4.60
31	-2.3	209.6	-209.6	-211.9	-221.6	4.60
32	-73.9	168.2	-168.2	-242.1	-250.3	3.35
33	72.9	105.8	-105.8	178.7	184.6	3.29
34	7.7	159.5	-159.5	167.1	175.5	**4.97**
35	-7.7	159.5	-159.5	-167.1	-175.5	**4.97**
36	-72.9	105.8	-105.8	-178.7	-184.6	3.29
37	124.9	107.2	-107.2	232.2	238.0	2.54
38	12.1	162.3	-162.3	174.4	182.8	4.79
39	-12.1	162.3	-162.3	-174.4	-182.8	4.79
40	-124.9	107.2	-107.2	-232.2	-238.0	2.54
41	124.9	107.2	-107.2	232.2	238.0	2.54
42	12.1	162.3	-162.3	174.4	182.8	4.79

43	-12.1	162.3	-162.3	-174.4	-182.8	4.79
44	-124.9	107.2	-107.2	-232.2	-238.0	2.54
45	72.9	105.8	-105.8	178.7	184.6	3.29
46	7.7	159.5	-159.5	167.1	175.5	**4.97**
47	-7.7	159.5	-159.5	-167.1	-175.5	**4.97**
48	-72.9	105.8	-105.8	-178.7	-184.6	3.29
49	75.7	73.4	-73.4	149.1	153.0	2.62
50	10.0	130.8	-130.8	140.8	147.4	4.72
51	-10.0	130.8	-130.8	-140.8	-147.4	4.72
52	-75.7	73.4	-73.4	-149.1	-153.0	2.62
53	129.8	74.9	-74.9	204.7	208.7	1.94
54	16.1	133.7	-133.7	149.8	156.6	4.51
55	-16.1	133.7	-133.7	-149.8	-156.6	4.51
56	-129.8	74.9	-74.9	-204.7	-208.7	1.94
57	129.8	74.9	-74.9	204.7	208.7	1.94
58	16.1	133.7	-133.7	149.8	156.6	4.51
59	-16.1	133.7	-133.7	-149.8	-156.6	4.51
60	-129.8	74.9	-74.9	-204.7	-208.7	1.94
61	75.7	73.4	-73.4	149.1	153.0	2.62
62	10.0	130.8	-130.8	140.8	147.4	4.72
63	-10.0	130.8	-130.8	-140.8	-147.4	4.72
64	-75.7	73.4	-73.4	-149.1	-153.0	2.62
65	79.0	56.4	-56.4	135.5	138.0	1.88
66	12.6	115.3	-115.3	127.9	133.2	4.19
67	-12.6	115.3	-115.3	-127.9	-133.2	4.19
68	-79.0	56.4	-56.4	-135.5	-138.0	1.88
69	135.9	57.8	-57.8	193.7	196.3	1.35
70	20.5	118.4	-118.4	138.8	144.4	3.96
71	-20.5	118.4	-118.4	-138.8	-144.4	3.96
72	-135.9	57.8	-57.8	-193.7	-196.3	1.35
73	135.9	57.8	-57.8	193.7	196.3	1.35
74	20.5	118.4	-118.4	138.8	144.4	3.96
75	-20.5	118.4	-118.4	-138.8	-144.4	3.96
76	-135.9	57.8	-57.8	-193.7	-196.3	1.35
77	79.0	56.4	-56.4	135.5	138.0	1.88
78	12.6	115.3	-115.3	127.9	133.2	4.19
79	-12.6	115.3	-115.3	-127.9	-133.2	4.19
80	-79.0	56.4	-56.4	-135.5	-138.0	1.88
81	72.8	52.5	-52.5	125.3	127.3	1.61
82	13.8	102.5	-102.5	116.3	120.6	3.71
83	-13.8	102.5	-102.5	-116.3	-120.6	3.71
84	-72.8	52.5	-52.5	-125.3	-127.3	1.61
85	123.1	54.0	-54.0	177.0	179.1	1.18
86	21.8	105.0	-105.0	126.8	131.3	3.51
87	-21.8	105.0	-105.0	-126.8	-131.3	3.51
88	-123.1	54.0	-54.0	-177.0	-179.1	1.18
89	123.1	54.0	-54.0	177.0	179.1	1.18

90	21.8	105.0	-105.0	126.8	131.3	3.51
91	-21.8	105.0	-105.0	-126.8	-131.3	3.51
92	-123.1	54.0	-54.0	-177.0	-179.1	1.18
93	72.8	52.5	-52.5	125.3	127.3	1.61
94	13.8	102.5	-102.5	116.3	120.6	3.71
95	-13.8	102.5	-102.5	-116.3	-120.6	3.71
96	-72.8	52.5	-52.5	-125.3	-127.3	1.61
97	84.0	43.8	-43.8	127.9	129.1	0.96
98	17.3	98.5	-98.5	115.7	119.3	3.11
99	-17.3	98.5	-98.5	-115.7	-119.3	3.11
100	-84.0	43.8	-43.8	-127.9	-129.1	0.96
101	142.6	45.1	-45.1	187.7	189.0	0.69
102	27.7	101.2	-101.2	128.9	132.6	2.89
103	-27.7	101.2	-101.2	-128.9	-132.6	2.89
104	-142.6	45.1	-45.1	-187.7	-189.0	0.69
105	142.6	45.1	-45.1	187.7	189.0	0.69
106	27.7	101.2	-101.2	128.9	132.6	2.89
107	-27.7	101.2	-101.2	-128.9	-132.6	2.89
108	-142.6	45.1	-45.1	-187.7	-189.0	0.69
109	84.0	43.8	-43.8	127.9	129.1	0.96
110	17.3	98.5	-98.5	115.7	119.3	3.11
111	-17.3	98.5	-98.5	-115.7	-119.3	3.11
112	-84.0	43.8	-43.8	-127.9	-129.1	0.96
113	85.6	40.2	-40.2	125.8	126.7	0.67
114	19.8	91.2	-91.2	111.0	113.9	2.57
115	-19.8	91.2	-91.2	-111.0	-113.9	2.57
116	-85.6	40.2	-40.2	-125.8	-126.7	0.67
117	144.4	41.5	-41.5	185.9	186.8	0.48
118	31.5	93.7	-93.7	125.2	128.2	2.37
119	-31.5	93.7	-93.7	-125.2	-128.2	2.37
120	-144.4	41.5	-41.5	-185.9	-186.8	0.48
121	144.4	41.5	-41.5	185.9	186.8	0.48
122	31.5	93.7	-93.7	125.2	128.2	2.37
123	-31.5	93.7	-93.7	-125.2	-128.2	2.37
124	-144.4	41.5	-41.5	-185.9	-186.8	0.48
125	85.6	40.2	-40.2	125.8	126.7	0.67
126	19.8	91.2	-91.2	111.0	113.9	2.57
127	-19.8	91.2	-91.2	-111.0	-113.9	2.57
128	-85.6	40.2	-40.2	-125.8	-126.7	0.67
129	87.9	36.6	-36.6	124.5	125.1	0.44
130	22.1	84.8	-84.8	106.9	109.1	2.12
131	-22.1	84.8	-84.8	-106.9	-109.1	2.12
132	-87.9	36.6	-36.6	-124.5	-125.1	0.44
133	147.7	37.9	-37.9	185.5	186.1	0.32
134	34.9	87.2	-87.2	122.1	124.4	1.94
135	-34.9	87.2	-87.2	-122.1	-124.4	1.94
136	-147.7	37.9	-37.9	-185.5	-186.1	0.32

137	147.7	37.9	-37.9	185.5	186.1	0.32
138	34.9	87.2	-87.2	122.1	124.4	1.94
139	-34.9	87.2	-87.2	-122.1	-124.4	1.94
140	-147.7	37.9	-37.9	-185.5	-186.1	0.32
141	87.9	36.6	-36.6	124.5	125.1	0.44
142	22.1	84.8	-84.8	106.9	109.1	2.12
143	-22.1	84.8	-84.8	-106.9	-109.1	2.12
144	-87.9	36.6	-36.6	-124.5	-125.1	0.44
145	91.7	32.7	-32.7	124.4	124.7	0.30
146	24.0	80.0	-80.0	104.0	105.9	1.81
147	-24.0	80.0	-80.0	-104.0	-105.9	1.81
148	-91.7	32.7	-32.7	-124.4	-124.7	0.30
149	155.1	33.7	-33.7	188.8	189.2	0.22
150	38.5	82.3	-82.3	120.8	122.8	1.63
151	-38.5	82.3	-82.3	-120.8	-122.8	1.63
152	-155.1	33.7	-33.7	-188.8	-189.2	0.22
153	155.1	33.7	-33.7	188.8	189.2	0.22
154	38.5	82.3	-82.3	120.8	122.8	1.63
155	-38.5	82.3	-82.3	-120.8	-122.8	1.63
156	-155.1	33.7	-33.7	-188.8	-189.2	0.22
157	91.7	32.7	-32.7	124.4	124.7	0.30
158	24.0	80.0	-80.0	104.0	105.9	1.81
159	-24.0	80.0	-80.0	-104.0	-105.9	1.81
160	-91.7	32.7	-32.7	-124.4	-124.7	0.30
161	73.9	36.2	-36.2	110.1	110.7	0.54
162	19.9	69.6	-69.6	89.5	91.0	1.71
163	-19.9	69.6	-69.6	-89.5	-91.0	1.71
164	-73.9	36.2	-36.2	-110.1	-110.7	0.54
165	121.8	37.1	-37.1	158.9	159.5	0.40
166	30.8	71.1	-71.1	101.9	103.5	1.55
167	-30.8	71.1	-71.1	-101.9	-103.5	1.55
168	-121.8	37.1	-37.1	-158.9	-159.5	0.40
169	121.8	37.1	-37.1	158.9	159.5	0.40
170	30.8	71.1	-71.1	101.9	103.5	1.55
171	-30.8	71.1	-71.1	-101.9	-103.5	1.55
172	-121.8	37.1	-37.1	-158.9	-159.5	0.40
173	73.9	36.2	-36.2	110.1	110.7	0.54
174	19.9	69.6	-69.6	89.5	91.0	1.71
175	-19.9	69.6	-69.6	-89.5	-91.0	1.71
176	-73.9	36.2	-36.2	-110.1	-110.7	0.54
177	93.0	26.3	-26.3	119.3	119.6	0.18
178	24.9	64.2	-64.2	89.1	90.2	1.25
179	-24.9	64.2	-64.2	-89.1	-90.2	1.25
180	-93.0	26.3	-26.3	-119.3	-119.6	0.18
181	153.6	27.1	-27.1	180.7	180.9	0.13
182	39.0	65.9	-65.9	104.8	106.0	1.11
183	-39.0	65.9	-65.9	-104.8	-106.0	1.11

184	-153.6	27.1	-27.1	-180.7	-180.9	0.13
185	153.6	27.1	-27.1	180.7	180.9	0.13
186	39.0	65.9	-65.9	104.8	106.0	1.11
187	-39.0	65.9	-65.9	-104.8	-106.0	1.11
188	-153.6	27.1	-27.1	-180.7	-180.9	0.13
189	93.0	26.3	-26.3	119.3	119.6	0.18
190	24.9	64.2	-64.2	89.1	90.2	1.25
191	-24.9	64.2	-64.2	-89.1	-90.2	1.25
192	-93.0	26.3	-26.3	-119.3	-119.6	0.18
193	92.0	19.5	-19.5	111.5	111.5	0.03
194	26.0	50.9	-50.9	76.9	77.5	0.82
195	-26.0	50.9	-50.9	-76.9	-77.5	0.82
196	-92.0	19.5	-19.5	-111.5	-111.5	0.03
197	151.6	20.2	-20.2	171.9	171.9	0.03
198	40.5	52.3	-52.3	92.8	93.4	0.71
199	-40.5	52.3	-52.3	-92.8	-93.4	0.71
200	-151.6	20.2	-20.2	-171.9	-171.9	0.03
201	151.6	20.2	-20.2	171.9	171.9	0.03
202	40.5	52.3	-52.3	92.8	93.4	0.71
203	-40.5	52.3	-52.3	-92.8	-93.4	0.71
204	-151.6	20.2	-20.2	-171.9	-171.9	0.03
205	92.0	19.5	-19.5	111.5	111.5	0.03
206	26.0	50.9	-50.9	76.9	77.5	0.82
207	-26.0	50.9	-50.9	-76.9	-77.5	0.82
208	-92.0	19.5	-19.5	-111.5	-111.5	0.03
209	91.5	9.2	-9.2	100.7	100.5	-0.13
210	27.4	34.0	-34.0	61.4	61.7	0.44
211	-27.4	34.0	-34.0	-61.4	-61.7	0.44
212	-91.5	9.2	-9.2	-100.7	-100.5	-0.13
213	150.0	9.7	-9.7	159.7	159.6	-0.08
214	42.3	35.1	-35.1	77.3	77.6	0.38
215	-42.3	35.1	-35.1	-77.3	-77.6	0.38
216	-150.0	9.7	-9.7	-159.7	-159.6	-0.08
217	150.0	9.7	-9.7	159.7	159.6	-0.08
218	42.3	35.1	-35.1	77.3	77.6	0.38
219	-42.3	35.1	-35.1	-77.3	-77.6	0.38
220	-150.0	9.7	-9.7	-159.7	-159.6	-0.08
221	91.5	9.2	-9.2	100.7	100.5	-0.13
222	27.4	34.0	-34.0	61.4	61.7	0.44
223	-27.4	34.0	-34.0	-61.4	-61.7	0.44
224	-91.5	9.2	-9.2	-100.7	-100.5	-0.13
225	108.4	-3.3	3.3	111.7	111.9	0.17
226	29.9	16.3	-16.3	46.2	46.3	0.21
227	-29.9	16.3	-16.3	-46.2	-46.3	0.21
228	-108.4	-3.3	3.3	-111.7	-111.9	0.17
229	179.6	-3.1	3.1	182.7	182.9	0.11
230	47.4	17.0	-17.0	64.4	64.6	0.18

231	-47.4	17.0	-17.0	-64.4	-64.6	0.18
232	-179.6	-3.1	3.1	-182.7	-182.9	0.11
233	179.6	-3.1	3.1	182.7	182.9	0.11
234	47.4	17.0	-17.0	64.4	64.6	0.18
235	-47.4	17.0	-17.0	-64.4	-64.6	0.18
236	-179.6	-3.1	3.1	-182.7	-182.9	0.11
237	108.4	-3.3	3.3	111.7	111.9	0.17
238	29.9	16.3	-16.3	46.2	46.3	0.21
239	-29.9	16.3	-16.3	-46.2	-46.3	0.21
240	-108.4	-3.3	3.3	-111.7	-111.9	0.17

Table B.3 M20 First and Second-Order Moments

M20						
Column	**M_{SD+D+L}**	**$M_{POSITIVE\ EQ.}$**	**$M_{NEGATIVE\ EQ.}$**	**First-Order Moment**	**Second-Order Moment**	**Percent**
1	30.5	353.0	-353.0	383.4	399.2	4.10
2	2.8	365.4	-365.4	368.1	384.3	4.38
3	-2.8	365.4	-365.4	-368.1	-384.3	4.38
4	-30.5	353.0	-353.0	-383.4	-399.2	4.10
5	50.2	354.0	-354.0	404.3	419.6	3.79
6	3.5	366.2	-366.2	369.7	385.3	4.21
7	-3.5	366.2	-366.2	-369.7	-385.3	4.21
8	-50.2	354.0	-354.0	-404.3	-419.6	3.79
9	50.2	354.0	-354.0	404.3	419.6	3.79
10	3.5	366.2	-366.2	369.7	385.3	4.21
11	-3.5	366.2	-366.2	-369.7	-385.3	4.21
12	-50.2	354.0	-354.0	-404.3	-419.6	3.79
13	30.5	353.0	-353.0	383.4	399.2	4.10
14	2.8	365.4	-365.4	368.1	384.3	4.38
15	-2.8	365.4	-365.4	-368.1	-384.3	4.38
16	-30.5	353.0	-353.0	-383.4	-399.2	4.10
17	73.1	218.6	-218.6	291.7	306.3	5.00
18	2.4	256.1	-256.1	258.5	275.2	6.44
19	-2.4	256.1	-256.1	-258.5	-275.2	6.44
20	-73.1	218.6	-218.6	-291.7	-306.3	5.00
21	128.7	219.4	-219.4	348.0	362.7	4.21
22	4.4	258.3	-258.3	262.7	279.4	6.36
23	-4.4	258.3	-258.3	-262.7	-279.4	6.36
24	-128.7	219.4	-219.4	-348.0	-362.7	4.21
25	128.7	219.4	-219.4	348.0	362.7	4.21
26	4.4	258.3	-258.3	262.7	279.4	6.36
27	-4.4	258.3	-258.3	-262.7	-279.4	6.36
28	-128.7	219.4	-219.4	-348.0	-362.7	4.21
29	73.1	218.6	-218.6	291.7	306.3	5.00
30	2.4	256.1	-256.1	258.5	275.2	6.44
31	-2.4	256.1	-256.1	-258.5	-275.2	6.44
32	-73.1	218.6	-218.6	-291.7	-306.3	5.00
33	74.1	141.3	-141.3	215.4	226.8	5.30
34	8.3	193.2	-193.2	201.5	216.2	7.30
35	-8.3	193.2	-193.2	-201.5	-216.2	7.30
36	-74.1	141.3	-141.3	-215.4	-226.8	5.30
37	127.0	142.7	-142.7	269.7	281.1	4.24
38	12.9	196.0	-196.0	208.8	223.6	7.08
39	-12.9	196.0	-196.0	-208.8	-223.6	7.08
40	-127.0	142.7	-142.7	-269.7	-281.1	4.24
41	127.0	142.7	-142.7	269.7	281.1	4.24
42	12.9	196.0	-196.0	208.8	223.6	7.08

43	-12.9	196.0	-196.0	-208.8	-223.6	7.08
44	-127.0	142.7	-142.7	-269.7	-281.1	4.24
45	74.1	141.3	-141.3	215.4	226.8	5.30
46	8.3	193.2	-193.2	201.5	216.2	7.30
47	-8.3	193.2	-193.2	-201.5	-216.2	7.30
48	-74.1	141.3	-141.3	-215.4	-226.8	5.30
49	76.6	97.3	-97.3	173.9	182.1	4.74
50	10.9	155.0	-155.0	165.9	178.1	**<u>7.35</u>**
51	-10.9	155.0	-155.0	-165.9	-178.1	**<u>7.35</u>**
52	-76.6	97.3	-97.3	-173.9	-182.1	4.74
53	131.4	98.8	-98.8	230.2	238.5	3.61
54	17.1	158.1	-158.1	175.2	187.5	7.05
55	-17.1	158.1	-158.1	-175.2	-187.5	7.05
56	-131.4	98.8	-98.8	-230.2	-238.5	3.61
57	131.4	98.8	-98.8	230.2	238.5	3.61
58	17.1	158.1	-158.1	175.2	187.5	7.05
59	-17.1	158.1	-158.1	-175.2	-187.5	7.05
60	-131.4	98.8	-98.8	-230.2	-238.5	3.61
61	76.6	97.3	-97.3	173.9	182.1	4.74
62	10.9	155.0	-155.0	165.9	178.1	**<u>7.35</u>**
63	-10.9	155.0	-155.0	-165.9	-178.1	**<u>7.35</u>**
64	-76.6	97.3	-97.3	-173.9	-182.1	4.74
65	79.7	72.3	-72.3	152.0	157.8	3.79
66	13.6	133.0	-133.0	146.5	156.6	6.86
67	-13.6	133.0	-133.0	-146.5	-156.6	6.86
68	-79.7	72.3	-72.3	-152.0	-157.8	3.79
69	136.9	73.7	-73.7	210.6	216.5	2.78
70	21.6	136.2	-136.2	157.8	168.0	6.50
71	-21.6	136.2	-136.2	-157.8	-168.0	6.50
72	-136.9	73.7	-73.7	-210.6	-216.5	2.78
73	136.9	73.7	-73.7	210.6	216.5	2.78
74	21.6	136.2	-136.2	157.8	168.0	6.50
75	-21.6	136.2	-136.2	-157.8	-168.0	6.50
76	-136.9	73.7	-73.7	-210.6	-216.5	2.78
77	79.7	72.3	-72.3	152.0	157.8	3.79
78	13.6	133.0	-133.0	146.5	156.6	6.86
79	-13.6	133.0	-133.0	-146.5	-156.6	6.86
80	-79.7	72.3	-72.3	-152.0	-157.8	3.79
81	75.5	62.9	-62.9	138.4	142.8	3.17
82	15.5	117.1	-117.1	132.6	140.8	6.20
83	-15.5	117.1	-117.1	-132.6	-140.8	6.20
84	-75.5	62.9	-62.9	-138.4	-142.8	3.17
85	127.4	64.5	-64.5	191.9	196.4	2.35
86	23.9	119.9	-119.9	143.8	152.3	5.86
87	-23.9	119.9	-119.9	-143.8	-152.3	5.86
88	-127.4	64.5	-64.5	-191.9	-196.4	2.35
89	127.4	64.5	-64.5	191.9	196.4	2.35

90	23.9	119.9	-119.9	143.8	152.3	5.86
91	-23.9	119.9	-119.9	-143.8	-152.3	5.86
92	-127.4	64.5	-64.5	-191.9	-196.4	2.35
93	75.5	62.9	-62.9	138.4	142.8	3.17
94	15.5	117.1	-117.1	132.6	140.8	6.20
95	-15.5	117.1	-117.1	-132.6	-140.8	6.20
96	-75.5	62.9	-62.9	-138.4	-142.8	3.17
97	85.8	52.8	-52.8	138.6	141.5	2.12
98	19.3	112.7	-112.7	132.0	139.0	5.36
99	-19.3	112.7	-112.7	-132.0	-139.0	5.36
100	-85.8	52.8	-52.8	-138.6	-141.5	2.12
101	145.4	54.2	-54.2	199.6	202.7	1.52
102	30.3	115.8	-115.8	146.0	153.3	5.00
103	-30.3	115.8	-115.8	-146.0	-153.3	5.00
104	-145.4	54.2	-54.2	-199.6	-202.7	1.52
105	145.4	54.2	-54.2	199.6	202.7	1.52
106	30.3	115.8	-115.8	146.0	153.3	5.00
107	-30.3	115.8	-115.8	-146.0	-153.3	5.00
108	-145.4	54.2	-54.2	-199.6	-202.7	1.52
109	85.8	52.8	-52.8	138.6	141.5	2.12
110	19.3	112.7	-112.7	132.0	139.0	5.36
111	-19.3	112.7	-112.7	-132.0	-139.0	5.36
112	-85.8	52.8	-52.8	-138.6	-141.5	2.12
113	88.3	48.8	-48.8	137.1	139.3	1.57
114	22.4	106.5	-106.5	128.9	134.9	4.63
115	-22.4	106.5	-106.5	-128.9	-134.9	4.63
116	-88.3	48.8	-48.8	-137.1	-139.3	1.57
117	148.6	50.3	-50.3	198.9	201.1	1.14
118	34.8	109.5	-109.5	144.3	150.5	4.27
119	-34.8	109.5	-109.5	-144.3	-150.5	4.27
120	-148.6	50.3	-50.3	-198.9	-201.1	1.14
121	148.6	50.3	-50.3	198.9	201.1	1.14
122	34.8	109.5	-109.5	144.3	150.5	4.27
123	-34.8	109.5	-109.5	-144.3	-150.5	4.27
124	-148.6	50.3	-50.3	-198.9	-201.1	1.14
125	88.3	48.8	-48.8	137.1	139.3	1.57
126	22.4	106.5	-106.5	128.9	134.9	4.63
127	-22.4	106.5	-106.5	-128.9	-134.9	4.63
128	-88.3	48.8	-48.8	-137.1	-139.3	1.57
129	91.1	44.9	-44.9	136.0	137.6	1.18
130	25.0	101.0	-101.0	126.1	131.2	4.04
131	-25.0	101.0	-101.0	-126.1	-131.2	4.04
132	-91.1	44.9	-44.9	-136.0	-137.6	1.18
133	152.7	46.4	-46.4	199.1	200.8	0.86
134	38.8	103.9	-103.9	142.7	148.0	3.70
135	-38.8	103.9	-103.9	-142.7	-148.0	3.70
136	-152.7	46.4	-46.4	-199.1	-200.8	0.86

137	152.7	46.4	-46.4	199.1	200.8	0.86
138	38.8	103.9	-103.9	142.7	148.0	3.70
139	-38.8	103.9	-103.9	-142.7	-148.0	3.70
140	-152.7	46.4	-46.4	-199.1	-200.8	0.86
141	91.1	44.9	-44.9	136.0	137.6	1.18
142	25.0	101.0	-101.0	126.1	131.2	4.04
143	-25.0	101.0	-101.0	-126.1	-131.2	4.04
144	-91.1	44.9	-44.9	-136.0	-137.6	1.18
145	94.0	41.1	-41.1	135.1	136.4	0.92
146	27.4	96.4	-96.4	123.7	128.2	3.62
147	-27.4	96.4	-96.4	-123.7	-128.2	3.62
148	-94.0	41.1	-41.1	-135.1	-136.4	0.92
149	158.1	42.3	-42.3	200.4	201.8	0.66
150	42.8	99.1	-99.1	141.9	146.5	3.28
151	-42.8	99.1	-99.1	-141.9	-146.5	3.28
152	-158.1	42.3	-42.3	-200.4	-201.8	0.66
153	158.1	42.3	-42.3	200.4	201.8	0.66
154	42.8	99.1	-99.1	141.9	146.5	3.28
155	-42.8	99.1	-99.1	-141.9	-146.5	3.28
156	-158.1	42.3	-42.3	-200.4	-201.8	0.66
157	94.0	41.1	-41.1	135.1	136.4	0.92
158	27.4	96.4	-96.4	123.7	128.2	3.62
159	-27.4	96.4	-96.4	-123.7	-128.2	3.62
160	-94.0	41.1	-41.1	-135.1	-136.4	0.92
161	85.9	42.5	-42.5	128.5	129.8	1.06
162	26.4	88.6	-88.6	115.1	118.9	3.36
163	-26.4	88.6	-88.6	-115.1	-118.9	3.36
164	-85.9	42.5	-42.5	-128.5	-129.8	1.06
165	142.1	43.7	-43.7	185.8	187.2	0.78
166	40.4	90.9	-90.9	131.3	135.3	3.05
167	-40.4	90.9	-90.9	-131.3	-135.3	3.05
168	-142.1	43.7	-43.7	-185.8	-187.2	0.78
169	142.1	43.7	-43.7	185.8	187.2	0.78
170	40.4	90.9	-90.9	131.3	135.3	3.05
171	-40.4	90.9	-90.9	-131.3	-135.3	3.05
172	-142.1	43.7	-43.7	-185.8	-187.2	0.78
173	85.9	42.5	-42.5	128.5	129.8	1.06
174	26.4	88.6	-88.6	115.1	118.9	3.36
175	-26.4	88.6	-88.6	-115.1	-118.9	3.36
176	-85.9	42.5	-42.5	-128.5	-129.8	1.06
177	98.2	36.5	-36.5	134.8	135.7	0.65
178	31.2	86.4	-86.4	117.6	121.0	2.86
179	-31.2	86.4	-86.4	-117.6	-121.0	2.86
180	-98.2	36.5	-36.5	-134.8	-135.7	0.65
181	163.1	37.6	-37.6	200.7	201.6	0.47
182	48.1	88.8	-88.8	136.9	140.3	2.55
183	-48.1	88.8	-88.8	-136.9	-140.3	2.55

184	-163.1	37.6	-37.6	-200.7	-201.6	0.47
185	163.1	37.6	-37.6	200.7	201.6	0.47
186	48.1	88.8	-88.8	136.9	140.3	2.55
187	-48.1	88.8	-88.8	-136.9	-140.3	2.55
188	-163.1	37.6	-37.6	-200.7	-201.6	0.47
189	98.2	36.5	-36.5	134.8	135.7	0.65
190	31.2	86.4	-86.4	117.6	121.0	2.86
191	-31.2	86.4	-86.4	-117.6	-121.0	2.86
192	-98.2	36.5	-36.5	-134.8	-135.7	0.65
193	99.4	33.9	-33.9	133.3	134.0	0.48
194	33.2	80.3	-80.3	113.5	116.2	2.39
195	-33.2	80.3	-80.3	-113.5	-116.2	2.39
196	-99.4	33.9	-33.9	-133.3	-134.0	0.48
197	164.1	35.0	-35.0	199.1	199.8	0.35
198	51.0	82.5	-82.5	133.4	136.3	2.12
199	-51.0	82.5	-82.5	-133.4	-136.3	2.12
200	-164.1	35.0	-35.0	-199.1	-199.8	0.35
201	164.1	35.0	-35.0	199.1	199.8	0.35
202	51.0	82.5	-82.5	133.4	136.3	2.12
203	-51.0	82.5	-82.5	-133.4	-136.3	2.12
204	-164.1	35.0	-35.0	-199.1	-199.8	0.35
205	99.4	33.9	-33.9	133.3	134.0	0.48
206	33.2	80.3	-80.3	113.5	116.2	2.39
207	-33.2	80.3	-80.3	-113.5	-116.2	2.39
208	-99.4	33.9	-33.9	-133.3	-134.0	0.48
209	101.5	30.6	-30.6	132.1	132.5	0.32
210	35.2	74.3	-74.3	109.5	111.7	2.00
211	-35.2	74.3	-74.3	-109.5	-111.7	2.00
212	-101.5	30.6	-30.6	-132.1	-132.5	0.32
213	166.8	31.6	-31.6	198.5	198.9	0.24
214	53.8	76.3	-76.3	130.1	132.3	1.75
215	-53.8	76.3	-76.3	-130.1	-132.3	1.75
216	-166.8	31.6	-31.6	-198.5	-198.9	0.24
217	166.8	31.6	-31.6	198.5	198.9	0.24
218	53.8	76.3	-76.3	130.1	132.3	1.75
219	-53.8	76.3	-76.3	-130.1	-132.3	1.75
220	-166.8	31.6	-31.6	-198.5	-198.9	0.24
221	101.5	30.6	-30.6	132.1	132.5	0.32
222	35.2	74.3	-74.3	109.5	111.7	2.00
223	-35.2	74.3	-74.3	-109.5	-111.7	2.00
224	-101.5	30.6	-30.6	-132.1	-132.5	0.32
225	105.2	27.2	-27.2	132.4	132.7	0.22
226	37.4	69.9	-69.9	107.3	109.1	1.71
227	-37.4	69.9	-69.9	-107.3	-109.1	1.71
228	-105.2	27.2	-27.2	-132.4	-132.7	0.22
229	174.3	27.9	-27.9	202.2	202.6	0.16
230	57.7	71.8	-71.8	129.6	131.5	1.48

231	-57.7	71.8	-71.8	-129.6	-131.5	1.48
232	-174.3	27.9	-27.9	-202.2	-202.6	0.16
233	174.3	27.9	-27.9	202.2	202.6	0.16
234	57.7	71.8	-71.8	129.6	131.5	1.48
235	-57.7	71.8	-71.8	-129.6	-131.5	1.48
236	-174.3	27.9	-27.9	-202.2	-202.6	0.16
237	105.2	27.2	-27.2	132.4	132.7	0.22
238	37.4	69.9	-69.9	107.3	109.1	1.71
239	-37.4	69.9	-69.9	-107.3	-109.1	1.71
240	-105.2	27.2	-27.2	-132.4	-132.7	0.22
241	84.5	31.0	-31.0	115.5	116.0	0.46
242	29.8	61.3	-61.3	91.1	92.6	1.64
243	-29.8	61.3	-61.3	-91.1	-92.6	1.64
244	-84.5	31.0	-31.0	-115.5	-116.0	0.46
245	136.3	31.8	-31.8	168.1	168.7	0.34
246	44.8	62.5	-62.5	107.3	108.8	1.44
247	-44.8	62.5	-62.5	-107.3	-108.8	1.44
248	-136.3	31.8	-31.8	-168.1	-168.7	0.34
249	136.3	31.8	-31.8	168.1	168.7	0.34
250	44.8	62.5	-62.5	107.3	108.8	1.44
251	-44.8	62.5	-62.5	-107.3	-108.8	1.44
252	-136.3	31.8	-31.8	-168.1	-168.7	0.34
253	84.5	31.0	-31.0	115.5	116.0	0.46
254	29.8	61.3	-61.3	91.1	92.6	1.64
255	-29.8	61.3	-61.3	-91.1	-92.6	1.64
256	-84.5	31.0	-31.0	-115.5	-116.0	0.46
257	105.6	23.0	-23.0	128.6	128.8	0.13
258	37.0	57.5	-57.5	94.5	95.6	1.19
259	-37.0	57.5	-57.5	-94.5	-95.6	1.19
260	-105.6	23.0	-23.0	-128.6	-128.8	0.13
261	171.0	23.6	-23.6	194.6	194.8	0.10
262	55.9	58.9	-58.9	114.8	115.9	1.01
263	-55.9	58.9	-58.9	-114.8	-115.9	1.01
264	-171.0	23.6	-23.6	-194.6	-194.8	0.10
265	171.0	23.6	-23.6	194.6	194.8	0.10
266	55.9	58.9	-58.9	114.8	115.9	1.01
267	-55.9	58.9	-58.9	-114.8	-115.9	1.01
268	-171.0	23.6	-23.6	-194.6	-194.8	0.10
269	105.6	23.0	-23.0	128.6	128.8	0.13
270	37.0	57.5	-57.5	94.5	95.6	1.19
271	-37.0	57.5	-57.5	-94.5	-95.6	1.19
272	-105.6	23.0	-23.0	-128.6	-128.8	0.13
273	104.1	16.6	-16.6	120.7	120.7	0.00
274	37.6	45.4	-45.4	83.0	83.6	0.79
275	-37.6	45.4	-45.4	-83.0	-83.6	0.79
276	-104.1	16.6	-16.6	-120.7	-120.7	0.00
277	168.2	17.2	-17.2	185.4	185.4	0.01

278	56.6	46.5	-46.5	103.2	103.9	0.66
279	-56.6	46.5	-46.5	-103.2	-103.9	0.66
280	-168.2	17.2	-17.2	-185.4	-185.4	0.01
281	168.2	17.2	-17.2	185.4	185.4	0.01
282	56.6	46.5	-46.5	103.2	103.9	0.66
283	-56.6	46.5	-46.5	-103.2	-103.9	0.66
284	-168.2	17.2	-17.2	-185.4	-185.4	0.01
285	104.1	16.6	-16.6	120.7	120.7	0.00
286	37.6	45.4	-45.4	83.0	83.6	0.79
287	-37.6	45.4	-45.4	-83.0	-83.6	0.79
288	-104.1	16.6	-16.6	-120.7	-120.7	0.00
289	103.4	6.9	-6.9	110.3	110.2	-0.14
290	38.7	29.7	-29.7	68.5	68.8	0.44
291	-38.7	29.7	-29.7	-68.5	-68.8	0.44
292	-103.4	6.9	-6.9	-110.3	-110.2	-0.14
293	166.1	7.3	-7.3	173.4	173.3	-0.09
294	57.9	30.6	-30.6	88.5	88.8	0.37
295	-57.9	30.6	-30.6	-88.5	-88.8	0.37
296	-166.1	7.3	-7.3	-173.4	-173.3	-0.09
297	166.1	7.3	-7.3	173.4	173.3	-0.09
298	57.9	30.6	-30.6	88.5	88.8	0.37
299	-57.9	30.6	-30.6	-88.5	-88.8	0.37
300	-166.1	7.3	-7.3	-173.4	-173.3	-0.09
301	103.4	6.9	-6.9	110.3	110.2	-0.14
302	38.7	29.7	-29.7	68.5	68.8	0.44
303	-38.7	29.7	-29.7	-68.5	-68.8	0.44
304	-103.4	6.9	-6.9	-110.3	-110.2	-0.14
305	122.1	-4.0	4.0	126.1	126.3	0.18
306	43.1	14.3	-14.3	57.4	57.6	0.26
307	-43.1	14.3	-14.3	-57.4	-57.6	0.26
308	-122.1	-4.0	4.0	-126.1	-126.3	0.18
309	198.3	-3.9	3.9	202.2	202.4	0.12
310	65.7	14.9	-14.9	80.6	80.8	0.21
311	-65.7	14.9	-14.9	-80.6	-80.8	0.21
312	-198.3	-3.9	3.9	-202.2	-202.4	0.12
313	198.3	-3.9	3.9	202.2	202.4	0.12
314	65.7	14.9	-14.9	80.6	80.8	0.21
315	-65.7	14.9	-14.9	-80.6	-80.8	0.21
316	-198.3	-3.9	3.9	-202.2	-202.4	0.12
317	122.1	-4.0	4.0	126.1	126.3	0.18
318	43.1	14.3	-14.3	57.4	57.6	0.26
319	-43.1	14.3	-14.3	-57.4	-57.6	0.26
320	-122.1	-4.0	4.0	-126.1	-126.3	0.18

Table B.4 M25 First and Second-Order Moments

M25						
Column	**M_{SD+D+L}**	**$M_{POSITIVE\ EQ.}$**	**$M_{NEGATIVE\ EQ.}$**	**First-Order Moment**	**Second-Order Moment**	**Percent**
1	31.3	422.8	-422.8	454.1	478.3	5.32
2	3.2	434.3	-434.3	437.6	462.2	5.63
3	-3.2	434.3	-434.3	-437.6	-462.2	5.63
4	-31.3	422.8	-422.8	-454.1	-478.3	5.32
5	51.3	423.9	-423.9	475.2	498.9	4.98
6	4.1	435.1	-435.1	439.2	463.2	5.46
7	-4.1	435.1	-435.1	-439.2	-463.2	5.46
8	-51.3	423.9	-423.9	-475.2	-498.9	4.98
9	51.3	423.9	-423.9	475.2	498.9	4.98
10	4.1	435.1	-435.1	439.2	463.2	5.46
11	-4.1	435.1	-435.1	-439.2	-463.2	5.46
12	-51.3	423.9	-423.9	-475.2	-498.9	4.98
13	31.3	422.8	-422.8	454.1	478.3	5.32
14	3.2	434.3	-434.3	437.6	462.2	5.63
15	-3.2	434.3	-434.3	-437.6	-462.2	5.63
16	-31.3	422.8	-422.8	-454.1	-478.3	5.32
17	71.9	277.0	-277.0	348.9	371.7	6.54
18	2.2	310.5	-310.5	312.7	337.9	8.04
19	-2.2	310.5	-310.5	-312.7	-337.9	8.04
20	-71.9	277.0	-277.0	-348.9	-371.7	6.54
21	127.1	277.6	-277.6	404.7	427.7	5.66
22	4.1	312.5	-312.5	316.6	341.8	7.97
23	-4.1	312.5	-312.5	-316.6	-341.8	7.97
24	-127.1	277.6	-277.6	-404.7	-427.7	5.66
25	127.1	277.6	-277.6	404.7	427.7	5.66
26	4.1	312.5	-312.5	316.6	341.8	7.97
27	-4.1	312.5	-312.5	-316.6	-341.8	7.97
28	-127.1	277.6	-277.6	-404.7	-427.7	5.66
29	71.9	277.0	-277.0	348.9	371.7	6.54
30	2.2	310.5	-310.5	312.7	337.9	8.04
31	-2.2	310.5	-310.5	-312.7	-337.9	8.04
32	-71.9	277.0	-277.0	-348.9	-371.7	6.54
33	74.7	185.1	-185.1	259.8	278.6	7.23
34	8.4	234.1	-234.1	242.5	265.2	9.35
35	-8.4	234.1	-234.1	-242.5	-265.2	9.35
36	-74.7	185.1	-185.1	-259.8	-278.6	7.23
37	128.1	186.5	-186.5	314.6	333.4	5.98
38	12.9	236.8	-236.8	249.7	272.4	9.12
39	-12.9	236.8	-236.8	-249.7	-272.4	9.12
40	-128.1	186.5	-186.5	-314.6	-333.4	5.98
41	128.1	186.5	-186.5	314.6	333.4	5.98
42	12.9	236.8	-236.8	249.7	272.4	9.12

43	-12.9	236.8	-236.8	-249.7	-272.4	9.12
44	-128.1	186.5	-186.5	-314.6	-333.4	5.98
45	74.7	185.1	-185.1	259.8	278.6	7.23
46	8.4	234.1	-234.1	242.5	265.2	9.35
47	-8.4	234.1	-234.1	-242.5	-265.2	9.35
48	-74.7	185.1	-185.1	-259.8	-278.6	7.23
49	76.8	128.4	-128.4	205.2	219.6	7.00
50	11.0	184.7	-184.7	195.8	215.0	**9.82**
51	-11.0	184.7	-184.7	-195.8	-215.0	**9.82**
52	-76.8	128.4	-128.4	-205.2	-219.6	7.00
53	131.7	129.9	-129.9	261.6	276.1	5.51
54	17.1	187.7	-187.7	204.8	224.2	9.47
55	-17.1	187.7	-187.7	-204.8	-224.2	9.47
56	-131.7	129.9	-129.9	-261.6	-276.1	5.51
57	131.7	129.9	-129.9	261.6	276.1	5.51
58	17.1	187.7	-187.7	204.8	224.2	9.47
59	-17.1	187.7	-187.7	-204.8	-224.2	9.47
60	-131.7	129.9	-129.9	-261.6	-276.1	5.51
61	76.8	128.4	-128.4	205.2	219.6	7.00
62	11.0	184.7	-184.7	195.8	215.0	**9.82**
63	-11.0	184.7	-184.7	-195.8	-215.0	**9.82**
64	-76.8	128.4	-128.4	-205.2	-219.6	7.00
65	79.5	93.2	-93.2	172.8	183.3	6.10
66	13.6	153.5	-153.5	167.2	183.2	9.57
67	-13.6	153.5	-153.5	-167.2	-183.2	9.57
68	-79.5	93.2	-93.2	-172.8	-183.3	6.10
69	136.6	94.6	-94.6	231.2	241.8	4.60
70	21.4	156.8	-156.8	178.2	194.4	9.13
71	-21.4	156.8	-156.8	-178.2	-194.4	9.13
72	-136.6	94.6	-94.6	-231.2	-241.8	4.60
73	136.6	94.6	-94.6	231.2	241.8	4.60
74	21.4	156.8	-156.8	178.2	194.4	9.13
75	-21.4	156.8	-156.8	-178.2	-194.4	9.13
76	-136.6	94.6	-94.6	-231.2	-241.8	4.60
77	79.5	93.2	-93.2	172.8	183.3	6.10
78	13.6	153.5	-153.5	167.2	183.2	9.57
79	-13.6	153.5	-153.5	-167.2	-183.2	9.57
80	-79.5	93.2	-93.2	-172.8	-183.3	6.10
81	76.8	75.4	-75.4	152.2	160.2	5.23
82	16.0	131.4	-131.4	147.4	160.5	8.91
83	-16.0	131.4	-131.4	-147.4	-160.5	8.91
84	-76.8	75.4	-75.4	-152.2	-160.2	5.23
85	129.7	77.0	-77.0	206.7	214.8	3.92
86	24.4	134.3	-134.3	158.7	172.1	8.44
87	-24.4	134.3	-134.3	-158.7	-172.1	8.44
88	-129.7	77.0	-77.0	-206.7	-214.8	3.92
89	129.7	77.0	-77.0	206.7	214.8	3.92

90	24.4	134.3	-134.3	158.7	172.1	8.44
91	-24.4	134.3	-134.3	-158.7	-172.1	8.44
92	-129.7	77.0	-77.0	-206.7	-214.8	3.92
93	76.8	75.4	-75.4	152.2	160.2	5.23
94	16.0	131.4	-131.4	147.4	160.5	8.91
95	-16.0	131.4	-131.4	-147.4	-160.5	8.91
96	-76.8	75.4	-75.4	-152.2	-160.2	5.23
97	86.0	61.3	-61.3	147.2	152.8	3.77
98	19.7	123.3	-123.3	143.0	154.3	7.91
99	-19.7	123.3	-123.3	-143.0	-154.3	7.91
100	-86.0	61.3	-61.3	-147.2	-152.8	3.77
101	145.7	62.7	-62.7	208.4	214.1	2.73
102	30.5	126.5	-126.5	157.1	168.7	7.40
103	-30.5	126.5	-126.5	-157.1	-168.7	7.40
104	-145.7	62.7	-62.7	-208.4	-214.1	2.73
105	145.7	62.7	-62.7	208.4	214.1	2.73
106	30.5	126.5	-126.5	157.1	168.7	7.40
107	-30.5	126.5	-126.5	-157.1	-168.7	7.40
108	-145.7	62.7	-62.7	-208.4	-214.1	2.73
109	86.0	61.3	-61.3	147.2	152.8	3.77
110	19.7	123.3	-123.3	143.0	154.3	7.91
111	-19.7	123.3	-123.3	-143.0	-154.3	7.91
112	-86.0	61.3	-61.3	-147.2	-152.8	3.77
113	89.1	55.5	-55.5	144.5	148.6	2.85
114	23.0	116.4	-116.4	139.5	149.2	6.95
115	-23.0	116.4	-116.4	-139.5	-149.2	6.95
116	-89.1	55.5	-55.5	-144.5	-148.6	2.85
117	149.7	57.1	-57.1	206.8	211.1	2.07
118	35.4	119.6	-119.6	155.0	165.0	6.44
119	-35.4	119.6	-119.6	-155.0	-165.0	6.44
120	-149.7	57.1	-57.1	-206.8	-211.1	2.07
121	149.7	57.1	-57.1	206.8	211.1	2.07
122	35.4	119.6	-119.6	155.0	165.0	6.44
123	-35.4	119.6	-119.6	-155.0	-165.0	6.44
124	-149.7	57.1	-57.1	-206.8	-211.1	2.07
125	89.1	55.5	-55.5	144.5	148.6	2.85
126	23.0	116.4	-116.4	139.5	149.2	6.95
127	-23.0	116.4	-116.4	-139.5	-149.2	6.95
128	-89.1	55.5	-55.5	-144.5	-148.6	2.85
129	92.0	51.3	-51.3	143.4	146.5	2.19
130	25.9	111.5	-111.5	137.4	145.9	6.17
131	-25.9	111.5	-111.5	-137.4	-145.9	6.17
132	-92.0	51.3	-51.3	-143.4	-146.5	2.19
133	154.1	52.9	-52.9	207.0	210.3	1.59
134	39.6	114.6	-114.6	154.2	163.0	5.68
135	-39.6	114.6	-114.6	-154.2	-163.0	5.68
136	-154.1	52.9	-52.9	-207.0	-210.3	1.59

137	154.1	52.9	-52.9	207.0	210.3	1.59
138	39.6	114.6	-114.6	154.2	163.0	5.68
139	-39.6	114.6	-114.6	-154.2	-163.0	5.68
140	-154.1	52.9	-52.9	-207.0	-210.3	1.59
141	92.0	51.3	-51.3	143.4	146.5	2.19
142	25.9	111.5	-111.5	137.4	145.9	6.17
143	-25.9	111.5	-111.5	-137.4	-145.9	6.17
144	-92.0	51.3	-51.3	-143.4	-146.5	2.19
145	94.6	47.8	-47.8	142.4	144.9	1.76
146	28.3	107.5	-107.5	135.8	143.4	5.60
147	-28.3	107.5	-107.5	-135.8	-143.4	5.60
148	-94.6	47.8	-47.8	-142.4	-144.9	1.76
149	158.7	49.1	-49.1	207.9	210.5	1.26
150	43.6	110.6	-110.6	154.2	162.1	5.11
151	-43.6	110.6	-110.6	-154.2	-162.1	5.11
152	-158.7	49.1	-49.1	-207.9	-210.5	1.26
153	158.7	49.1	-49.1	207.9	210.5	1.26
154	43.6	110.6	-110.6	154.2	162.1	5.11
155	-43.6	110.6	-110.6	-154.2	-162.1	5.11
156	-158.7	49.1	-49.1	-207.9	-210.5	1.26
157	94.6	47.8	-47.8	142.4	144.9	1.76
158	28.3	107.5	-107.5	135.8	143.4	5.60
159	-28.3	107.5	-107.5	-135.8	-143.4	5.60
160	-94.6	47.8	-47.8	-142.4	-144.9	1.76
161	88.8	48.4	-48.4	137.2	139.7	1.83
162	28.3	100.3	-100.3	128.6	135.4	5.25
163	-28.3	100.3	-100.3	-128.6	-135.4	5.25
164	-88.8	48.4	-48.4	-137.2	-139.7	1.83
165	146.5	49.8	-49.8	196.3	199.0	1.35
166	42.7	102.9	-102.9	145.6	152.6	4.80
167	-42.7	102.9	-102.9	-145.6	-152.6	4.80
168	-146.5	49.8	-49.8	-196.3	-199.0	1.35
169	146.5	49.8	-49.8	196.3	199.0	1.35
170	42.7	102.9	-102.9	145.6	152.6	4.80
171	-42.7	102.9	-102.9	-145.6	-152.6	4.80
172	-146.5	49.8	-49.8	-196.3	-199.0	1.35
173	88.8	48.4	-48.4	137.2	139.7	1.83
174	28.3	100.3	-100.3	128.6	135.4	5.25
175	-28.3	100.3	-100.3	-128.6	-135.4	5.25
176	-88.8	48.4	-48.4	-137.2	-139.7	1.83
177	99.8	42.5	-42.5	142.3	144.1	1.29
178	33.1	98.7	-98.7	131.8	138.0	4.68
179	-33.1	98.7	-98.7	-131.8	-138.0	4.68
180	-99.8	42.5	-42.5	-142.3	-144.1	1.29
181	165.5	43.7	-43.7	209.2	211.1	0.93
182	50.4	101.4	-101.4	151.8	158.2	4.21
183	-50.4	101.4	-101.4	-151.8	-158.2	4.21

184	-165.5	43.7	-43.7	-209.2	-211.1	0.93
185	165.5	43.7	-43.7	209.2	211.1	0.93
186	50.4	101.4	-101.4	151.8	158.2	4.21
187	-50.4	101.4	-101.4	-151.8	-158.2	4.21
188	-165.5	43.7	-43.7	-209.2	-211.1	0.93
189	99.8	42.5	-42.5	142.3	144.1	1.29
190	33.1	98.7	-98.7	131.8	138.0	4.68
191	-33.1	98.7	-98.7	-131.8	-138.0	4.68
192	-99.8	42.5	-42.5	-142.3	-144.1	1.29
193	102.0	40.4	-40.4	142.4	143.9	1.06
194	35.7	94.0	-94.0	129.7	135.1	4.16
195	-35.7	94.0	-94.0	-129.7	-135.1	4.16
196	-102.0	40.4	-40.4	-142.4	-143.9	1.06
197	167.9	41.7	-41.7	209.6	211.2	0.77
198	54.0	96.6	-96.6	150.6	156.2	3.71
199	-54.0	96.6	-96.6	-150.6	-156.2	3.71
200	-167.9	41.7	-41.7	-209.6	-211.2	0.77
201	167.9	41.7	-41.7	209.6	211.2	0.77
202	54.0	96.6	-96.6	150.6	156.2	3.71
203	-54.0	96.6	-96.6	-150.6	-156.2	3.71
204	-167.9	41.7	-41.7	-209.6	-211.2	0.77
205	102.0	40.4	-40.4	142.4	143.9	1.06
206	35.7	94.0	-94.0	129.7	135.1	4.16
207	-35.7	94.0	-94.0	-129.7	-135.1	4.16
208	-102.0	40.4	-40.4	-142.4	-143.9	1.06
209	104.5	38.4	-38.4	142.9	144.1	0.87
210	38.1	90.2	-90.2	128.3	133.0	3.70
211	-38.1	90.2	-90.2	-128.3	-133.0	3.70
212	-104.5	38.4	-38.4	-142.9	-144.1	0.87
213	171.4	39.6	-39.6	211.0	212.3	0.63
214	57.4	92.7	-92.7	150.1	155.0	3.28
215	-57.4	92.7	-92.7	-150.1	-155.0	3.28
216	-171.4	39.6	-39.6	-211.0	-212.3	0.63
217	171.4	39.6	-39.6	211.0	212.3	0.63
218	57.4	92.7	-92.7	150.1	155.0	3.28
219	-57.4	92.7	-92.7	-150.1	-155.0	3.28
220	-171.4	39.6	-39.6	-211.0	-212.3	0.63
221	104.5	38.4	-38.4	142.9	144.1	0.87
222	38.1	90.2	-90.2	128.3	133.0	3.70
223	-38.1	90.2	-90.2	-128.3	-133.0	3.70
224	-104.5	38.4	-38.4	-142.9	-144.1	0.87
225	107.1	36.2	-36.2	143.3	144.4	0.72
226	40.3	87.2	-87.2	127.5	131.7	3.34
227	-40.3	87.2	-87.2	-127.5	-131.7	3.34
228	-107.1	36.2	-36.2	-143.3	-144.4	0.72
229	176.4	37.2	-37.2	213.6	214.7	0.52
230	61.1	89.7	-89.7	150.7	155.2	2.94

231	-61.1	89.7	-89.7	-150.7	-155.2	2.94
232	-176.4	37.2	-37.2	-213.6	-214.7	0.52
233	176.4	37.2	-37.2	213.6	214.7	0.52
234	61.1	89.7	-89.7	150.7	155.2	2.94
235	-61.1	89.7	-89.7	-150.7	-155.2	2.94
236	-176.4	37.2	-37.2	-213.6	-214.7	0.52
237	107.1	36.2	-36.2	143.3	144.4	0.72
238	40.3	87.2	-87.2	127.5	131.7	3.34
239	-40.3	87.2	-87.2	-127.5	-131.7	3.34
240	-107.1	36.2	-36.2	-143.3	-144.4	0.72
241	97.4	38.0	-38.0	135.4	136.6	0.91
242	37.4	80.6	-80.6	118.0	121.7	3.16
243	-37.4	80.6	-80.6	-118.0	-121.7	3.16
244	-97.4	38.0	-38.0	-135.4	-136.6	0.91
245	157.7	39.1	-39.1	196.8	198.1	0.66
246	55.7	82.6	-82.6	138.3	142.2	2.79
247	-55.7	82.6	-82.6	-138.3	-142.2	2.79
248	-157.7	39.1	-39.1	-196.8	-198.1	0.66
249	157.7	39.1	-39.1	196.8	198.1	0.66
250	55.7	82.6	-82.6	138.3	142.2	2.79
251	-55.7	82.6	-82.6	-138.3	-142.2	2.79
252	-157.7	39.1	-39.1	-196.8	-198.1	0.66
253	97.4	38.0	-38.0	135.4	136.6	0.91
254	37.4	80.6	-80.6	118.0	121.7	3.16
255	-37.4	80.6	-80.6	-118.0	-121.7	3.16
256	-97.4	38.0	-38.0	-135.4	-136.6	0.91
257	110.6	32.3	-32.3	142.9	143.7	0.56
258	43.2	78.5	-78.5	121.7	125.0	2.70
259	-43.2	78.5	-78.5	-121.7	-125.0	2.70
260	-110.6	32.3	-32.3	-142.9	-143.7	0.56
261	179.9	33.2	-33.2	213.1	214.0	0.40
262	64.8	80.5	-80.5	145.4	148.8	2.34
263	-64.8	80.5	-80.5	-145.4	-148.8	2.34
264	-179.9	33.2	-33.2	-213.1	-214.0	0.40
265	179.9	33.2	-33.2	213.1	214.0	0.40
266	64.8	80.5	-80.5	145.4	148.8	2.34
267	-64.8	80.5	-80.5	-145.4	-148.8	2.34
268	-179.9	33.2	-33.2	-213.1	-214.0	0.40
269	110.6	32.3	-32.3	142.9	143.7	0.56
270	43.2	78.5	-78.5	121.7	125.0	2.70
271	-43.2	78.5	-78.5	-121.7	-125.0	2.70
272	-110.6	32.3	-32.3	-142.9	-143.7	0.56
273	111.4	29.7	-29.7	141.2	141.7	0.41
274	44.9	72.6	-72.6	117.5	120.1	2.28
275	-44.9	72.6	-72.6	-117.5	-120.1	2.28
276	-111.4	29.7	-29.7	-141.2	-141.7	0.41
277	180.3	30.6	-30.6	210.9	211.6	0.30

278	67.0	74.5	-74.5	141.5	144.2	1.96
279	-67.0	74.5	-74.5	-141.5	-144.2	1.96
280	-180.3	30.6	-30.6	-210.9	-211.6	0.30
281	180.3	30.6	-30.6	210.9	211.6	0.30
282	67.0	74.5	-74.5	141.5	144.2	1.96
283	-67.0	74.5	-74.5	-141.5	-144.2	1.96
284	-180.3	30.6	-30.6	-210.9	-211.6	0.30
285	111.4	29.7	-29.7	141.2	141.7	0.41
286	44.9	72.6	-72.6	117.5	120.1	2.28
287	-44.9	72.6	-72.6	-117.5	-120.1	2.28
288	-111.4	29.7	-29.7	-141.2	-141.7	0.41
289	113.3	27.1	-27.1	140.3	140.7	0.28
290	46.6	67.5	-67.5	114.1	116.3	1.91
291	-46.6	67.5	-67.5	-114.1	-116.3	1.91
292	-113.3	27.1	-27.1	-140.3	-140.7	0.28
293	182.6	27.9	-27.9	210.5	211.0	0.20
294	69.3	69.2	-69.2	138.6	140.8	1.63
295	-69.3	69.2	-69.2	-138.6	-140.8	1.63
296	-182.6	27.9	-27.9	-210.5	-211.0	0.20
297	182.6	27.9	-27.9	210.5	211.0	0.20
298	69.3	69.2	-69.2	138.6	140.8	1.63
299	-69.3	69.2	-69.2	-138.6	-140.8	1.63
300	-182.6	27.9	-27.9	-210.5	-211.0	0.20
301	113.3	27.1	-27.1	140.3	140.7	0.28
302	46.6	67.5	-67.5	114.1	116.3	1.91
303	-46.6	67.5	-67.5	-114.1	-116.3	1.91
304	-113.3	27.1	-27.1	-140.3	-140.7	0.28
305	117.0	24.5	-24.5	141.6	141.8	0.18
306	49.0	64.2	-64.2	113.2	115.1	1.63
307	-49.0	64.2	-64.2	-113.2	-115.1	1.63
308	-117.0	24.5	-24.5	-141.6	-141.8	0.18
309	190.1	25.2	-25.2	215.3	215.6	0.14
310	73.5	66.0	-66.0	139.5	141.4	1.38
311	-73.5	66.0	-66.0	-139.5	-141.4	1.38
312	-190.1	25.2	-25.2	-215.3	-215.6	0.14
313	190.1	25.2	-25.2	215.3	215.6	0.14
314	73.5	66.0	-66.0	139.5	141.4	1.38
315	-73.5	66.0	-66.0	-139.5	-141.4	1.38
316	-190.1	25.2	-25.2	-215.3	-215.6	0.14
317	117.0	24.5	-24.5	141.6	141.8	0.18
318	49.0	64.2	-64.2	113.2	115.1	1.63
319	-49.0	64.2	-64.2	-113.2	-115.1	1.63
320	-117.0	24.5	-24.5	-141.6	-141.8	0.18
321	93.6	28.2	-28.2	121.9	122.4	0.41
322	38.5	56.5	-56.5	94.9	96.4	1.59
323	-38.5	56.5	-56.5	-94.9	-96.4	1.59
324	-93.6	28.2	-28.2	-121.9	-122.4	0.41

325	148.3	28.9	-28.9	177.2	177.7	0.30
326	56.3	57.6	-57.6	113.9	115.4	1.36
327	-56.3	57.6	-57.6	-113.9	-115.4	1.36
328	-148.3	28.9	-28.9	-177.2	-177.7	0.30
329	148.3	28.9	-28.9	177.2	177.7	0.30
330	56.3	57.6	-57.6	113.9	115.4	1.36
331	-56.3	57.6	-57.6	-113.9	-115.4	1.36
332	-148.3	28.9	-28.9	-177.2	-177.7	0.30
333	93.6	28.2	-28.2	121.9	122.4	0.41
334	38.5	56.5	-56.5	94.9	96.4	1.59
335	-38.5	56.5	-56.5	-94.9	-96.4	1.59
336	-93.6	28.2	-28.2	-121.9	-122.4	0.41
337	116.6	20.2	-20.2	136.8	136.9	0.10
338	47.5	52.5	-52.5	100.0	101.1	1.15
339	-47.5	52.5	-52.5	-100.0	-101.1	1.15
340	-116.6	20.2	-20.2	-136.8	-136.9	0.10
341	185.3	20.7	-20.7	206.0	206.1	0.08
342	69.8	53.7	-53.7	123.5	124.7	0.96
343	-69.8	53.7	-53.7	-123.5	-124.7	0.96
344	-185.3	20.7	-20.7	-206.0	-206.1	0.08
345	185.3	20.7	-20.7	206.0	206.1	0.08
346	69.8	53.7	-53.7	123.5	124.7	0.96
347	-69.8	53.7	-53.7	-123.5	-124.7	0.96
348	-185.3	20.7	-20.7	-206.0	-206.1	0.08
349	116.6	20.2	-20.2	136.8	136.9	0.10
350	47.5	52.5	-52.5	100.0	101.1	1.15
351	-47.5	52.5	-52.5	-100.0	-101.1	1.15
352	-116.6	20.2	-20.2	-136.8	-136.9	0.10
353	114.7	13.9	-13.9	128.5	128.5	-0.02
354	47.6	40.7	-40.7	88.3	89.0	0.78
355	-47.6	40.7	-40.7	-88.3	-89.0	0.78
356	-114.7	13.9	-13.9	-128.5	-128.5	-0.02
357	181.9	14.3	-14.3	196.2	196.2	-0.01
358	69.9	41.7	-41.7	111.6	112.3	0.64
359	-69.9	41.7	-41.7	-111.6	-112.3	0.64
360	-181.9	14.3	-14.3	-196.2	-196.2	-0.01
361	181.9	14.3	-14.3	196.2	196.2	-0.01
362	69.9	41.7	-41.7	111.6	112.3	0.64
363	-69.9	41.7	-41.7	-111.6	-112.3	0.64
364	-181.9	14.3	-14.3	-196.2	-196.2	-0.01
365	114.7	13.9	-13.9	128.5	128.5	-0.02
366	47.6	40.7	-40.7	88.3	89.0	0.78
367	-47.6	40.7	-40.7	-88.3	-89.0	0.78
368	-114.7	13.9	-13.9	-128.5	-128.5	-0.02
369	113.8	4.9	-4.9	118.7	118.5	-0.15
370	48.5	26.1	-26.1	74.6	75.0	0.46
371	-48.5	26.1	-26.1	-74.6	-75.0	0.46

372	-113.8	4.9	-4.9	-118.7	-118.5	-0.15
373	179.4	5.3	-5.3	184.6	184.5	-0.10
374	70.7	26.8	-26.8	97.5	97.9	0.37
375	-70.7	26.8	-26.8	-97.5	-97.9	0.37
376	-179.4	5.3	-5.3	-184.6	-184.5	-0.10
377	179.4	5.3	-5.3	184.6	184.5	-0.10
378	70.7	26.8	-26.8	97.5	97.9	0.37
379	-70.7	26.8	-26.8	-97.5	-97.9	0.37
380	-179.4	5.3	-5.3	-184.6	-184.5	-0.10
381	113.8	4.9	-4.9	118.7	118.5	-0.15
382	48.5	26.1	-26.1	74.6	75.0	0.46
383	-48.5	26.1	-26.1	-74.6	-75.0	0.46
384	-113.8	4.9	-4.9	-118.7	-118.5	-0.15
385	133.9	-4.5	4.5	138.4	138.7	0.19
386	54.5	12.7	-12.7	67.2	67.4	0.30
387	-54.5	12.7	-12.7	-67.2	-67.4	0.30
388	-133.9	-4.5	4.5	-138.4	-138.7	0.19
389	213.7	-4.5	4.5	218.2	218.5	0.13
390	80.8	13.1	-13.1	93.9	94.2	0.24
391	-80.8	13.1	-13.1	-93.9	-94.2	0.24
392	-213.7	-4.5	4.5	-218.2	-218.5	0.13
393	213.7	-4.5	4.5	218.2	218.5	0.13
394	80.8	13.1	-13.1	93.9	94.2	0.24
395	-80.8	13.1	-13.1	-93.9	-94.2	0.24
396	-213.7	-4.5	4.5	-218.2	-218.5	0.13
397	133.9	-4.5	4.5	138.4	138.7	0.19
398	54.5	12.7	-12.7	67.2	67.4	0.30
399	-54.5	12.7	-12.7	-67.2	-67.4	0.30
400	-133.9	-4.5	4.5	-138.4	-138.7	0.19

Table B.5 M30 First and Second-Order Moments

M30						
Column	**M_{SD+D+L}**	**$M_{POSITIVE\ EQ.}$**	**$M_{NEGATIVE\ EQ.}$**	**First-Order Moment**	**Second-Order Moment**	**Percent**
1	32.0	474.5	-474.5	506.4	539.8	6.59
2	3.6	484.6	-484.6	488.3	522.2	6.94
3	-3.6	484.6	-484.6	-488.3	-522.2	6.94
4	-32.0	474.5	-474.5	-506.4	-539.8	6.59
5	52.2	475.6	-475.6	527.8	560.6	6.22
6	4.6	485.3	-485.3	489.9	523.1	6.77
7	-4.6	485.3	-485.3	-489.9	-523.1	6.77
8	-52.2	475.6	-475.6	-527.8	-560.6	6.22
9	52.2	475.6	-475.6	527.8	560.6	6.22
10	4.6	485.3	-485.3	489.9	523.1	6.77
11	-4.6	485.3	-485.3	-489.9	-523.1	6.77
12	-52.2	475.6	-475.6	-527.8	-560.6	6.22
13	32.0	474.5	-474.5	506.4	539.8	6.59
14	3.6	484.6	-484.6	488.3	522.2	6.94
15	-3.6	484.6	-484.6	-488.3	-522.2	6.94
16	-32.0	474.5	-474.5	-506.4	-539.8	6.59
17	70.5	325.8	-325.8	396.4	428.3	8.05
18	1.9	354.1	-354.1	356.0	390.3	9.63
19	-1.9	354.1	-354.1	-356.0	-390.3	9.63
20	-70.5	325.8	-325.8	-396.4	-428.3	8.05
21	125.1	326.4	-326.4	451.5	483.5	7.09
22	3.7	355.8	-355.8	359.4	393.8	9.57
23	-3.7	355.8	-355.8	-359.4	-393.8	9.57
24	-125.1	326.4	-326.4	-451.5	-483.5	7.09
25	125.1	326.4	-326.4	451.5	483.5	7.09
26	3.7	355.8	-355.8	359.4	393.8	9.57
27	-3.7	355.8	-355.8	-359.4	-393.8	9.57
28	-125.1	326.4	-326.4	-451.5	-483.5	7.09
29	70.5	325.8	-325.8	396.4	428.3	8.05
30	1.9	354.1	-354.1	356.0	390.3	9.63
31	-1.9	354.1	-354.1	-356.0	-390.3	9.63
32	-70.5	325.8	-325.8	-396.4	-428.3	8.05
33	74.9	225.4	-225.4	300.3	327.5	9.08
34	8.2	268.6	-268.6	276.8	308.1	11.33
35	-8.2	268.6	-268.6	-276.8	-308.1	11.33
36	-74.9	225.4	-225.4	-300.3	-327.5	9.08
37	128.7	226.5	-226.5	355.2	382.5	7.68
38	12.5	271.0	-271.0	283.5	314.9	11.10
39	-12.5	271.0	-271.0	-283.5	-314.9	11.10
40	-128.7	226.5	-226.5	-355.2	-382.5	7.68
41	128.7	226.5	-226.5	355.2	382.5	7.68
42	12.5	271.0	-271.0	283.5	314.9	11.10

43	-12.5	271.0	-271.0	-283.5	-314.9	11.10
44	-128.7	226.5	-226.5	-355.2	-382.5	7.68
45	74.9	225.4	-225.4	300.3	327.5	9.08
46	8.2	268.6	-268.6	276.8	308.1	11.33
47	-8.2	268.6	-268.6	-276.8	-308.1	11.33
48	-74.9	225.4	-225.4	-300.3	-327.5	9.08
49	76.7	158.8	-158.8	235.5	257.3	9.23
50	10.8	210.0	-210.0	220.8	247.9	12.25
51	-10.8	210.0	-210.0	-220.8	-247.9	12.25
52	-76.7	158.8	-158.8	-235.5	-257.3	9.23
53	131.6	160.2	-160.2	291.8	313.6	7.48
54	16.6	212.8	-212.8	229.4	256.6	11.88
55	-16.6	212.8	-212.8	-229.4	-256.6	11.88
56	-131.6	160.2	-160.2	-291.8	-313.6	7.48
57	131.6	160.2	-160.2	291.8	313.6	7.48
58	16.6	212.8	-212.8	229.4	256.6	11.88
59	-16.6	212.8	-212.8	-229.4	-256.6	11.88
60	-131.6	160.2	-160.2	-291.8	-313.6	7.48
61	76.7	158.8	-158.8	235.5	257.3	9.23
62	10.8	210.0	-210.0	220.8	247.9	12.25
63	-10.8	210.0	-210.0	-220.8	-247.9	12.25
64	-76.7	158.8	-158.8	-235.5	-257.3	9.23
65	79.0	114.6	-114.6	193.6	210.2	8.59
66	13.3	170.2	-170.2	183.5	206.3	**<u>12.40</u>**
67	-13.3	170.2	-170.2	-183.5	-206.3	**<u>12.40</u>**
68	-79.0	114.6	-114.6	-193.6	-210.2	8.59
69	135.6	115.9	-115.9	251.5	268.3	6.65
70	20.6	173.3	-173.3	193.9	217.0	11.88
71	-20.6	173.3	-173.3	-193.9	-217.0	11.88
72	-135.6	115.9	-115.9	-251.5	-268.3	6.65
73	135.6	115.9	-115.9	251.5	268.3	6.65
74	20.6	173.3	-173.3	193.9	217.0	11.88
75	-20.6	173.3	-173.3	-193.9	-217.0	11.88
76	-135.6	115.9	-115.9	-251.5	-268.3	6.65
77	79.0	114.6	-114.6	193.6	210.2	8.59
78	13.3	170.2	-170.2	183.5	206.3	**<u>12.40</u>**
79	-13.3	170.2	-170.2	-183.5	-206.3	**<u>12.40</u>**
80	-79.0	114.6	-114.6	-193.6	-210.2	8.59
81	77.3	87.9	-87.9	165.3	178.0	7.67
82	15.9	141.3	-141.3	157.1	175.9	11.93
83	-15.9	141.3	-141.3	-157.1	-175.9	11.93
84	-77.3	87.9	-87.9	-165.3	-178.0	7.67
85	130.7	89.5	-89.5	220.2	233.0	5.84
86	24.1	144.0	-144.0	168.1	187.2	11.33
87	-24.1	144.0	-144.0	-168.1	-187.2	11.33
88	-130.7	89.5	-89.5	-220.2	-233.0	5.84
89	130.7	89.5	-89.5	220.2	233.0	5.84

90	24.1	144.0	-144.0	168.1	187.2	11.33
91	-24.1	144.0	-144.0	-168.1	-187.2	11.33
92	-130.7	89.5	-89.5	-220.2	-233.0	5.84
93	77.3	87.9	-87.9	165.3	178.0	7.67
94	15.9	141.3	-141.3	157.1	175.9	11.93
95	-15.9	141.3	-141.3	-157.1	-175.9	11.93
96	-77.3	87.9	-87.9	-165.3	-178.0	7.67
97	85.4	68.4	-68.4	153.8	162.9	5.94
98	19.4	127.5	-127.5	146.9	162.9	10.91
99	-19.4	127.5	-127.5	-146.9	-162.9	10.91
100	-85.4	68.4	-68.4	-153.8	-162.9	5.94
101	144.8	69.8	-69.8	214.6	223.9	4.33
102	29.8	130.6	-130.6	160.4	176.8	10.22
103	-29.8	130.6	-130.6	-160.4	-176.8	10.22
104	-144.8	69.8	-69.8	-214.6	-223.9	4.33
105	144.8	69.8	-69.8	214.6	223.9	4.33
106	29.8	130.6	-130.6	160.4	176.8	10.22
107	-29.8	130.6	-130.6	-160.4	-176.8	10.22
108	-144.8	69.8	-69.8	-214.6	-223.9	4.33
109	85.4	68.4	-68.4	153.8	162.9	5.94
110	19.4	127.5	-127.5	146.9	162.9	10.91
111	-19.4	127.5	-127.5	-146.9	-162.9	10.91
112	-85.4	68.4	-68.4	-153.8	-162.9	5.94
113	88.8	58.9	-58.9	147.7	154.5	4.60
114	22.8	117.8	-117.8	140.6	154.3	9.73
115	-22.8	117.8	-117.8	-140.6	-154.3	9.73
116	-88.8	58.9	-58.9	-147.7	-154.5	4.60
117	149.4	60.4	-60.4	209.8	216.8	3.32
118	34.7	120.9	-120.9	155.6	169.6	9.03
119	-34.7	120.9	-120.9	-155.6	-169.6	9.03
120	-149.4	60.4	-60.4	-209.8	-216.8	3.32
121	149.4	60.4	-60.4	209.8	216.8	3.32
122	34.7	120.9	-120.9	155.6	169.6	9.03
123	-34.7	120.9	-120.9	-155.6	-169.6	9.03
124	-149.4	60.4	-60.4	-209.8	-216.8	3.32
125	88.8	58.9	-58.9	147.7	154.5	4.60
126	22.8	117.8	-117.8	140.6	154.3	9.73
127	-22.8	117.8	-117.8	-140.6	-154.3	9.73
128	-88.8	58.9	-58.9	-147.7	-154.5	4.60
129	91.8	53.5	-53.5	145.3	150.5	3.54
130	25.7	112.2	-112.2	137.8	149.8	8.66
131	-25.7	112.2	-112.2	-137.8	-149.8	8.66
132	-91.8	53.5	-53.5	-145.3	-150.5	3.54
133	153.8	55.0	-55.0	208.8	214.1	2.55
134	39.0	115.2	-115.2	154.2	166.5	7.98
135	-39.0	115.2	-115.2	-154.2	-166.5	7.98
136	-153.8	55.0	-55.0	-208.8	-214.1	2.55

137	153.8	55.0	-55.0	208.8	214.1	2.55
138	39.0	115.2	-115.2	154.2	166.5	7.98
139	-39.0	115.2	-115.2	-154.2	-166.5	7.98
140	-153.8	55.0	-55.0	-208.8	-214.1	2.55
141	91.8	53.5	-53.5	145.3	150.5	3.54
142	25.7	112.2	-112.2	137.8	149.8	8.66
143	-25.7	112.2	-112.2	-137.8	-149.8	8.66
144	-91.8	53.5	-53.5	-145.3	-150.5	3.54
145	94.0	50.0	-50.0	144.0	148.1	2.81
146	28.0	108.5	-108.5	136.5	147.1	7.83
147	-28.0	108.5	-108.5	-136.5	-147.1	7.83
148	-94.0	50.0	-50.0	-144.0	-148.1	2.81
149	157.6	51.4	-51.4	209.0	213.2	2.01
150	42.7	111.5	-111.5	154.2	165.3	7.16
151	-42.7	111.5	-111.5	-154.2	-165.3	7.16
152	-157.6	51.4	-51.4	-209.0	-213.2	2.01
153	157.6	51.4	-51.4	209.0	213.2	2.01
154	42.7	111.5	-111.5	154.2	165.3	7.16
155	-42.7	111.5	-111.5	-154.2	-165.3	7.16
156	-157.6	51.4	-51.4	-209.0	-213.2	2.01
157	94.0	50.0	-50.0	144.0	148.1	2.81
158	28.0	108.5	-108.5	136.5	147.1	7.83
159	-28.0	108.5	-108.5	-136.5	-147.1	7.83
160	-94.0	50.0	-50.0	-144.0	-148.1	2.81
161	90.0	50.3	-50.3	140.2	144.0	2.68
162	28.7	102.5	-102.5	131.2	140.8	7.26
163	-28.7	102.5	-102.5	-131.2	-140.8	7.26
164	-90.0	50.3	-50.3	-140.2	-144.0	2.68
165	148.4	51.7	-51.7	200.2	204.1	1.96
166	43.0	105.2	-105.2	148.2	158.0	6.63
167	-43.0	105.2	-105.2	-148.2	-158.0	6.63
168	-148.4	51.7	-51.7	-200.2	-204.1	1.96
169	148.4	51.7	-51.7	200.2	204.1	1.96
170	43.0	105.2	-105.2	148.2	158.0	6.63
171	-43.0	105.2	-105.2	-148.2	-158.0	6.63
172	-148.4	51.7	-51.7	-200.2	-204.1	1.96
173	90.0	50.3	-50.3	140.2	144.0	2.68
174	28.7	102.5	-102.5	131.2	140.8	7.26
175	-28.7	102.5	-102.5	-131.2	-140.8	7.26
176	-90.0	50.3	-50.3	-140.2	-144.0	2.68
177	99.6	44.6	-44.6	144.2	147.0	1.96
178	33.2	101.1	-101.1	134.2	143.1	6.57
179	-33.2	101.1	-101.1	-134.2	-143.1	6.57
180	-99.6	44.6	-44.6	-144.2	-147.0	1.96
181	165.2	45.9	-45.9	211.0	214.0	1.41
182	50.1	103.9	-103.9	154.0	163.2	5.93
183	-50.1	103.9	-103.9	-154.0	-163.2	5.93

184	-165.2	45.9	-45.9	-211.0	-214.0	1.41
185	165.2	45.9	-45.9	211.0	214.0	1.41
186	50.1	103.9	-103.9	154.0	163.2	5.93
187	-50.1	103.9	-103.9	-154.0	-163.2	5.93
188	-165.2	45.9	-45.9	-211.0	-214.0	1.41
189	99.6	44.6	-44.6	144.2	147.0	1.96
190	33.2	101.1	-101.1	134.2	143.1	6.57
191	-33.2	101.1	-101.1	-134.2	-143.1	6.57
192	-99.6	44.6	-44.6	-144.2	-147.0	1.96
193	102.4	42.1	-42.1	144.5	146.9	1.64
194	36.1	96.7	-96.7	132.8	140.7	5.98
195	-36.1	96.7	-96.7	-132.8	-140.7	5.98
196	-102.4	42.1	-42.1	-144.5	-146.9	1.64
197	168.5	43.4	-43.4	211.9	214.4	1.19
198	54.1	99.4	-99.4	153.5	161.7	5.36
199	-54.1	99.4	-99.4	-153.5	-161.7	5.36
200	-168.5	43.4	-43.4	-211.9	-214.4	1.19
201	168.5	43.4	-43.4	211.9	214.4	1.19
202	54.1	99.4	-99.4	153.5	161.7	5.36
203	-54.1	99.4	-99.4	-153.5	-161.7	5.36
204	-168.5	43.4	-43.4	-211.9	-214.4	1.19
205	102.4	42.1	-42.1	144.5	146.9	1.64
206	36.1	96.7	-96.7	132.8	140.7	5.98
207	-36.1	96.7	-96.7	-132.8	-140.7	5.98
208	-102.4	42.1	-42.1	-144.5	-146.9	1.64
209	105.0	39.9	-39.9	144.9	146.9	1.40
210	38.6	93.2	-93.2	131.8	139.0	5.48
211	-38.6	93.2	-93.2	-131.8	-139.0	5.48
212	-105.0	39.9	-39.9	-144.9	-146.9	1.40
213	172.2	41.1	-41.1	213.3	215.5	1.01
214	57.7	95.8	-95.8	153.5	161.0	4.88
215	-57.7	95.8	-95.8	-153.5	-161.0	4.88
216	-172.2	41.1	-41.1	-213.3	-215.5	1.01
217	172.2	41.1	-41.1	213.3	215.5	1.01
218	57.7	95.8	-95.8	153.5	161.0	4.88
219	-57.7	95.8	-95.8	-153.5	-161.0	4.88
220	-172.2	41.1	-41.1	-213.3	-215.5	1.01
221	105.0	39.9	-39.9	144.9	146.9	1.40
222	38.6	93.2	-93.2	131.8	139.0	5.48
223	-38.6	93.2	-93.2	-131.8	-139.0	5.48
224	-105.0	39.9	-39.9	-144.9	-146.9	1.40
225	107.2	38.4	-38.4	145.6	147.4	1.24
226	40.8	91.1	-91.1	131.8	138.5	5.09
227	-40.8	91.1	-91.1	-131.8	-138.5	5.09
228	-107.2	38.4	-38.4	-145.6	-147.4	1.24
229	176.3	39.4	-39.4	215.7	217.6	0.89
230	61.2	93.6	-93.6	154.9	161.8	4.50

231	-61.2	93.6	-93.6	-154.9	-161.8	4.50
232	-176.3	39.4	-39.4	-215.7	-217.6	0.89
233	176.3	39.4	-39.4	215.7	217.6	0.89
234	61.2	93.6	-93.6	154.9	161.8	4.50
235	-61.2	93.6	-93.6	-154.9	-161.8	4.50
236	-176.3	39.4	-39.4	-215.7	-217.6	0.89
237	107.2	38.4	-38.4	145.6	147.4	1.24
238	40.8	91.1	-91.1	131.8	138.5	5.09
239	-40.8	91.1	-91.1	-131.8	-138.5	5.09
240	-107.2	38.4	-38.4	-145.6	-147.4	1.24
241	100.1	41.1	-41.1	141.2	143.3	1.48
242	39.1	86.8	-86.8	126.0	132.1	4.87
243	-39.1	86.8	-86.8	-126.0	-132.1	4.87
244	-100.1	41.1	-41.1	-141.2	-143.3	1.48
245	161.9	42.3	-42.3	204.2	206.4	1.08
246	57.8	89.0	-89.0	146.8	153.2	4.32
247	-57.8	89.0	-89.0	-146.8	-153.2	4.32
248	-161.9	42.3	-42.3	-204.2	-206.4	1.08
249	161.9	42.3	-42.3	204.2	206.4	1.08
250	57.8	89.0	-89.0	146.8	153.2	4.32
251	-57.8	89.0	-89.0	-146.8	-153.2	4.32
252	-161.9	42.3	-42.3	-204.2	-206.4	1.08
253	100.1	41.1	-41.1	141.2	143.3	1.48
254	39.1	86.8	-86.8	126.0	132.1	4.87
255	-39.1	86.8	-86.8	-126.0	-132.1	4.87
256	-100.1	41.1	-41.1	-141.2	-143.3	1.48
257	111.7	37.8	-37.8	149.5	151.1	1.08
258	44.8	87.6	-87.6	132.3	138.1	4.35
259	-44.8	87.6	-87.6	-132.3	-138.1	4.35
260	-111.7	37.8	-37.8	-149.5	-151.1	1.08
261	181.7	38.8	-38.8	220.6	222.3	0.77
262	66.6	89.9	-89.9	156.5	162.5	3.81
263	-66.6	89.9	-89.9	-156.5	-162.5	3.81
264	-181.7	38.8	-38.8	-220.6	-222.3	0.77
265	181.7	38.8	-38.8	220.6	222.3	0.77
266	66.6	89.9	-89.9	156.5	162.5	3.81
267	-66.6	89.9	-89.9	-156.5	-162.5	3.81
268	-181.7	38.8	-38.8	-220.6	-222.3	0.77
269	111.7	37.8	-37.8	149.5	151.1	1.08
270	44.8	87.6	-87.6	132.3	138.1	4.35
271	-44.8	87.6	-87.6	-132.3	-138.1	4.35
272	-111.7	37.8	-37.8	-149.5	-151.1	1.08
273	113.5	36.9	-36.9	150.4	151.8	0.93
274	47.0	84.7	-84.7	131.6	136.7	3.89
275	-47.0	84.7	-84.7	-131.6	-136.7	3.89
276	-113.5	36.9	-36.9	-150.4	-151.8	0.93
277	183.5	38.0	-38.0	221.4	222.9	0.67

278	69.5	86.9	-86.9	156.4	161.6	3.39
279	-69.5	86.9	-86.9	-156.4	-161.6	3.39
280	-183.5	38.0	-38.0	-221.4	-222.9	0.67
281	183.5	38.0	-38.0	221.4	222.9	0.67
282	69.5	86.9	-86.9	156.4	161.6	3.39
283	-69.5	86.9	-86.9	-156.4	-161.6	3.39
284	-183.5	38.0	-38.0	-221.4	-222.9	0.67
285	113.5	36.9	-36.9	150.4	151.8	0.93
286	47.0	84.7	-84.7	131.6	136.7	3.89
287	-47.0	84.7	-84.7	-131.6	-136.7	3.89
288	-113.5	36.9	-36.9	-150.4	-151.8	0.93
289	115.7	34.7	-34.7	150.5	151.6	0.78
290	49.0	81.2	-81.2	130.2	134.8	3.49
291	-49.0	81.2	-81.2	-130.2	-134.8	3.49
292	-115.7	34.7	-34.7	-150.5	-151.6	0.78
293	186.5	35.8	-35.8	222.2	223.5	0.56
294	72.4	83.3	-83.3	155.7	160.4	3.02
295	-72.4	83.3	-83.3	-155.7	-160.4	3.02
296	-186.5	35.8	-35.8	-222.2	-223.5	0.56
297	186.5	35.8	-35.8	222.2	223.5	0.56
298	72.4	83.3	-83.3	155.7	160.4	3.02
299	-72.4	83.3	-83.3	-155.7	-160.4	3.02
300	-186.5	35.8	-35.8	-222.2	-223.5	0.56
301	115.7	34.7	-34.7	150.5	151.6	0.78
302	49.0	81.2	-81.2	130.2	134.8	3.49
303	-49.0	81.2	-81.2	-130.2	-134.8	3.49
304	-115.7	34.7	-34.7	-150.5	-151.6	0.78
305	118.2	31.9	-31.9	150.1	151.0	0.65
306	51.1	77.8	-77.8	128.9	133.0	3.17
307	-51.1	77.8	-77.8	-128.9	-133.0	3.17
308	-118.2	31.9	-31.9	-150.1	-151.0	0.65
309	191.1	32.8	-32.8	223.9	224.9	0.46
310	75.8	79.9	-79.9	155.7	160.0	2.72
311	-75.8	79.9	-79.9	-155.7	-160.0	2.72
312	-191.1	32.8	-32.8	-223.9	-224.9	0.46
313	191.1	32.8	-32.8	223.9	224.9	0.46
314	75.8	79.9	-79.9	155.7	160.0	2.72
315	-75.8	79.9	-79.9	-155.7	-160.0	2.72
316	-191.1	32.8	-32.8	-223.9	-224.9	0.46
317	118.2	31.9	-31.9	150.1	151.0	0.65
318	51.1	77.8	-77.8	128.9	133.0	3.17
319	-51.1	77.8	-77.8	-128.9	-133.0	3.17
320	-118.2	31.9	-31.9	-150.1	-151.0	0.65
321	107.0	32.9	-32.9	140.0	141.1	0.82
322	46.7	71.2	-71.2	117.9	121.5	3.04
323	-46.7	71.2	-71.2	-117.9	-121.5	3.04
324	-107.0	32.9	-32.9	-140.0	-141.1	0.82

325	170.3	33.8	-33.8	204.1	205.3	0.60
326	68.1	72.9	-72.9	141.0	144.7	2.62
327	-68.1	72.9	-72.9	-141.0	-144.7	2.62
328	-170.3	33.8	-33.8	-204.1	-205.3	0.60
329	170.3	33.8	-33.8	204.1	205.3	0.60
330	68.1	72.9	-72.9	141.0	144.7	2.62
331	-68.1	72.9	-72.9	-141.0	-144.7	2.62
332	-170.3	33.8	-33.8	-204.1	-205.3	0.60
333	107.0	32.9	-32.9	140.0	141.1	0.82
334	46.7	71.2	-71.2	117.9	121.5	3.04
335	-46.7	71.2	-71.2	-117.9	-121.5	3.04
336	-107.0	32.9	-32.9	-140.0	-141.1	0.82
337	121.0	28.0	-28.0	149.0	149.7	0.50
338	53.4	69.5	-69.5	122.9	126.0	2.58
339	-53.4	69.5	-69.5	-122.9	-126.0	2.58
340	-121.0	28.0	-28.0	-149.0	-149.7	0.50
341	193.5	28.7	-28.7	222.3	223.0	0.35
342	78.4	71.2	-71.2	149.6	152.9	2.19
343	-78.4	71.2	-71.2	-149.6	-152.9	2.19
344	-193.5	28.7	-28.7	-222.3	-223.0	0.35
345	193.5	28.7	-28.7	222.3	223.0	0.35
346	78.4	71.2	-71.2	149.6	152.9	2.19
347	-78.4	71.2	-71.2	-149.6	-152.9	2.19
348	-193.5	28.7	-28.7	-222.3	-223.0	0.35
349	121.0	28.0	-28.0	149.0	149.7	0.50
350	53.4	69.5	-69.5	122.9	126.0	2.58
351	-53.4	69.5	-69.5	-122.9	-126.0	2.58
352	-121.0	28.0	-28.0	-149.0	-149.7	0.50
353	121.5	26.4	-26.4	148.0	148.5	0.37
354	54.7	65.1	-65.1	119.8	122.4	2.18
355	-54.7	65.1	-65.1	-119.8	-122.4	2.18
356	-121.5	26.4	-26.4	-148.0	-148.5	0.37
357	193.4	27.2	-27.2	220.6	221.2	0.27
358	79.9	66.7	-66.7	146.6	149.3	1.84
359	-79.9	66.7	-66.7	-146.6	-149.3	1.84
360	-193.4	27.2	-27.2	-220.6	-221.2	0.27
361	193.4	27.2	-27.2	220.6	221.2	0.27
362	79.9	66.7	-66.7	146.6	149.3	1.84
363	-79.9	66.7	-66.7	-146.6	-149.3	1.84
364	-193.4	27.2	-27.2	-220.6	-221.2	0.27
365	121.5	26.4	-26.4	148.0	148.5	0.37
366	54.7	65.1	-65.1	119.8	122.4	2.18
367	-54.7	65.1	-65.1	-119.8	-122.4	2.18
368	-121.5	26.4	-26.4	-148.0	-148.5	0.37
369	123.2	24.9	-24.9	148.1	148.4	0.25
370	56.2	61.6	-61.6	117.8	120.0	1.83
371	-56.2	61.6	-61.6	-117.8	-120.0	1.83

372	-123.2	24.9	-24.9	-148.1	-148.4	0.25
373	195.4	25.6	-25.6	221.0	221.4	0.18
374	81.9	63.1	-63.1	145.0	147.3	1.54
375	-81.9	63.1	-63.1	-145.0	-147.3	1.54
376	-195.4	25.6	-25.6	-221.0	-221.4	0.18
377	195.4	25.6	-25.6	221.0	221.4	0.18
378	81.9	63.1	-63.1	145.0	147.3	1.54
379	-81.9	63.1	-63.1	-145.0	-147.3	1.54
380	-195.4	25.6	-25.6	-221.0	-221.4	0.18
381	123.2	24.9	-24.9	148.1	148.4	0.25
382	56.2	61.6	-61.6	117.8	120.0	1.83
383	-56.2	61.6	-61.6	-117.8	-120.0	1.83
384	-123.2	24.9	-24.9	-148.1	-148.4	0.25
385	127.0	22.7	-22.7	149.6	149.9	0.16
386	58.7	59.1	-59.1	117.8	119.6	1.57
387	-58.7	59.1	-59.1	-117.8	-119.6	1.57
388	-127.0	22.7	-22.7	-149.6	-149.9	0.16
389	202.9	23.3	-23.3	226.1	226.4	0.12
390	86.3	60.6	-60.6	146.8	148.8	1.31
391	-86.3	60.6	-60.6	-146.8	-148.8	1.31
392	-202.9	23.3	-23.3	-226.1	-226.4	0.12
393	202.9	23.3	-23.3	226.1	226.4	0.12
394	86.3	60.6	-60.6	146.8	148.8	1.31
395	-86.3	60.6	-60.6	-146.8	-148.8	1.31
396	-202.9	23.3	-23.3	-226.1	-226.4	0.12
397	127.0	22.7	-22.7	149.6	149.9	0.16
398	58.7	59.1	-59.1	117.8	119.6	1.57
399	-58.7	59.1	-59.1	-117.8	-119.6	1.57
400	-127.0	22.7	-22.7	-149.6	-149.9	0.16
401	101.3	25.5	-25.5	126.8	127.2	0.37
402	45.7	51.4	-51.4	97.1	98.6	1.54
403	-45.7	51.4	-51.4	-97.1	-98.6	1.54
404	-101.3	25.5	-25.5	-126.8	-127.2	0.37
405	157.9	26.0	-26.0	184.0	184.5	0.28
406	65.6	52.4	-52.4	118.0	119.6	1.30
407	-65.6	52.4	-52.4	-118.0	-119.6	1.30
408	-157.9	26.0	-26.0	-184.0	-184.5	0.28
409	157.9	26.0	-26.0	184.0	184.5	0.28
410	65.6	52.4	-52.4	118.0	119.6	1.30
411	-65.6	52.4	-52.4	-118.0	-119.6	1.30
412	-157.9	26.0	-26.0	-184.0	-184.5	0.28
413	101.3	25.5	-25.5	126.8	127.2	0.37
414	45.7	51.4	-51.4	97.1	98.6	1.54
415	-45.7	51.4	-51.4	-97.1	-98.6	1.54
416	-101.3	25.5	-25.5	-126.8	-127.2	0.37
417	125.8	17.4	-17.4	143.1	143.3	0.08
418	56.3	47.1	-47.1	103.4	104.5	1.12

419	-56.3	47.1	-47.1	-103.4	-104.5	1.12
420	-125.8	17.4	-17.4	-143.1	-143.3	0.08
421	196.8	17.8	-17.8	214.7	214.8	0.06
422	81.1	48.1	-48.1	129.2	130.4	0.92
423	-81.1	48.1	-48.1	-129.2	-130.4	0.92
424	-196.8	17.8	-17.8	-214.7	-214.8	0.06
425	196.8	17.8	-17.8	214.7	214.8	0.06
426	81.1	48.1	-48.1	129.2	130.4	0.92
427	-81.1	48.1	-48.1	-129.2	-130.4	0.92
428	-196.8	17.8	-17.8	-214.7	-214.8	0.06
429	125.8	17.4	-17.4	143.1	143.3	0.08
430	56.3	47.1	-47.1	103.4	104.5	1.12
431	-56.3	47.1	-47.1	-103.4	-104.5	1.12
432	-125.8	17.4	-17.4	-143.1	-143.3	0.08
433	123.5	11.3	-11.3	134.9	134.8	-0.04
434	56.1	35.8	-35.8	91.9	92.6	0.77
435	-56.1	35.8	-35.8	-91.9	-92.6	0.77
436	-123.5	11.3	-11.3	-134.9	-134.8	-0.04
437	193.0	11.7	-11.7	204.7	204.6	-0.02
438	80.7	36.6	-36.6	117.3	118.1	0.62
439	-80.7	36.6	-36.6	-117.3	-118.1	0.62
440	-193.0	11.7	-11.7	-204.7	-204.6	-0.02
441	193.0	11.7	-11.7	204.7	204.6	-0.02
442	80.7	36.6	-36.6	117.3	118.1	0.62
443	-80.7	36.6	-36.6	-117.3	-118.1	0.62
444	-193.0	11.7	-11.7	-204.7	-204.6	-0.02
445	123.5	11.3	-11.3	134.9	134.8	-0.04
446	56.1	35.8	-35.8	91.9	92.6	0.77
447	-56.1	35.8	-35.8	-91.9	-92.6	0.77
448	-123.5	11.3	-11.3	-134.9	-134.8	-0.04
449	122.4	3.4	-3.4	125.9	125.7	-0.15
450	56.7	22.6	-22.6	79.4	79.7	0.47
451	-56.7	22.6	-22.6	-79.4	-79.7	0.47
452	-122.4	3.4	-3.4	-125.9	-125.7	-0.15
453	190.1	3.7	-3.7	193.8	193.6	-0.10
454	81.1	23.2	-23.2	104.4	104.7	0.37
455	-81.1	23.2	-23.2	-104.4	-104.7	0.37
456	-190.1	3.7	-3.7	-193.8	-193.6	-0.10
457	190.1	3.7	-3.7	193.8	193.6	-0.10
458	81.1	23.2	-23.2	104.4	104.7	0.37
459	-81.1	23.2	-23.2	-104.4	-104.7	0.37
460	-190.1	3.7	-3.7	-193.8	-193.6	-0.10
461	122.4	3.4	-3.4	125.9	125.7	-0.15
462	56.7	22.6	-22.6	79.4	79.7	0.47
463	-56.7	22.6	-22.6	-79.4	-79.7	0.47
464	-122.4	3.4	-3.4	-125.9	-125.7	-0.15
465	143.8	-4.6	4.6	148.4	148.7	0.19

466	64.1	11.2	-11.2	75.3	75.6	0.33
467	-64.1	11.2	-11.2	-75.3	-75.6	0.33
468	-143.8	-4.6	4.6	-148.4	-148.7	0.19
469	226.1	-4.6	4.6	230.7	231.1	0.14
470	93.0	11.5	-11.5	104.6	104.9	0.25
471	-93.0	11.5	-11.5	-104.6	-104.9	0.25
472	-226.1	-4.6	4.6	-230.7	-231.1	0.14
473	226.1	-4.6	4.6	230.7	231.1	0.14
474	93.0	11.5	-11.5	104.6	104.9	0.25
475	-93.0	11.5	-11.5	-104.6	-104.9	0.25
476	-226.1	-4.6	4.6	-230.7	-231.1	0.14
477	143.8	-4.6	4.6	148.4	148.7	0.19
478	64.1	11.2	-11.2	75.3	75.6	0.33
479	-64.1	11.2	-11.2	-75.3	-75.6	0.33
480	-143.8	-4.6	4.6	-148.4	-148.7	0.19

Table B.6 TM5 First and Second-Order Moments

TM5						
Column	**M_{SD+D+L}**	**$M_{POSITIVE\ EQ.}$**	**$M_{NEGATIVE\ EQ.}$**	**First-Order Moment**	**Second-Order Moment**	**Percent**
1	23.0	129.7	-129.7	152.7	157.4	3.11
2	0.0	136.9	-136.9	-136.9	-141.7	3.53
3	0.0	136.9	-136.9	136.9	141.7	3.53
4	-23.0	129.7	-129.7	-152.7	-157.4	3.11
5	41.5	131.1	-131.1	172.6	177.2	2.68
6	-0.2	138.9	-138.9	-139.1	-143.6	3.21
7	0.2	138.9	-138.9	139.1	143.6	3.21
8	-41.5	131.1	-131.1	-172.6	-177.2	2.68
9	41.5	131.1	-131.1	172.6	177.2	2.68
10	-0.2	138.9	-138.9	-139.1	-143.6	3.21
11	0.2	138.9	-138.9	139.1	143.6	3.21
12	-41.5	131.1	-131.1	-172.6	-177.2	2.68
13	23.0	129.7	-129.7	152.7	157.4	3.11
14	0.0	136.9	-136.9	-136.9	-141.7	3.53
15	0.0	136.9	-136.9	136.9	141.7	3.53
16	-23.0	129.7	-129.7	-152.7	-157.4	3.11
17	62.2	61.6	-61.6	123.8	127.0	2.62
18	-0.7	83.4	-83.4	-84.0	-88.2	**4.95**
19	0.7	83.4	-83.4	84.0	88.2	**4.95**
20	-62.2	61.6	-61.6	-123.8	-127.0	2.62
21	114.7	64.7	-64.7	179.4	182.7	1.85
22	-0.9	89.4	-89.4	-90.3	-94.6	4.73
23	0.9	89.4	-89.4	90.3	94.6	4.73
24	-114.7	64.7	-64.7	-179.4	-182.7	1.85
25	114.7	64.7	-64.7	179.4	182.7	1.85
26	-0.9	89.4	-89.4	-90.3	-94.6	4.73
27	0.9	89.4	-89.4	90.3	94.6	4.73
28	-114.7	64.7	-64.7	-179.4	-182.7	1.85
29	62.2	61.6	-61.6	123.8	127.0	2.62
30	-0.7	83.4	-83.4	-84.0	-88.2	**4.95**
31	0.7	83.4	-83.4	84.0	88.2	**4.95**
32	-62.2	61.6	-61.6	-123.8	-127.0	2.62
33	54.7	26.7	-26.7	81.5	82.5	1.22
34	0.4	50.2	-50.2	50.6	52.6	4.05
35	-0.4	50.2	-50.2	-50.6	-52.6	4.05
36	-54.7	26.7	-26.7	-81.5	-82.5	1.22
37	100.9	30.2	-30.2	131.2	132.3	0.87
38	0.9	56.7	-56.7	57.6	59.9	4.05
39	-0.9	56.7	-56.7	-57.6	-59.9	4.05
40	-100.9	30.2	-30.2	-131.2	-132.3	0.87
41	100.9	30.2	-30.2	131.2	132.3	0.87
42	0.9	56.7	-56.7	57.6	59.9	4.05

43	-0.9	56.7	-56.7	-57.6	-59.9	4.05
44	-100.9	30.2	-30.2	-131.2	-132.3	0.87
45	54.7	26.7	-26.7	81.5	82.5	1.22
46	0.4	50.2	-50.2	50.6	52.6	4.05
47	-0.4	50.2	-50.2	-50.6	-52.6	4.05
48	-54.7	26.7	-26.7	-81.5	-82.5	1.22
49	54.1	8.6	-8.6	62.8	62.4	-0.58
50	1.0	29.0	-29.0	30.0	30.5	1.57
51	-1.0	29.0	-29.0	-30.0	-30.5	1.57
52	-54.1	8.6	-8.6	-62.8	-62.4	-0.58
53	99.5	11.8	-11.8	111.4	111.2	-0.21
54	1.8	34.8	-34.8	36.6	37.3	2.01
55	-1.8	34.8	-34.8	-36.6	-37.3	2.01
56	-99.5	11.8	-11.8	-111.4	-111.2	-0.21
57	99.5	11.8	-11.8	111.4	111.2	-0.21
58	1.8	34.8	-34.8	36.6	37.3	2.01
59	-1.8	34.8	-34.8	-36.6	-37.3	2.01
60	-99.5	11.8	-11.8	-111.4	-111.2	-0.21
61	54.1	8.6	-8.6	62.8	62.4	-0.58
62	1.0	29.0	-29.0	30.0	30.5	1.57
63	-1.0	29.0	-29.0	-30.0	-30.5	1.57
64	-54.1	8.6	-8.6	-62.8	-62.4	-0.58
65	67.7	-6.4	6.4	74.1	74.8	1.00
66	0.0	12.5	-12.5	-12.5	-12.4	-0.82
67	0.0	12.5	-12.5	12.5	12.4	-0.82
68	-67.7	-6.4	6.4	-74.1	-74.8	1.00
69	125.2	-3.7	3.7	128.9	129.6	0.51
70	0.8	17.6	-17.6	18.5	18.6	0.52
71	-0.8	17.6	-17.6	-18.5	-18.6	0.52
72	-125.2	-3.7	3.7	-128.9	-129.6	0.51
73	125.2	-3.7	3.7	128.9	129.6	0.51
74	0.8	17.6	-17.6	18.5	18.6	0.52
75	-0.8	17.6	-17.6	-18.5	-18.6	0.52
76	-125.2	-3.7	3.7	-128.9	-129.6	0.51
77	67.7	-6.4	6.4	74.1	74.8	1.00
78	0.0	12.5	-12.5	-12.5	-12.4	-0.82
79	0.0	12.5	-12.5	12.5	12.4	-0.82
80	-67.7	-6.4	6.4	-74.1	-74.8	1.00

* All calculations are on the bottom of columns

Table B.7 TM10 First and Second-Order Moments

TM10						
Column	**M_{SD+D+L}**	**$M_{POSITIVE\ EQ.}$**	**$M_{NEGATIVE\ EQ.}$**	**First-Order Moment**	**Second-Order Moment**	**Percent**
1	23.6	191.8	-191.8	215.4	231.0	7.25
2	0.5	198.5	-198.5	199.0	214.8	7.95
3	-0.5	198.5	-198.5	-199.0	-214.8	7.95
4	-23.6	191.8	-191.8	-215.4	-231.0	7.25
5	42.8	193.2	-193.2	236.0	251.3	6.47
6	0.6	200.5	-200.5	201.1	216.2	7.53
7	-0.6	200.5	-200.5	-201.1	-216.2	7.53
8	-42.8	193.2	-193.2	-236.0	-251.3	6.47
9	42.8	193.2	-193.2	236.0	251.3	6.47
10	0.6	200.5	-200.5	201.1	216.2	7.53
11	-0.6	200.5	-200.5	-201.1	-216.2	7.53
12	-42.8	193.2	-193.2	-236.0	-251.3	6.47
13	23.6	191.8	-191.8	215.4	231.0	7.25
14	0.5	198.5	-198.5	199.0	214.8	7.95
15	-0.5	198.5	-198.5	-199.0	-214.8	7.95
16	-23.6	191.8	-191.8	-215.4	-231.0	7.25
17	62.5	108.7	-108.7	171.1	184.5	7.84
18	0.0	130.0	-130.0	-130.0	-145.5	11.88
19	0.0	130.0	-130.0	130.0	145.5	11.88
20	-62.5	108.7	-108.7	-171.1	-184.5	7.84
21	116.9	111.7	-111.7	228.6	242.2	5.95
22	0.4	136.1	-136.1	136.5	152.3	11.52
23	-0.4	136.1	-136.1	-136.5	-152.3	11.52
24	-116.9	111.7	-111.7	-228.6	-242.2	5.95
25	116.9	111.7	-111.7	228.6	242.2	5.95
26	0.4	136.1	-136.1	136.5	152.3	11.52
27	-0.4	136.1	-136.1	-136.5	-152.3	11.52
28	-116.9	111.7	-111.7	-228.6	-242.2	5.95
29	62.5	108.7	-108.7	171.1	184.5	7.84
30	0.0	130.0	-130.0	-130.0	-145.5	11.88
31	0.0	130.0	-130.0	130.0	145.5	11.88
32	-62.5	108.7	-108.7	-171.1	-184.5	7.84
33	56.0	62.1	-62.1	118.1	126.8	7.35
34	1.6	89.1	-89.1	90.7	102.5	**12.91**
35	-1.6	89.1	-89.1	-90.7	-102.5	**12.91**
36	-56.0	62.1	-62.1	-118.1	-126.8	7.35
37	103.8	66.2	-66.2	169.9	179.0	5.32
38	3.1	96.9	-96.9	100.0	112.4	12.45
39	-3.1	96.9	-96.9	-100.0	-112.4	12.45
40	-103.8	66.2	-66.2	-169.9	-179.0	5.32
41	103.8	66.2	-66.2	169.9	179.0	5.32

42	3.1	96.9	-96.9	100.0	112.4	12.45
43	-3.1	96.9	-96.9	-100.0	-112.4	12.45
44	-103.8	66.2	-66.2	-169.9	-179.0	5.32
45	56.0	62.1	-62.1	118.1	126.8	7.35
46	1.6	89.1	-89.1	90.7	102.5	**12.91**
47	-1.6	89.1	-89.1	-90.7	-102.5	**12.91**
48	-56.0	62.1	-62.1	-118.1	-126.8	7.35
49	57.4	38.5	-38.5	95.9	100.4	4.73
50	2.0	67.0	-67.0	69.0	76.8	11.39
51	-2.0	67.0	-67.0	-69.0	-76.8	11.39
52	-57.4	38.5	-38.5	-95.9	-100.4	4.73
53	106.8	42.9	-42.9	149.6	154.7	3.36
54	3.9	75.3	-75.3	79.2	88.0	11.10
55	-3.9	75.3	-75.3	-79.2	-88.0	11.10
56	-106.8	42.9	-42.9	-149.6	-154.7	3.36
57	106.8	42.9	-42.9	149.6	154.7	3.36
58	3.9	75.3	-75.3	79.2	88.0	11.10
59	-3.9	75.3	-75.3	-79.2	-88.0	11.10
60	-106.8	42.9	-42.9	-149.6	-154.7	3.36
61	57.4	38.5	-38.5	95.9	100.4	4.73
62	2.0	67.0	-67.0	69.0	76.8	11.39
63	-2.0	67.0	-67.0	-69.0	-76.8	11.39
64	-57.4	38.5	-38.5	-95.9	-100.4	4.73
65	59.9	25.7	-25.7	85.6	87.3	2.00
66	2.5	55.4	-55.4	57.9	62.9	8.75
67	-2.5	55.4	-55.4	-57.9	-62.9	8.75
68	-59.9	25.7	-25.7	-85.6	-87.3	2.00
69	111.7	30.1	-30.1	141.9	144.1	1.56
70	5.2	63.9	-63.9	69.1	75.1	8.74
71	-5.2	63.9	-63.9	-69.1	-75.1	8.74
72	-111.7	30.1	-30.1	-141.9	-144.1	1.56
73	111.7	30.1	-30.1	141.9	144.1	1.56
74	5.2	63.9	-63.9	69.1	75.1	8.74
75	-5.2	63.9	-63.9	-69.1	-75.1	8.74
76	-111.7	30.1	-30.1	-141.9	-144.1	1.56
77	59.9	25.7	-25.7	85.6	87.3	2.00
78	2.5	55.4	-55.4	57.9	62.9	8.75
79	-2.5	55.4	-55.4	-57.9	-62.9	8.75
80	-59.9	25.7	-25.7	-85.6	-87.3	2.00
81	49.1	22.7	-22.7	71.8	72.5	1.05
82	2.5	45.3	-45.3	47.8	50.9	6.47
83	-2.5	45.3	-45.3	-47.8	-50.9	6.47
84	-49.1	22.7	-22.7	-71.8	-72.5	1.05
85	90.3	26.1	-26.1	116.4	117.6	0.99
86	4.9	51.6	-51.6	56.5	60.2	6.69
87	-4.9	51.6	-51.6	-56.5	-60.2	6.69
88	-90.3	26.1	-26.1	-116.4	-117.6	0.99

89	90.3	26.1	-26.1	116.4	117.6	0.99
90	4.9	51.6	-51.6	56.5	60.2	6.69
91	-4.9	51.6	-51.6	-56.5	-60.2	6.69
92	-90.3	26.1	-26.1	-116.4	-117.6	0.99
93	49.1	22.7	-22.7	71.8	72.5	1.05
94	2.5	45.3	-45.3	47.8	50.9	6.47
95	-2.5	45.3	-45.3	-47.8	-50.9	6.47
96	-49.1	22.7	-22.7	-71.8	-72.5	1.05
97	60.6	14.4	-14.4	75.0	74.3	-0.83
98	3.1	40.0	-40.0	43.1	44.7	3.87
99	-3.1	40.0	-40.0	-43.1	-44.7	3.87
100	-60.6	14.4	-14.4	-75.0	-74.3	-0.83
101	111.6	18.0	-18.0	129.7	129.4	-0.21
102	6.3	47.0	-47.0	53.2	55.6	4.39
103	-6.3	47.0	-47.0	-53.2	-55.6	4.39
104	-111.6	18.0	-18.0	-129.7	-129.4	-0.21
105	111.6	18.0	-18.0	129.7	129.4	-0.21
106	6.3	47.0	-47.0	53.2	55.6	4.39
107	-6.3	47.0	-47.0	-53.2	-55.6	4.39
108	-111.6	18.0	-18.0	-129.7	-129.4	-0.21
109	60.6	14.4	-14.4	75.0	74.3	-0.83
110	3.1	40.0	-40.0	43.1	44.7	3.87
111	-3.1	40.0	-40.0	-43.1	-44.7	3.87
112	-60.6	14.4	-14.4	-75.0	-74.3	-0.83
113	59.3	9.3	-9.3	68.6	67.5	-1.55
114	3.5	30.9	-30.9	34.5	34.9	1.35
115	-3.5	30.9	-30.9	-34.5	-34.9	1.35
116	-59.3	9.3	-9.3	-68.6	-67.5	-1.55
117	109.2	12.4	-12.4	121.7	120.8	-0.67
118	7.1	36.9	-36.9	43.9	44.9	2.09
119	-7.1	36.9	-36.9	-43.9	-44.9	2.09
120	-109.2	12.4	-12.4	-121.7	-120.8	-0.67
121	109.2	12.4	-12.4	121.7	120.8	-0.67
122	7.1	36.9	-36.9	43.9	44.9	2.09
123	-7.1	36.9	-36.9	-43.9	-44.9	2.09
124	-109.2	12.4	-12.4	-121.7	-120.8	-0.67
125	59.3	9.3	-9.3	68.6	67.5	-1.55
126	3.5	30.9	-30.9	34.5	34.9	1.35
127	-3.5	30.9	-30.9	-34.5	-34.9	1.35
128	-59.3	9.3	-9.3	-68.6	-67.5	-1.55
129	57.4	3.2	-3.2	60.6	59.4	-2.03
130	4.2	21.0	-21.0	25.2	25.0	-0.85
131	-4.2	21.0	-21.0	-25.2	-25.0	-0.85
132	-57.4	3.2	-3.2	-60.6	-59.4	-2.03
133	105.3	5.8	-5.8	111.2	110.1	-0.98
134	8.0	25.9	-25.9	33.9	34.0	0.27
135	-8.0	25.9	-25.9	-33.9	-34.0	0.27

136	-105.3	5.8	-5.8	-111.2	-110.1	-0.98
137	105.3	5.8	-5.8	111.2	110.1	-0.98
138	8.0	25.9	-25.9	33.9	34.0	0.27
139	-8.0	25.9	-25.9	-33.9	-34.0	0.27
140	-105.3	5.8	-5.8	-111.2	-110.1	-0.98
141	57.4	3.2	-3.2	60.6	59.4	-2.03
142	4.2	21.0	-21.0	25.2	25.0	-0.85
143	-4.2	21.0	-21.0	-25.2	-25.0	-0.85
144	-57.4	3.2	-3.2	-60.6	-59.4	-2.03
145	71.9	-6.2	6.2	78.1	79.1	1.30
146	4.0	10.2	-10.2	14.1	13.8	-2.04
147	-4.0	10.2	-10.2	-14.1	-13.8	-2.04
148	-71.9	-6.2	6.2	-78.1	-79.1	1.30
149	132.9	-4.0	4.0	136.9	137.8	0.68
150	8.5	14.5	-14.5	23.0	22.9	-0.34
151	-8.5	14.5	-14.5	-23.0	-22.9	-0.34
152	-132.9	-4.0	4.0	-136.9	-137.8	0.68
153	132.9	-4.0	4.0	136.9	137.8	0.68
154	8.5	14.5	-14.5	23.0	22.9	-0.34
155	-8.5	14.5	-14.5	-23.0	-22.9	-0.34
156	-132.9	-4.0	4.0	-136.9	-137.8	0.68
157	71.9	-6.2	6.2	78.1	79.1	1.30
158	4.0	10.2	-10.2	14.1	13.8	-2.04
159	-4.0	10.2	-10.2	-14.1	-13.8	-2.04
160	-71.9	-6.2	6.2	-78.1	-79.1	1.30

Table B.8 TM15 First and Second-Order Moments

TM15						
Column	**M_{SD+D+L}**	**$M_{POSITIVE\ EQ.}$**	**$M_{NEGATIVE\ EQ.}$**	**First-Order Moment**	**Second-Order Moment**	**Percent**
1	24.8	333.4	-333.4	358.2	398.5	11.26
2	1.1	338.6	-338.6	339.8	380.3	11.92
3	-1.1	338.6	-338.6	-339.8	-380.3	11.92
4	-24.8	333.4	-333.4	-358.2	-398.5	11.26
5	44.6	334.8	-334.8	379.3	419.1	10.47
6	1.4	340.4	-340.4	341.7	381.3	11.57
7	-1.4	340.4	-340.4	-341.7	-381.3	11.57
8	-44.6	334.8	-334.8	-379.3	-419.1	10.47
9	44.6	334.8	-334.8	379.3	419.1	10.47
10	1.4	340.4	-340.4	341.7	381.3	11.57
11	-1.4	340.4	-340.4	-341.7	-381.3	11.57
12	-44.6	334.8	-334.8	-379.3	-419.1	10.47
13	24.8	333.4	-333.4	358.2	398.5	11.26
14	1.1	338.6	-338.6	339.8	380.3	11.92
15	-1.1	338.6	-338.6	-339.8	-380.3	11.92
16	-24.8	333.4	-333.4	-358.2	-398.5	11.26
17	60.7	225.3	-225.3	286.0	323.4	13.06
18	-0.2	241.3	-241.3	-241.5	-281.0	16.36
19	0.2	241.3	-241.3	241.5	281.0	16.36
20	-60.7	225.3	-225.3	-286.0	-323.4	13.06
21	115.5	227.5	-227.5	343.0	380.6	10.96
22	0.4	246.1	-246.1	246.4	286.3	16.17
23	-0.4	246.1	-246.1	-246.4	-286.3	16.17
24	-115.5	227.5	-227.5	-343.0	-380.6	10.96
25	115.5	227.5	-227.5	343.0	380.6	10.96
26	0.4	246.1	-246.1	246.4	286.3	16.17
27	-0.4	246.1	-246.1	-246.4	-286.3	16.17
28	-115.5	227.5	-227.5	-343.0	-380.6	10.96
29	60.7	225.3	-225.3	286.0	323.4	13.06
30	-0.2	241.3	-241.3	-241.5	-281.0	16.36
31	0.2	241.3	-241.3	241.5	281.0	16.36
32	-60.7	225.3	-225.3	-286.0	-323.4	13.06
33	57.3	148.5	-148.5	205.8	235.8	14.57
34	2.0	171.9	-171.9	173.9	207.5	19.33
35	-2.0	171.9	-171.9	-173.9	-207.5	19.33
36	-57.3	148.5	-148.5	-205.8	-235.8	14.57
37	106.4	152.1	-152.1	258.5	288.8	11.75
38	3.5	178.9	-178.9	182.4	216.8	18.86
39	-3.5	178.9	-178.9	-182.4	-216.8	18.86
40	-106.4	152.1	-152.1	-258.5	-288.8	11.75
41	106.4	152.1	-152.1	258.5	288.8	11.75
42	3.5	178.9	-178.9	182.4	216.8	18.86

43	-3.5	178.9	-178.9	-182.4	-216.8	18.86
44	-106.4	152.1	-152.1	-258.5	-288.8	11.75
45	57.3	148.5	-148.5	205.8	235.8	14.57
46	2.0	171.9	-171.9	173.9	207.5	19.33
47	-2.0	171.9	-171.9	-173.9	-207.5	19.33
48	-57.3	148.5	-148.5	-205.8	-235.8	14.57
49	57.8	97.1	-97.1	154.9	176.5	13.94
50	2.3	124.3	-124.3	126.5	152.7	**20.72**
51	-2.3	124.3	-124.3	-126.5	-152.7	**20.72**
52	-57.8	97.1	-97.1	-154.9	-176.5	13.94
53	108.0	101.3	-101.3	209.3	231.5	10.62
54	4.3	132.3	-132.3	136.7	164.1	20.07
55	-4.3	132.3	-132.3	-136.7	-164.1	20.07
56	-108.0	101.3	-101.3	-209.3	-231.5	10.62
57	108.0	101.3	-101.3	209.3	231.5	10.62
58	4.3	132.3	-132.3	136.7	164.1	20.07
59	-4.3	132.3	-132.3	-136.7	-164.1	20.07
60	-108.0	101.3	-101.3	-209.3	-231.5	10.62
61	57.8	97.1	-97.1	154.9	176.5	13.94
62	2.3	124.3	-124.3	126.5	152.7	**20.72**
63	-2.3	124.3	-124.3	-126.5	-152.7	**20.72**
64	-57.8	97.1	-97.1	-154.9	-176.5	13.94
65	59.6	64.1	-64.1	123.8	137.9	11.40
66	2.3	94.5	-94.5	96.8	116.3	20.15
67	-2.3	94.5	-94.5	-96.8	-116.3	20.15
68	-59.6	64.1	-64.1	-123.8	-137.9	11.40
69	112.8	68.4	-68.4	181.2	196.1	8.18
70	5.0	103.6	-103.6	108.6	129.6	19.38
71	-5.0	103.6	-103.6	-108.6	-129.6	19.38
72	-112.8	68.4	-68.4	-181.2	-196.1	8.18
73	112.8	68.4	-68.4	181.2	196.1	8.18
74	5.0	103.6	-103.6	108.6	129.6	19.38
75	-5.0	103.6	-103.6	-108.6	-129.6	19.38
76	-112.8	68.4	-68.4	-181.2	-196.1	8.18
77	59.6	64.1	-64.1	123.8	137.9	11.40
78	2.3	94.5	-94.5	96.8	116.3	20.15
79	-2.3	94.5	-94.5	-96.8	-116.3	20.15
80	-59.6	64.1	-64.1	-123.8	-137.9	11.40
81	45.2	49.5	-49.5	94.8	104.2	9.98
82	3.0	72.4	-72.4	75.4	88.9	17.95
83	-3.0	72.4	-72.4	-75.4	-88.9	17.95
84	-45.2	49.5	-49.5	-94.8	-104.2	9.98
85	83.0	53.4	-53.4	136.4	146.5	7.44
86	5.3	79.1	-79.1	84.4	99.1	17.40
87	-5.3	79.1	-79.1	-84.4	-99.1	17.40
88	-83.0	53.4	-53.4	-136.4	-146.5	7.44
89	83.0	53.4	-53.4	136.4	146.5	7.44

90	5.3	79.1	-79.1	84.4	99.1	17.40
91	-5.3	79.1	-79.1	-84.4	-99.1	17.40
92	-83.0	53.4	-53.4	-136.4	-146.5	7.44
93	45.2	49.5	-49.5	94.8	104.2	9.98
94	3.0	72.4	-72.4	75.4	88.9	17.95
95	-3.0	72.4	-72.4	-75.4	-88.9	17.95
96	-45.2	49.5	-49.5	-94.8	-104.2	9.98
97	62.0	32.1	-32.1	94.1	98.3	4.50
98	3.6	64.4	-64.4	68.1	78.0	14.61
99	-3.6	64.4	-64.4	-68.1	-78.0	14.61
100	-62.0	32.1	-32.1	-94.1	-98.3	4.50
101	115.6	36.7	-36.7	152.3	157.3	3.32
102	7.4	73.7	-73.7	81.0	92.6	14.29
103	-7.4	73.7	-73.7	-81.0	-92.6	14.29
104	-115.6	36.7	-36.7	-152.3	-157.3	3.32
105	115.6	36.7	-36.7	152.3	157.3	3.32
106	7.4	73.7	-73.7	81.0	92.6	14.29
107	-7.4	73.7	-73.7	-81.0	-92.6	14.29
108	-115.6	36.7	-36.7	-152.3	-157.3	3.32
109	62.0	32.1	-32.1	94.1	98.3	4.50
110	3.6	64.4	-64.4	68.1	78.0	14.61
111	-3.6	64.4	-64.4	-68.1	-78.0	14.61
112	-62.0	32.1	-32.1	-94.1	-98.3	4.50
113	60.1	24.5	-24.5	84.6	86.1	1.81
114	4.7	54.5	-54.5	59.2	65.7	11.01
115	-4.7	54.5	-54.5	-59.2	-65.7	11.01
116	-60.1	24.5	-24.5	-84.6	-86.1	1.81
117	111.2	29.0	-29.0	140.2	142.5	1.64
118	9.1	63.0	-63.0	72.1	80.1	11.06
119	-9.1	63.0	-63.0	-72.1	-80.1	11.06
120	-111.2	29.0	-29.0	-140.2	-142.5	1.64
121	111.2	29.0	-29.0	140.2	142.5	1.64
122	9.1	63.0	-63.0	72.1	80.1	11.06
123	-9.1	63.0	-63.0	-72.1	-80.1	11.06
124	-111.2	29.0	-29.0	-140.2	-142.5	1.64
125	60.1	24.5	-24.5	84.6	86.1	1.81
126	4.7	54.5	-54.5	59.2	65.7	11.01
127	-4.7	54.5	-54.5	-59.2	-65.7	11.01
128	-60.1	24.5	-24.5	-84.6	-86.1	1.81
129	60.8	19.1	-19.1	80.0	79.7	-0.30
130	5.3	48.0	-48.0	53.2	57.4	7.88
131	-5.3	48.0	-48.0	-53.2	-57.4	7.88
132	-60.8	19.1	-19.1	-80.0	-79.7	-0.30
133	112.7	23.4	-23.4	136.0	136.5	0.33
134	10.2	56.2	-56.2	66.3	71.9	8.30
135	-10.2	56.2	-56.2	-66.3	-71.9	8.30
136	-112.7	23.4	-23.4	-136.0	-136.5	0.33

137	112.7	23.4	-23.4	136.0	136.5	0.33
138	10.2	56.2	-56.2	66.3	71.9	8.30
139	-10.2	56.2	-56.2	-66.3	-71.9	8.30
140	-112.7	23.4	-23.4	-136.0	-136.5	0.33
141	60.8	19.1	-19.1	80.0	79.7	-0.30
142	5.3	48.0	-48.0	53.2	57.4	7.88
143	-5.3	48.0	-48.0	-53.2	-57.4	7.88
144	-60.8	19.1	-19.1	-80.0	-79.7	-0.30
145	63.4	15.8	-15.8	79.2	78.1	-1.39
146	5.8	44.3	-44.3	50.1	53.0	5.68
147	-5.8	44.3	-44.3	-50.1	-53.0	5.68
148	-63.4	15.8	-15.8	-79.2	-78.1	-1.39
149	118.0	19.8	-19.8	137.9	137.4	-0.37
150	11.5	52.4	-52.4	63.9	67.9	6.28
151	-11.5	52.4	-52.4	-63.9	-67.9	6.28
152	-118.0	19.8	-19.8	-137.9	-137.4	-0.37
153	118.0	19.8	-19.8	137.9	137.4	-0.37
154	11.5	52.4	-52.4	63.9	67.9	6.28
155	-11.5	52.4	-52.4	-63.9	-67.9	6.28
156	-118.0	19.8	-19.8	-137.9	-137.4	-0.37
157	63.4	15.8	-15.8	79.2	78.1	-1.39
158	5.8	44.3	-44.3	50.1	53.0	5.68
159	-5.8	44.3	-44.3	-50.1	-53.0	5.68
160	-63.4	15.8	-15.8	-79.2	-78.1	-1.39
161	52.0	17.4	-17.4	69.4	68.8	-0.86
162	5.2	38.7	-38.7	43.9	45.9	4.50
163	-5.2	38.7	-38.7	-43.9	-45.9	4.50
164	-52.0	17.4	-17.4	-69.4	-68.8	-0.86
165	95.2	20.6	-20.6	115.8	115.7	-0.15
166	9.8	44.5	-44.5	54.4	57.1	5.01
167	-9.8	44.5	-44.5	-54.4	-57.1	5.01
168	-95.2	20.6	-20.6	-115.8	-115.7	-0.15
169	95.2	20.6	-20.6	115.8	115.7	-0.15
170	9.8	44.5	-44.5	54.4	57.1	5.01
171	-9.8	44.5	-44.5	-54.4	-57.1	5.01
172	-95.2	20.6	-20.6	-115.8	-115.7	-0.15
173	52.0	17.4	-17.4	69.4	68.8	-0.86
174	5.2	38.7	-38.7	43.9	45.9	4.50
175	-5.2	38.7	-38.7	-43.9	-45.9	4.50
176	-52.0	17.4	-17.4	-69.4	-68.8	-0.86
177	64.1	11.6	-11.6	75.7	74.5	-1.62
178	6.3	35.3	-35.3	41.6	42.8	2.76
179	-6.3	35.3	-35.3	-41.6	-42.8	2.76
180	-64.1	11.6	-11.6	-75.7	-74.5	-1.62
181	117.6	14.8	-14.8	132.4	131.6	-0.67
182	12.3	41.6	-41.6	53.9	55.7	3.38
183	-12.3	41.6	-41.6	-53.9	-55.7	3.38

184	-117.6	14.8	-14.8	-132.4	-131.6	-0.67
185	117.6	14.8	-14.8	132.4	131.6	-0.67
186	12.3	41.6	-41.6	53.9	55.7	3.38
187	-12.3	41.6	-41.6	-53.9	-55.7	3.38
188	-117.6	14.8	-14.8	-132.4	-131.6	-0.67
189	64.1	11.6	-11.6	75.7	74.5	-1.62
190	6.3	35.3	-35.3	41.6	42.8	2.76
191	-6.3	35.3	-35.3	-41.6	-42.8	2.76
192	-64.1	11.6	-11.6	-75.7	-74.5	-1.62
193	62.7	8.9	-8.9	71.5	70.3	-1.77
194	6.7	28.9	-28.9	35.6	35.9	0.78
195	-6.7	28.9	-28.9	-35.6	-35.9	0.78
196	-62.7	8.9	-8.9	-71.5	-70.3	-1.77
197	115.0	11.6	-11.6	126.6	125.6	-0.82
198	12.9	34.3	-34.3	47.2	47.9	1.51
199	-12.9	34.3	-34.3	-47.2	-47.9	1.51
200	-115.0	11.6	-11.6	-126.6	-125.6	-0.82
201	115.0	11.6	-11.6	126.6	125.6	-0.82
202	12.9	34.3	-34.3	47.2	47.9	1.51
203	-12.9	34.3	-34.3	-47.2	-47.9	1.51
204	-115.0	11.6	-11.6	-126.6	-125.6	-0.82
205	62.7	8.9	-8.9	71.5	70.3	-1.77
206	6.7	28.9	-28.9	35.6	35.9	0.78
207	-6.7	28.9	-28.9	-35.6	-35.9	0.78
208	-62.7	8.9	-8.9	-71.5	-70.3	-1.77
209	60.7	3.1	-3.1	63.8	62.5	-1.99
210	7.2	19.8	-19.8	27.0	26.8	-0.91
211	-7.2	19.8	-19.8	-27.0	-26.8	-0.91
212	-60.7	3.1	-3.1	-63.8	-62.5	-1.99
213	110.9	5.5	-5.5	116.4	115.2	-0.99
214	13.6	24.3	-24.3	37.8	37.9	0.11
215	-13.6	24.3	-24.3	-37.8	-37.9	0.11
216	-110.9	5.5	-5.5	-116.4	-115.2	-0.99
217	110.9	5.5	-5.5	116.4	115.2	-0.99
218	13.6	24.3	-24.3	37.8	37.9	0.11
219	-13.6	24.3	-24.3	-37.8	-37.9	0.11
220	-110.9	5.5	-5.5	-116.4	-115.2	-0.99
221	60.7	3.1	-3.1	63.8	62.5	-1.99
222	7.2	19.8	-19.8	27.0	26.8	-0.91
223	-7.2	19.8	-19.8	-27.0	-26.8	-0.91
224	-60.7	3.1	-3.1	-63.8	-62.5	-1.99
225	75.9	-6.8	6.8	82.7	83.7	1.23
226	7.7	8.4	-8.4	16.1	15.9	-1.61
227	-7.7	8.4	-8.4	-16.1	-15.9	-1.61
228	-75.9	-6.8	6.8	-82.7	-83.7	1.23
229	139.8	-4.9	4.9	144.7	145.6	0.66
230	15.4	12.3	-12.3	27.7	27.6	-0.23

231	-15.4	12.3	-12.3	-27.7	-27.6	-0.23
232	-139.8	-4.9	4.9	-144.7	-145.6	0.66
233	139.8	-4.9	4.9	144.7	145.6	0.66
234	15.4	12.3	-12.3	27.7	27.6	-0.23
235	-15.4	12.3	-12.3	-27.7	-27.6	-0.23
236	-139.8	-4.9	4.9	-144.7	-145.6	0.66
237	75.9	-6.8	6.8	82.7	83.7	1.23
238	7.7	8.4	-8.4	16.1	15.9	-1.61
239	-7.7	8.4	-8.4	-16.1	-15.9	-1.61
240	-75.9	-6.8	6.8	-82.7	-83.7	1.23

Appendix C

Verification of Second-Order Analysis

Table C.1 M10-First-Order Analysis Moment on Column Number Four

	Moment on Base (kN.m)	**Moment on Top (kN.m)**
Live Load	-5.85	12.27
Super Imposed Load	-8.77	18.41
Dead Load	-13.84	29.14
Earthquake Load	-227.2	-46.3

Table C.2 M10-Verification on Second-Order Analysis on Column Number Four

Parameter	**Value**
$\sum P$	60633kN
I_{Column}	$0.04374m^4$
I_{Beam}	8.58×10^{-3} m^4
E_{Column}	26.6×10^{6} kN/m^2
E_{Beam}	23×10^{6} kN/m^2
G_A(middle)	10.4
K(unbraced)	1.68
P_{ek} (middle)	351952kN
G_A (edge)	20.8
K (unbraced)	1.8
P_{ek} (edge)	306590kN
$\sum P_{ek}$	5268336kN
B_2	1.012
C_m	0.41
P	2330kN
K (braced)	0.70
P_e	2027245kN
B_1	0.41 (Take B_1=1)
M_u	-260.2kN.m
M_u (SAP2000)	-260.3kN.m
%error	0.04 %
Acceptance Criteria	10%
Comment	OK

Table C.3 M15-First-Order Analysis Moment on Column Number Four

	Moment on Base (kN.m)	Moment on Top (kN.m)
Live Load	-6.1	12.7
Super Imposed Load	-9.1	19.1
Dead Load	-14.4	30.3
Earthquake Load	-289	-96.8

Table C.4 M15-Verification on Second-Order Analysis on Column Number Four

Parameter	Value
$\sum P$	93083kN
I_{Column}	$0.066m^4$
I_{Beam}	8.58×10^{-3} m^4
E_{Column}	26.6×10^{6} kN/m^2
E_{Beam}	23×10^{6} kN/m^2
G_A(middle)	15.7
K(unbraced)	1.75
P_{ek} (middle)	489431kN
G_A (edge)	31.4
K (unbraced)	1.88
P_{ek} (edge)	424084kN
$\sum P_{ek}$	7308120kN
B_2	1.013
C_m	0.41
P	3803kN
K (braced)	0.7
P_e	3058943kN
B_1	0.41 (Take B_1=1)
M_u	-322.4kN.m
M_u (SAP2000)	-327.4kN.m
%error	1.5 %
Acceptance Criteria	10%
Comment	OK

Table C.5 M20-First-Order Analysis Moment on Column Number Four

	Moment on Base (kN.m)	**Moment on Top (kN.m)**
Live Load	-6.3	13.1
Super Imposed Load	-9.4	19.7
Dead Load	-14.8	31.2
Earthquake Load	-352.9	-154.5

Table B.6 M20-Verification on Second-Order Analysis on Column Number Four

Parameter	**Value**
$\sum P$	126961kN
I_{Column}	$0.097m^4$
I_{Beam}	8.58×10^{-3} m^4
E_{Column}	26.6×10^{6} kN/m^2
E_{Beam}	23×10^{6} kN/m^2
G_A(middle)	23
K(unbraced)	1.82
P_{ek} (middle)	665047kN
G_A (edge)	46
K (unbraced)	1.91
P_{ek} (edge)	603849kN
$\sum P_{ek}$	10151168kN
B_2	1.013
C_m	0.41
P	5461kN
K (braced)	0.7
P_e	4495719kN
B_1	0.41 (Take B_1=1)
M_u	-389kN.m
M_u (SAP2000)	-399kN.m
%error	2.5 %
Acceptance Criteria	10%
Comment	OK

Table C.7 M25-First-Order Analysis Moment on Column Number Four

	Moment on Base (kN.m)	**Moment on Top (kN.m)**
Live Load	-6.4	13.4
Super Imposed Load	-9.6	20.1
Dead Load	-15.2	31.9
Earthquake Load	-422.8	-219.7

TableC.8 M25-Verification on Second-Order Analysis on Column Number Four

Parameter	**Value**
$\sum P$	162403kN
I_{Column}	$0.138m^4$
I_{Beam}	8.58×10^{-3} m^4
E_{Column}	26.6×10^{6} kN/m^2
E_{Beam}	23×10^{6} kN/m^2
G_A(middle)	32.8
K(unbraced)	1.88
P_{ek} (middle)	886720kN
G_A (edge)	65.6
K (unbraced)	1.92
P_{ek} (edge)	850159kN
$\sum P_{ek}$	13895032kN
B_2	1.012
C_m	0.41
P	7284kN
K (braced)	0.7
P_e	6395972kN
B_1	0.41 (Take B_1=1)
M_u	-459kN.m
M_u (SAP2000)	-478.3kN.m
%error	4 %
Acceptance Criteria	10%
Comment	OK

Table C.9 M30-First-Order Analysis Moment on Column Number Four

	Moment on Base (kN.m)	**Moment on Top (kN.m)**
Live Load	-6.57	13.7
Super Imposed Load	-9.86	20.6
Dead Load	-15.5	32.7
Earthquake Load	-474	-277

Table C.10 M30-Verification on Second-Order Analysis on Column Number Four

Parameter	**Value**
$\sum P$	199545kN
I_{Column}	$0.19m^4$
I_{Beam}	8.58×10^{-3} m^4
E_{Column}	26.6×10^{6} kN/m^2
E_{Beam}	23×10^{6} kN/m^2
G_A(middle)	45.2
K(unbraced)	1.9
P_{ek} (middle)	1195280kN
G_A (edge)	90.4
K (unbraced)	1.95
P_{ek} (edge)	1134770kN
$\sum P_{ek}$	18640401kN
B_2	1.011
C_m	0.41
P	9260kN
K (braced)	0.7
P_e	8806048kN
B_1	0.41 (Take B_1=1)
M_u	-511kN.m
M_u (SAP2000)	-539kN.m
%error	5.2 %
Acceptance Criteria	10%
Comment	OK

جامعة النجاح الوطنية

كلية الدراسات العليا

اثار P – دلتا في الخرسانة المسلحة لاطارات البوابة الزلزالية

إعداد

صهيب محمد ابو قبيطة

إشراف

د. عبد الرزاق طوقان

قدمت هذه الأطروحة استكمالا لمتطلبات الحصول على درجة الماجستير في هندسة الإنشاءات بكلية الدراسات العليا في جامعة النجاح الوطنية في نابلس، فلسطين.

2019

اثار P – دلتا في الخرسانة المسلحة لاطارات البوابة الزلزالية

إعداد

صهيب محمد ابو قبيطة

إشراف

د. عبد الرزاق طوقان

الملخص

تأثير P-Delta هو تأثير غير خطي من الدرجة الثانية والذي يتواجد في أية منشأ عندما يتعرض الى أحمال محورية و عزوم ويكون تأثيره أكبر في المباني المرتفعة. المباني متعددة الطوابق تنتشر بشكل كبير لإيواء العدد الكبير من السكان اللذين يحتاجون الى سكن خاصة في العواصم والمدن الكبيرة. لذلك، لدراسة تأثير عدد الطوابق على تحليل P-Delta ، تأثير P-Delta تم دراسته على ستة نماذج متعددة الطوابق من البوابات الخرسانية المسلحة والتي تتدرج من خمسة طوابق الى ثلاثين طابق والتي تخضع لحد الفترة الأساسية المنصوص عليها في ASCE 7 مقابل دراسة نفس الستة النماذج السابقة غير أنها لا تخضع لحد الفترة الأساسية.

تقع فلسطين في منطقة نشطة زلزاليا حيث أنها تقع على امتداد صدع البحر الميت والذي يعد من أنشط الصدوع الزلزالية في منطقة الشرق الأوسط. لذلك، تم تطبيق أحمال زلزالية على جميع النماذج والتي تم حساب قيمها باستخدام تحليل طيف الإستجابة بالتوافق مع IBC 2015 و ASCE 7. العزم من تحليل الدرجة الأولى و تحليل الدرجة الثانية تم حسابه على العمود الحرج لجميع النماذج ونسبة الزيادة في العزم من تحليل الدرجة الأولى الى تحليل الدرجة الثانية تم حسابه. تم إستخدام برنامج التحليل الإنشائي SAP2000 19.0 بالتوافق مع الحسابات اليدوية.

كنتيجة نهائية، على الأرجح، المهندسين الإنشائيين لن يواجهوا مشاكل مع P-Delta اذا تم بناء منشاءات إطارات بوابات خرسانية مسلحة حتى 25 طابق والتي تخضع للكود وحتى 8 طوابق والتي لاتخضع للكود.